



**Institute of
Applied Physics**

Friedrich-Schiller-Universität Jena

Optical System Design Fundamentals

Lecture 6: Aberrations: classification, diagrams and identification in real images

2024 / 06 / 11

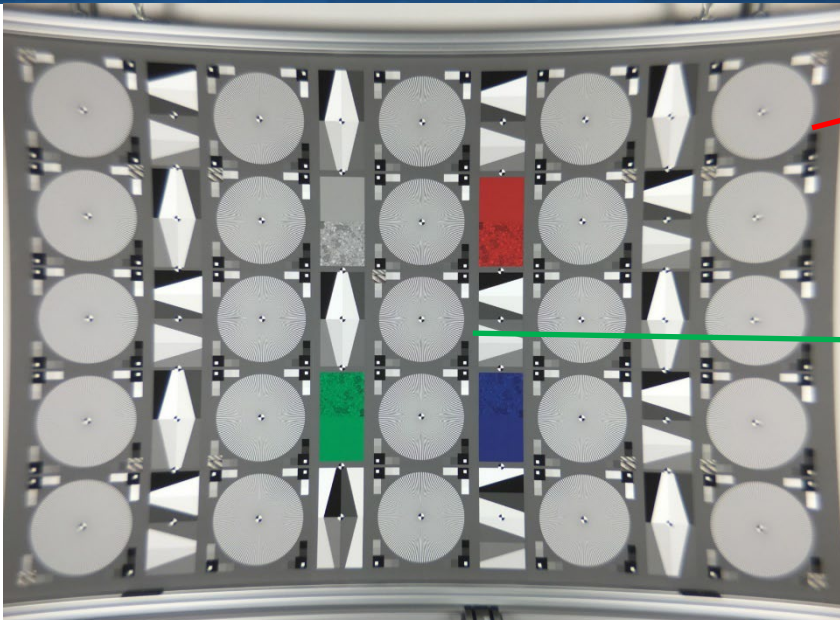
Vladan Blahnik

Preliminary Schedule - OSDF 2024

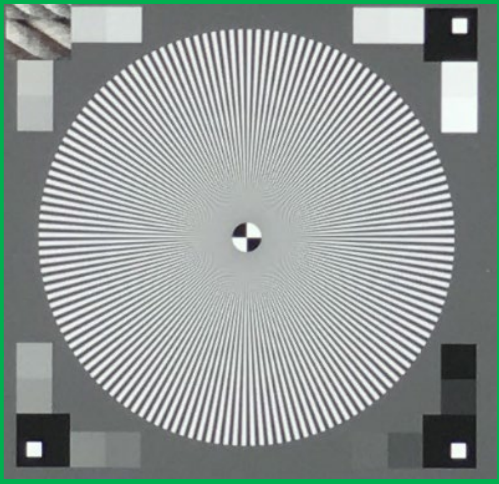
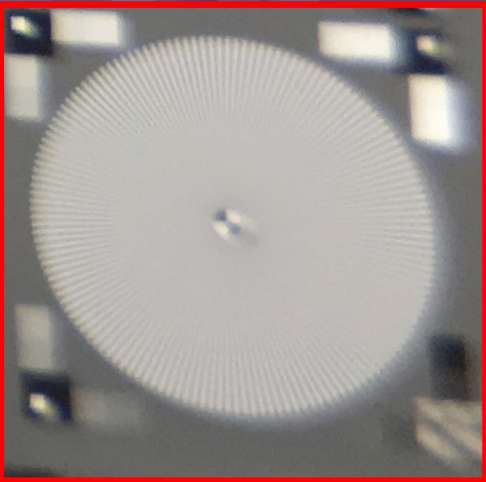
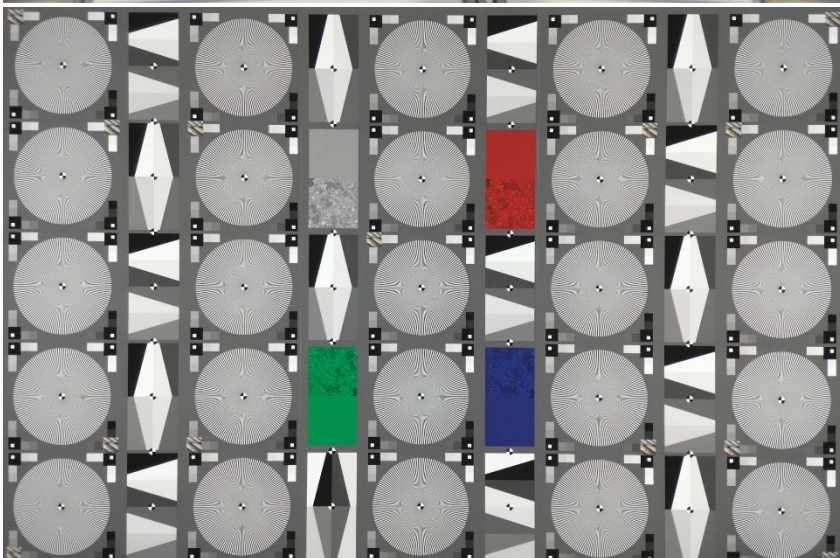
1	07.05.2024	Optical Imaging Fundamentals	Fermat principle, modeling light propagation with ray and wave model; diffraction; Snell's law, total internal reflection, light propagation in optical system, raytracing; ray and wave propagation in optical systems; pinhole camera; central perspective projection; étendue, f-number and numerical aperture, focal length; ideal projection laws; fish-eye imaging; anamorphic projection; perspective distortion, Panini projection; massive ray-tracing based imaging model	(S) (optional)
2	14.05.2024	The ideal image	Paraxial approximation, principal planes, entrance and exit pupil, paraxial imaging equations; Scheimpflug condition; paraxial matrix formulation; Delano diagram; Aplanatic imaging: Abbe sine condition, numerical aperture, sine scaled pupil for microscope imaging	(S)
3	21.05.2024	First order layout, system structures and properties	application of imaging equations; examples: layout of visual imaging system; layout of microscope lens and illumination system; telecentricity, "4f-setups"; tele and reversed tele (retrofocus) system; depth of field, bokeh; equivalence to multi-perspective 3D image acquisition; focusing methods of optical systems; afocal systems; connecting optical (sub-)systems: eye to afocal system; illumination system and its matching to projection optics); zoom systems; first order aberrations (focus and magnification error) and their compensation: lens breathing, aperture ramping; scaling laws of optical imaging	S
4	28.05.2024	Imaging model including diffraction	Gabor analytical signal; coherence function; degree of coherence; Rayleigh-Sommerfeld diffraction; optical system transfer as complex, linear operator; Fraunhofer-, Fresnel-approximation and high-NA field transfer wave-optical imaging equations for non-coherent, coherent and partially coherent imaging; isoplanatic patches, Hopkins Transfer Function for partially coherent imaging, optical transfer functions for non-coherent and coherent imaging; ideal wave-optical imaging equations; Fourier-Optics; spatial filtering; Abbe theory of image formation in microscope, phase contrast microscopy	S
5	04.06.2024	Wavefront deformation, Optical Transfer Function, Point Spread Function and performance criteria	wave aberrations, Zernike polynomials, measurement of system quality; point spread function (PSF), optical transfer function (OTF) and modulation transfer function (MTF); optical system performance criteria based on PSF and MTF: Strehl definition, Rayleigh and Marechal criteria, 2-point resolution, MTF-based criteria, coupling efficiency / insertion loss at photonics interface	S
6	11.06.2024	Aberrations: Classification, diagrams and identification in real images	measurement of wave front deformation: Shack-Hartmann sensor, Fizeau interferometer Symmetry considerations as basis for aberration theory; Seidel polynomial, chromatic aberrations; surface contributions and Pegel diagram, stop-shift-equation; Longitudinal and transverse aberrations, spot diagram; computing aberrations with Hamilton Eikonal Function; examples: defocus, plane parallel plate longitudinal and lateral chromatic aberration, Abbe diagram, dispersion fit; achromat and apochromat aberration in real images of (extended) objects	no
7	18.06.2024	Optimization process and correction principles	pre- and post-computer era correction methodology, merit function, system specification, initial setups, opto-mechanical constraints, damped-least-square optimization; symmetry principles, lens bending, aplanatic surface insertion, lens splitting, aspheres and freeforms	S
8	25.06.2024	Aberration correction and optical system structure	Petzval theorem, field flattening, achromat and apochromat, sensitivity analysis, diffractive elements; system structure of optical systems, e.g. photographic lenses, microscopic objectives, lithographic systems, eyepieces, scan systems, telescopes, endoscopes	(S)
9	02.07.2024	Tolerancing and straylight analysis	optical technology constraints, sensitivity analysis, statistical fundamentals, compensators, Monte-Carlo analysis, Design-To-Cost; false light; ghost analysis in optical systems; AR coating; opto-mechanical straylight prevention	S

Aberrations

„Bad“



„Good“



Institute of
Applied Physics

Friedrich-Schiller-Universität Jena

Aberrations

- Classification / types of imperfections / aberrations
- Representation (e.g. in Optical Design Software)
- What is the impact of aberration types on imaging?
- How to minimize in optical design and during lens manufacturing?

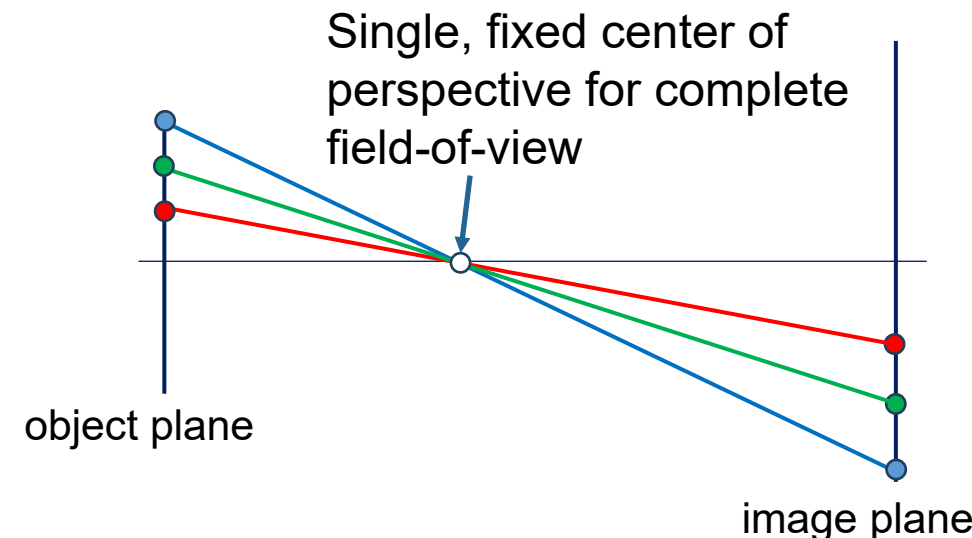
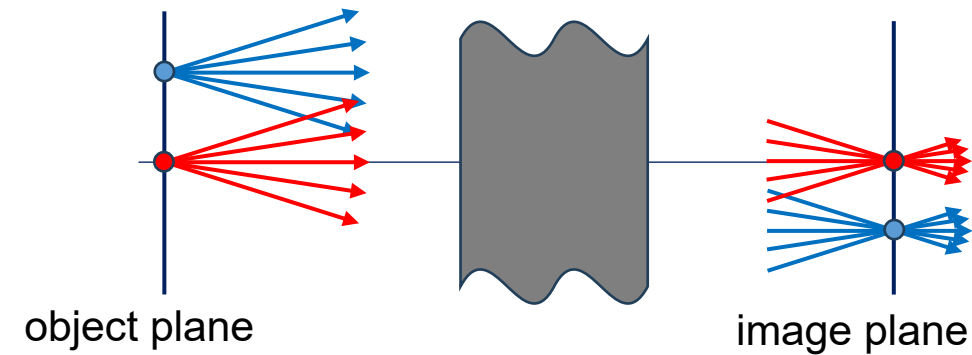
Ideal Imaging between planes

Berek (1930), Grundlagen der Praktischen Optik [Fundamentals of Practical Optics]; p. 4

For an axis-perpendicular plane to be ideally imaged, the following conditions must be met:

1. **every point** on the plane must be imaged **stigmatically**;
2. the **entirety** of the image points must again **fill a plane** perpendicular to the axis;
3. the ratio of the distance between any two image points to the distance of the associated object points, the **magnification**, must be **constant** within the entire image plane.

“stigmatic imaging” means “a point object is imaged again perfectly onto a point” for any aperture



Berek (1930), Grundlagen der Praktischen Optik
[Fundamentals of Practical Optics]; p. 4

For an axis-perpendicular plane to be ideally imaged, the following conditions must be met:

1. **every point** on the plane must be imaged **stigmatically**;
2. the **entirety** of the image points must again **fill a plane** perpendicular to the axis;
3. the ratio of the distance between any two image points to the distance of the associated object points, the **magnification**, must be **constant** within the entire image plane.

Paraxial approximations:

$$ni = n'i' \quad [\text{SL,appr}] \quad (\text{approximated Snell's law } n \sin i = n' \sin i')$$

$$u = \frac{h}{s}, \quad u' = \frac{h}{s'}, \quad \varphi = \frac{h}{r}. \quad [\text{NA,appr}] \quad (\text{small } h, \tan u \approx u \dots)$$

consequently, as sag scales quadratically with surface height h :

$$\text{sag} = r - \sqrt{r^2 - h^2} = r \left(1 - \sqrt{1 - \frac{h^2}{r^2}} \right) \approx r \left(\frac{h^2}{2r^2} + \dots \right) \approx \frac{h^2}{2r}$$

Proven, that paraxial imaging fulfills conditions for ideal imaging.

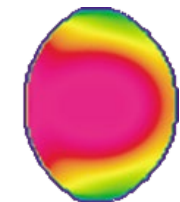
Without approximations we have **nonlinear** relations, e.g. with $\sin i = i - \frac{i^3}{6} + \frac{i^5}{120} - \dots$ and we have **induced effects**.

Lens pupil function including wavefront deformation and optical system transfer functions PSF and OTF

monochromatic PSF

$$PSF(x - m\xi, \lambda) = \left| \iint_{\text{lens pupil}} d\alpha d\beta L(\alpha, \lambda) \exp(-i2\pi w[\alpha \cdot (x - m\xi)]) \right|^2$$

lens pupil function



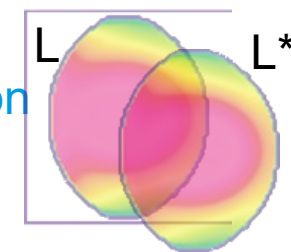
$L(\alpha, \lambda) = L_0(\alpha, \lambda) \exp(i2\pi W(\alpha))$

lens pupil shape wavefront deviation

$\xi \in \mathbb{R}^2$ object coordinates (ob),
 $\alpha \in \mathbb{R}^2$ entrance pupil coordinates (EP)
 $\alpha' \in \mathbb{R}^2$ exit pupil coordinates (AP)
 $x \in \mathbb{R}^2$ image coordinates (im)

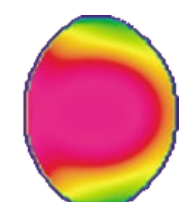
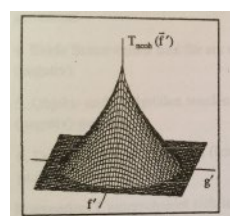
monochromatic OTF

Autocorrelation
of lens pupil
function



monochromatic MTF (Modulation) monochromatic PTF (Phase)

$$OTF(\alpha, \lambda) = \iint_{\text{pupil}} d\bar{\alpha} L(\bar{\alpha} + \alpha, \lambda) L^*(\bar{\alpha}, \lambda) = MTF(\alpha, \lambda) \exp(i2\pi PTF(\alpha, \lambda))$$



$L(\alpha, \lambda) = L_0(\alpha, \lambda) \exp(i2\pi W(\alpha))$

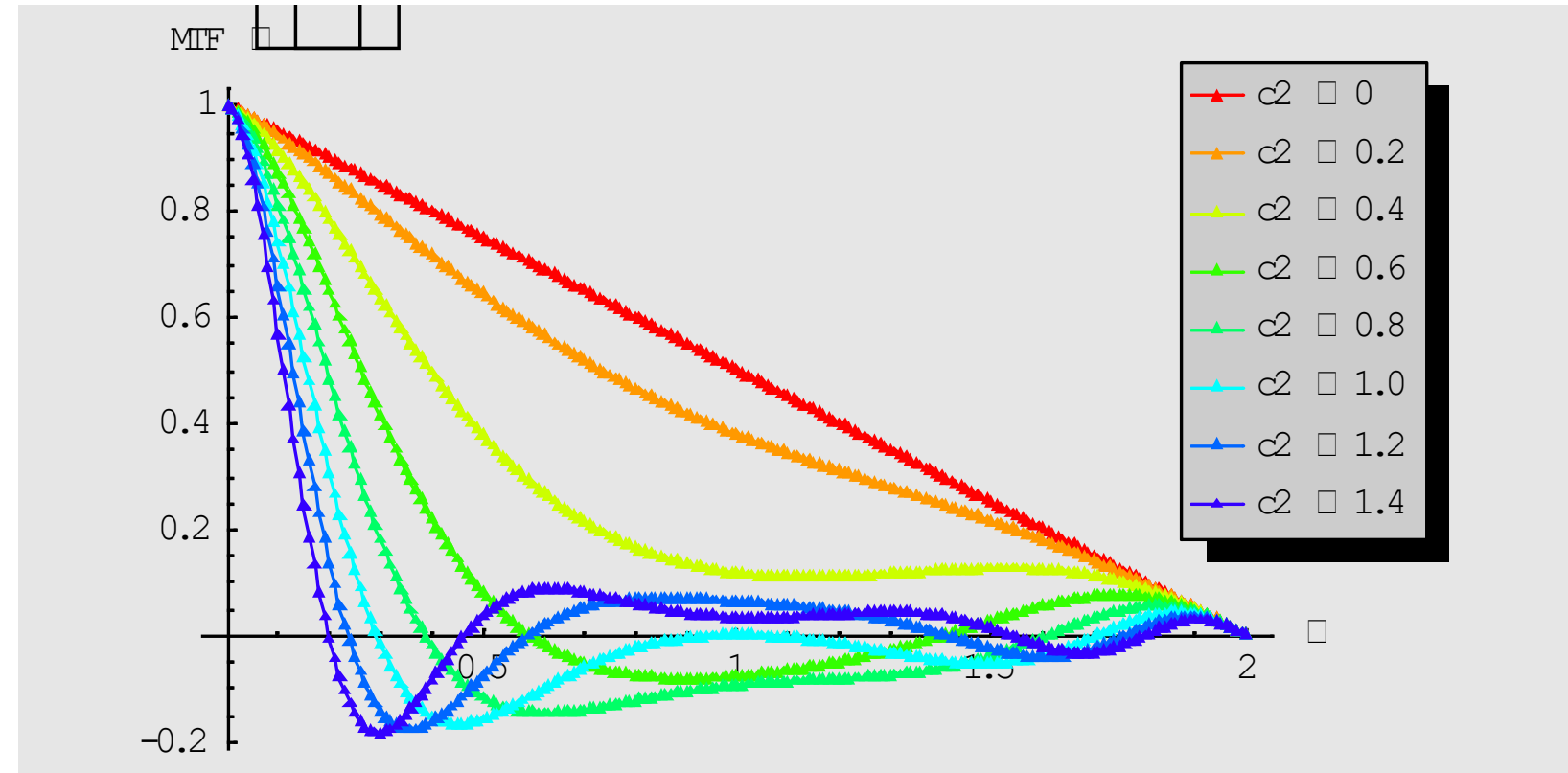
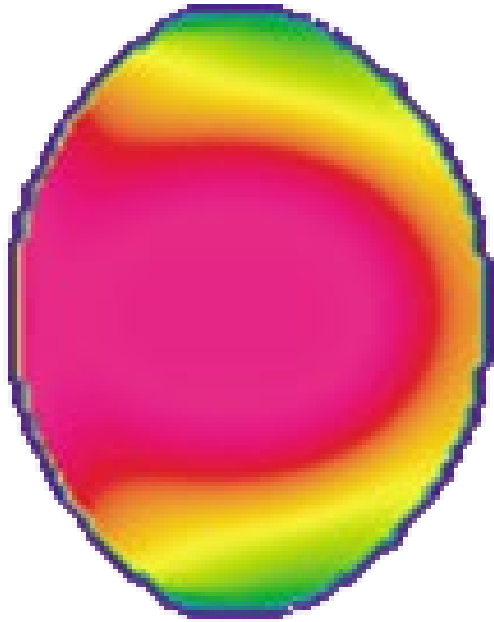
lens pupil shape wavefront deviation

“resolution parameter”

$$w = \frac{NA_{im}}{\lambda} = \frac{1}{2K\lambda}$$

magnification m

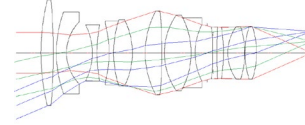
Controlling the wavefront deformation



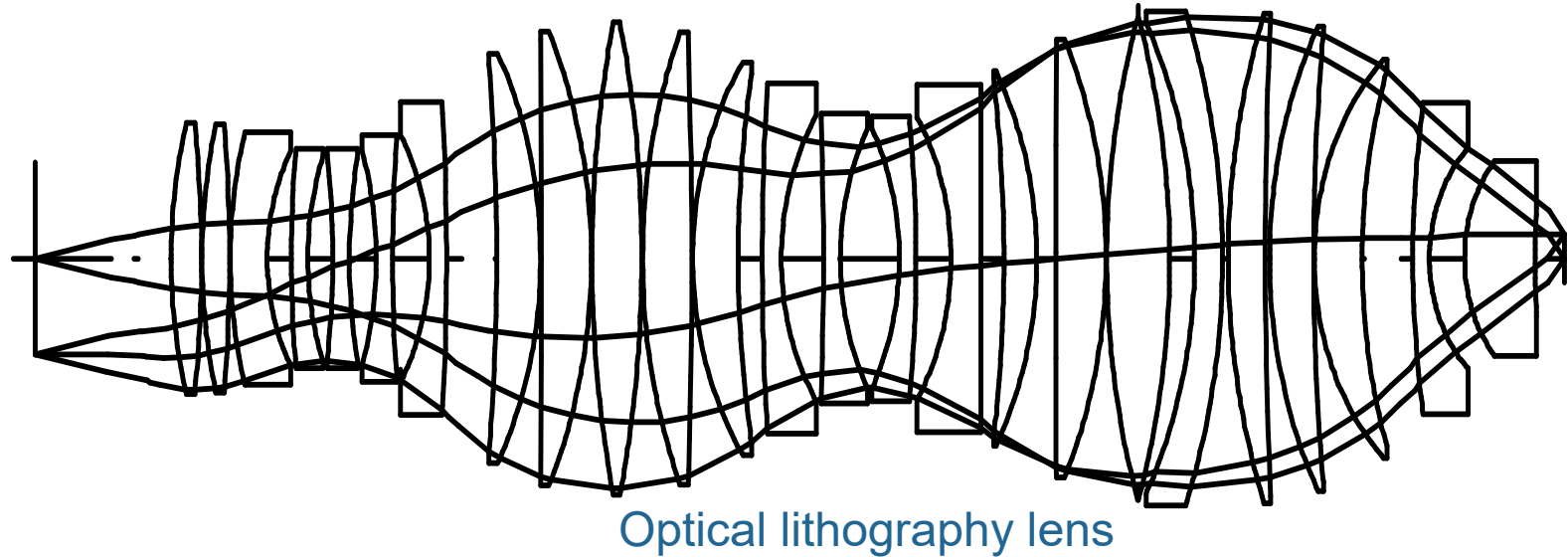
Fractions of the wavelength already significantly deteriorate contrast transfer.

Optical design problem for **camera lens**: For optical path lengths of ca. 100mm control wavefront deformation in the order of $<1\mu\text{m}$ (0.001mm), that is $\Delta\text{OPL}/\text{OPL} \approx 10^{-5}$
(over complete pupil and complete field and all wavelengths and all focusing distances and eventually all zoom positions)

Controlling the wavefront deformation



Camera lens



Optical lithography lens

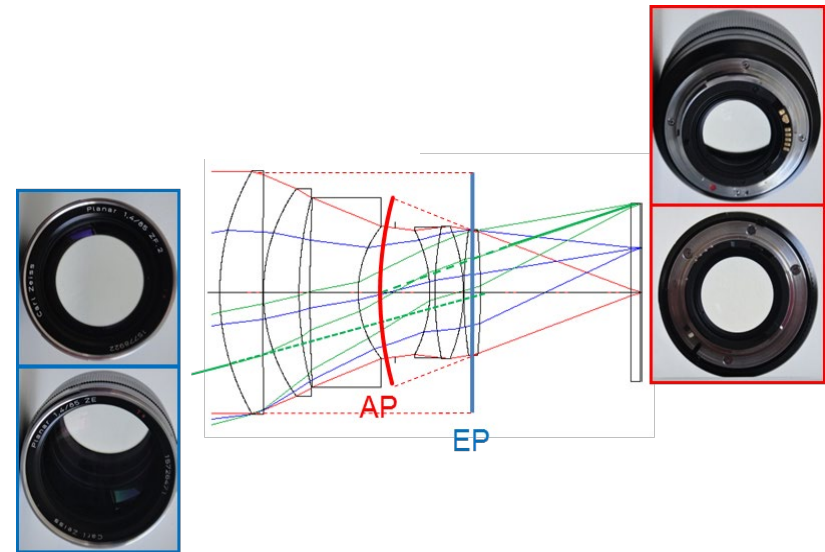
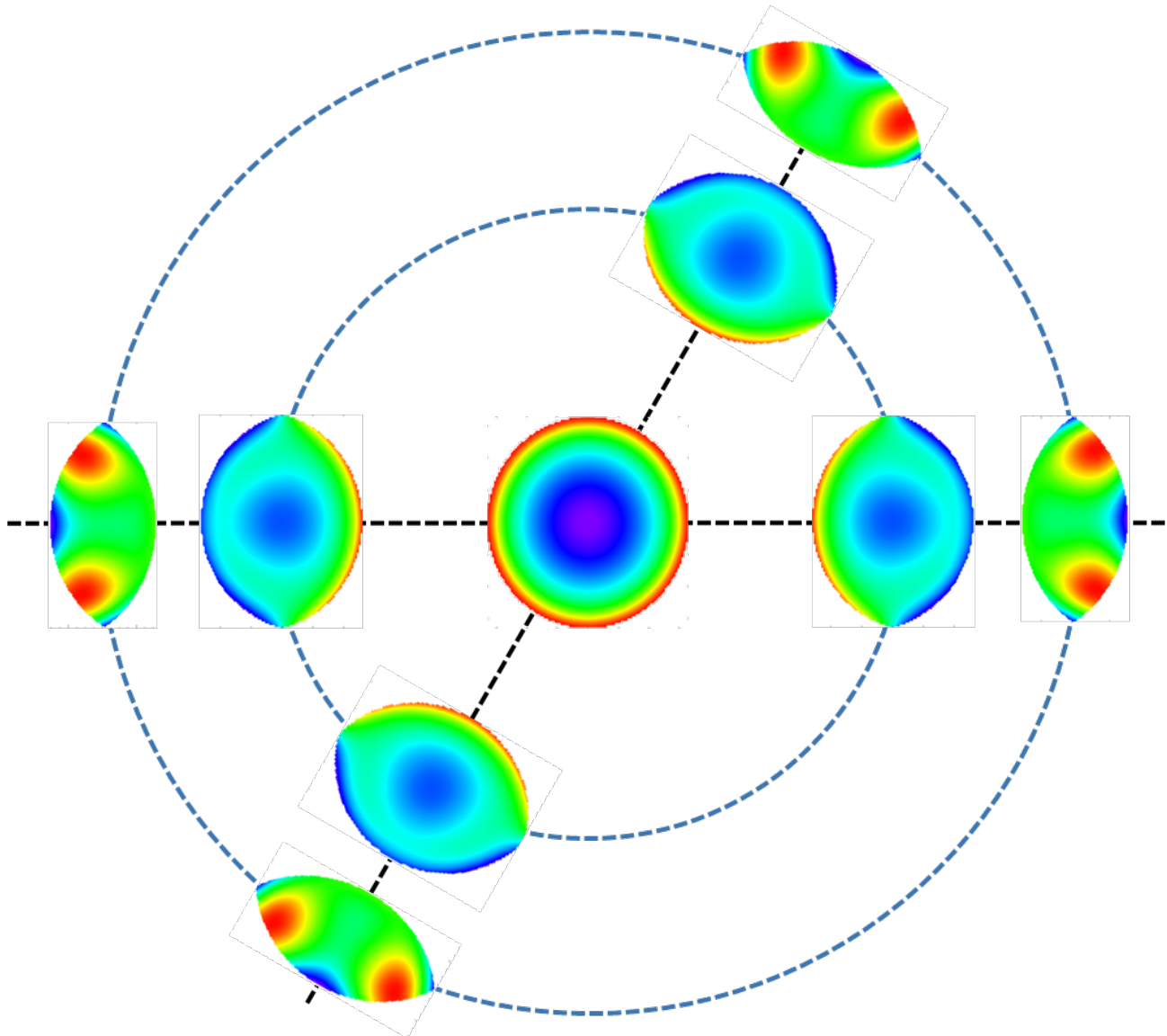
Fractions of the wavelength already significantly deteriorate contrast transfer.

Optical design problem for **lithography lens**: For optical path lengths of ca. 1000mm control wavefront deformation in the order of $<0.1\text{nm}$ (0.0000001mm), that is $\Delta\text{OPL}/\text{OPL} \approx 10^{-10}$
(over complete pupil and complete field)

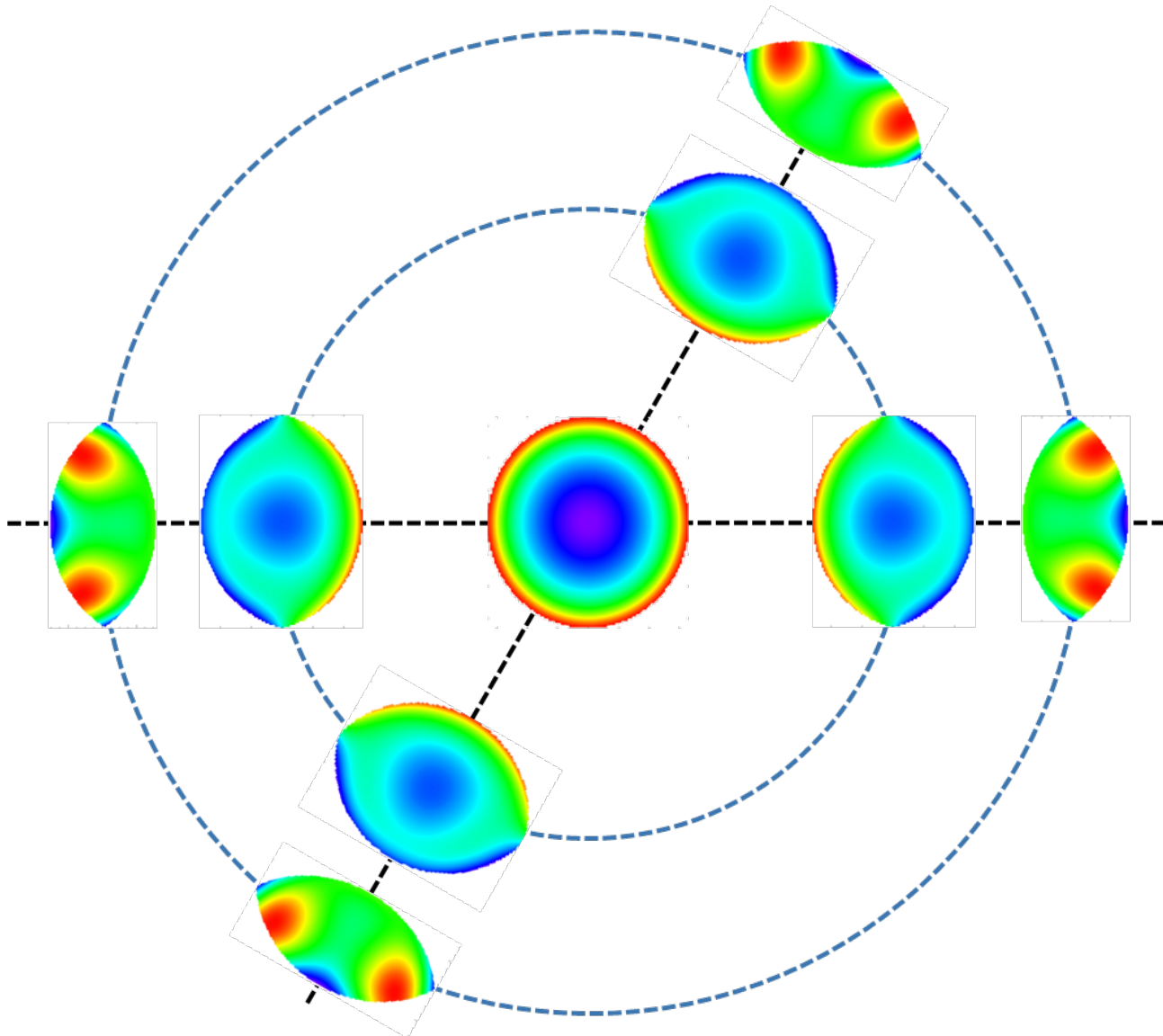
Fractions of the wavelength already significantly deteriorate contrast transfer.

Optical design problem for **camera lens**: For optical path lengths of ca. 100mm control wavefront deformation in the order of $<1\mu\text{m}$ (0.001mm), that is $\Delta\text{OPL}/\text{OPL} \approx 10^{-5}$
(over complete pupil and complete field and all wavelengths and all focusing distances and eventually all zoom positions)

Aberration of rotational symmetric system



Aberration of rotational symmetric system



$$\text{pupil } \vec{\alpha} = \begin{pmatrix} \alpha \\ \beta \end{pmatrix}$$

$$\text{object } \vec{\xi} = \begin{pmatrix} \xi \\ \eta \end{pmatrix}$$

Aberration function in general depends on 4 variables

$$W(\vec{\alpha}, \vec{\xi}) = W(\alpha, \beta, \xi, \eta).$$

Polar coordinates:

$$\text{pupil } \vec{\alpha} = \begin{pmatrix} r \\ \varphi \end{pmatrix}$$

$$\text{object } \vec{\xi} = \begin{pmatrix} \rho \\ \vartheta \end{pmatrix}$$

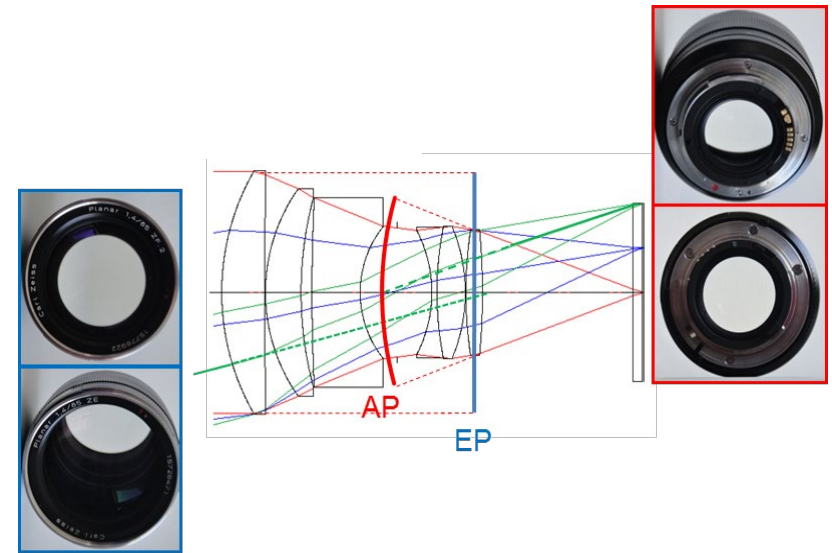
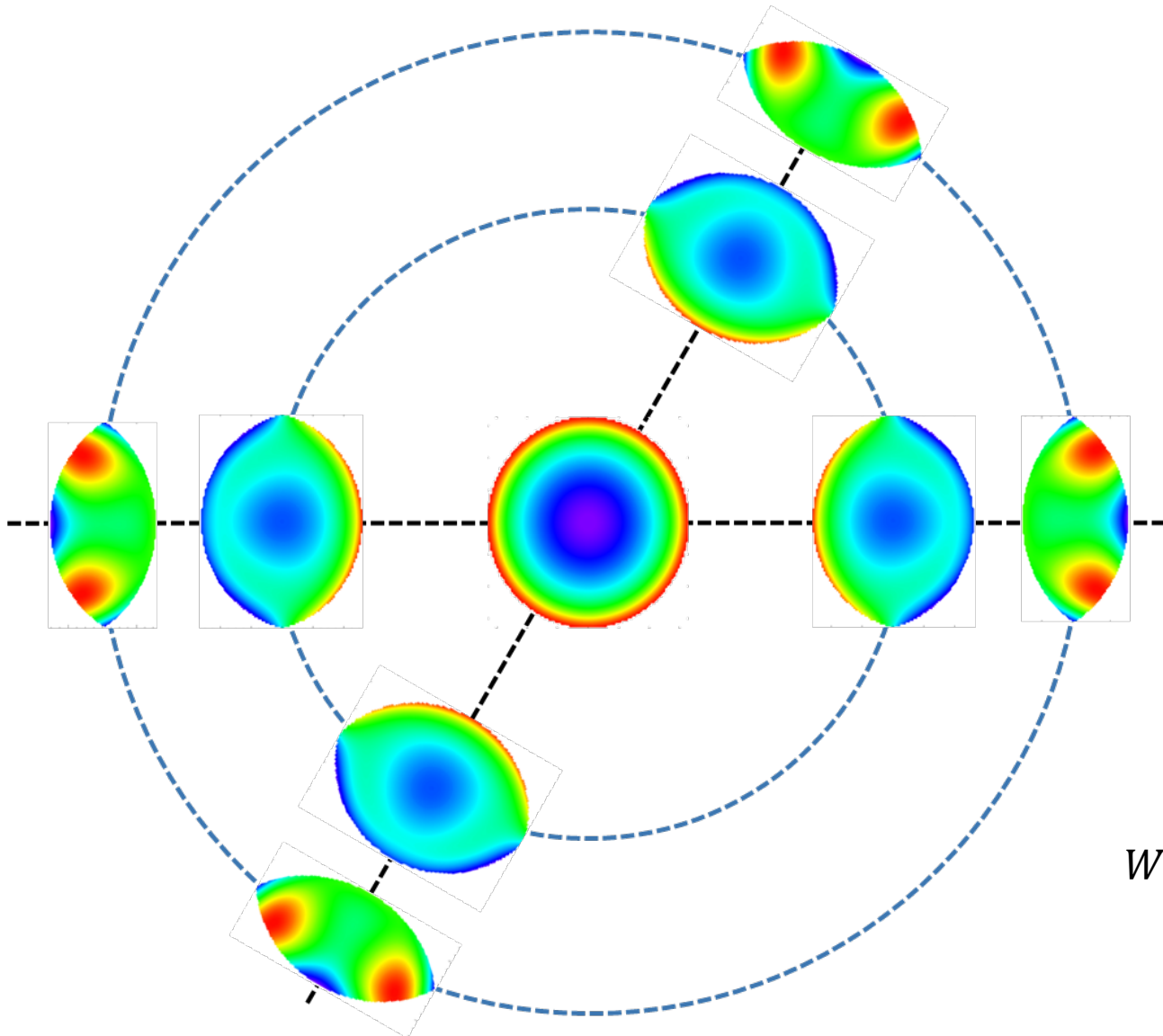
For a rotational symmetric system the aberration function is invariant for the scalar products of the variables:

$$W(\vec{\alpha} \cdot \vec{\alpha}, \vec{\alpha} \cdot \vec{\xi}, \vec{\xi} \cdot \vec{\xi})$$

with respect to a rotation of the field (or of the pupil)

$$R_\vartheta = \begin{pmatrix} \cos \vartheta & \sin \vartheta \\ -\sin \vartheta & \cos \vartheta \end{pmatrix}$$

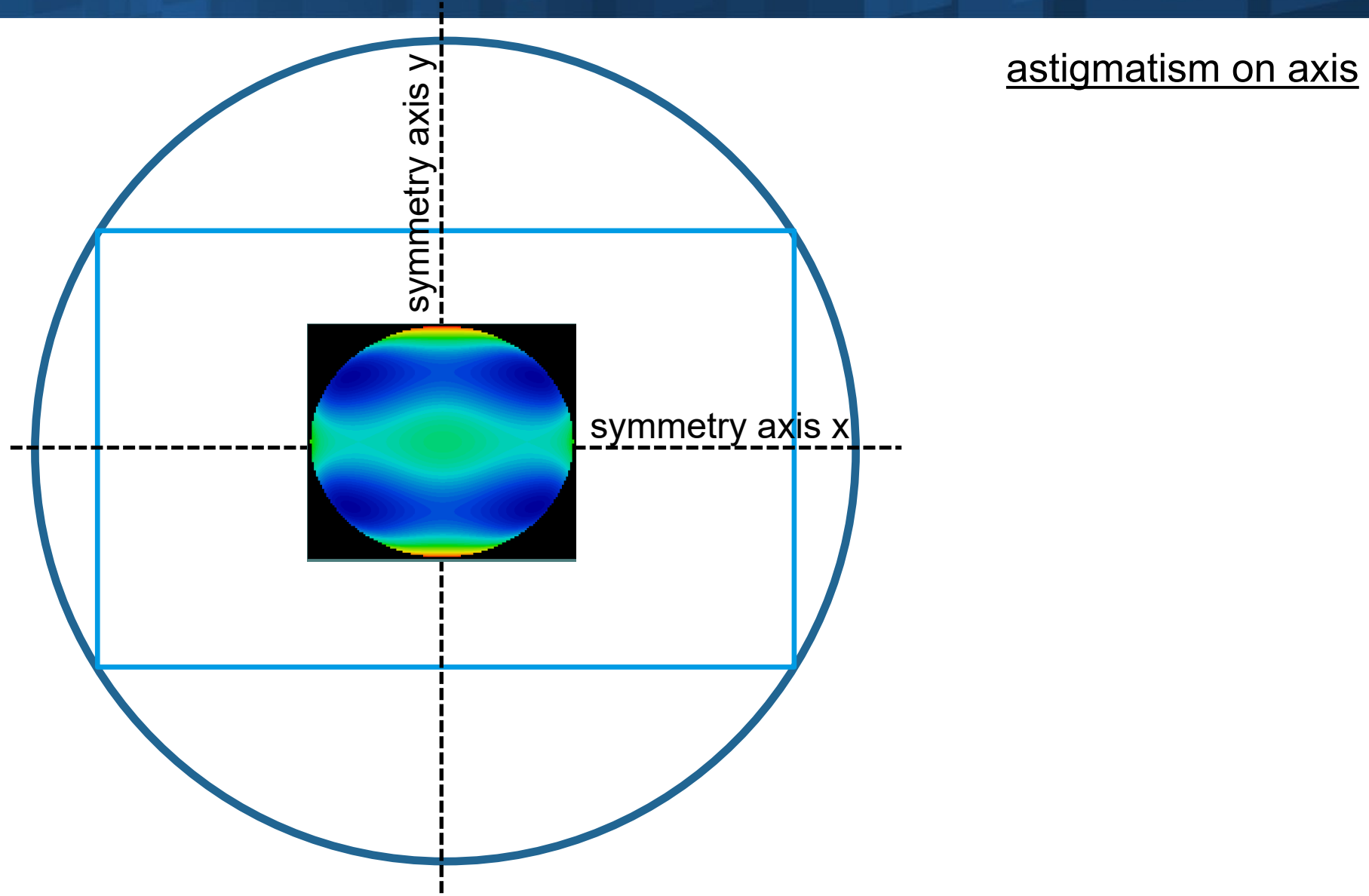
Aberration of rotational symmetric system



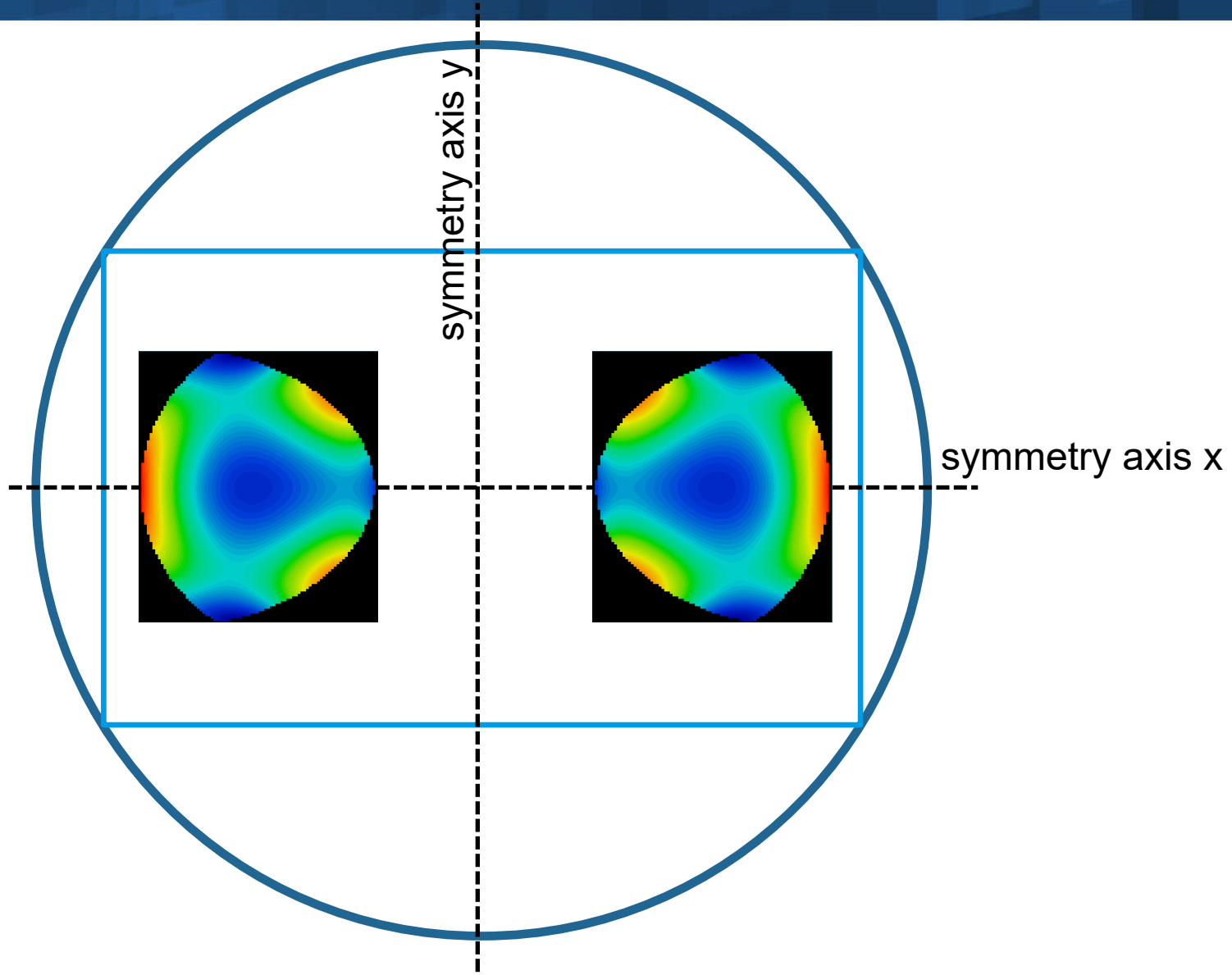
Rotationally symmetric system:
function of 3 variables

$$W(\vec{\alpha} \cdot \vec{\alpha}, \vec{\alpha} \cdot \vec{\xi}, \vec{\xi} \cdot \vec{\xi}) = \sum_{l=0}^{\infty} \sum_{k=0}^{\infty} \sum_{j=0}^{\infty} c_{2j,k,2l} |\vec{\xi}|^{2j} (\vec{\xi} \cdot \vec{\alpha})^k |\vec{\alpha}|^{2l}$$

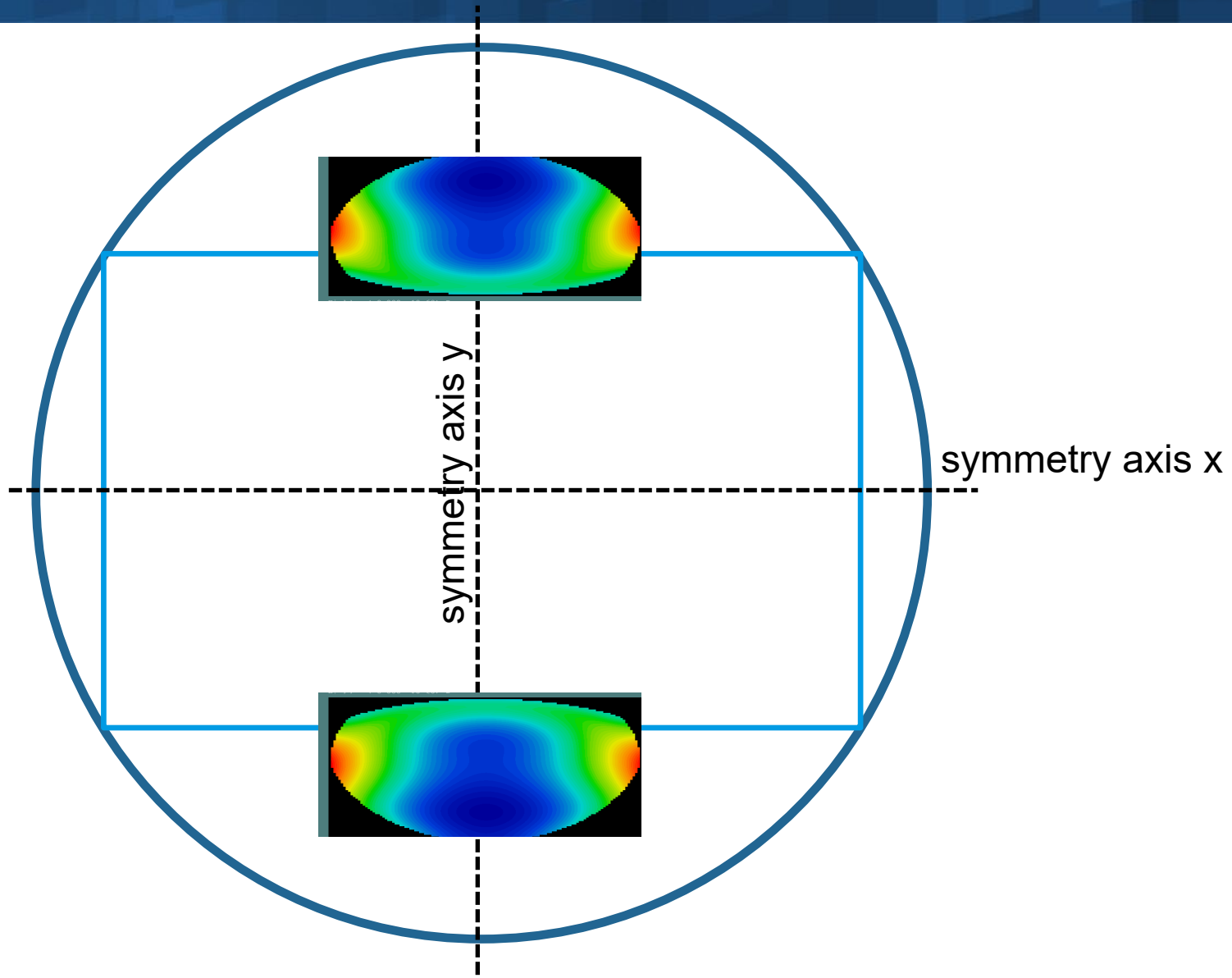
Anamorphic lens symmetry (nominal design)



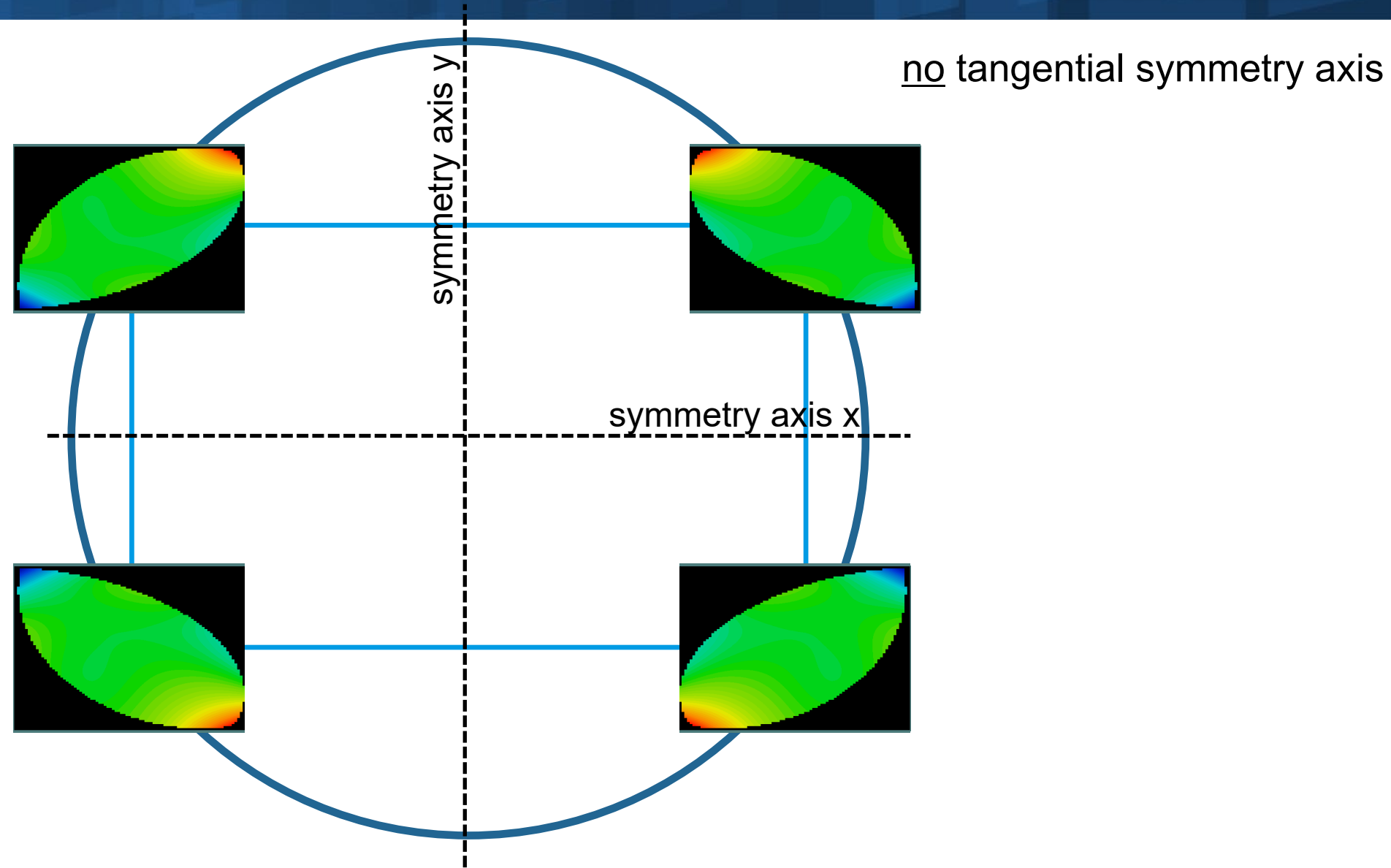
Anamorphic lens symmetry (nominal design)



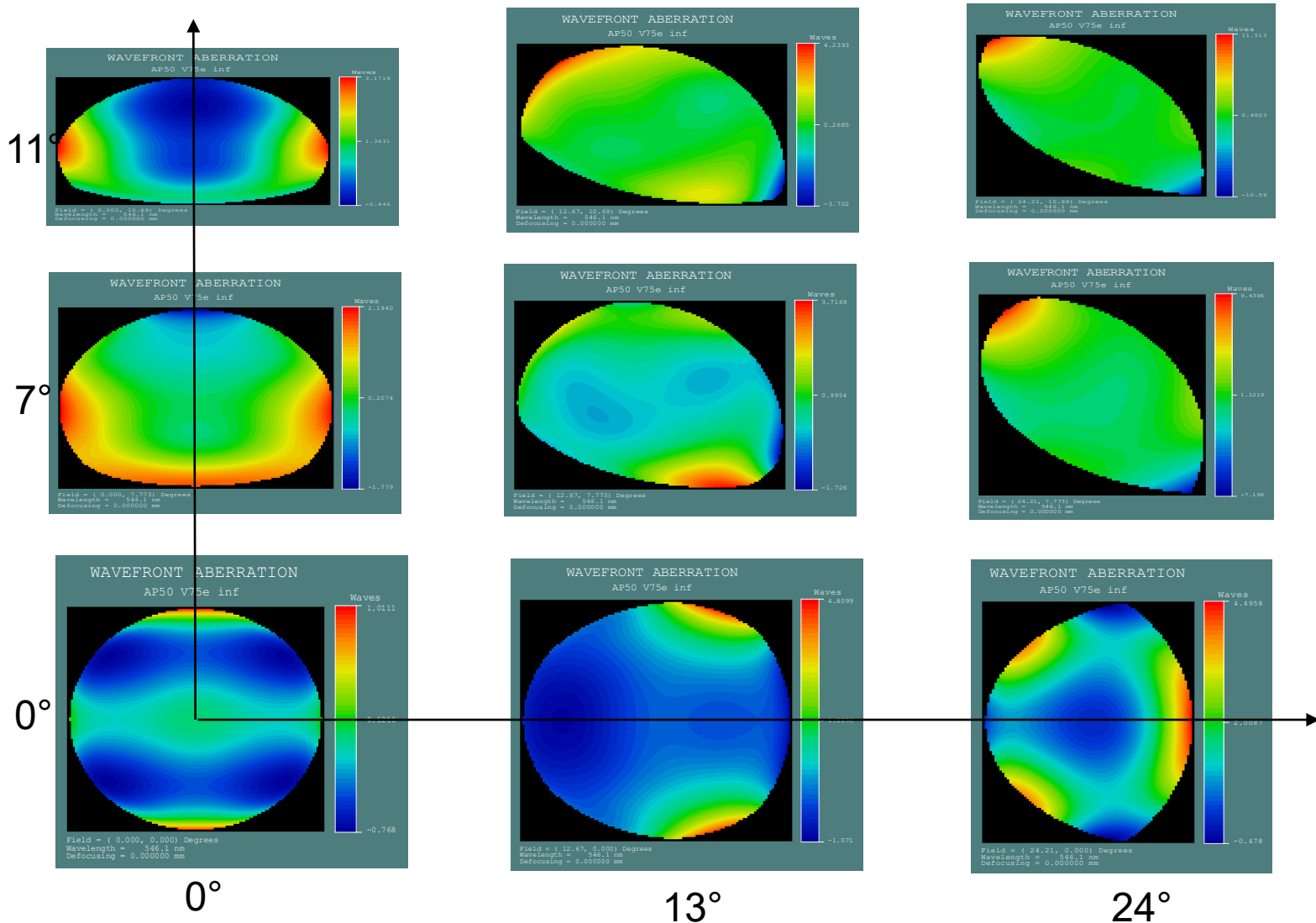
Anamorphic lens symmetry (nominal design)

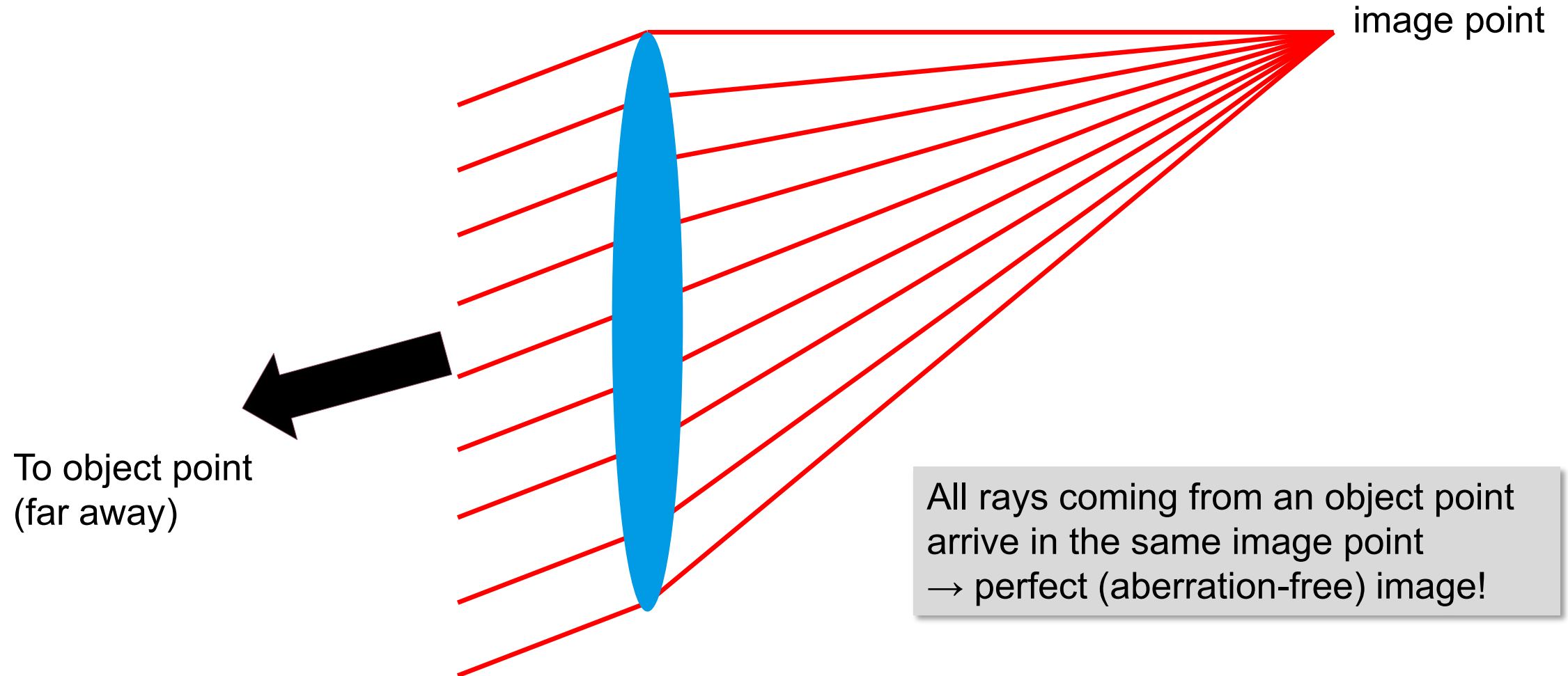


Anamorphic lens symmetry (nominal design)

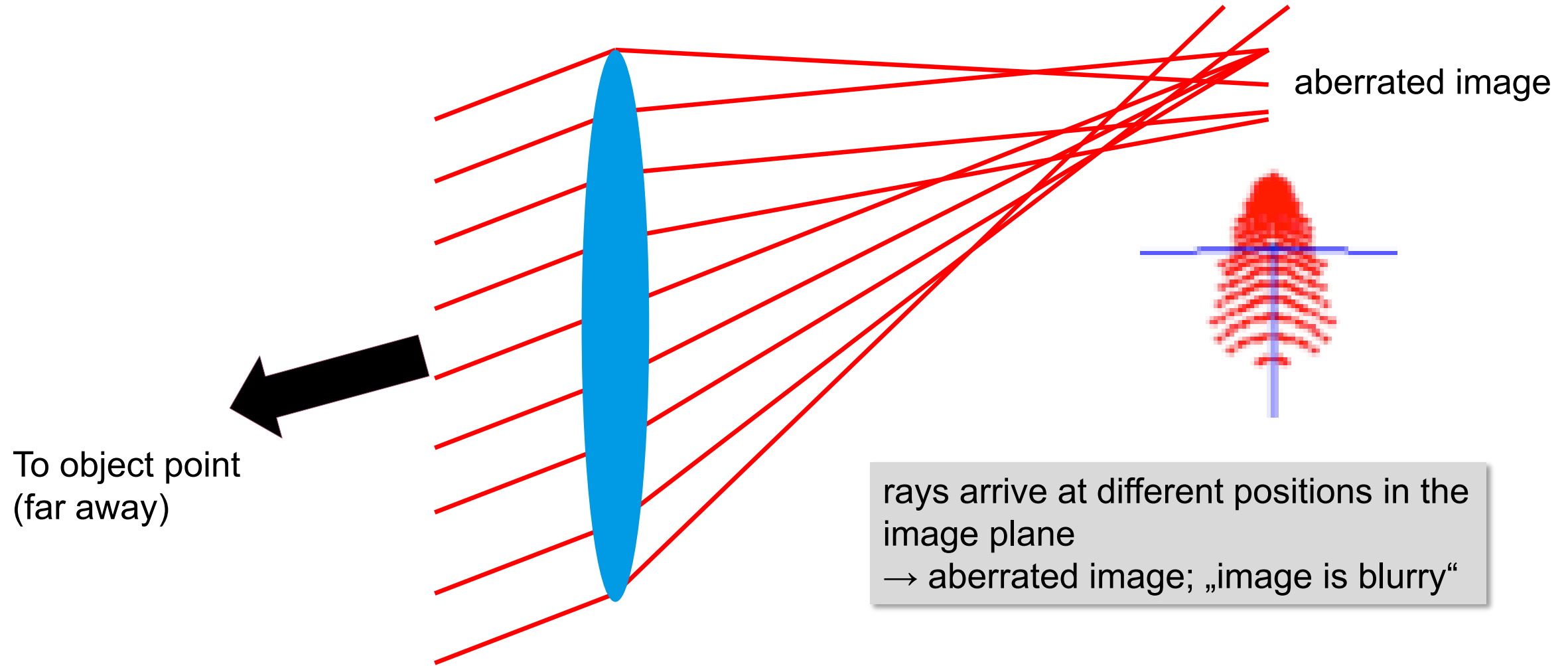


Pupil over field: anamorphic lens

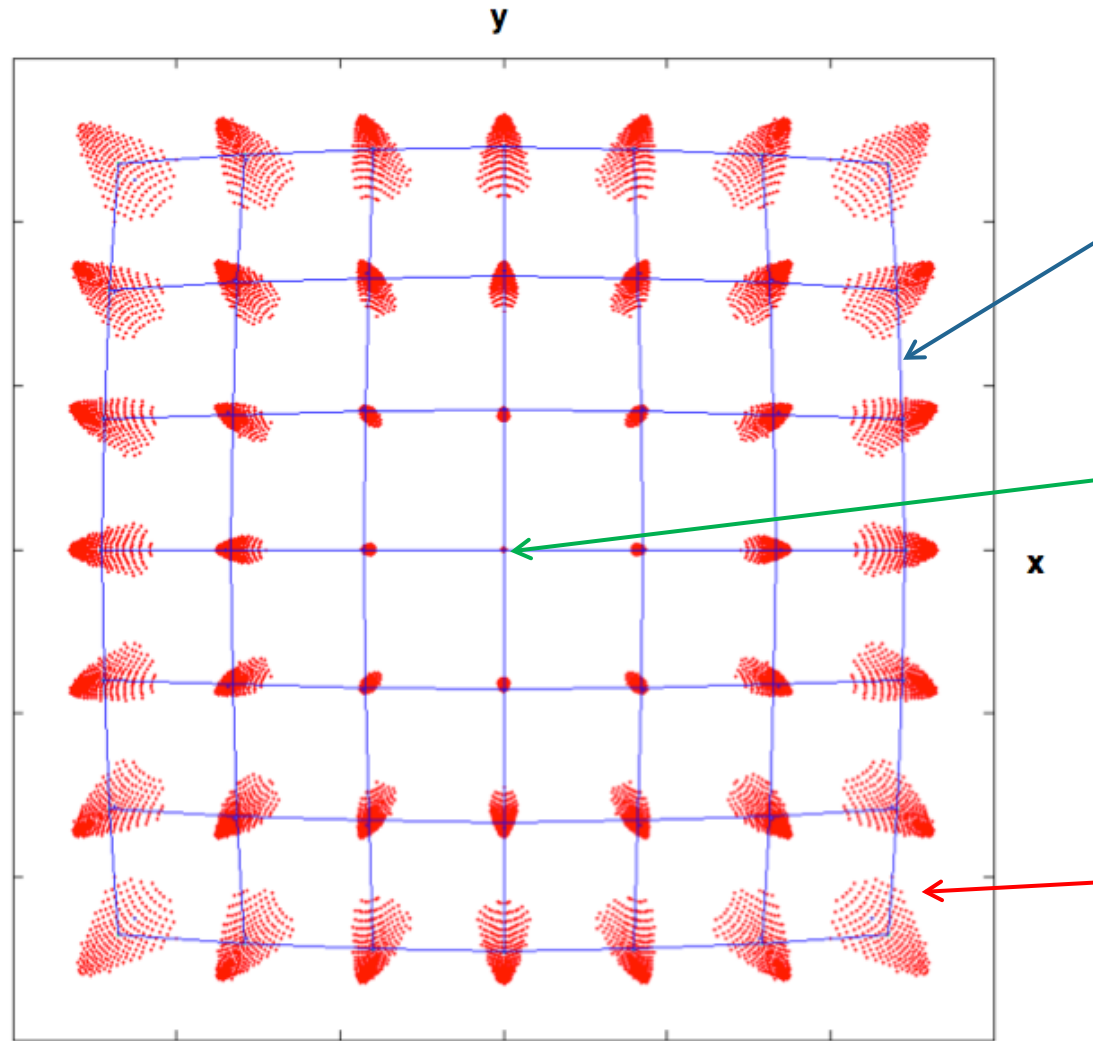




Aberration (spot diagram)



Aberration „Spot diagram“: not all rays from one object point come together in the image plane

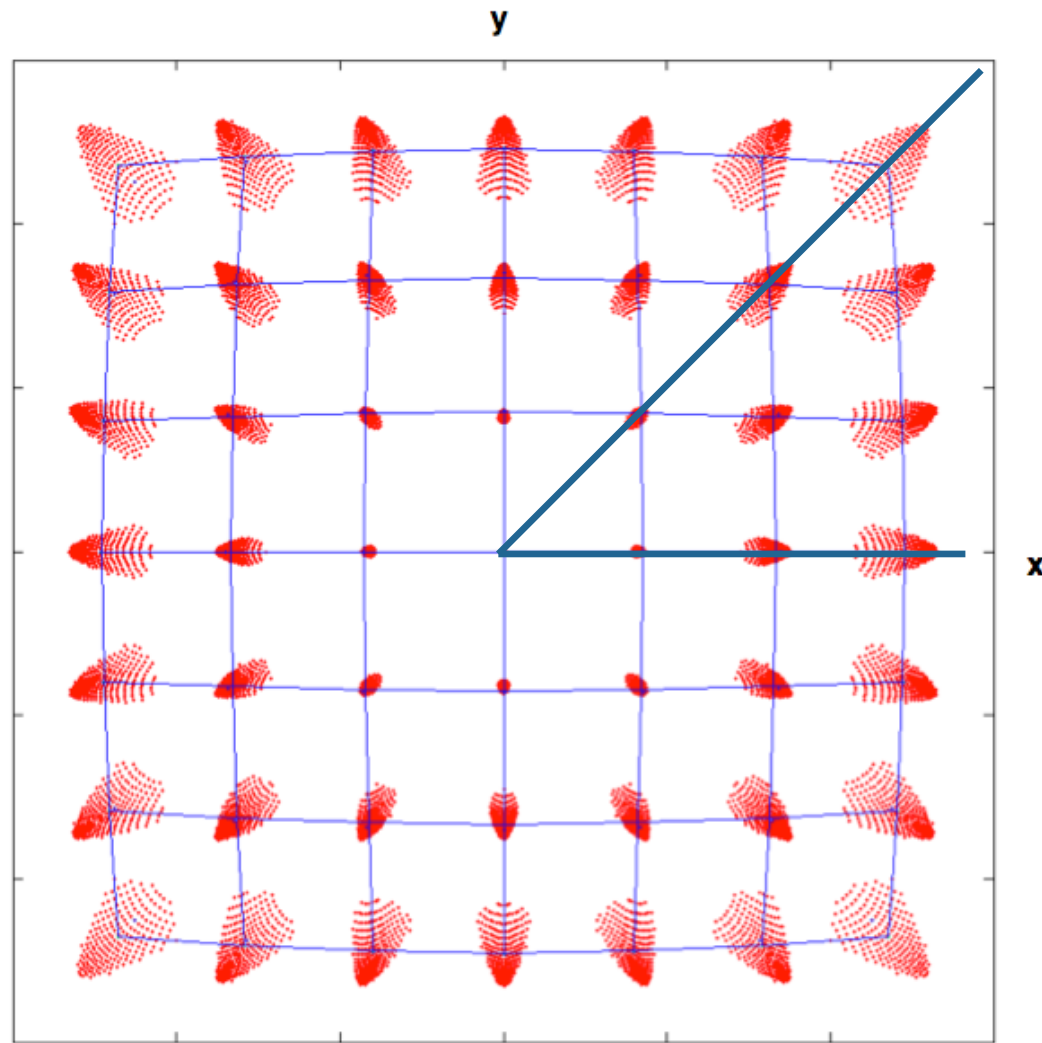


imaged lines are not straight: **distortion**

all rays entering the lens from one object point come together at center of field
→ sharp image in center

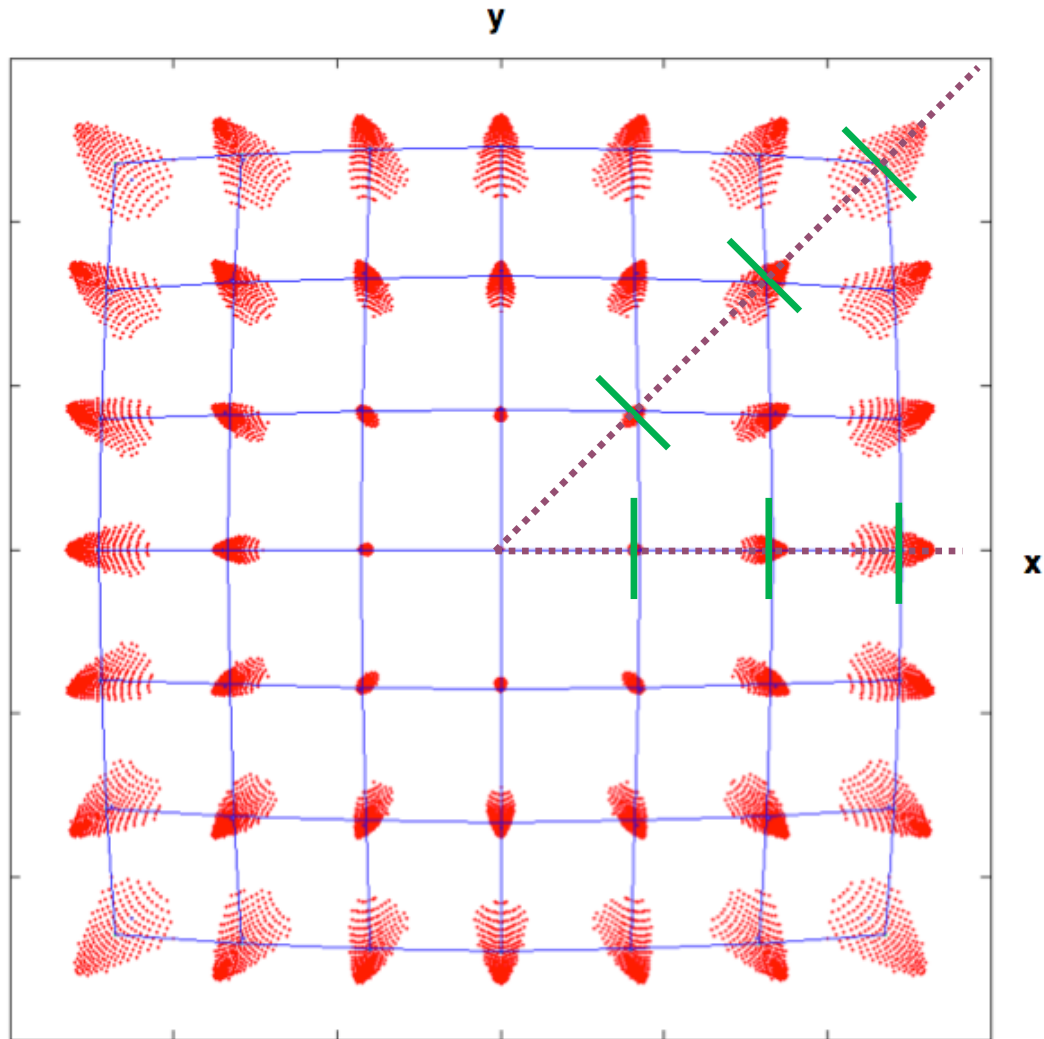
rays deviate towards corner of field
→ blurry image at edges

Aberration: Tangential and Sagittal directions of rotational symmetric lens



Tangential (or meridional) directions:
From center of field outside

Aberration: Tangential and Sagittal directions of rotational symmetric lens



Sagittal direction:
Perpendicular to tangential direction.

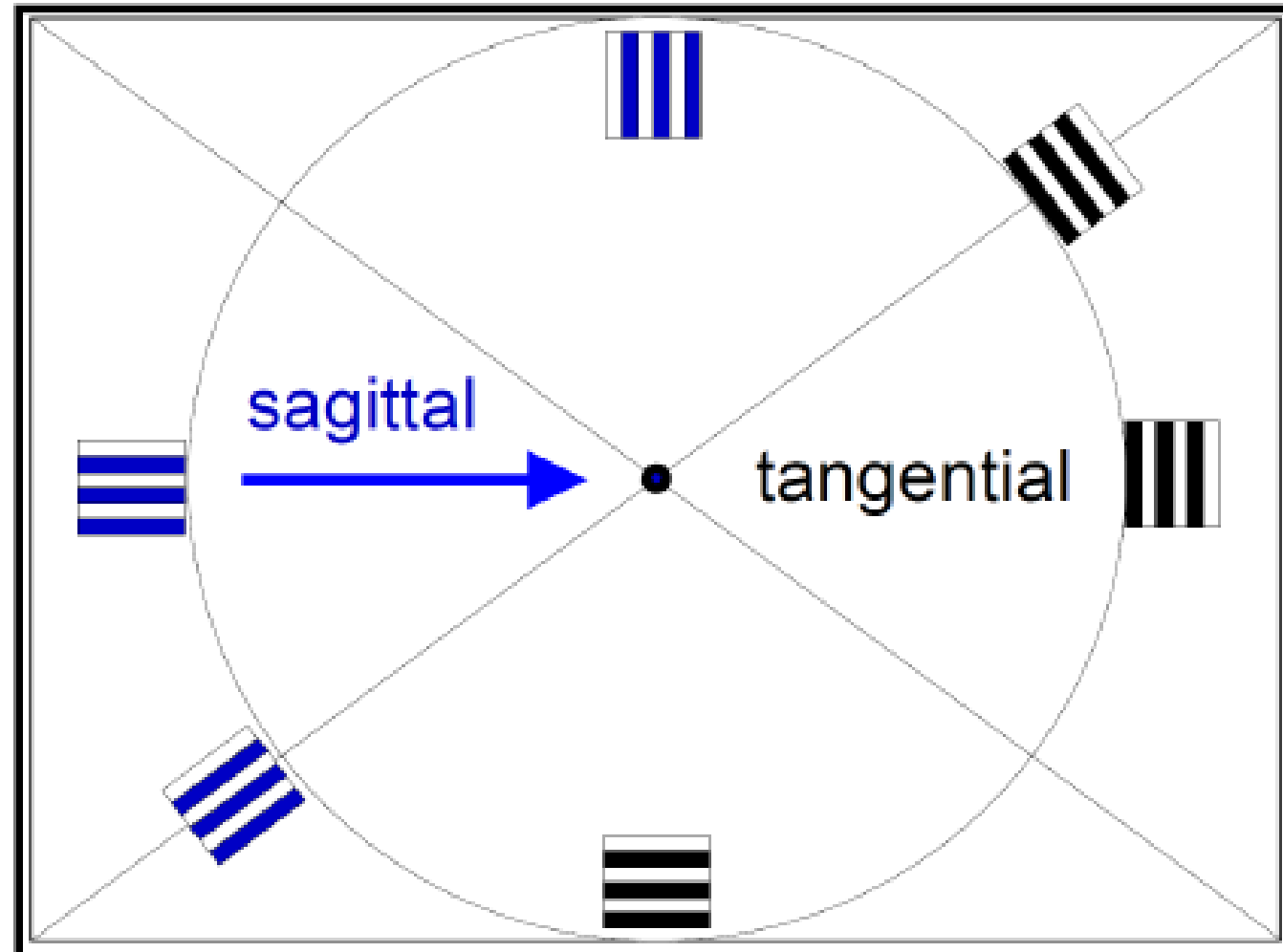
In a ray aberration diagram the sagittal direction is usually drawn through the chief ray (in general the sagittal curve changes for other reference points).

In a rotational symmetric lens

- the sagittal curves are symmetric) around the chief ray reference point
- the tangential curves remain do only depend on image height, but not on azimuth

Test structure orientation for MTF-evaluation

Tangential and Sagittal directions of rotational symmetric lens

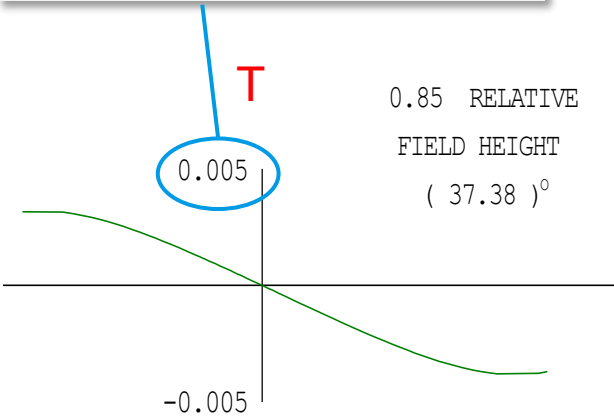


H. Nasse (2008).
„How to read MTF
curves“

The periodic modulation is perpendicular to the direction correspondingly.

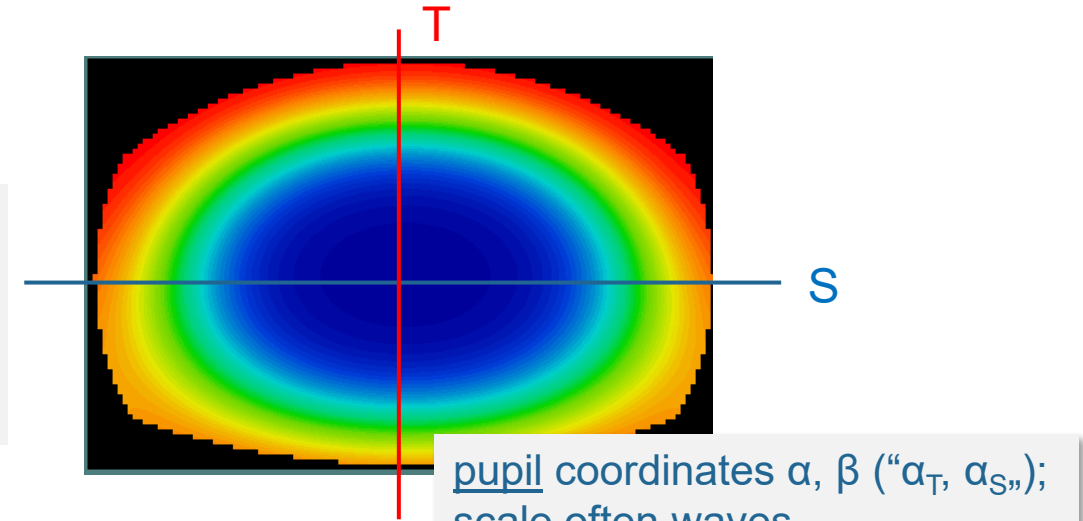
Ray aberration and wavefront deviation

image coordinates $\Delta x, \Delta y$;
scale often millimeter,
e.g. $0.005\text{mm} = 5\mu\text{m}$

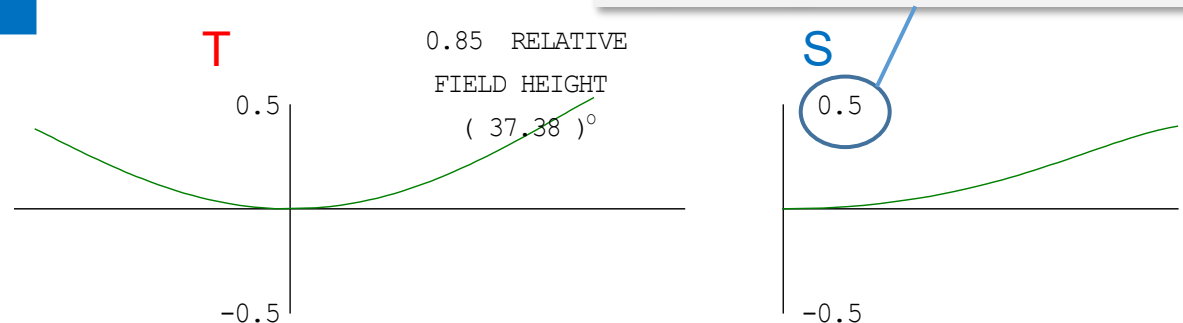


Ray aberration

$$\begin{pmatrix} \Delta x \\ \Delta y \end{pmatrix} = \frac{\lambda R}{n} \nabla W = \frac{\lambda R}{n} \begin{pmatrix} \frac{\partial W}{\partial \alpha} \\ \frac{\partial W}{\partial \beta} \end{pmatrix}$$

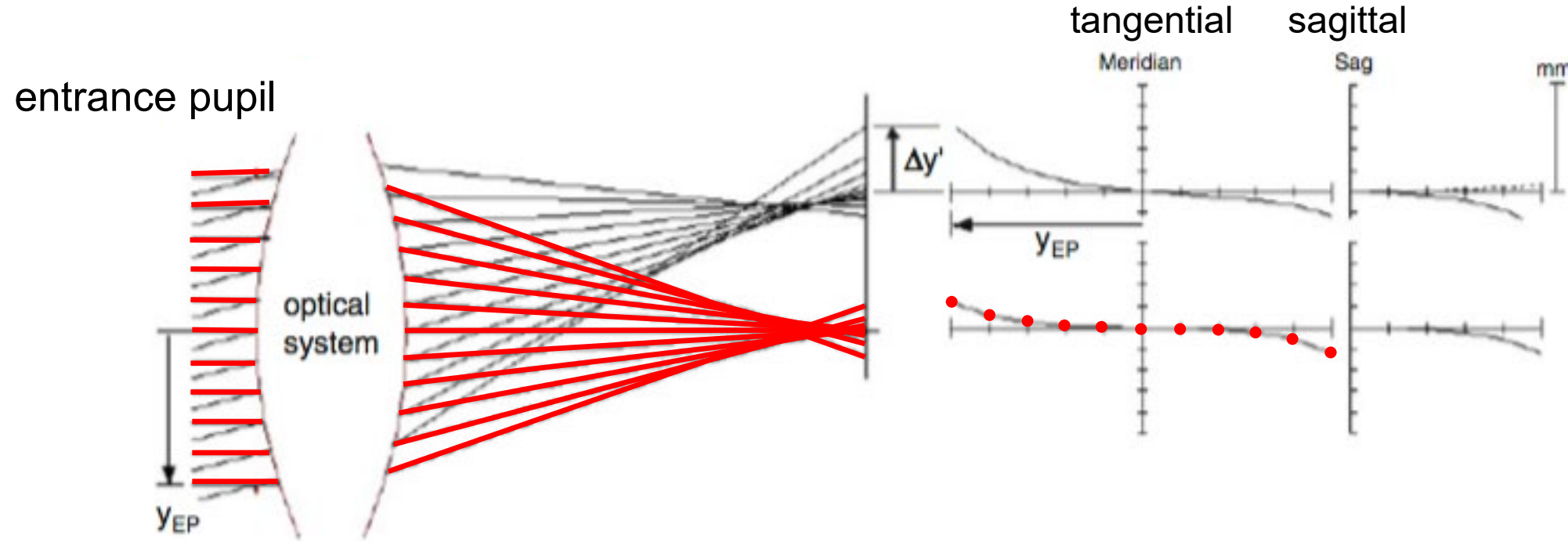


pupil coordinates α, β (" α_T, α_S ");
scale often waves,
e.g. $0.5\lambda_{\text{ref}}$ (reference wavelength)

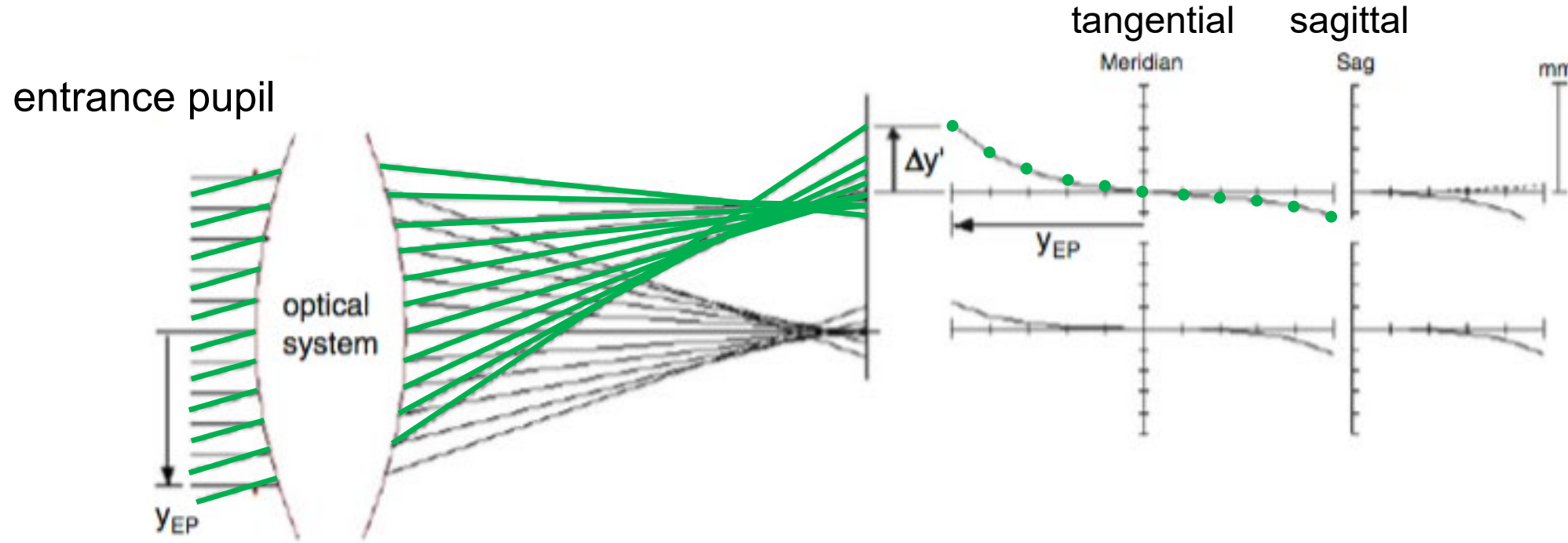


Wavefront deviation (optical path difference)

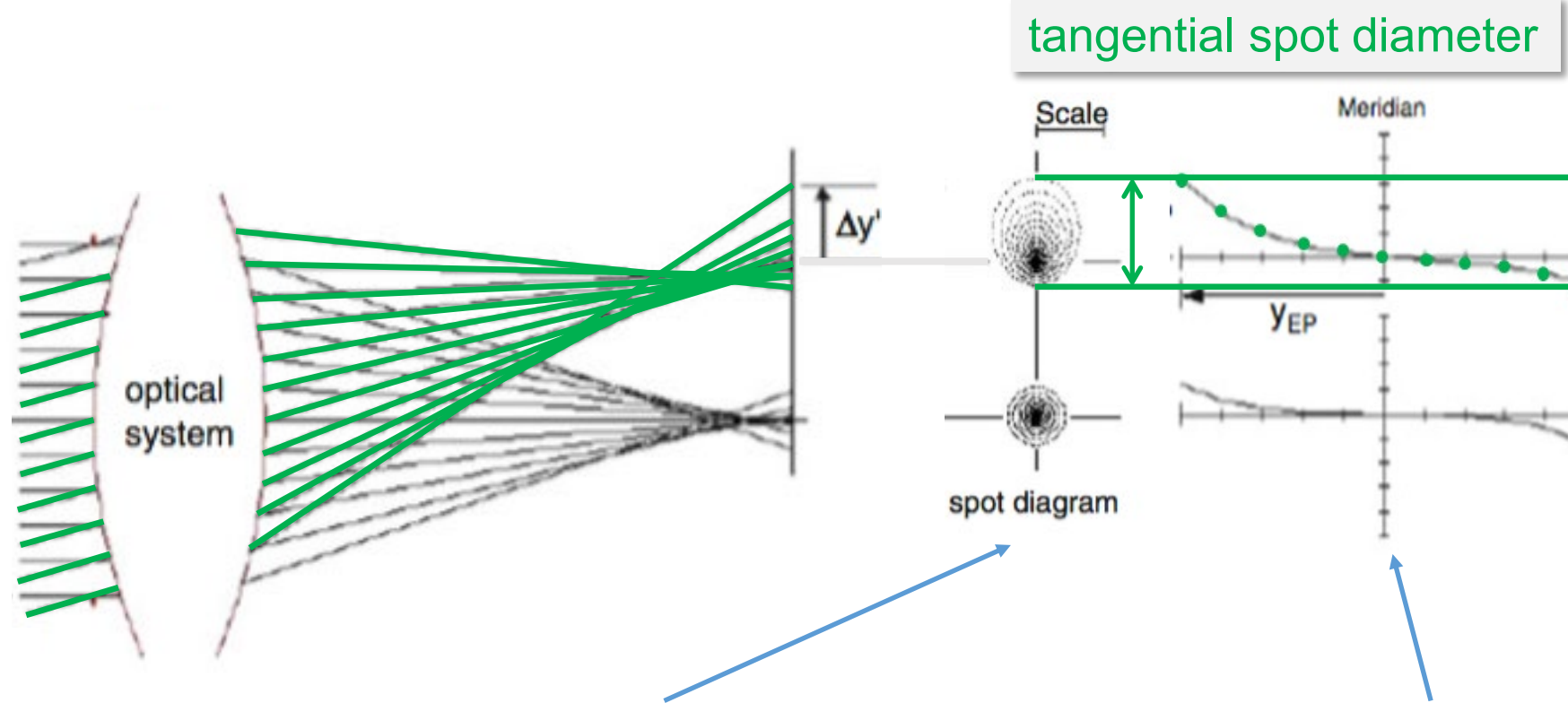
Aberration diagram (lateral ray deviation)



Aberration diagram (lateral ray deviation)



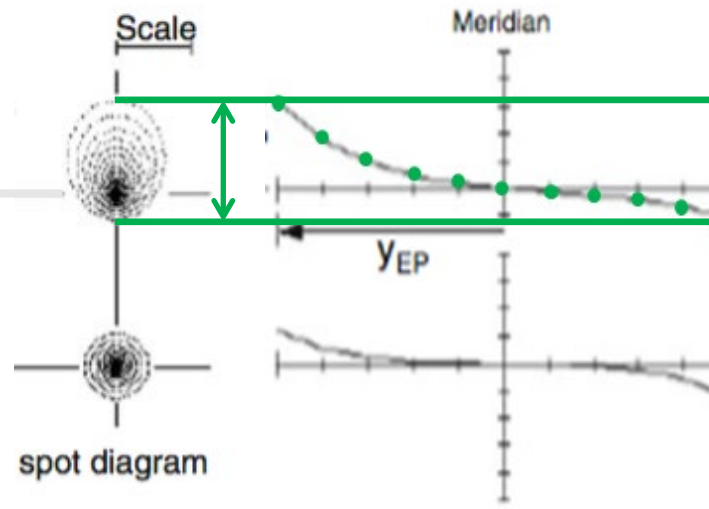
Aberration and spot diagram



Spot diagram:

- + evaluation of complete pupil
- aberration types harder/impossible to classify
- Polychromatic visualization either problematic (on-top) or additional plots required

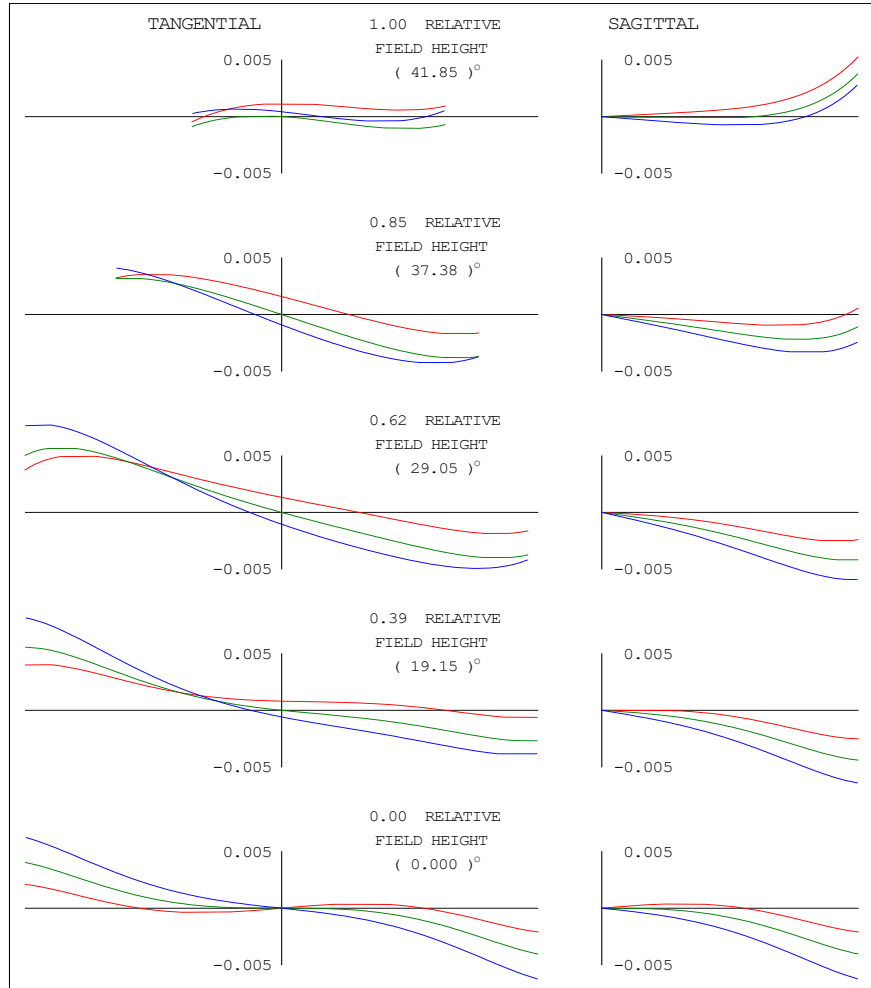
tangential spot diameter



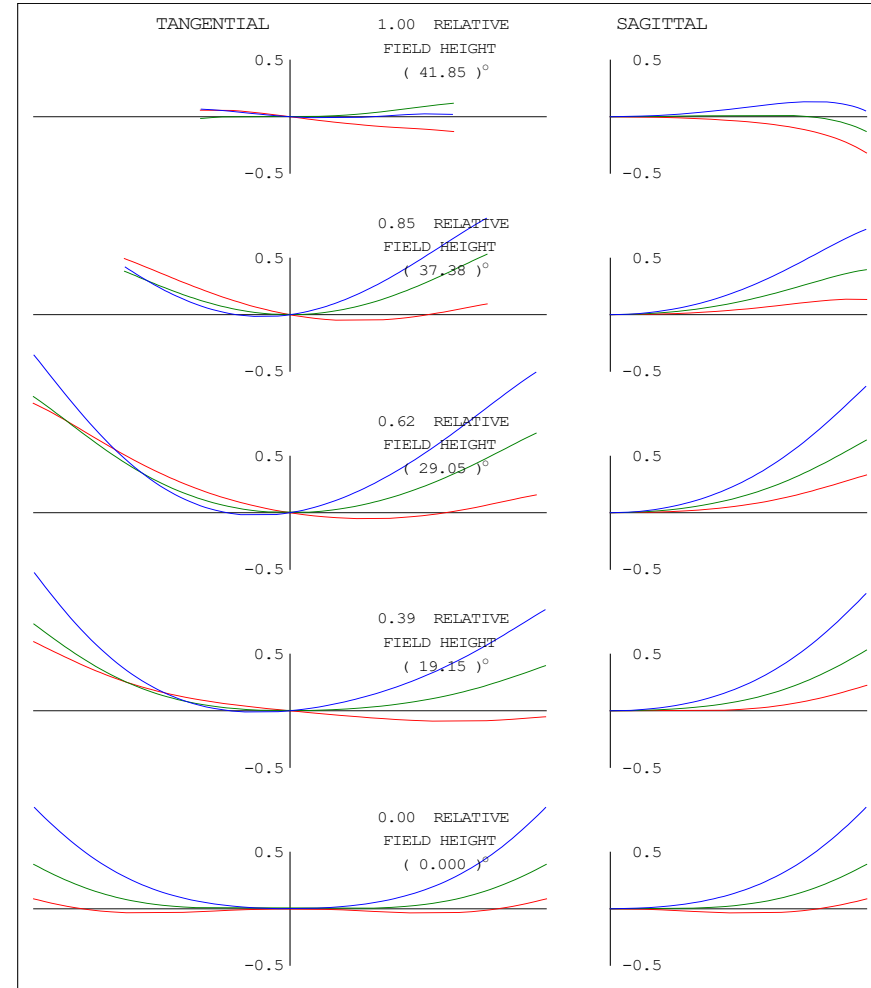
aberration diagram:

- only tangential and sagittal direction
- + aberration types can be identified
- + good polychromatic visualization

Ray aberration and wavefront deviation



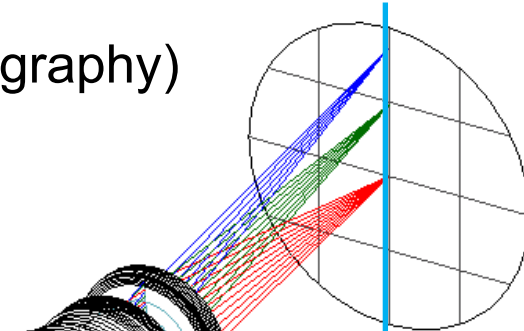
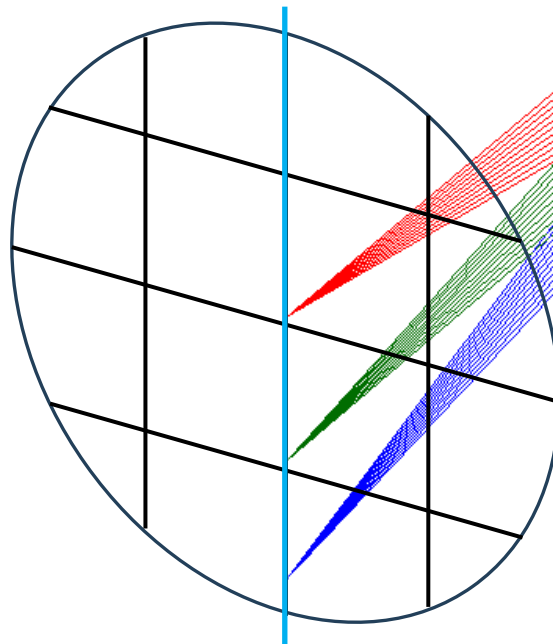
Ray aberration



Wavefront deviation (optical path difference)

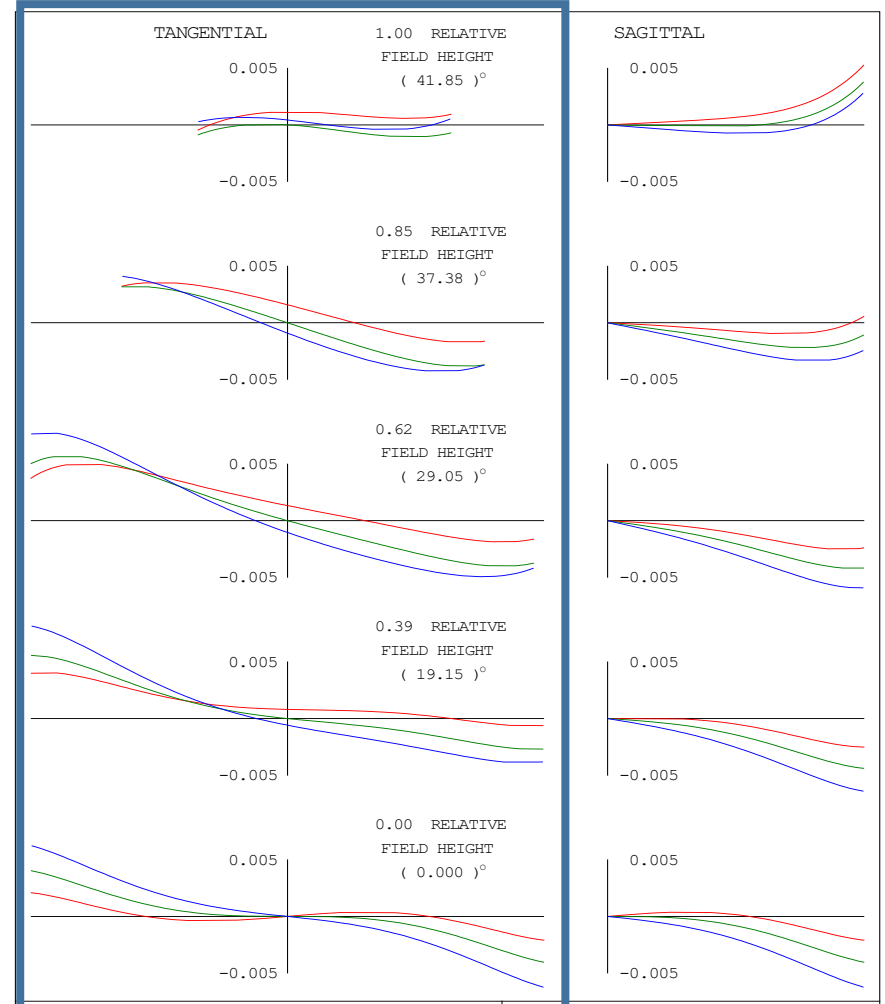
Rotational-symmetric system: Tangential (meridional) rays

“meridional”: along a meridian (geography)
= along north-south direction



- Tangential plane contains:
- object and image point
 - chief ray
 - optical axis

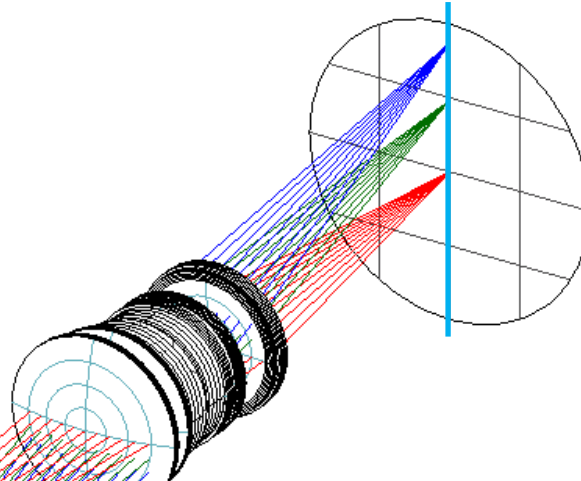
Tangential (meridional)



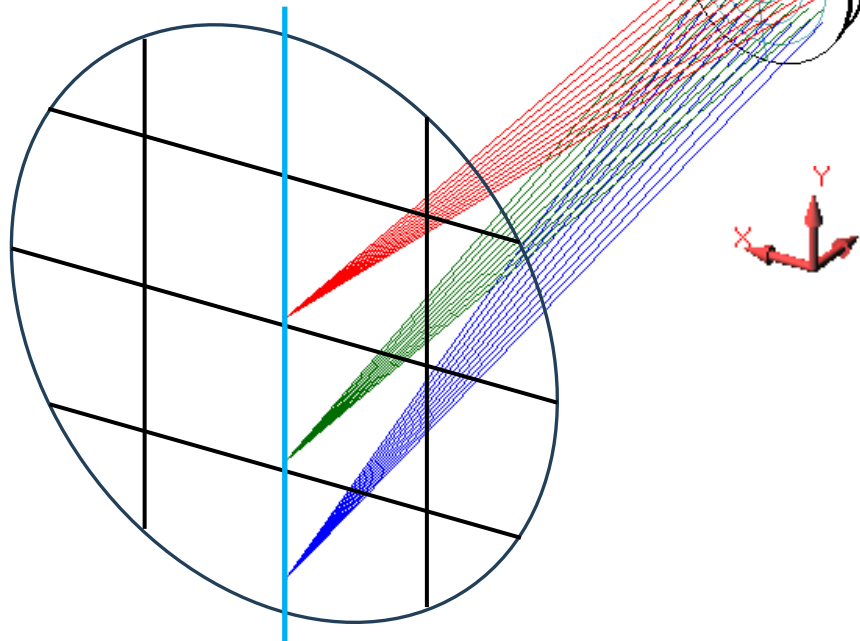
Ray aberration

Rotational-symmetric system: Sagittal rays

“sagitta” lat. “arrow”



Sagittal ray perpendicular to tangential rays



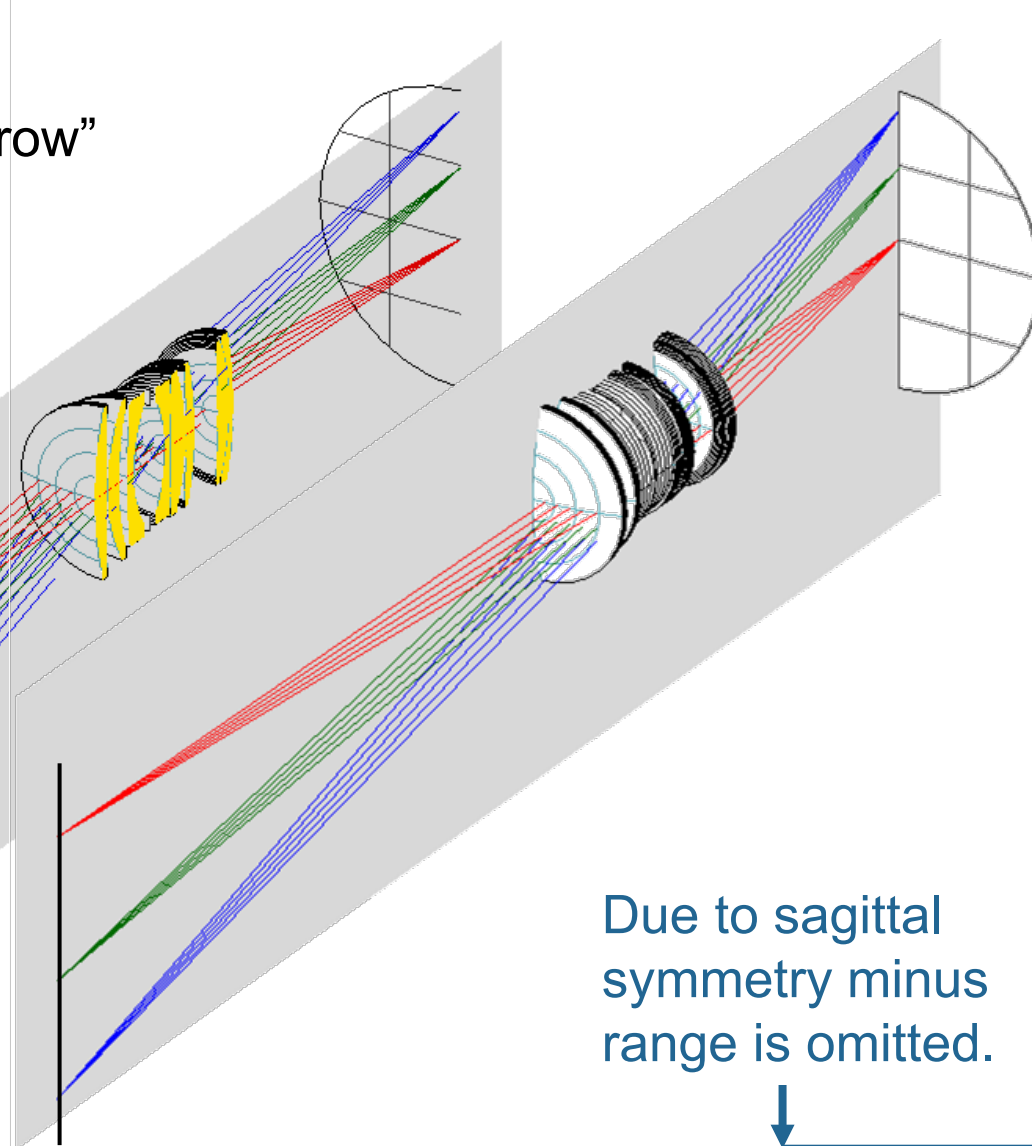
Sagittal plane contains:

- object and image point
- chief ray

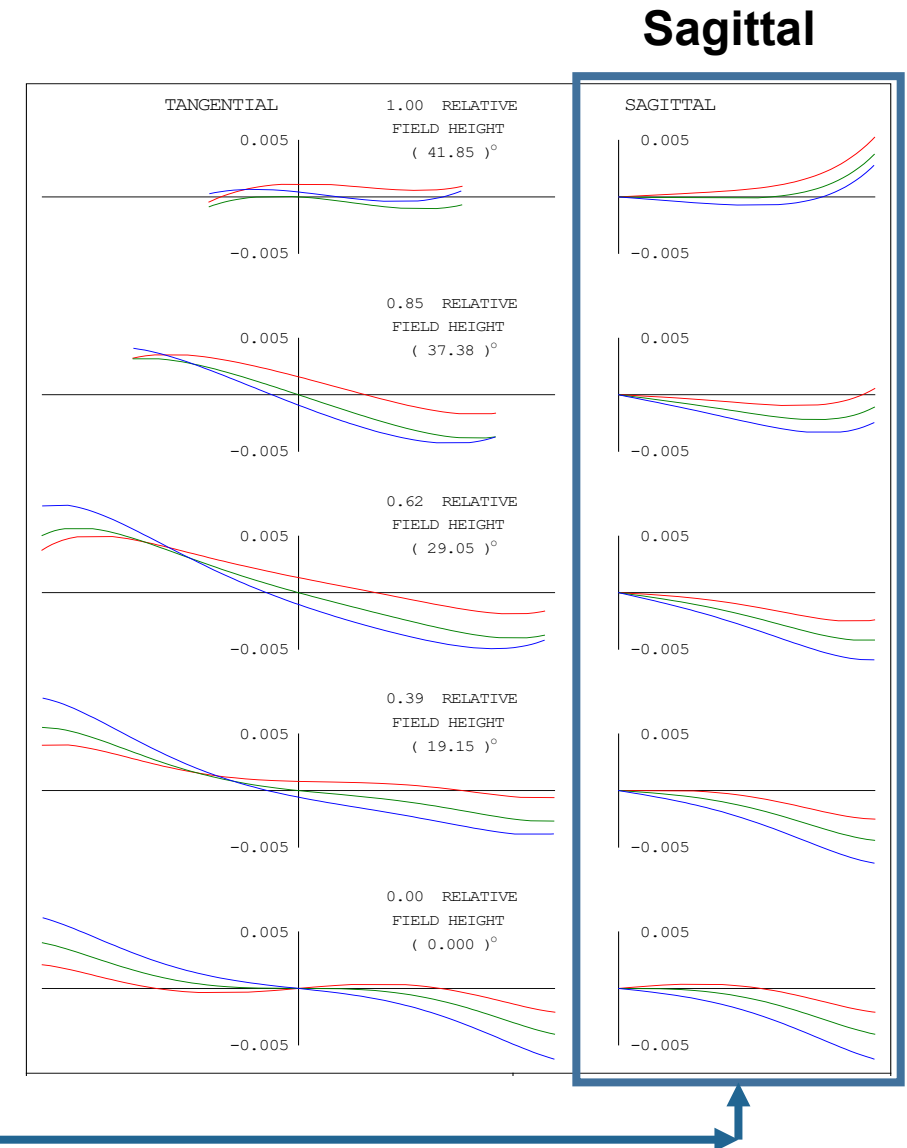
Unlike the tangential plane it does not include the (complete) optical axis

Symmetry around tangential plane for sagittal rays

“sagitta” lat. “arrow”

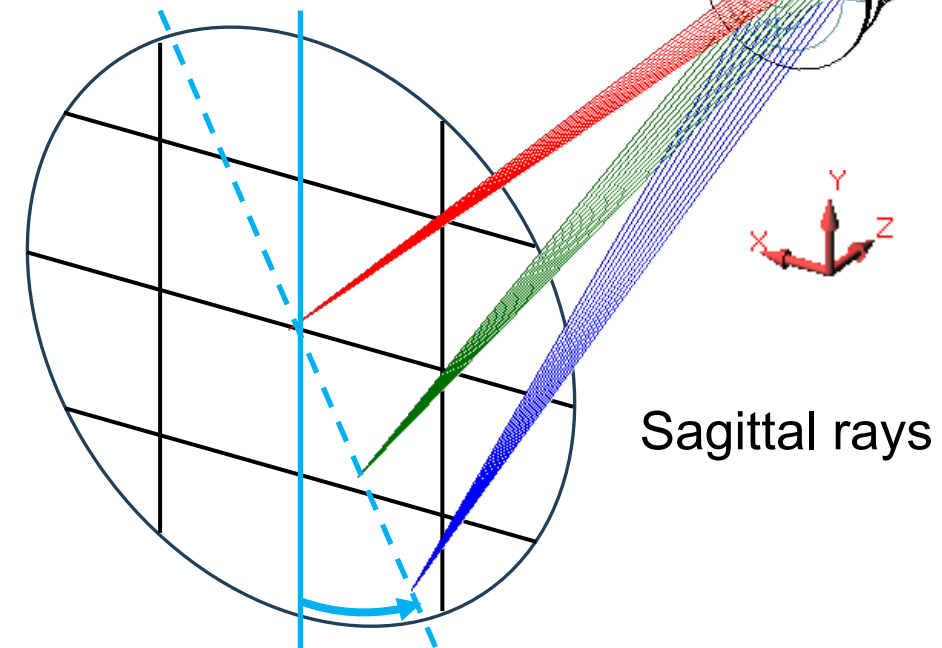
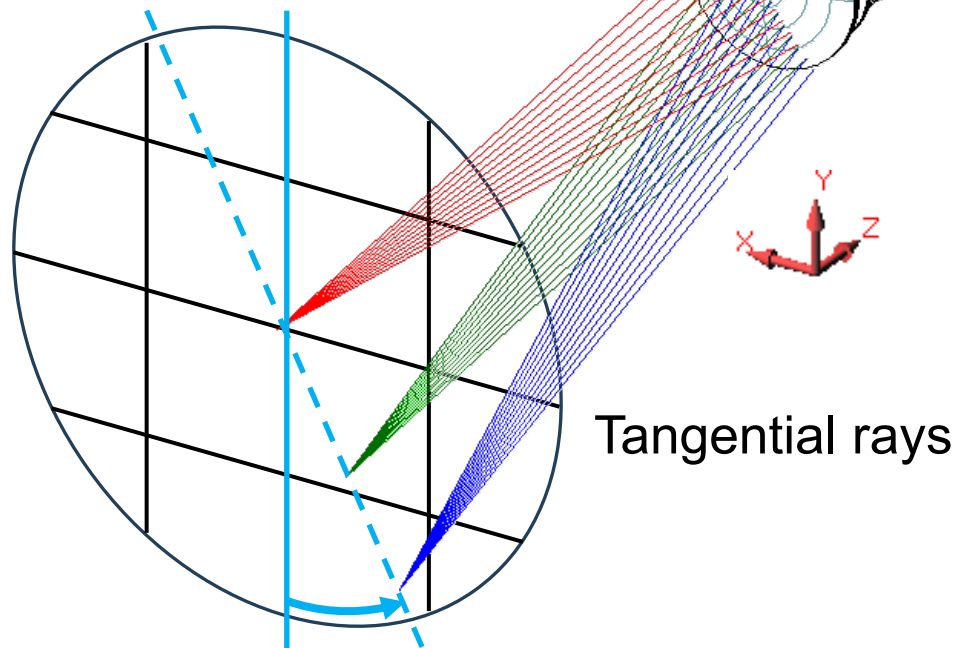


Due to sagittal
symmetry minus
range is omitted.



Rotational-symmetric system: Invariance with object azimuth angle

Rotate all object points keeping the same object heights:
The system symmetry remains.
All aberrations and the pupil shape are invariant with rotating the tangential plane.



Classification of aberrations

$$W(\alpha^2, \alpha \cdot \xi, \xi^2) = w_{200} \alpha^2 + w_{400} \alpha^4 + w_{310} \alpha^2 \alpha \cdot \xi + w_{202} \alpha^2 \xi^2 + w_{020} (\alpha \cdot \xi)^2 + w_{013} \alpha \cdot \xi \xi^2 + \dots$$

Rotationally symmetric system:
function of 3 variables

$$W(\vec{\alpha} \cdot \vec{\alpha}, \vec{\alpha} \cdot \vec{\xi}, \vec{\xi} \cdot \vec{\xi}) = \sum_{l=0}^{\infty} \sum_{k=0}^{\infty} \sum_{j=0}^{\infty} c_{2j,k,2l} |\vec{\xi}|^{2j} (\vec{\xi} \cdot \vec{\alpha})^k |\vec{\alpha}|^{2l}$$

Classification as a function of $\alpha^2, \alpha \cdot \xi, \xi^2$ “Seidel form”

Seidel was the first to formulate and publish an explicit form for calculating the five monochromatic third order (Seidel) aberrations.

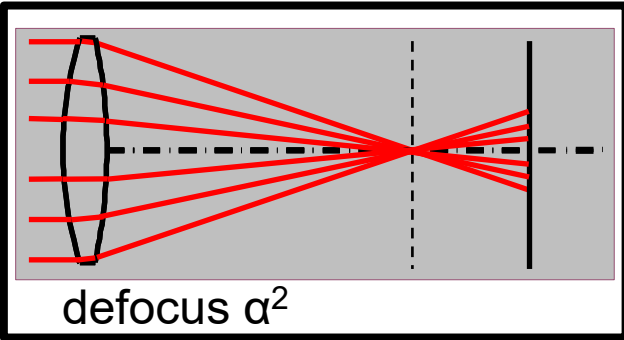


Ludwig von Seidel (1821 - 1896)

Classification of aberrations

$$W(\alpha^2, \alpha \cdot \xi, \xi^2) = w_{200} \alpha^2 + w_{400} \alpha^4 + w_{310} \alpha^2 \alpha \cdot \xi + w_{202} \alpha^2 \xi^2 + w_{020} (\alpha \cdot \xi)^2 + w_{013} \alpha \cdot \xi \xi^2 + \dots$$

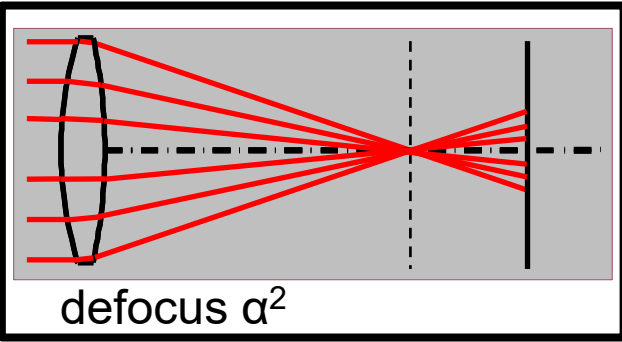
1st order monochromatic:



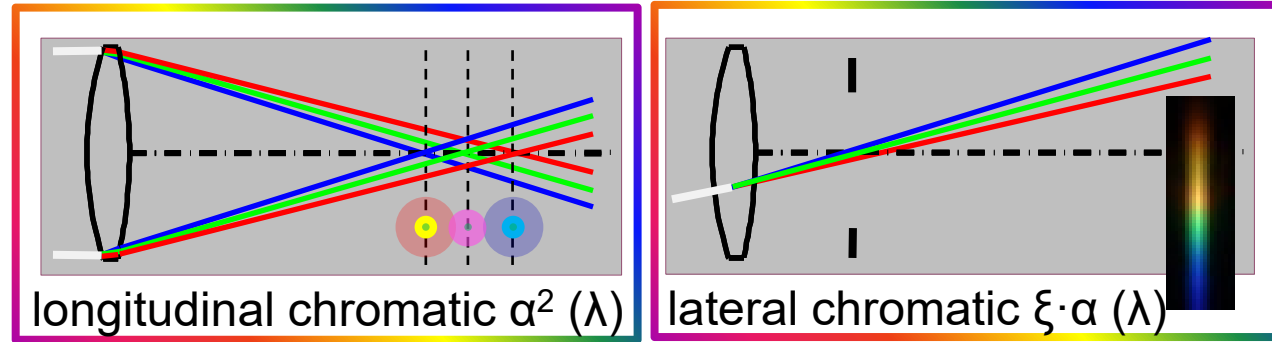
Classification of aberrations

$$W(\alpha^2, \alpha \cdot \xi, \xi^2) = w_{200} \alpha^2 + w_{400} \alpha^4 + w_{310} \alpha^2 \alpha \cdot \xi + w_{202} \alpha^2 \xi^2 + w_{020} (\alpha \cdot \xi)^2 + w_{013} \alpha \cdot \xi \xi^2 + \dots$$

1st order monochromatic:



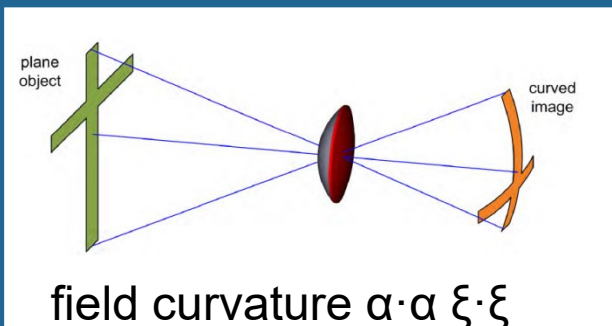
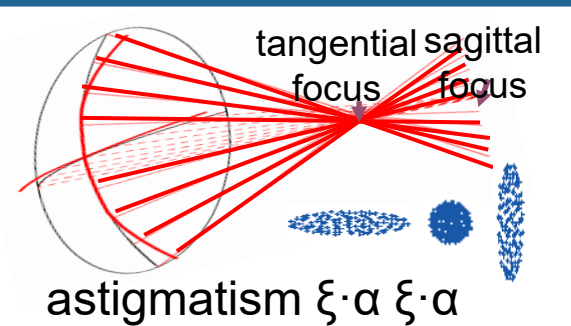
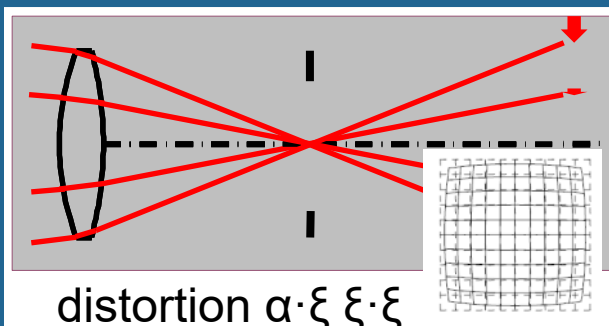
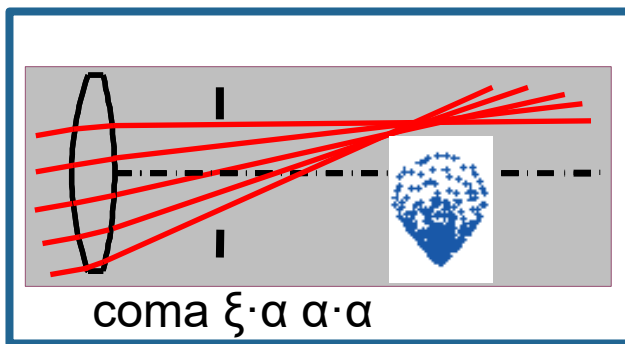
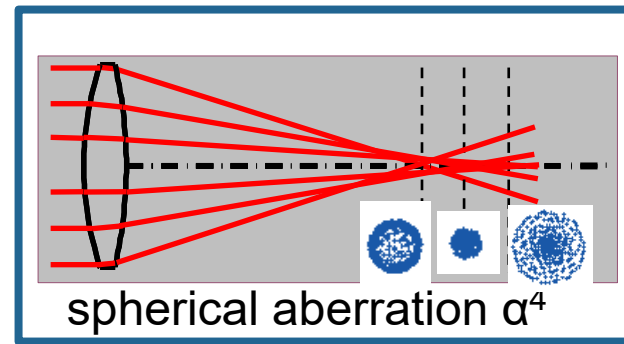
1st order
chromatic:



Classification of aberrations

$$W(\alpha^2, \alpha \cdot \xi, \xi^2) = w_{200} \alpha^2 + w_{400} \alpha^4 + w_{310} \alpha^2 \alpha \cdot \xi + w_{202} \alpha^2 \xi^2 + w_{020} (\alpha \cdot \xi)^2 + w_{013} \alpha \cdot \xi \xi^2 + \dots$$

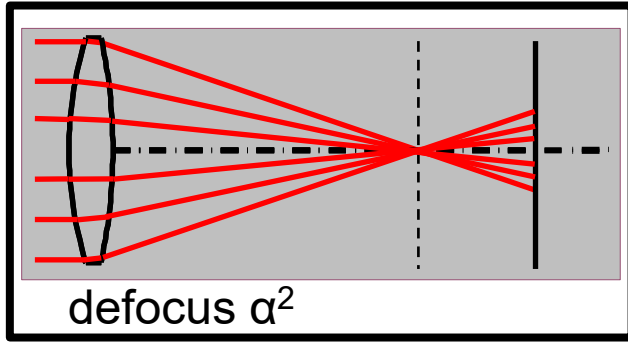
3rd order
monochromatic:



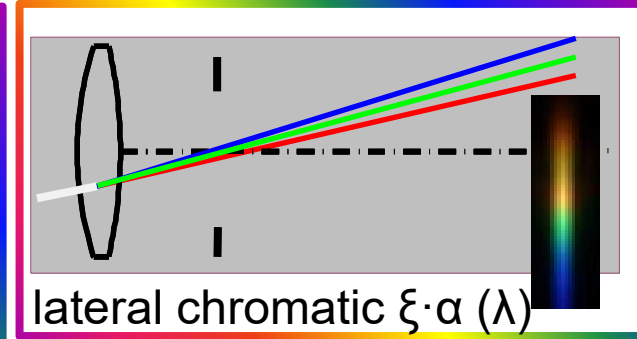
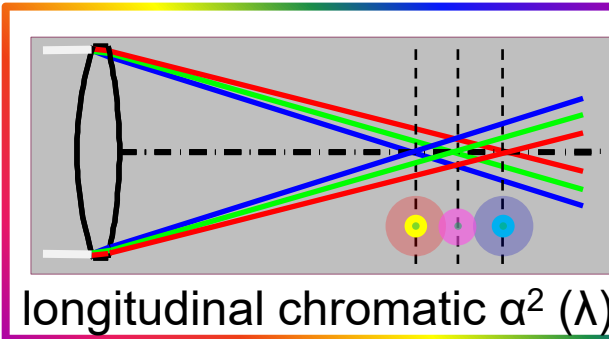
Classification of aberrations

$$W(\alpha^2, \alpha \cdot \xi, \xi^2) = w_{200} \alpha^2 + w_{400} \alpha^4 + w_{310} \alpha^2 \alpha \cdot \xi + w_{202} \alpha^2 \xi^2 + w_{020} (\alpha \cdot \xi)^2 + w_{013} \alpha \cdot \xi \xi^2 + \dots$$

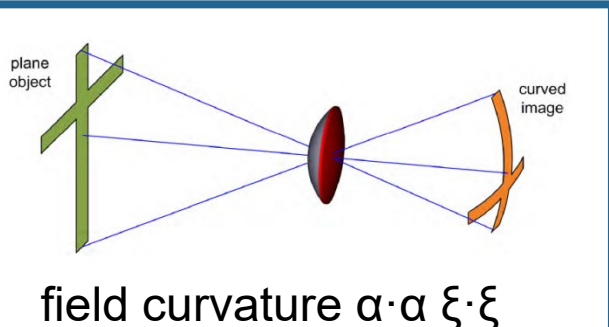
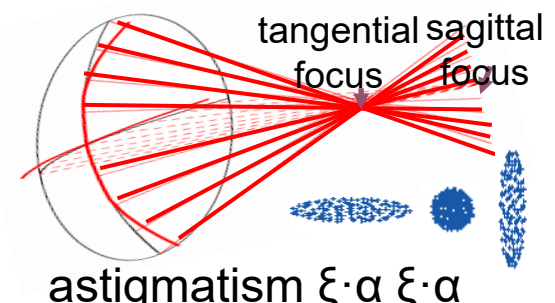
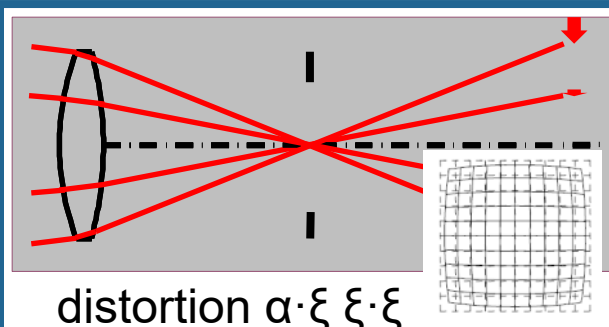
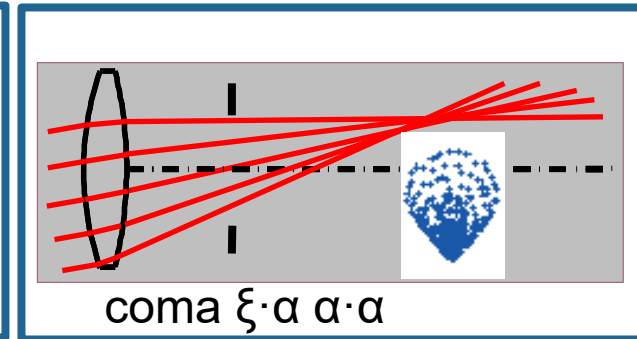
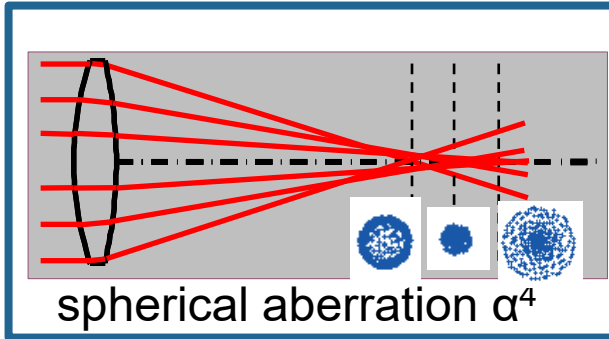
1st order monochromatic:



1st order chromatic:



3rd order monochromatic:



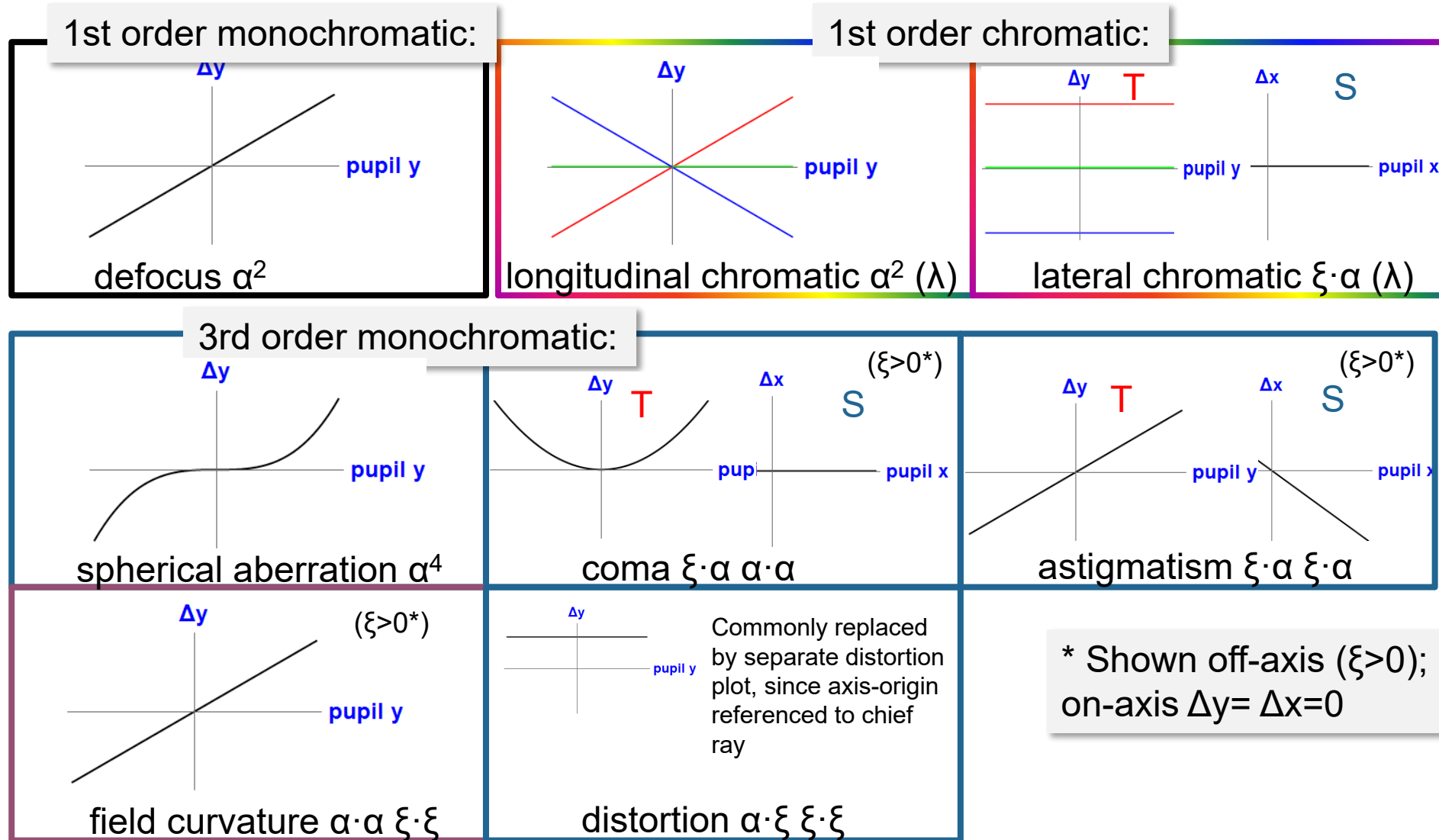
5th order: 9 types

7th order: 14 types

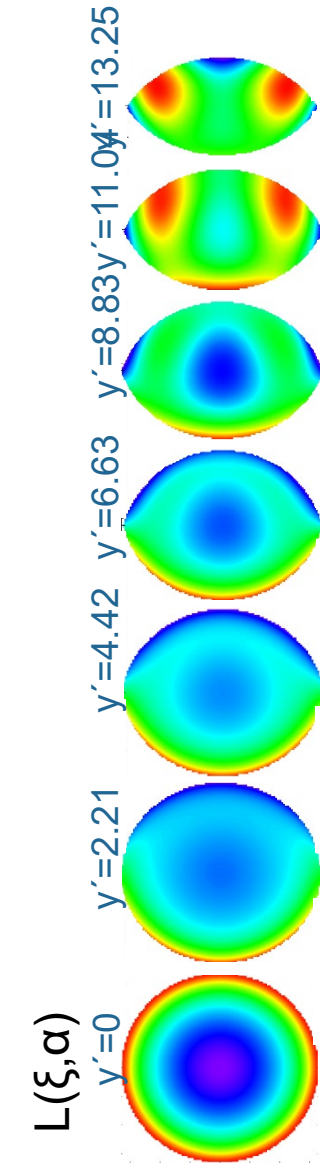
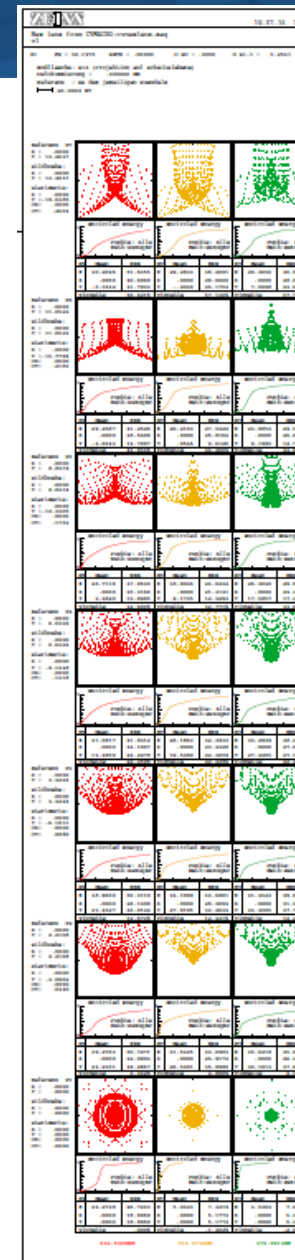
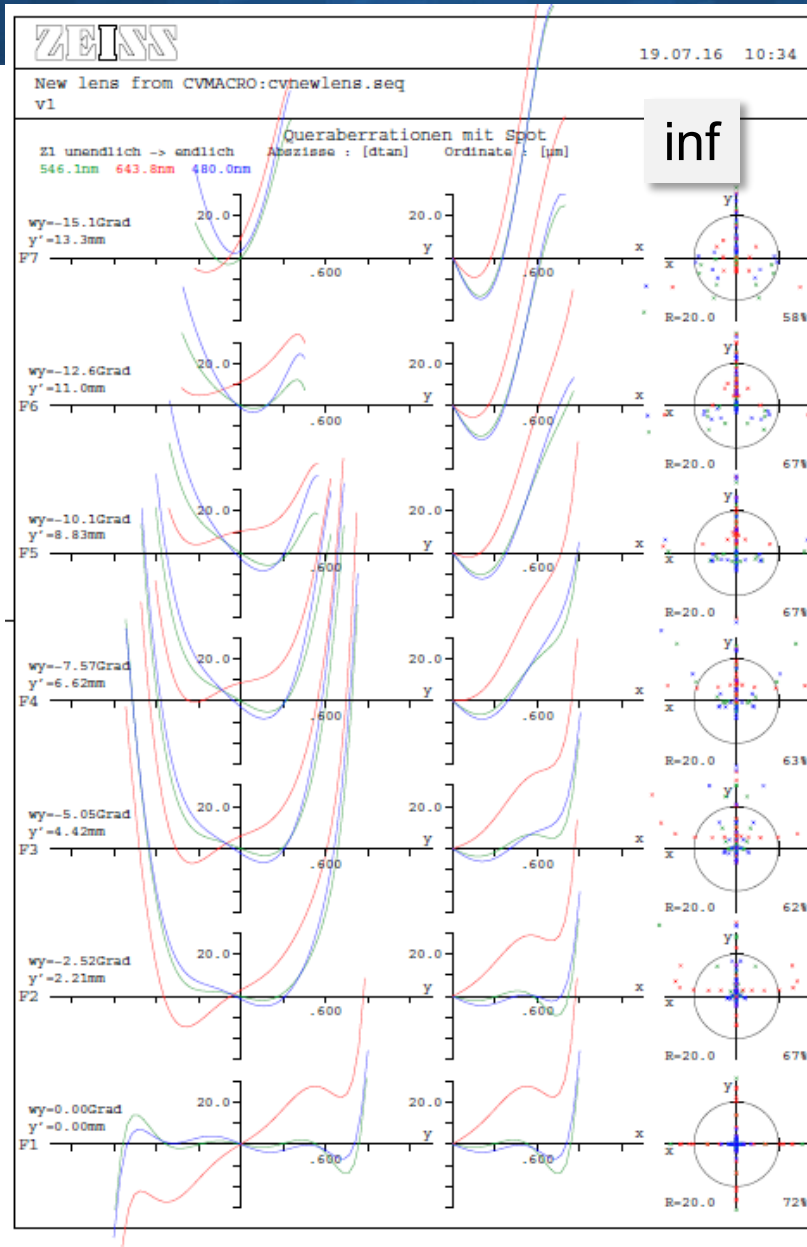
...
n'th order $(n+3)(n+5)/8-1$

Classification of aberrations

Ray aberration graphs

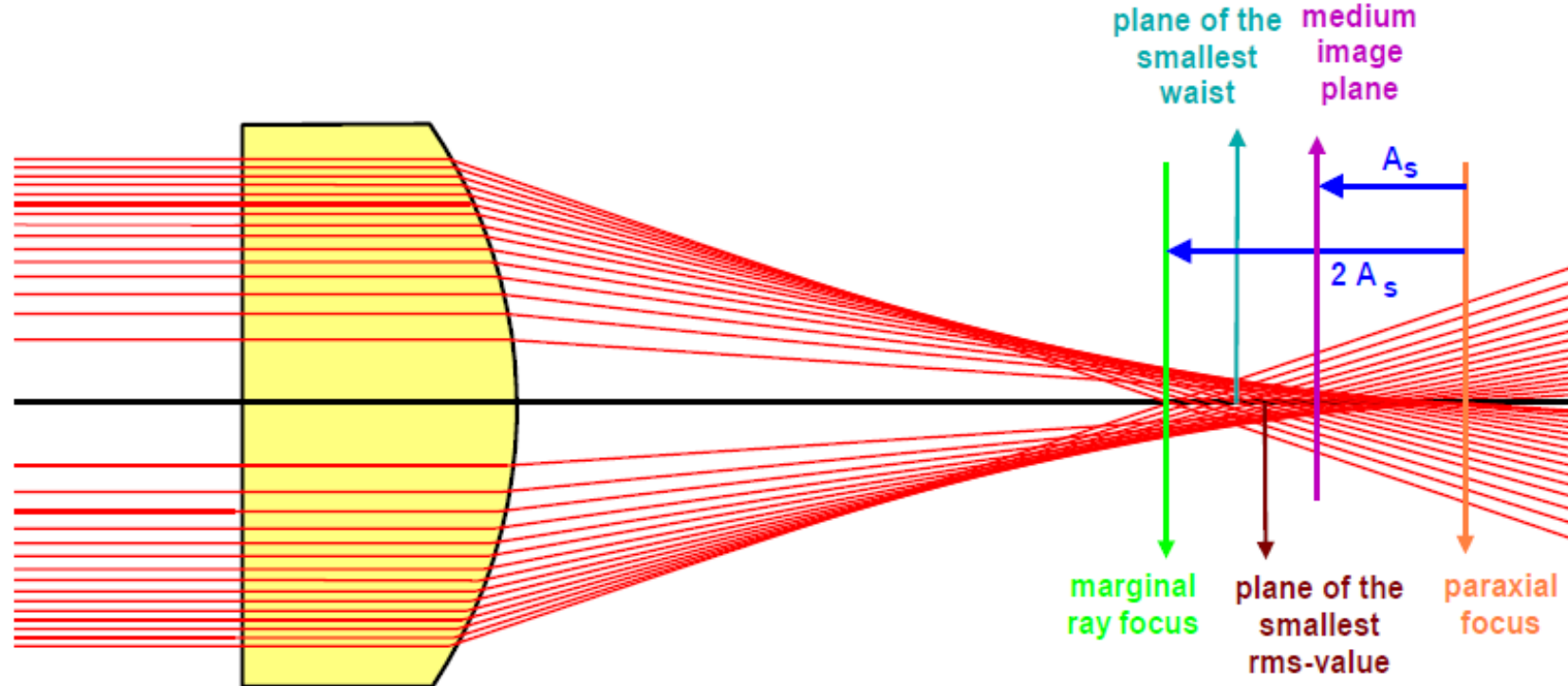


Aberration diagram and spot diagram



PSF(x)

Spherical Aberration



With spherical aberration the optimum focus position changes when you stop down the lens.

„Aberration free“ Lens (almost)



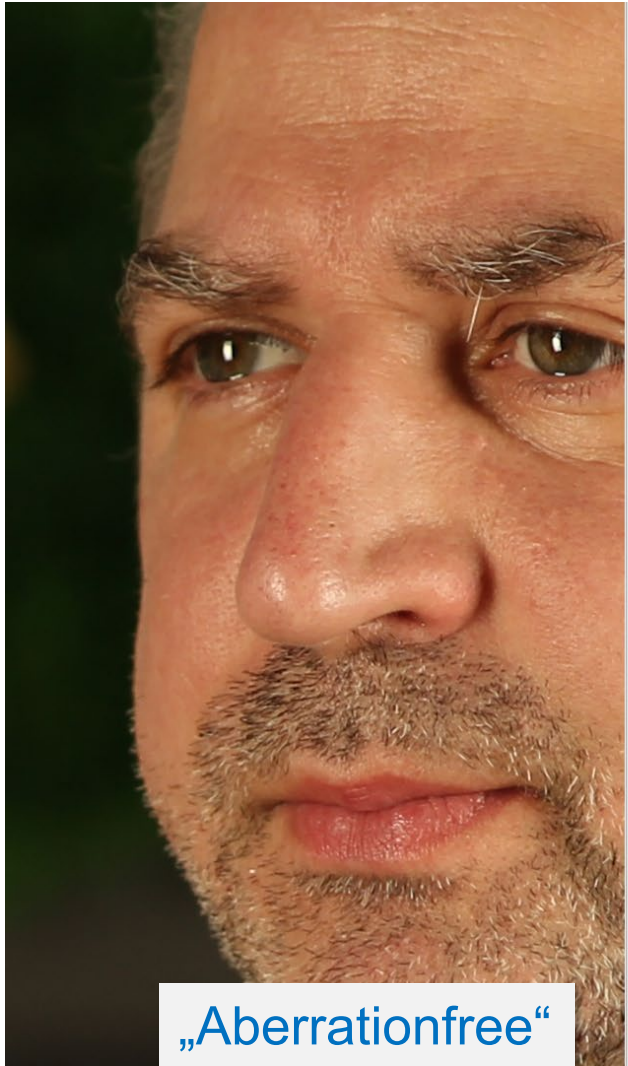
Lens with spherical aberration („+“-sign)



Lens with spherical aberration („-“-sign)



Spherical aberration: Best focus



„Aberrationfree“

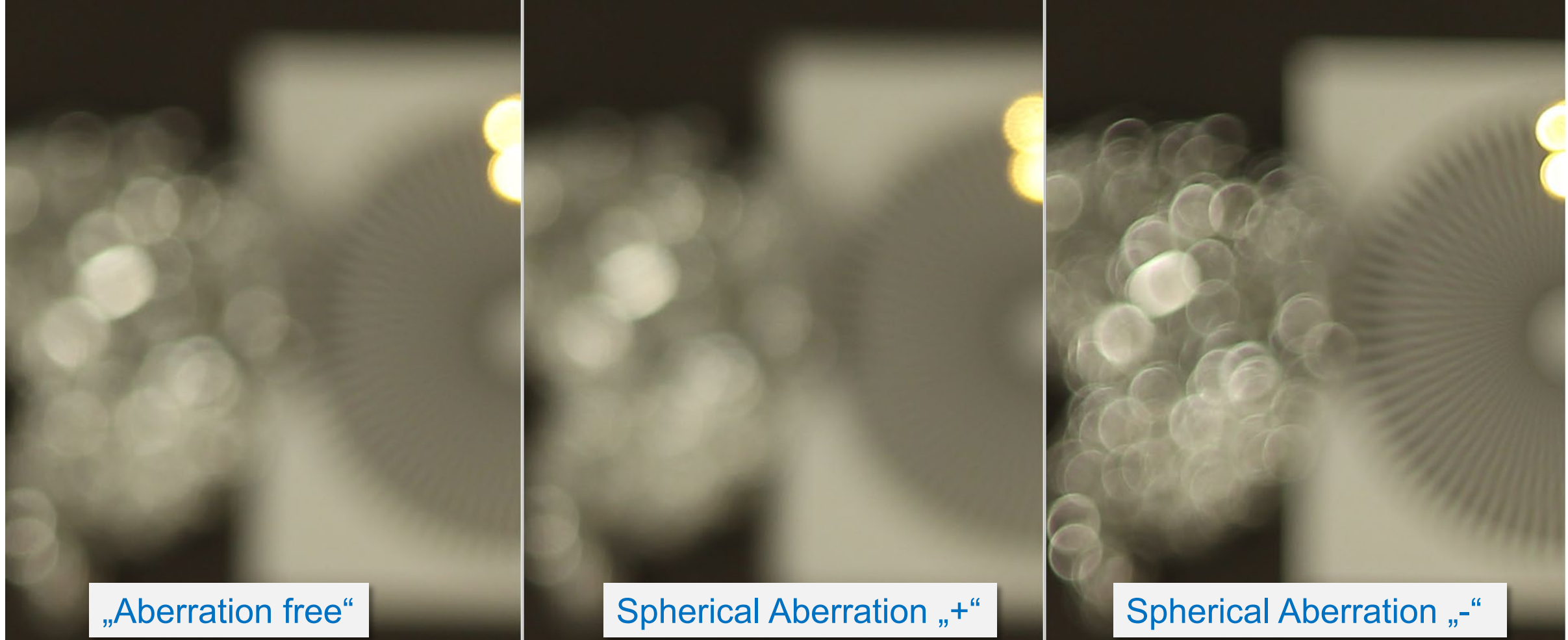


Sph. Aberr. „+“

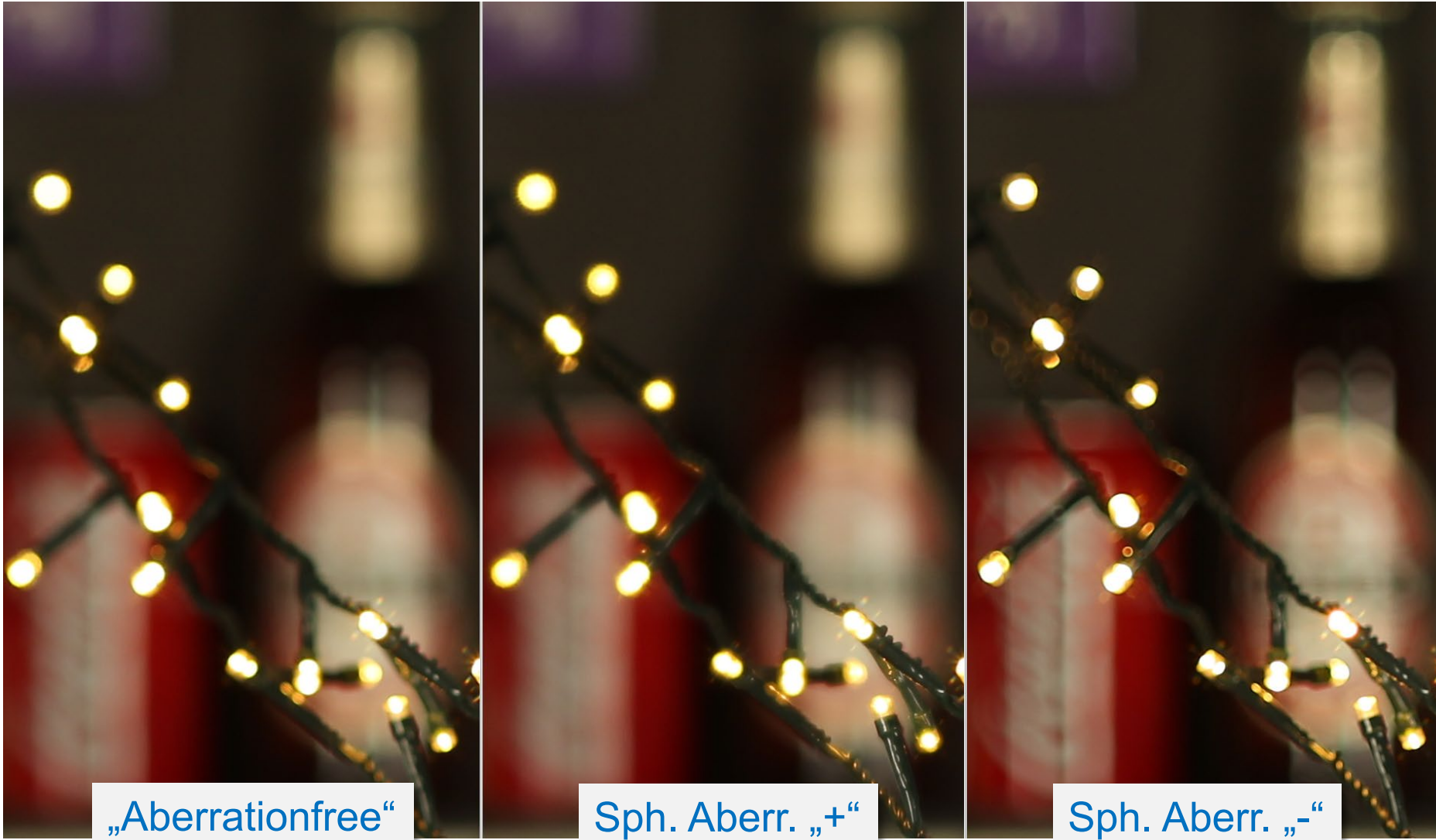


Sph. Aberr. „-“

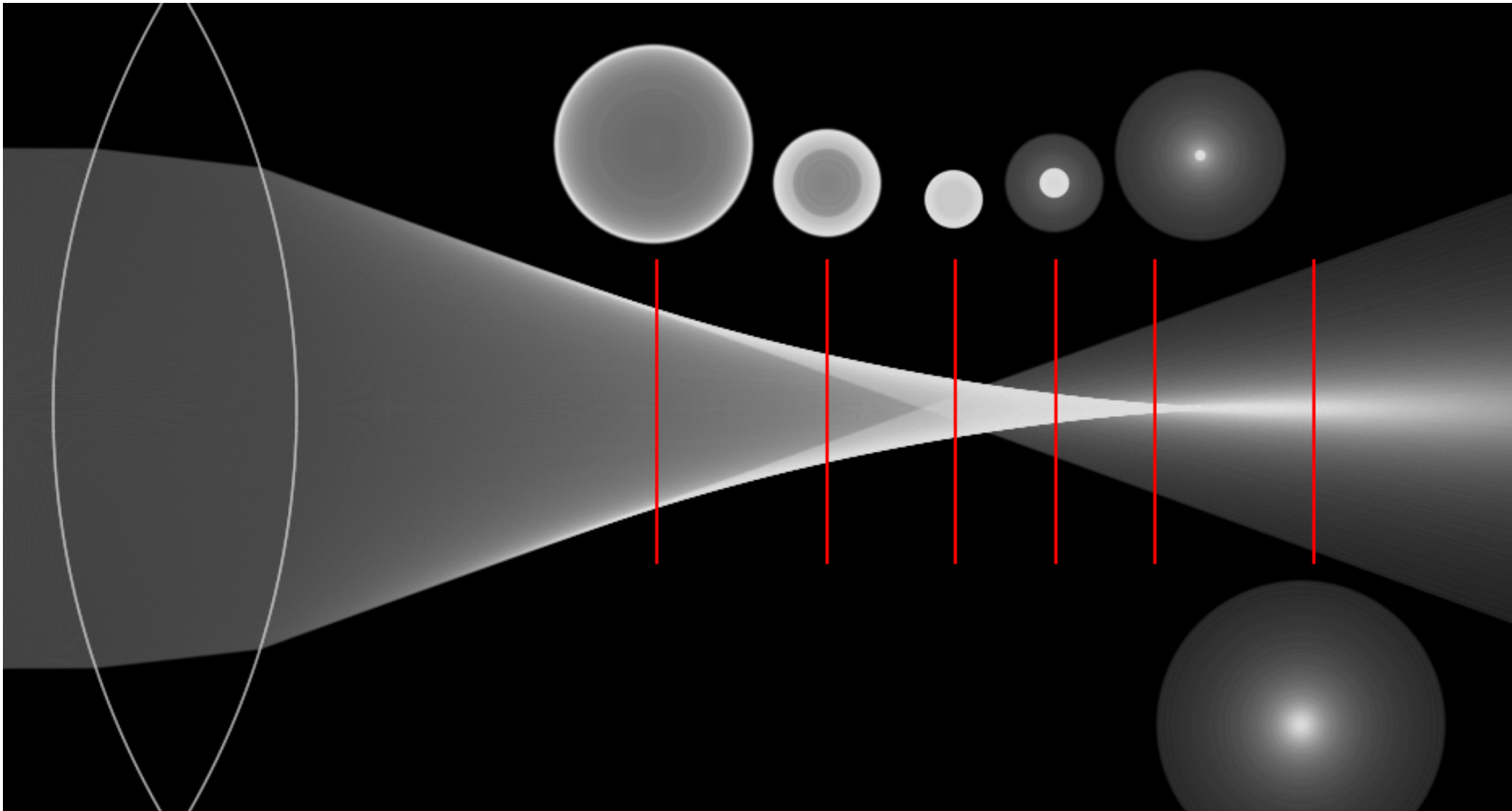
Spherical aberration: background



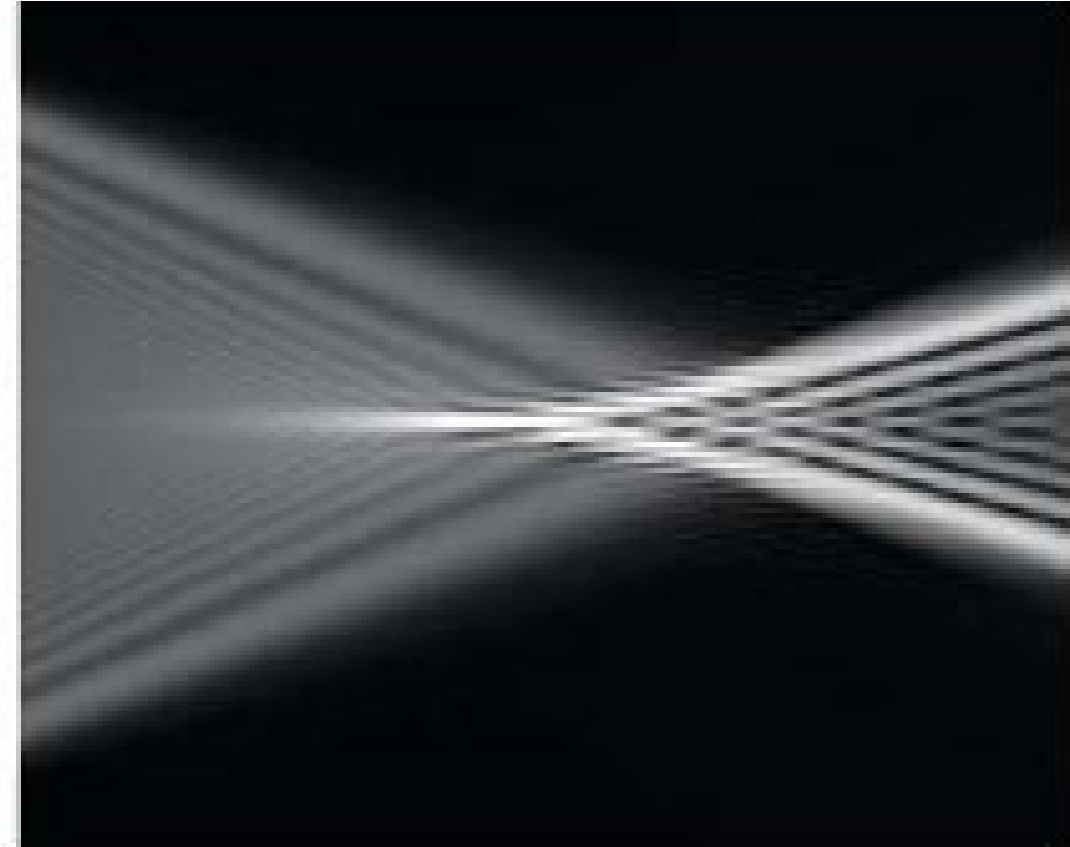
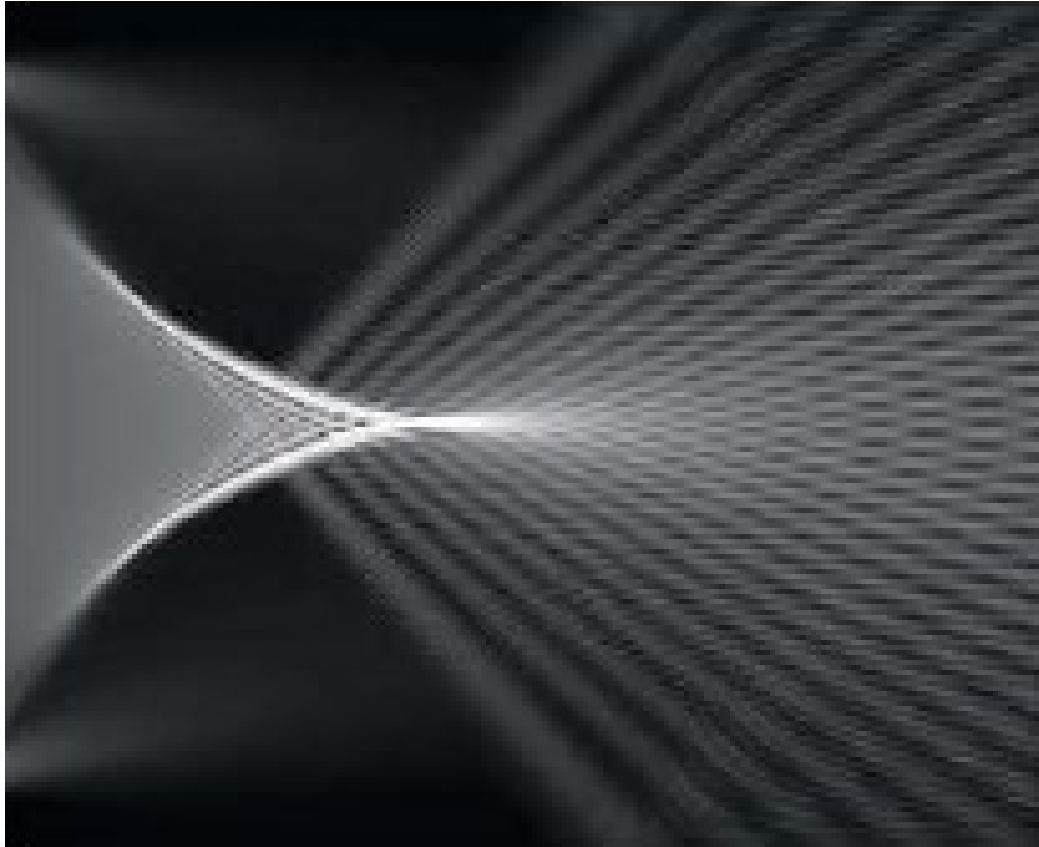
Spherical aberration: background



Spherical aberration through focus



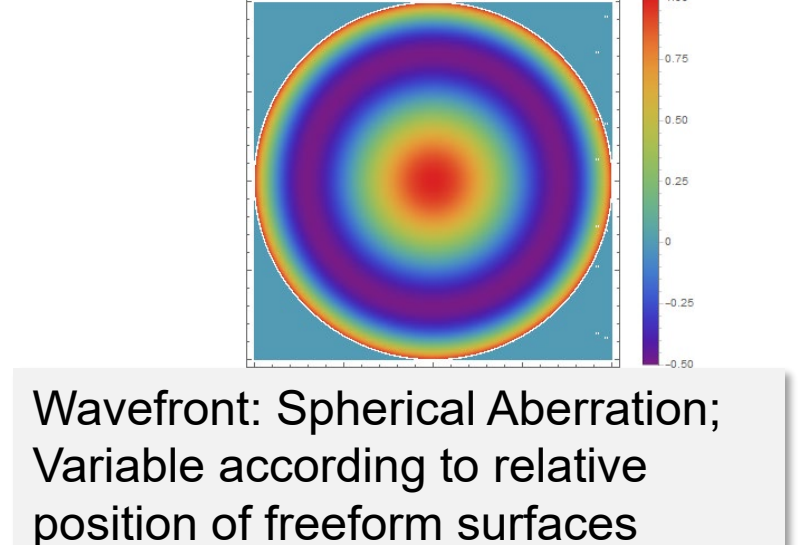
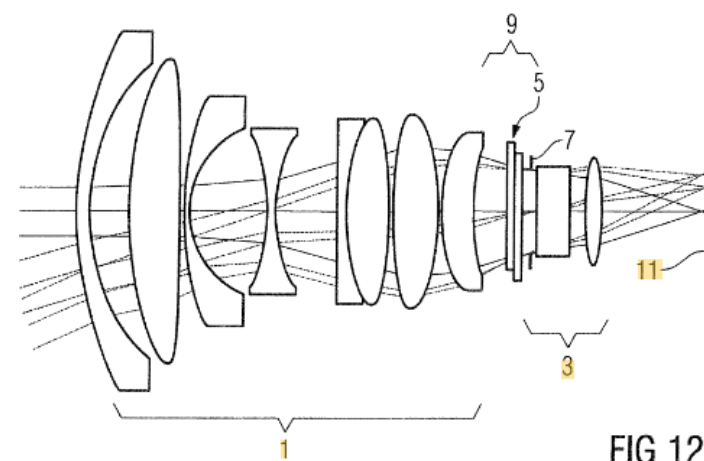
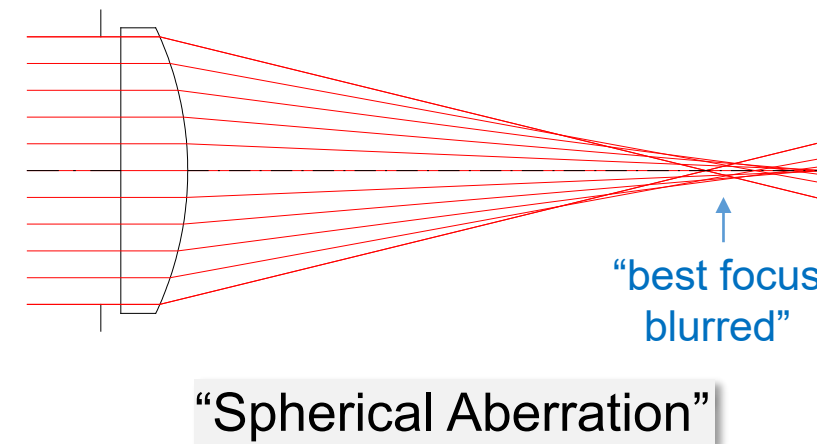
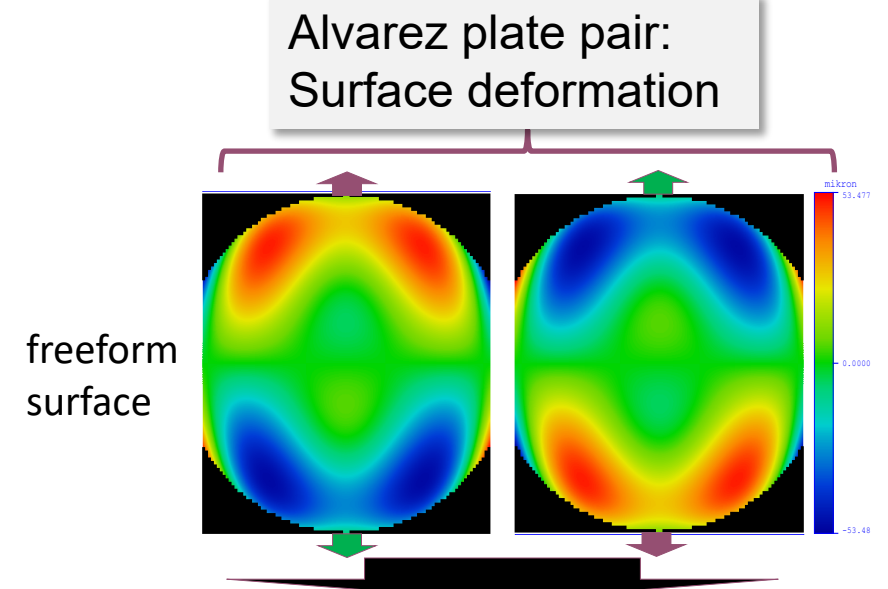
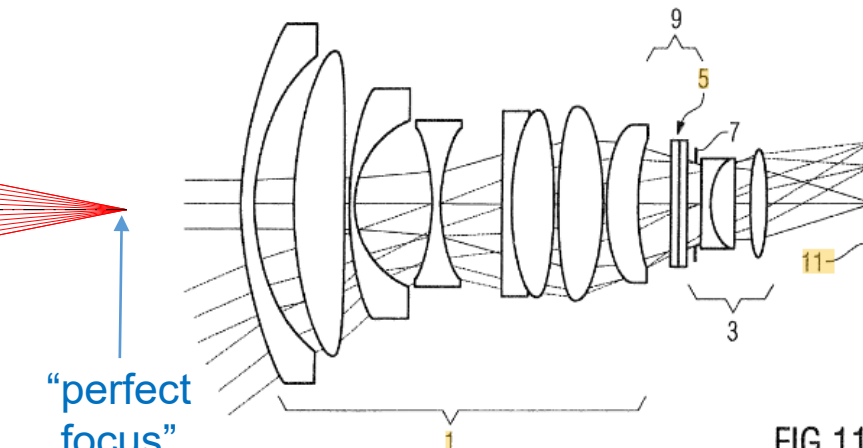
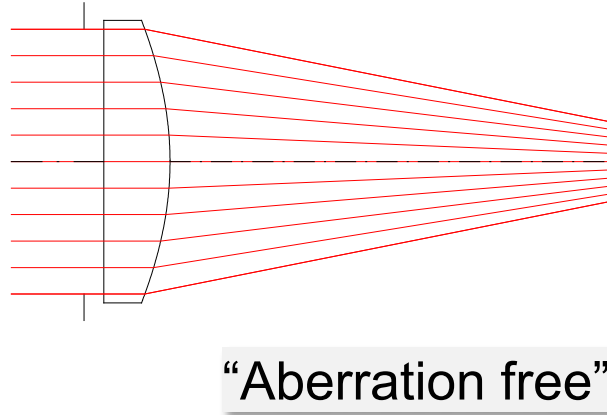
Spherical aberration through focus



Through focus intensity of positive and negative spherical aberration including diffraction.

The fine structures depend on the amount of spherical aberration and wavelength.

Vary spherical aberration of lens with Alvarez manipulator



Effect of spherical aberration



$Z9 = 0$



$Z9 = 0.4 \lambda$



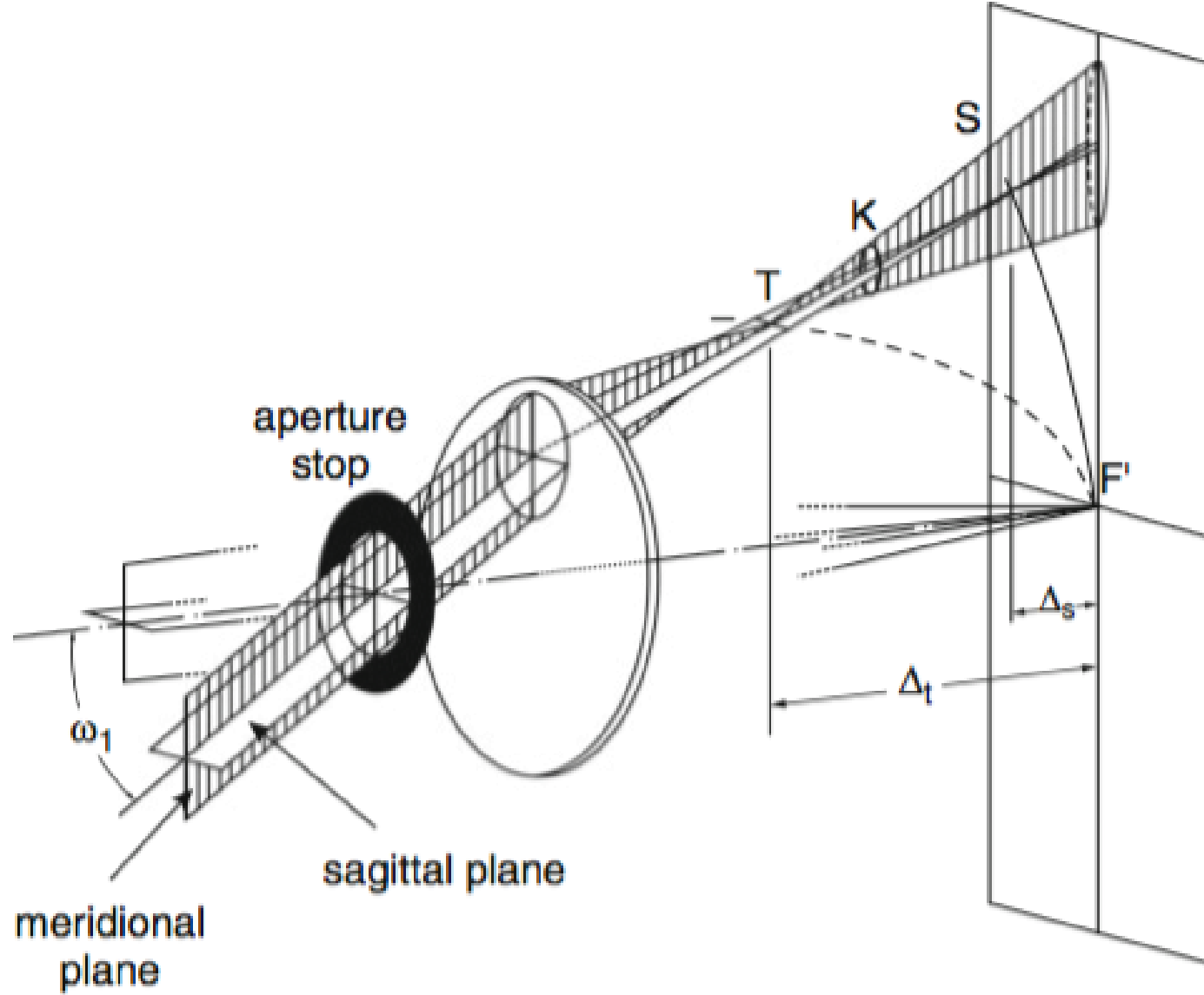
$Z9 = 0.7 \lambda$



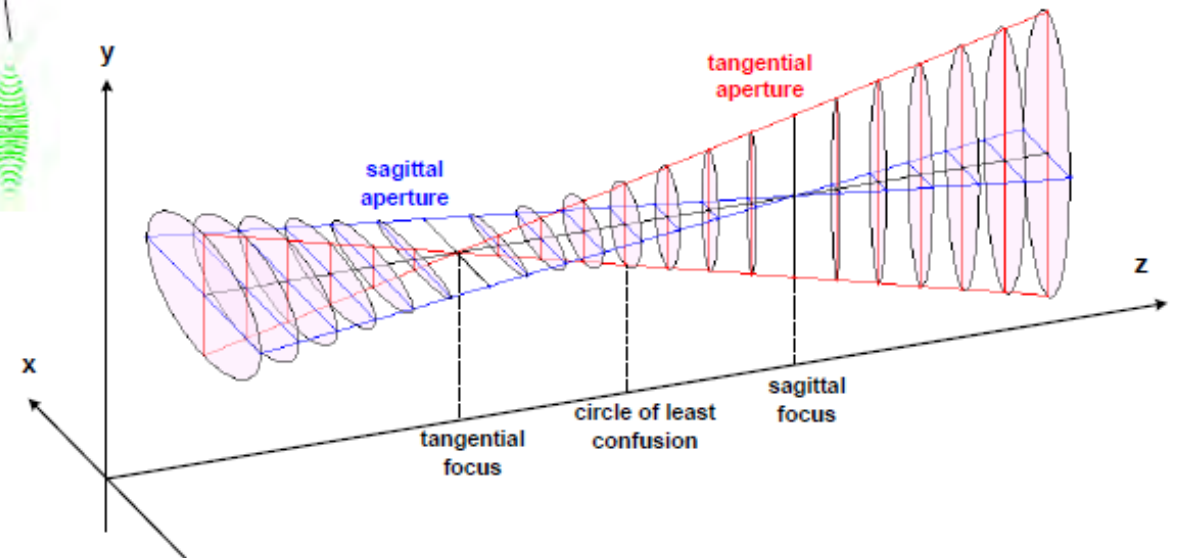
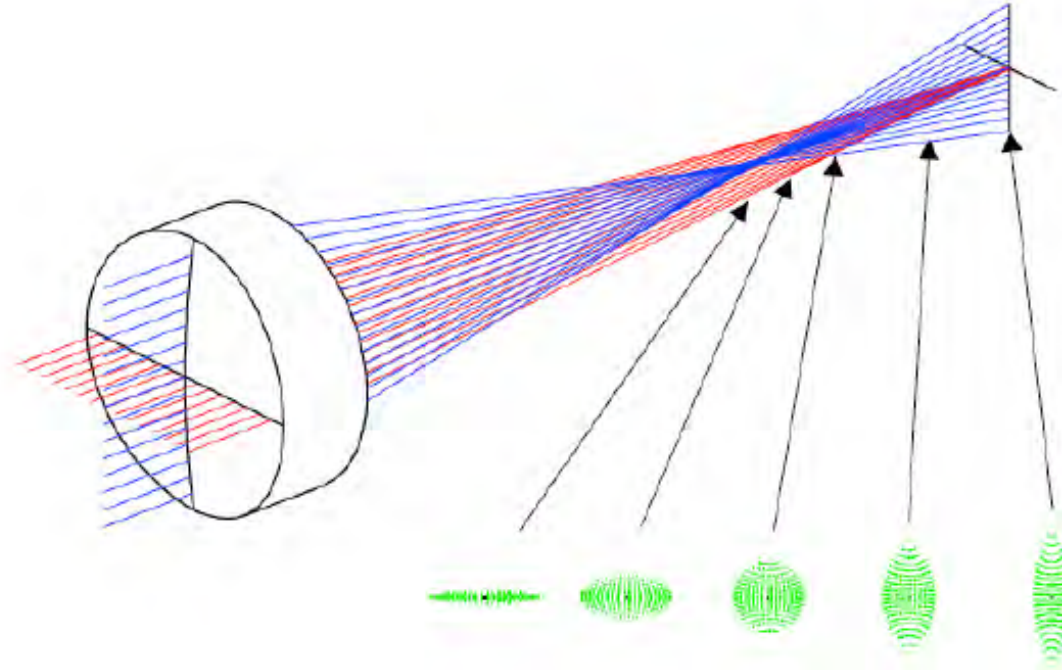
$Z9 = 1.0 \lambda$

Effect of
increasing
spherical
aberration (“Z9”).

Astigmatism

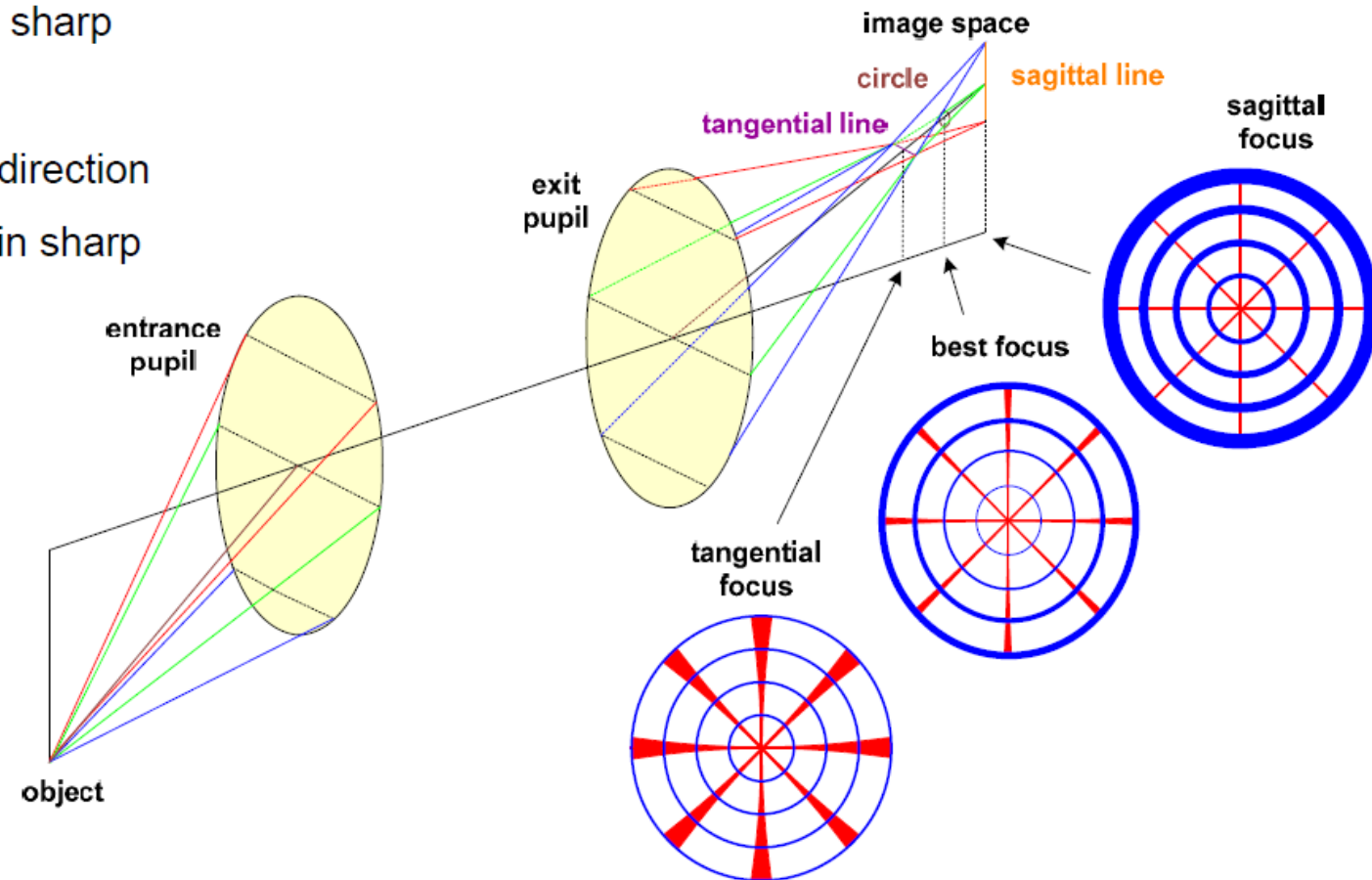


Astigmatism

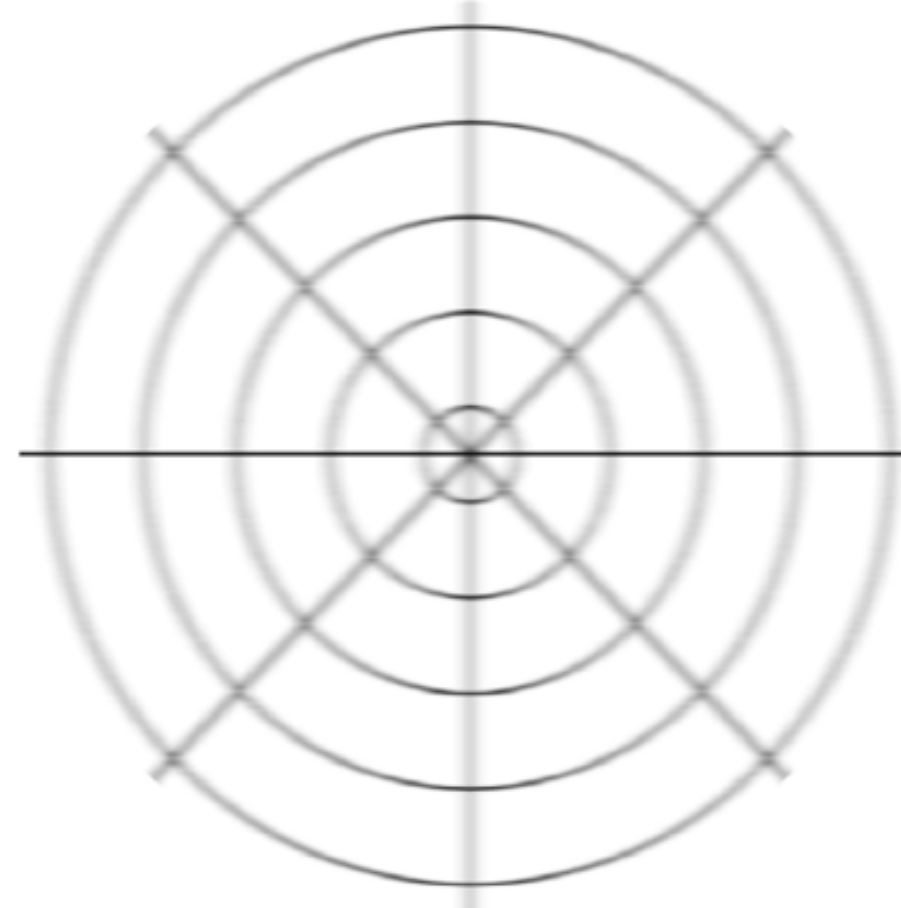
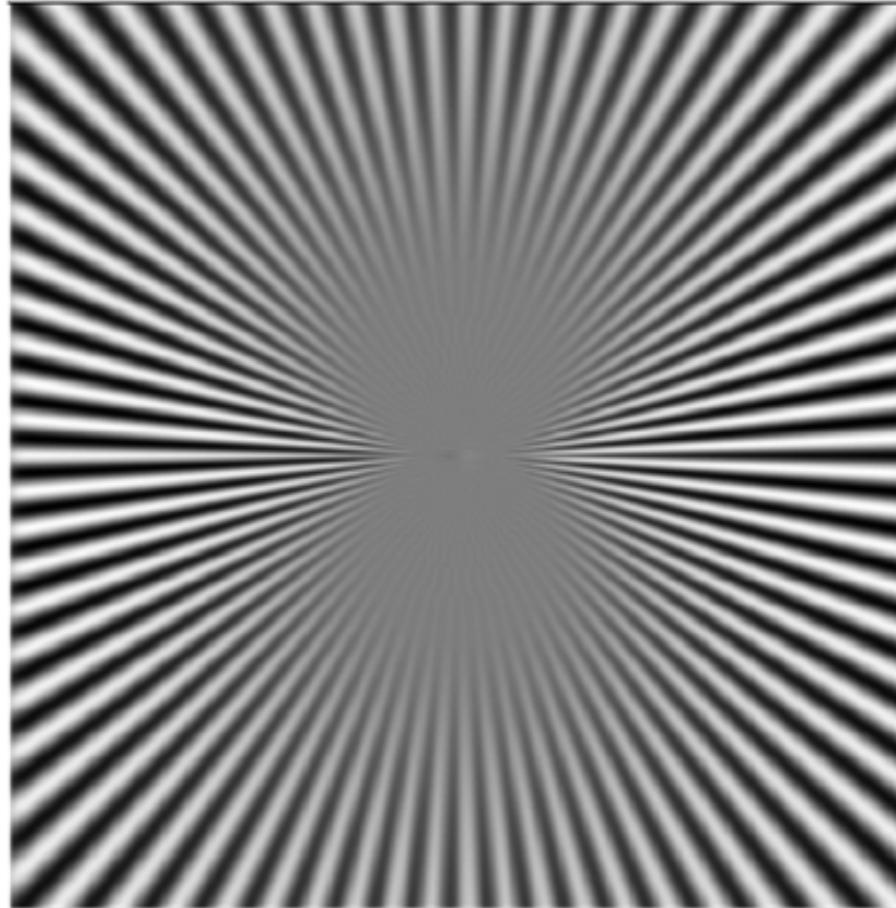


Astigmatism

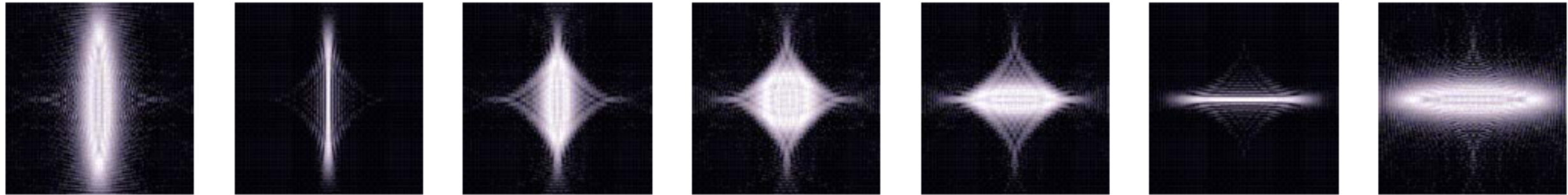
- Imaging of a polar grid in different planes
- Tangential focus:
 - blur in azimuthal direction
 - rings remain sharp
- Sagittal focus:
 - blur in radial direction
 - spokes remain sharp



Astigmatism + Defocus
Such that horizontal lines are sharp, vertical blurred



Astigmatism: Wave-optical PSF through focus



sagittaler
Fokus

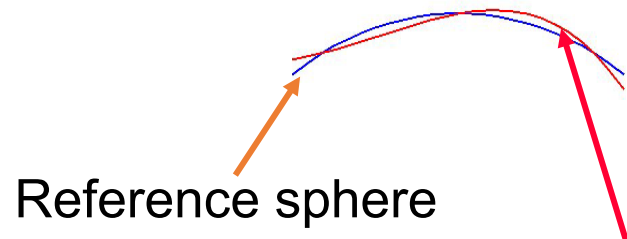
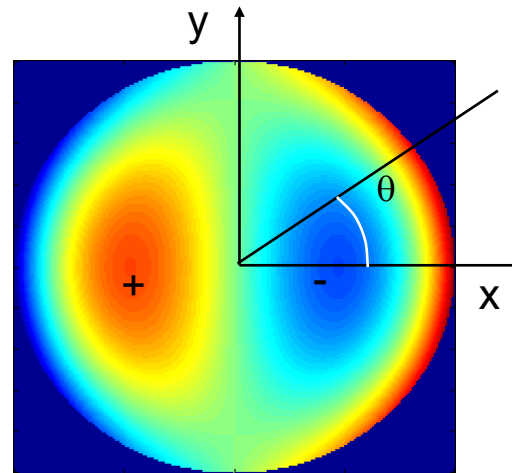
„least confusion“

tangentialer
Fokus



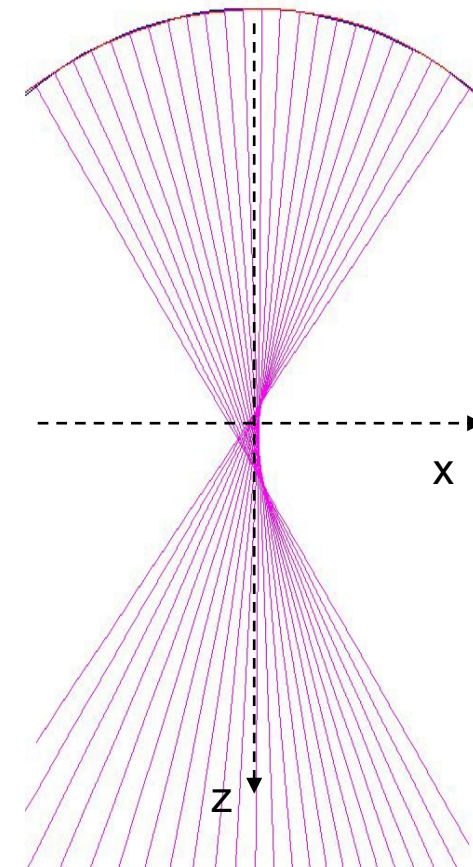
coma: $Z_7 \quad (3r^3 - 2r) \cdot \cos \theta$

Wavefront deformation in pupil

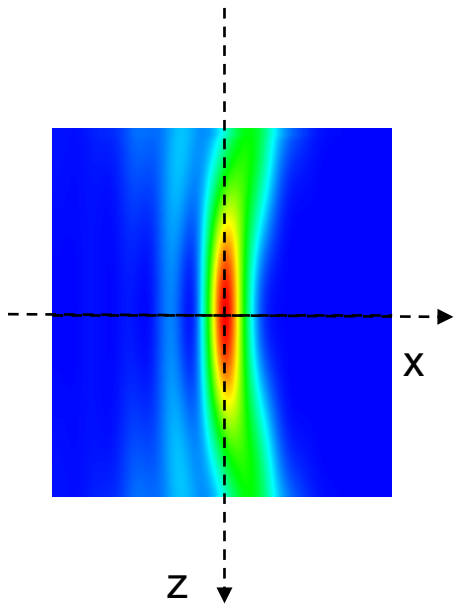


wavefront with coma

Ray trace



Aerial image



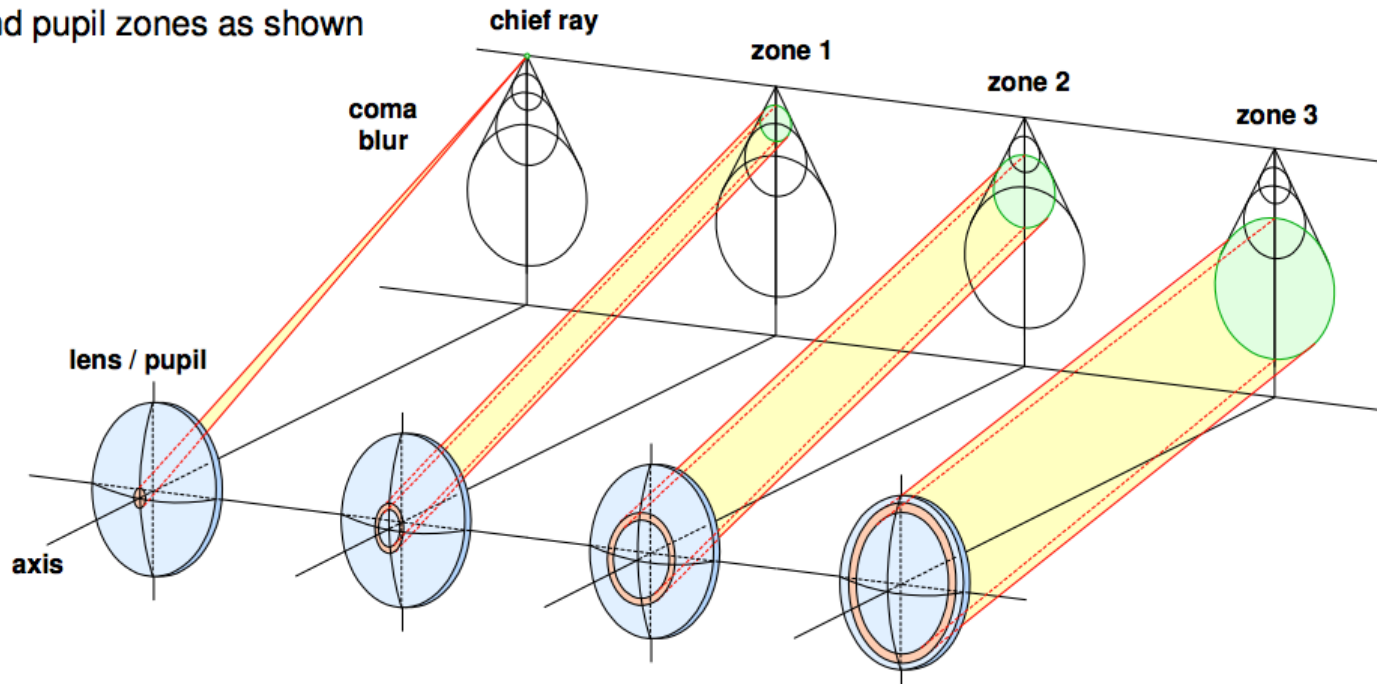
Aerial image
through focus.
„Banana shape“.

Coma

$$K(\vec{x}, \vec{\xi}, z) = \iint d\alpha L_0(\vec{\xi}, \vec{\alpha}) \exp\left(i \frac{2\pi}{\lambda} W(\vec{\xi}, \vec{\alpha})\right) \exp\left(-i \frac{\pi}{\lambda} z NA^2 \vec{\alpha} \cdot \vec{\alpha}\right) \exp\left(-i 2\pi w \vec{\alpha} \cdot (\vec{x} - m\vec{\xi})\right)$$

with $W(\vec{\alpha}, \vec{\xi}) = c_{coma} \vec{\xi} \cdot \vec{\alpha} \vec{\alpha} \cdot \vec{\alpha}$

- Coma aberration: for oblique bundles and finite aperture due to asymmetry
- Primary effect: coma grows linear with field size y
- Systems with large field of view: coma hard to correct
- Relation of spot circles and pupil zones as shown

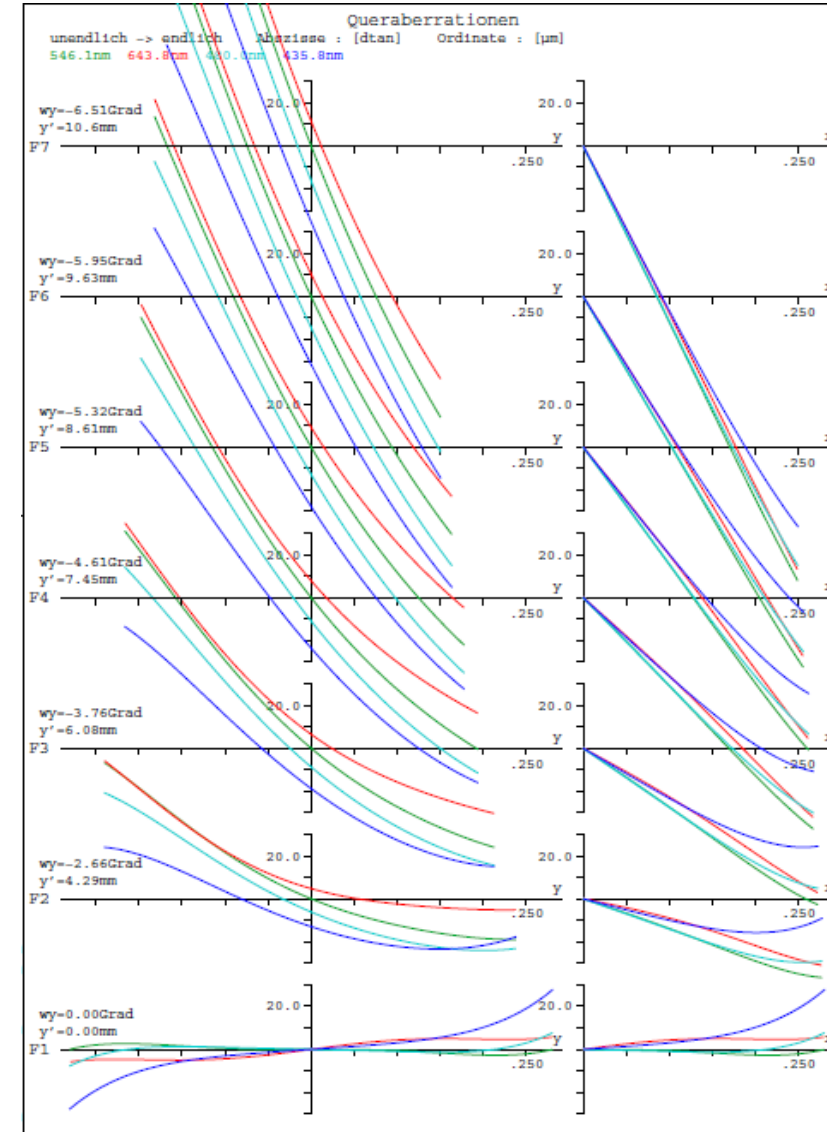
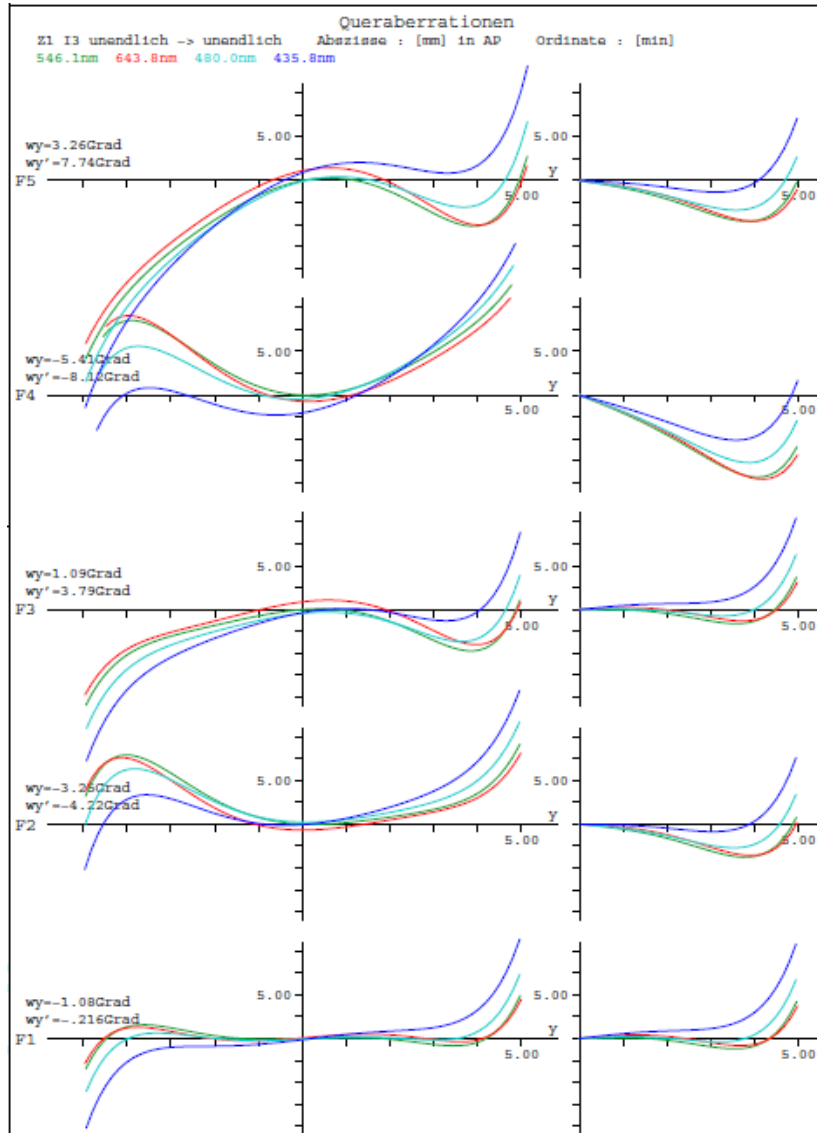


$$\begin{aligned} K(\vec{x}, \vec{\xi}, z) \\ = \iint d\alpha L_0(\vec{\xi}, \vec{\alpha}) \exp\left(-i \frac{\pi}{\lambda} [z NA^2 \vec{\alpha}^2 \right. \\ \left. + 2NA \vec{\alpha} \cdot (\vec{x} - m\vec{\xi}) + 2c_{coma} \vec{\xi} \cdot \vec{\alpha} \vec{\alpha} \cdot \vec{\alpha}] \right) \end{aligned}$$

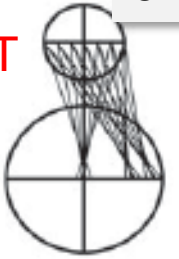
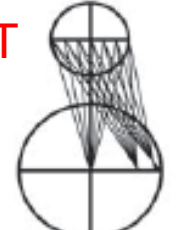
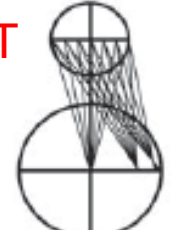
Small α :
 magnification shift $m \rightarrow m + \frac{c_{coma}}{NA}$

$\alpha \rightarrow 1$:
 Focus shift $z \rightarrow z + \frac{2c_{coma} |\vec{\xi}|}{NA^2}$

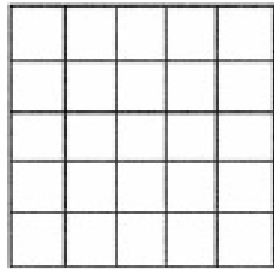
Examples of Optical System Aberration Diagrams



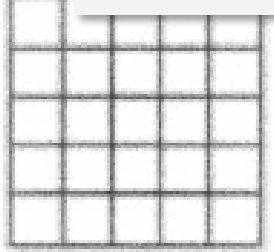
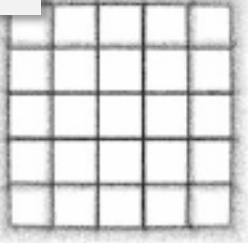
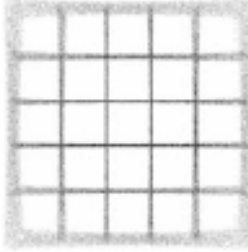
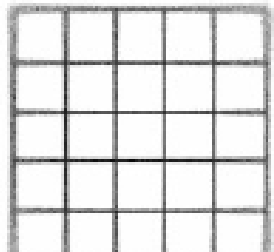
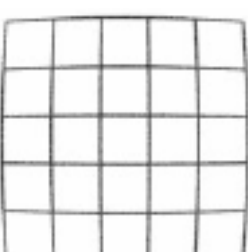
Classification of aberrations

3rd order monochromatic:		
		spherical aberration α^4
		coma $\xi \cdot \alpha$ $\alpha \cdot \alpha$
		astigmatism $\xi \cdot \alpha$ $\xi \cdot \alpha$
		field curvature $\alpha \cdot \alpha$ $\xi \cdot \xi$
		distortion $\alpha \cdot \xi$ $\xi \cdot \xi$

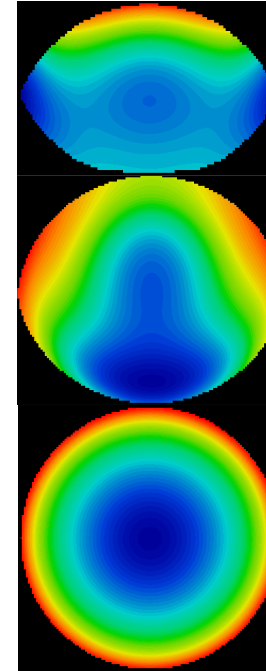
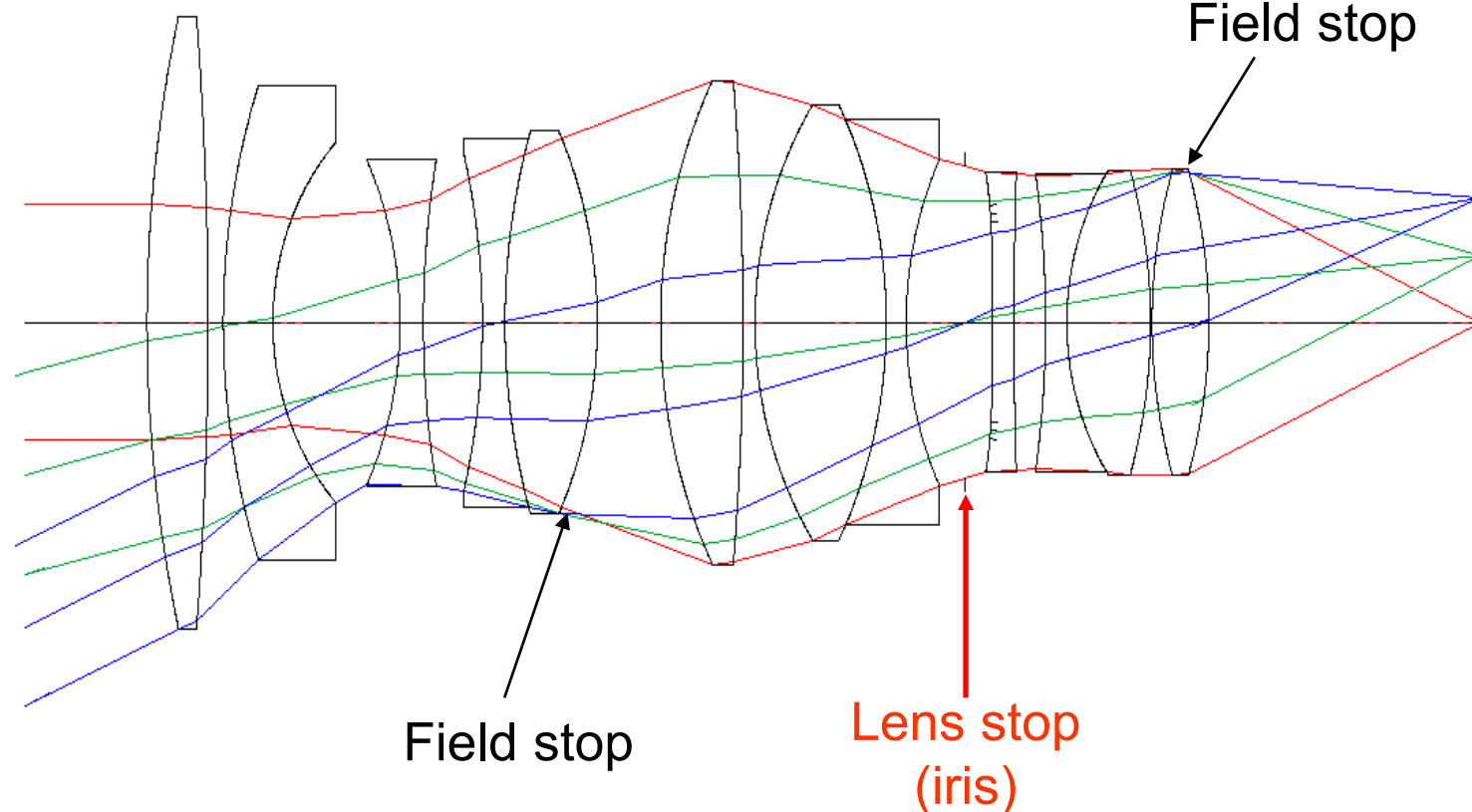
Classification of aberrations



ideal

3rd order monochromatic:		
 spherical aberration α^4	 coma $\xi \cdot \alpha$ $\alpha \cdot \alpha$	 astigmatism $\xi \cdot \alpha$ $\xi \cdot \alpha$
 field curvature $\alpha \cdot \alpha$ $\xi \cdot \xi$	 distortion $\alpha \cdot \xi$ $\xi \cdot \xi$	

Lens pupil (shape and wavefront aberration)



Real objects are complicated. The lens as well (pupil shape, aberrations,...)
How can the image be calculated?

Characterizing wavefront deformation by a set of orthogonal functions: Zernike Polynomials $Z_{n,m}(r, \varphi)$

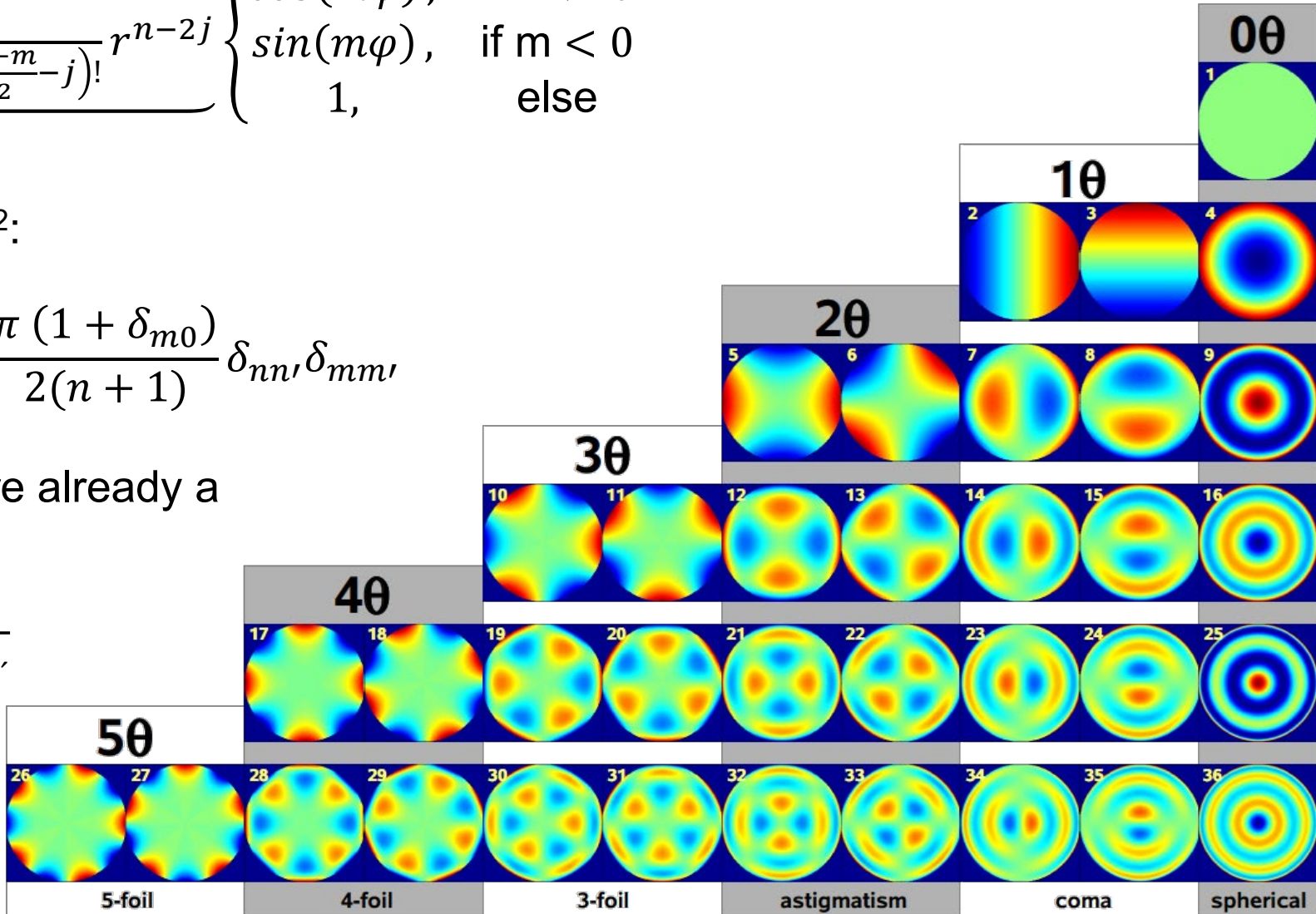
$$Z_{n,m}(r, \varphi) = \sum_{j=0}^{\frac{n-m}{2}} \underbrace{(-1)^j \frac{(n-j)!}{j! \left(\frac{n+m}{2}-j\right)! \left(\frac{n-m}{2}-j\right)!} r^{n-2j}}_{R_n^m(r)} \begin{cases} \cos(m\varphi), & \text{if } m > 0 \\ \sin(m\varphi), & \text{if } m < 0 \\ 1, & \text{else} \end{cases}$$

Orthogonal system with respect to L^2 :

$$\int_0^1 \int_0^{2\pi} Z_n^m(r, \varphi) Z_{n'}^{m'*}(r, \varphi) d\varphi r dr = \frac{\pi (1 + \delta_{m0})}{2(n+1)} \delta_{nn'} \delta_{mm'}$$

For fixed m the radial polynomials are already a complete orthogonal system:

$$\int_0^1 R_n^m(r) R_{n'}^m(r) r dr = \frac{1}{2(n+1)\delta_{n,n'}}$$



Frits Zernike introduced in 1934 his famous phase contrast microscopy method (honored with Nobel prize).

Zernike, F. (1934). *Beugungstheorie des Schneidenverfahrens und seiner verbesserten Form, der Phasenkontrastmethode*, Physica I, S. 689-704.

Zernike approximated the surface deviations of a circular mirror surface, the treated phase object, from perfect shape with an orthogonal functional system of polynomials, which are now named after him. He describes this orthogonal system, which is defined as eigenfunctions of a self-adjoint, rotationally symmetrical differential operator, as a generalization of the (one-dimensional) Legendre polynomials. Zernike's student Nijboer later (1942) used this orthogonal system for a diffraction-optical theory of aberrations. The representation of wave aberration according to Zernike polynomials has been standard in optics for some time. In optics textbooks, new "derivations" of these polynomials are given "from the requirement of orthogonality and invariance alone" (Born / Wolf (1999)).

Physica I, pp. 689-704 (1934), translated by Anthony Yen *

The translator wishes to thank Frits Zernike (Junior) for encouraging and editing the translation, and Shinn-Sheng Yu for typesetting the text using LATEX and reproducing the graphs using *Mathematica*

DIFFRACTION THEORY OF THE KNIFE-EDGE TEST AND ITS IMPROVED FORM, THE PHASE-CONTRAST METHOD

by F. ZERNIKE

Physical Laboratory of University of Groningen

Abstract

On the basis of Abbe's diffraction theory of optical imaging, the appearance of shaped small deviations is evaluated with Foucault's knife-edge procedure and The orthogonal "circle polynomials" are found and applied to the diffraction p

The well-known knife-edge procedure for the testing of concave optical systems, was given by Foucault in 1859¹.

A spherical concave mirror is set up in such a way that it is displaced somewhat laterally from its center of curvature. One the



Scalar product definition

Different vector spaces

$$\mathbb{R}^3 \text{ (linear Algebra): } \vec{a} \cdot \vec{b} = \begin{pmatrix} a_1 \\ a_2 \\ a_3 \end{pmatrix} \cdot \begin{pmatrix} b_1 \\ b_2 \\ b_3 \end{pmatrix} = a_1 b_1 + a_2 b_2 + a_3 b_3$$

L^2

(Lebesgue space with quadratic Norm;
Hilbert space of square integrable functions)

$$\langle f | g \rangle = \int_a^b f(x) g(x) dx$$

Scalar product on L^2



e.g. orthogonal:

$$\begin{pmatrix} 1 \\ 0 \\ 0 \end{pmatrix} \cdot \begin{pmatrix} 0 \\ 1 \\ 0 \end{pmatrix} = 0$$

e.g. orthogonal:
Legendre-Polynomials,
Zernike-Polynomials,
Eigen-functions of a
vibrating membrane
(Bessel-Functions);
Schmidt-Gram
orthogonalization method

given wavefront deformation
(analytical form)

functional approximation with
orthogonal functions F_j

$$W(r, \varphi) \approx W_{appr}(r, \varphi) = \sum_{j=1}^N c_j f_j(r, \varphi)$$

Formally coefficients c_j can be calculated
directly from wavefront deformation function W
with the chosen system of orthogonal functions

$$c_j = \int_{r=0}^1 \int_{\varphi=0}^{2\pi} W(r, \varphi) f_j(r, \varphi) r dr d\varphi$$

Orthogonalization method (Gram-Schmidt)

General orthogonalization method of functions by Gram-Schmidt algorithm:

Definition of inner product of two functions:

$$\langle F_1, F_2 \rangle = \frac{1}{\pi} \int F_1 \cdot F_2 r dr d\phi$$

Start: first new function Y' and normalization for Y : $Y'_1 = Z_1$

$$Y_1 = \frac{Y'_1}{\sqrt{\langle Y_1, Y_1 \rangle}}$$

Second new function: linear combination of old function and lower order new functions and normalization:

$$Y'_2 = Z_2 - \langle Z_2, Y_1 \rangle Y_1$$

$$Y_2 = \frac{Y'_2}{\sqrt{\langle Y_2, Y_2 \rangle}}$$

General step, analogous:

$$Y'_n = Z_n - \sum_{m=1}^{n-1} \langle Z_n, Y_m \rangle Y_m$$

$$Y_n = \frac{Y'_n}{\sqrt{\langle Y_n, Y_n \rangle}}$$

Zernike polynomials as eigenfunctions of a the self-adjoint Zernike differential operator

The Zernike differential operator is

$$Z_2 = (1 - r^2) \frac{\partial^2}{\partial r^2} - \left(\frac{1}{r} - 3r \right) \frac{\partial}{\partial r} + \frac{1}{r^2} \frac{\partial^2}{\partial \varphi^2}$$

It is self-adjoint on the unit circle $0 \leq |r| \leq 1$:

$$Z_n^m(r, \varphi) = R_n^m(r) \cdot \begin{cases} \sin(m\varphi) & \text{für } m > 0 \\ \cos(m\varphi) & \text{für } m < 0 \\ 1 & \text{für } m = 0 \end{cases}$$

Eigenfunctions of self-adjoint Zernike-Differential-Operator are the Zernike Polynomials: an orthogonal set of equations

(paper by Zernike / Brinckmann)

$$\int_0^1 \int_0^{2\pi} Z_n^m(r, \phi) Z_{n'}^{m'*}(r, \phi) d\phi r dr = \frac{\pi (1 + \delta_{m0})}{2(n+1)} \delta_{nn'} \delta_{mm'}$$

Zernike Polynomials, first 16 functions

n	m	$N_{n,m}$	Polar	cartesian	Fringe-#
0	0	$1/\pi$	1	1	Z1
1	-1	$4/\pi$	$r \cos \varphi$	y	Z2
1	1	$4/\pi$	$r \sin \varphi$	x	Z3
2	0	$3/\pi$	$2r^2 - 1$	$2x^2 + 2y^2 - 1$	Z4
2	-2	$6/\pi$	$r^2 \cos 2\varphi$	$y^2 - x^2$	Z5
2	2	$6/\pi$	$r^2 \sin 2\varphi$	$2xy$	Z6
3	-1	$8/\pi$	$(3r^3 - 2r) \cos \varphi$	$3y^3 - 2y + 3x^2y$	Z7
3	1	$8/\pi$	$(3r^3 - 2r) \sin \varphi$	$3x^3 - 2x + 3xy^2$	Z8
4	0	$5/\pi$	$6r^4 - 6r^2 + 1$	$6x^4 + 6y^4 + 12x^2y^2 - 6x^2 - 6y^2 + 1$	Z9
3	-3	$8/\pi$	$r^3 \cos 3\varphi$	$y^3 - 3x^2y$	Z10
3	3	$8/\pi$	$r^3 \sin 3\varphi$	$3xy^2 - x^3$	Z11
4	-2	$10/\pi$	$(4r^4 - 3r^2) \cos 2\varphi$	$4y^4 - 4x^4 + 3x^2 - 3y^2 - 4x^2y^2$	Z12
4	2	$10/\pi$	$(4r^4 - 3r^2) \sin 2\varphi$	$8xy^3 + 8x^3y - 6xy$	Z13
5	-1	$12/\pi$	$(10r^5 - 12r^3 + 3r) \cos \varphi$		Z14
5	1	$12/\pi$	$(10r^5 - 12r^3 + 3r) \sin \varphi$		Z15
6	0	$7/\pi$	$20r^6 - 30r^4 + 12r^2 - 1$		Z16

Zernike polynomials and Seidel 3rd order aberrations

„Zernike name“

	Fringe-#	n	m	normalization*	waviness	1	ρ	ρ^2	ρ^3	ρ^4
tilt	2	1	1	1,27	1		1			
defocus	4	2	0	0,95	0	-1		2		
astigmatism	5	2	2	1,91	2			1		
coma	7	3	1	2,55	1		-2		3	
spher. abb.	9	4	0	1,59	0	1		-6		6
total	10	0	0	0,55	0					

„Seidel name“



- magnification (error), distortion
- defocus, field curvature
- astigmatism
- coma
- spherical aberration

Seidel aberrations are a function of 3 variables (ρ, φ, ξ):

(ρ, φ) for pupil and ξ for object height

Zernike polynomials are a function of 2 variables: (ρ, φ) for pupil

For a certain object height $\xi = \xi_0$ one representation can be transformed to the other,

$$Z(\rho, \varphi, \xi_0) \leftrightarrow S(\rho, \varphi, \xi_0)$$

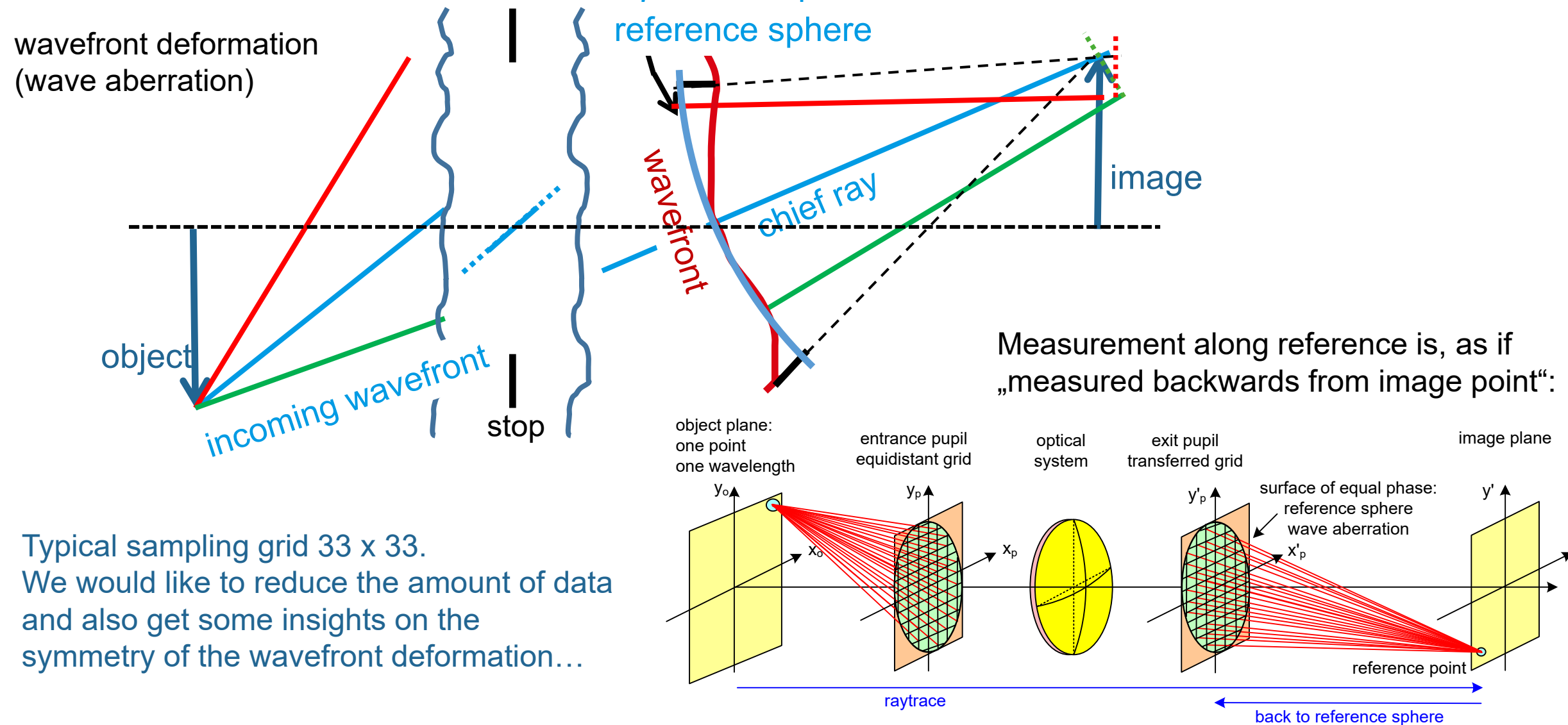
$$W(\vec{\alpha} \cdot \vec{\alpha}, \vec{\alpha} \cdot \vec{\xi}, \vec{\xi} \cdot \vec{\xi}) = W(r^2, r\rho \cos \varphi, \rho^2)$$

Because of $\cos^2 \varphi = \frac{1}{2}(1 + \cos 2\varphi)$ any higher order monomials $\cos^m \varphi$ can be expressed by $\cos m\varphi$

Technically besides transforming the polynomials / monomials, also the convention for the azimuthal part is different („ $\cos^2 \varphi$ “ and „ $\cos(2\varphi)$ “) and needs to be done properly.

This transformation can be done without problems, there is a one-to-one relationship (since we have polynomials in both cases). Sometimes confusions arise when aberrations are labeled same (e.g. „coma“) but field dependence is ignored or the transformation is not done properly.

Computation of wavefront deformation

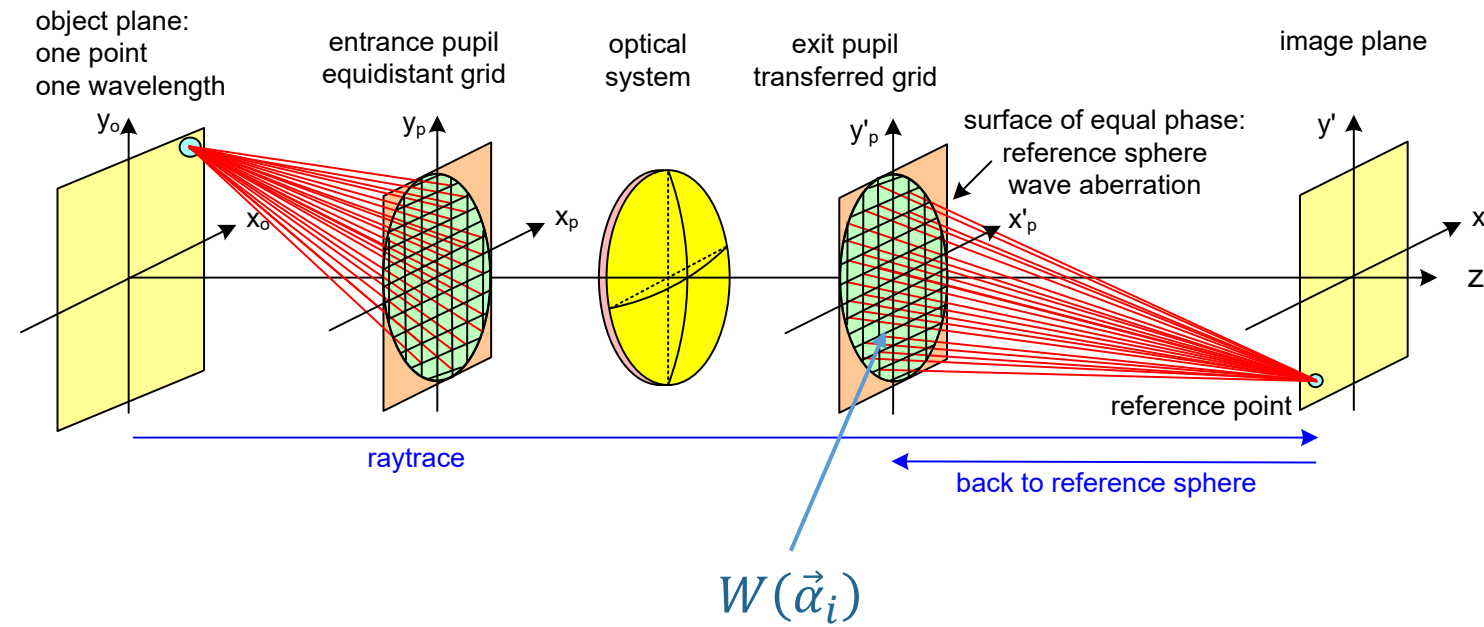


Numerical computation of the Zernike coefficients

A function $W(\vec{\alpha})$ shall be expressed by a set of orthonormal functions $Z_i(\vec{\alpha})$ as

$$W(\vec{\alpha}) = \sum_j c_j Z_j(\vec{\alpha}), \quad \text{with} \quad c_j = \langle W(\vec{\alpha}) | Z_j(\vec{\alpha}) \rangle = \iint W(\vec{\alpha}) Z_j(\vec{\alpha}) d\vec{\alpha}.$$

According to the ray tracing data the aberration $W(\vec{\alpha})$ is determined on a grid of sampling points $\vec{\alpha}_i$. From the n values of $W(\vec{\alpha}_i)$ at the positions $\vec{\alpha}_i$ the wave front deformation $W(\vec{\alpha})$ is expressed by k Zernike Polynomials $Z_j(\vec{\alpha})$ in the form $W(\vec{\alpha}) = \sum_{j=1}^k c_j Z_j(\vec{\alpha})$ by determining the coefficients c_j solving a system of linear equations.



Numerical computation of the Zernike coefficients

A function $W(\vec{\alpha})$ shall be expressed by a set of orthonormal functions $Z_i(\vec{\alpha})$ as

$$W(\vec{\alpha}) = \sum_j c_j Z_j(\vec{\alpha}), \quad \text{with} \quad c_j = \langle W(\vec{\alpha}) | Z_j(\vec{\alpha}) \rangle = \iint W(\vec{\alpha}) Z_j(\vec{\alpha}) d\vec{\alpha}.$$

According to the ray tracing data the aberration $W(\vec{\alpha})$ is determined on a grid of sampling points $\vec{\alpha}_i$. From the n values of $W(\vec{\alpha}_i)$ at the positions $\vec{\alpha}_i$ the wave front deformation $W(\vec{\alpha})$ is expressed by k Zernike Polynomials $Z_j(\vec{\alpha})$ in the form

$W(\vec{\alpha}) = \sum_{j=1}^k c_j Z_j(\vec{\alpha})$ by determining the coefficients c_j solving a system of linear equations:

$$\begin{pmatrix} Z_1(\vec{\alpha}_1) & Z_2(\vec{\alpha}_1) & \cdot & \cdot & Z_k(\vec{\alpha}_1) \\ Z_1(\vec{\alpha}_2) & Z_2(\vec{\alpha}_2) & \cdot & \cdot & Z_k(\vec{\alpha}_2) \\ \cdot & \cdot & \cdot & \cdot & \cdot \\ \cdot & \cdot & \cdot & \cdot & \cdot \\ Z_1(\vec{\alpha}_n) & Z_2(\vec{\alpha}_n) & \cdot & \cdot & Z_k(\vec{\alpha}_n) \end{pmatrix} \begin{pmatrix} c_1 \\ c_2 \\ \cdot \\ \cdot \\ c_k \end{pmatrix} = \begin{pmatrix} W(\vec{\alpha}_1) \\ W(\vec{\alpha}_2) \\ \cdot \\ \cdot \\ W(\vec{\alpha}_n) \end{pmatrix}$$

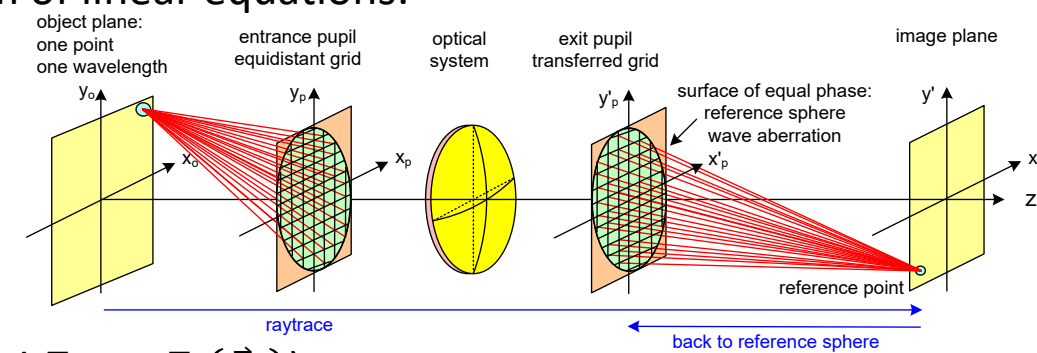
or written in component form with summation rule (with $W_j = W(\vec{\alpha}_j)$ and $Z_{ij} = Z_j(\vec{\alpha}_i)$)

$$W_i = Z_{ij} c_j \quad \text{respectively in matrix-/vector-form:} \quad \vec{W} = Z \vec{c}$$

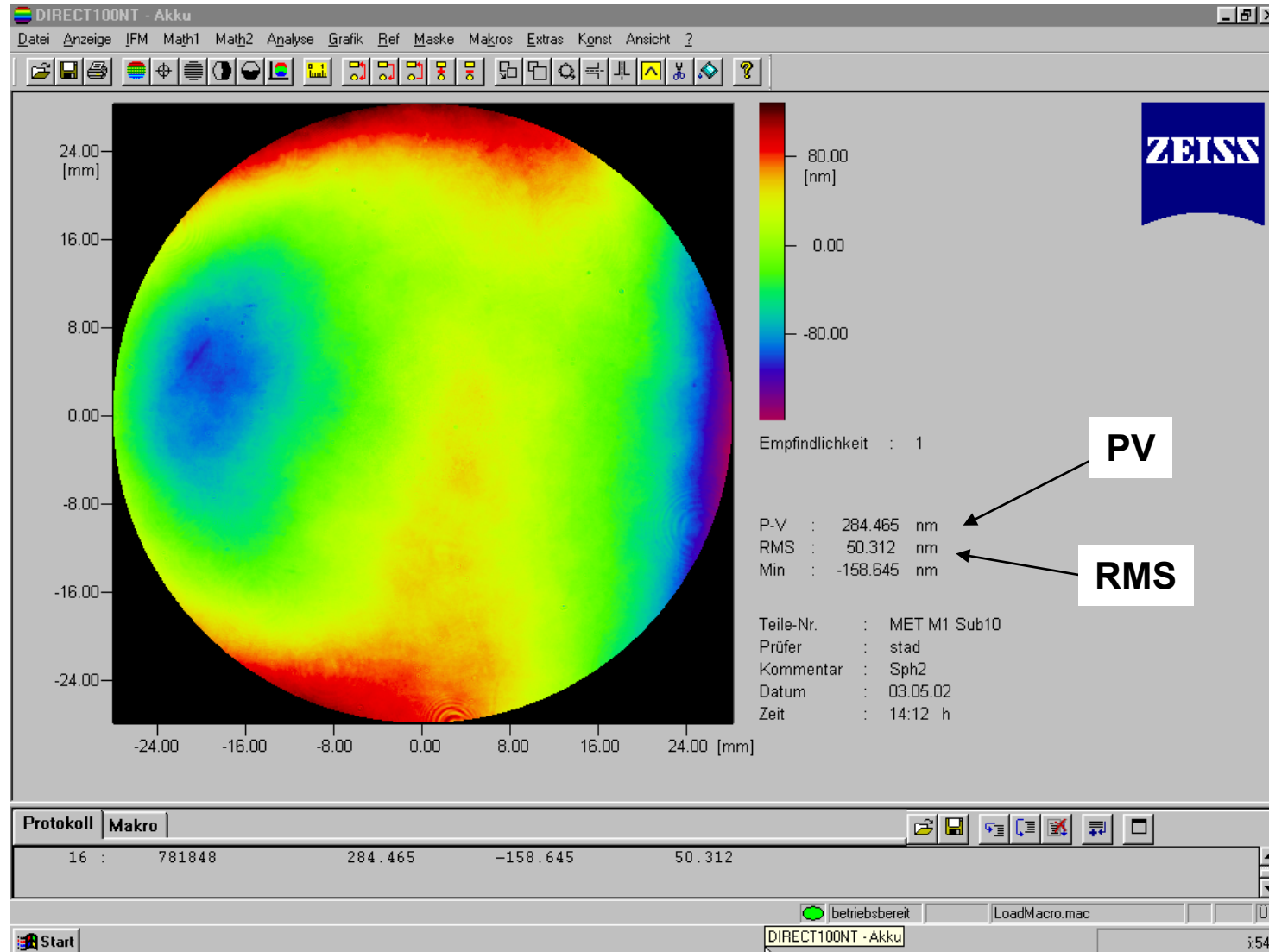
The system of equations is solved with the pseudo inverse Z^* applied, $Z^* \vec{W} = Z^* Z \vec{c}$, yielding the coefficient vector

$$\vec{c} = (Z^* Z)^{-1} Z^* \vec{W}$$

Different solution methods, e.g. singular value decomposition, cf. Press, Teutolsky, Vetterling, Flannery (1992), p. 59 ff.).
 For a sampling grid of 33 x 33 points and 36 Zernike polynomials the matrix has (36,999) lines and columns.



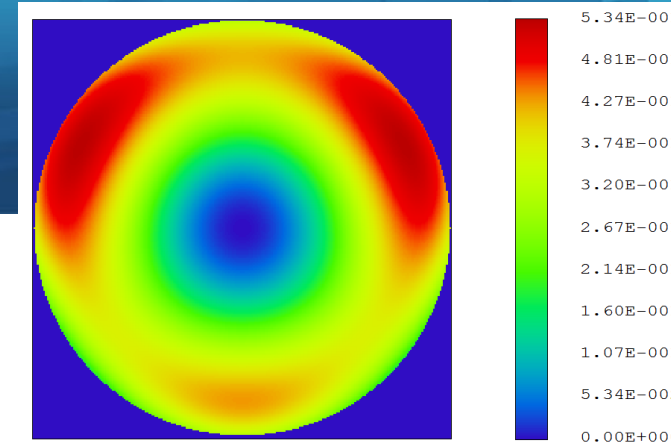
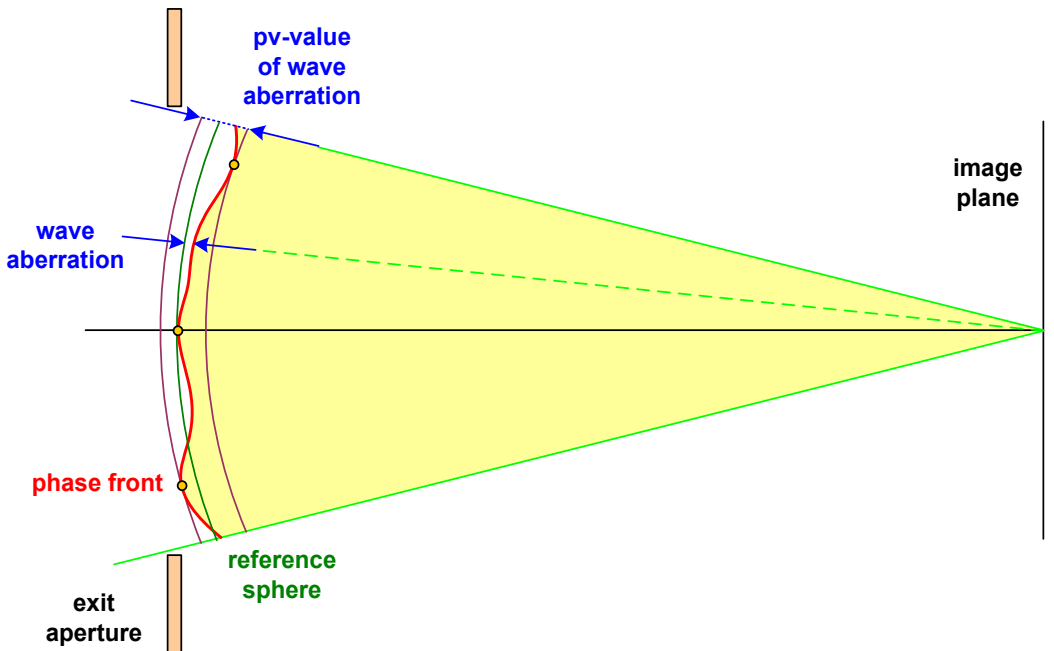
Wavefront Analysis (measurement data)



Wave Aberration and quality criteria

- Quality assessment:

- peak valley value (PV)
- rms value, area average
- Zernike decomposition for detailed analysis



- Mean quadratic wave deviation (W_{Rms} , root mean square)

$$W_{rms} = \sqrt{\langle W^2 \rangle - \langle W \rangle^2} = \sqrt{\frac{1}{A_{Exp}} \int [W(x_p, y_p) - W_{mean}(x_p, y_p)]^2 dx_p dy_p}$$

with pupil area $A_{Exp} = \int dx dy$

- Peak valley value W_{pv} : largest difference

$$W_{pv} = \max \left[W(x_p, y_p) | (x_p, y_p)_{\min \max} \right]$$

- General case with apodization:

$$W_{rms} = \sqrt{\frac{1}{A_{Exp}^{(w)}} \int I_{Exp}(x_p, y_p) \cdot [W(x_p, y_p) - W_{mean}^{(w)}(x_p, y_p)]^2 dx_p dy_p}$$

weighting of local phase deviations with intensity

Calculation of mean values standard deviations of wavefront deformation data

Mean value

Integral notation

$$\langle W \rangle = \frac{1}{A} \int W \, dA$$

2nd moment

$$\langle W^2 \rangle = \frac{1}{A} \int |W|^2 \, dA$$

Marechal approximation
of Strehl ratio

$$D = \frac{1}{A} \int (W - \langle W \rangle)^2 \, dA$$

Discrete computation with $\langle W \rangle = \frac{1}{A} \int W \, dA = \sum_{j=1}^N p_j W(\alpha_j) \mu(dA)$ and $\sum_{j=1}^N p_j = 1$, with $p_j \geq 0$

$$\langle W \rangle = \sum_{j=1}^N p_j W(\alpha_j)$$

$$\langle W^2 \rangle = \sum_{j=1}^N p_j |W(\alpha_j)|^2$$

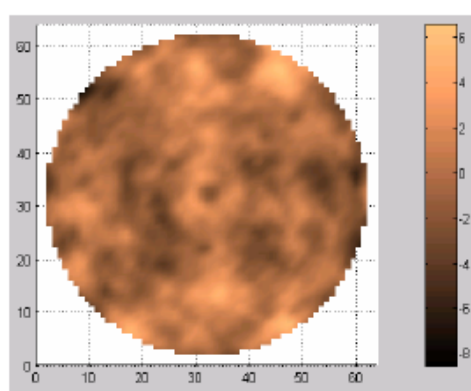
std dev

$$\Delta W = \sqrt{\frac{1}{N-1} \sum_{j=1}^N (W(\alpha_j) - \langle W \rangle)^2}$$
$$= \sqrt{\frac{1}{N-1} \sum_{j=1}^N (W(\alpha_j)^2 - N\langle W \rangle^2)}$$

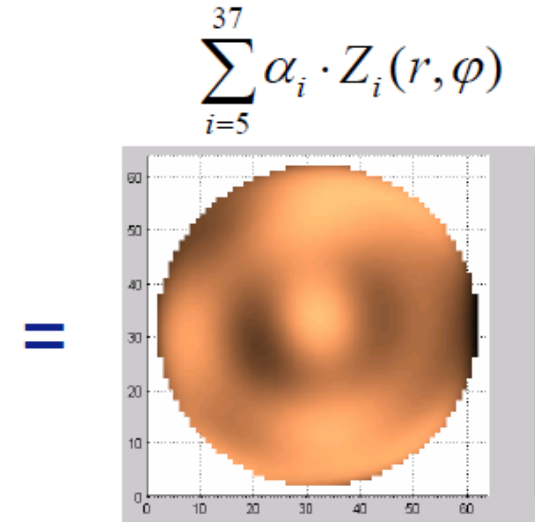
RMS (root mean square) deviation of wavefront expressed by Zernike approximation and residual high orders summarized in “residual rms”

$$RMS_{\text{Wavefront}}^2 = RMS_{\text{Zernike}}^2 + RMS_{\text{residual}}^2$$

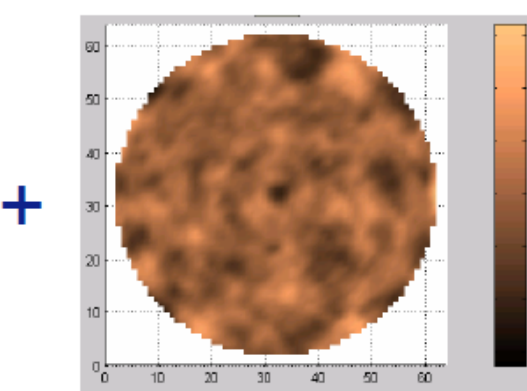
Measured wavefront



Zernike synthesis



Residual wavefront

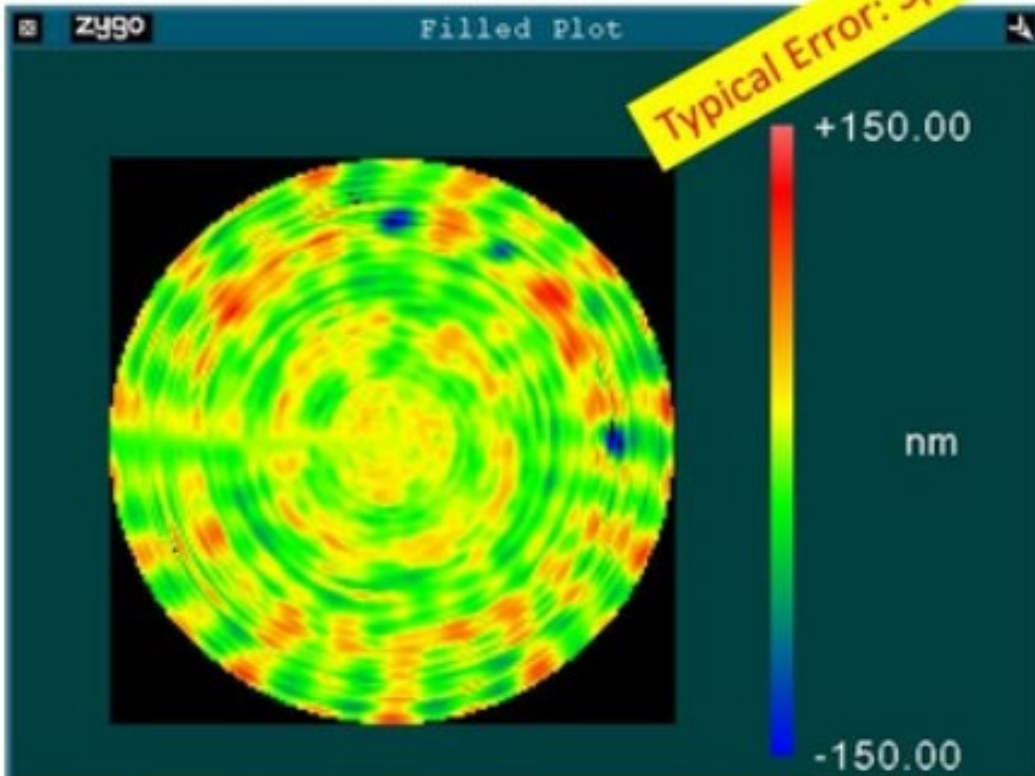


$$\sqrt{1.19^2 + 1.45^2} = 1.87$$

Effect of different optics manufacturing technology on mid spatial frequency residuals

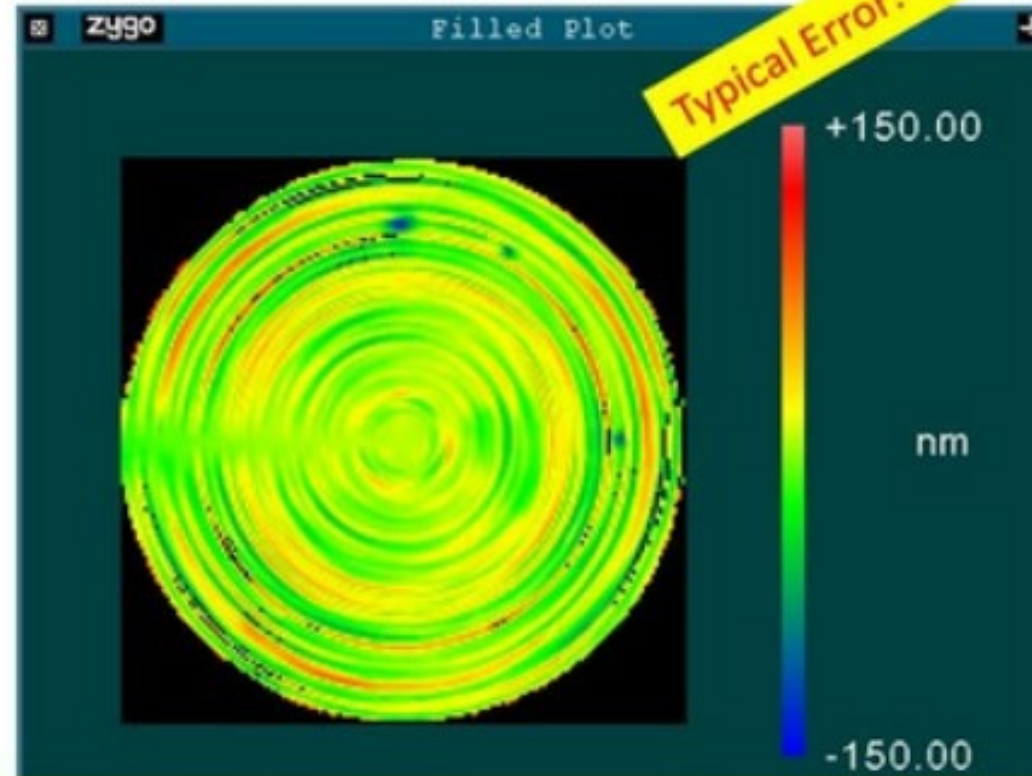
Glass Optic grinded and polished

PV = 313 nm RMS = 27 nm



Metall Optic – diamond turned

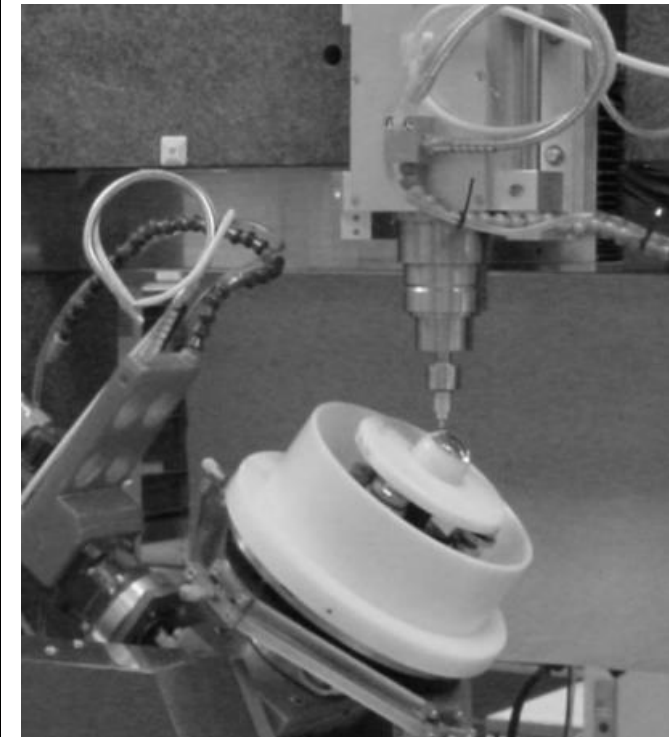
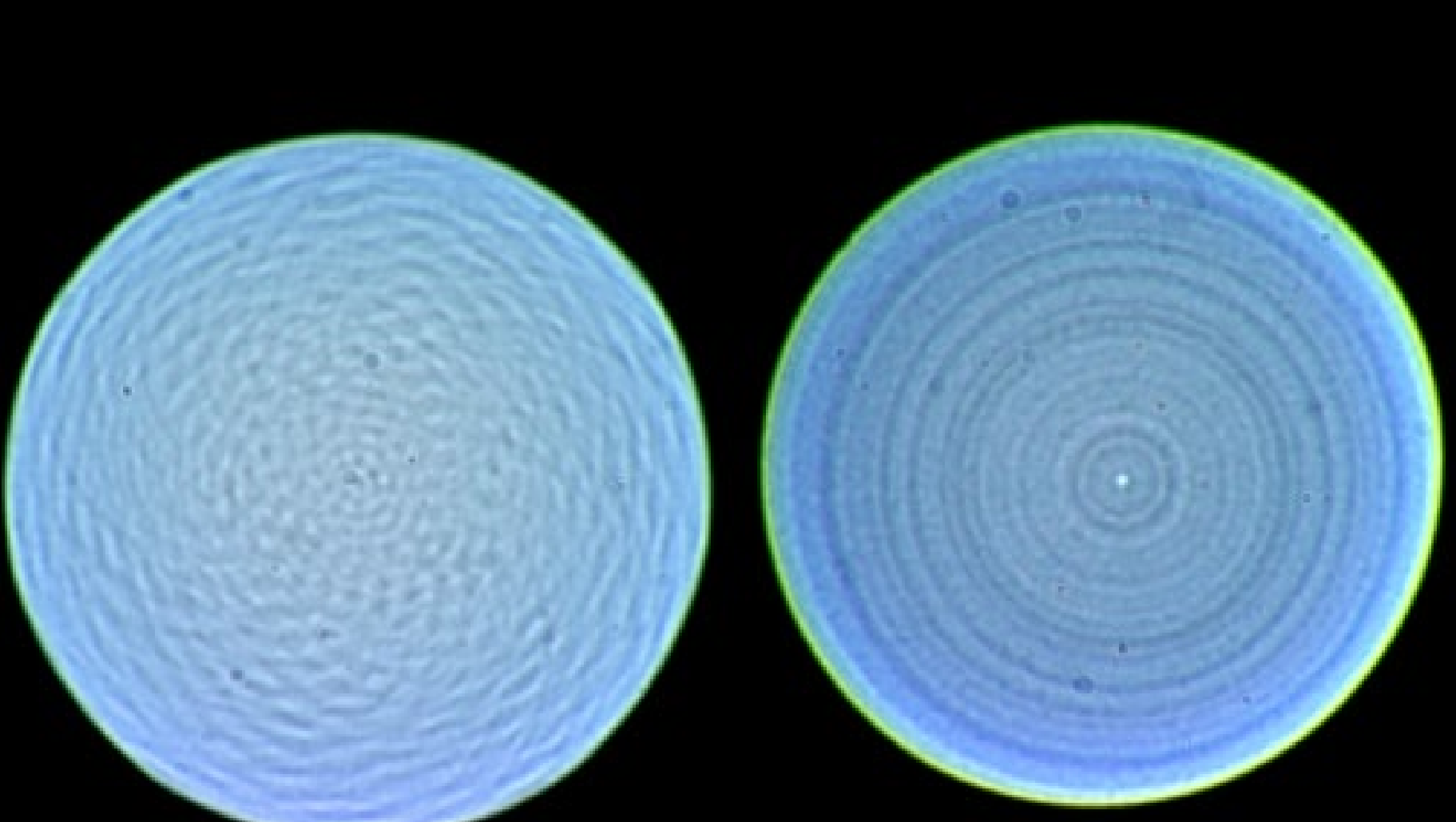
PV = 234 nm RMS = 26 nm



[151x151] matrix (0,2 mm per pixel) = 30x30 mm; Piston, Tilt and Power subtracted

Fine structures in Out-of-Focus Highlights (defocus PSF)

Optical manufacturing polishing residuals



Small polishing tools
(required for
aspherical surfaces)

$$\text{PSF}(\vec{x}, \vec{\xi}, z) = \left| \iint d\alpha L_0(\vec{\xi}, \vec{\alpha}) \exp\left(i \frac{2\pi}{\lambda} W(\vec{\xi}, \vec{\alpha})\right) \exp\left(-i \frac{\pi}{\lambda} z NA^2 \vec{\alpha} \cdot \vec{\alpha}\right) \exp\left(-i 2\pi w \vec{\alpha} \cdot (\vec{x} - m\vec{\xi})\right) \right|^2$$

Strehl ratio

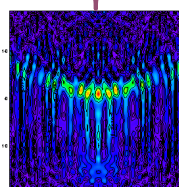
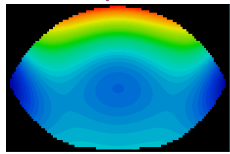
ics

ität Jena

Karl Strehl,
1864-1940

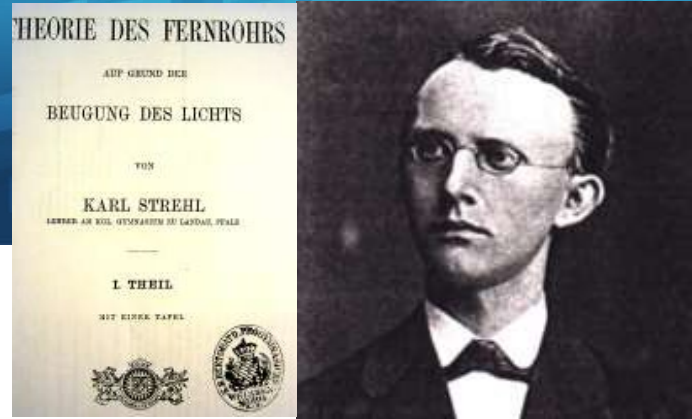
The PSF („point spread function“) is related to wave aberration W and pupil shape L_0 as follows:

$$PSF(x, \xi) = \left| \iint_{\text{lens pupil}} d\alpha L(\xi, \alpha) \exp\left(-i2\pi \frac{NA'}{\lambda} \alpha \cdot (x - m\xi)\right) \right|^2$$

monochromatic PSF lens pupil function magnification m
 

$$L(\xi, \alpha) = L_0(\xi, \alpha) \exp(i2\pi W(\xi, \alpha))$$

lens pupil shape & wavefront deviation
 transmission distribution (units of λ)



coordinates (all $\in \mathbb{R}^2$):

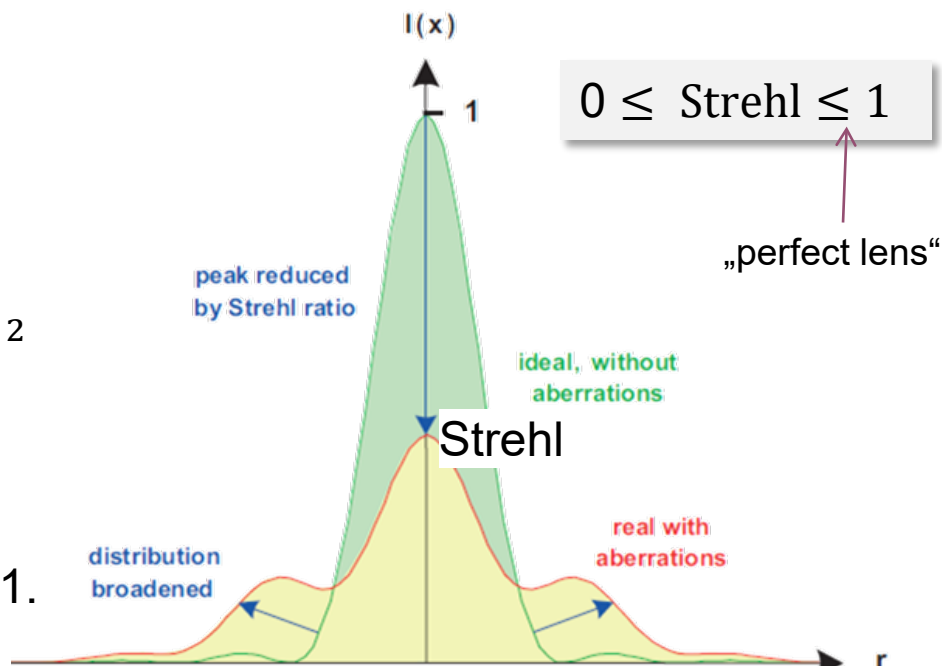
- ξ object
- x image
- α pupil (angular direction)*

*normalized, such that $0 \leq |\alpha| \leq 1$

The Strehl ratio is defined as the normalized value of PSF(0) at the center of this distribution at $x = m\xi$:

$$\text{Strehl} = \frac{1}{F} \left| \iint_{\text{lens pupil}} d\alpha L_0(\alpha) \exp(i2\pi W(\alpha)) \right|^2$$

with the normalization $F = \left| \iint_{\text{lens pupil}} d\alpha L_0(\alpha) \right|^2$, such that $0 \leq \text{Strehl} \leq 1$.



Strehl definition: Marechal approximation for not too large aberrations

For weak aberrations $\ll \lambda$ the Strehl ratio can be approximated by an expansion up to the second order of the exponential function $\exp(x)=1+x+x^2/2+\dots$ which yields

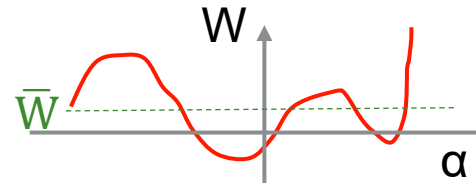
$$\text{Strehl} = 1 - 4\pi^2 \left(\frac{\overline{L_0(L_0 W^2)} - (\overline{L_0 W})^2}{(\overline{L_0})^2} \right)$$

The „averaging bar“ denotes the integral of the corresponding function over the pupil region: $\bar{f} = \iint_{\text{lens pupil}} d\alpha f(\alpha)$

For a homogeneous amplitude distribution* $\overline{L_0}=1$

we obtain the **Marechal approximation**

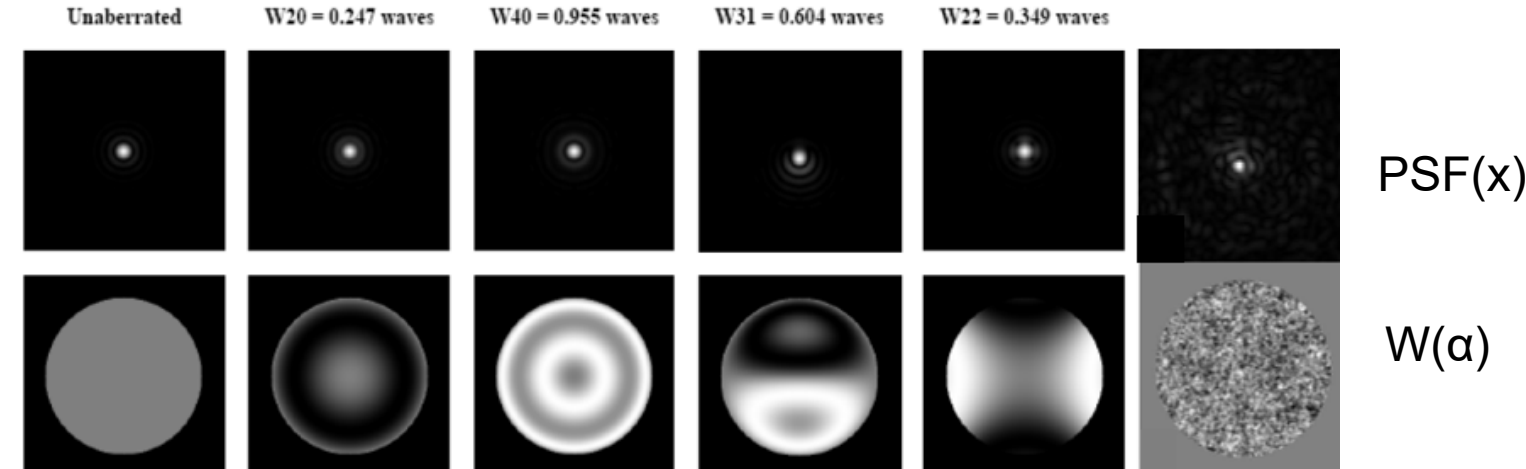
*even for a non-homogeneous amplitude distribution the Marechal approximation is applicable for most relevant applications



According to this approximation the Strehl ratio depends only on the root-mean-square of the wavefront deformation and not on the aberration type. It even applies to high-frequent statistical wavefront deformations.

Example: For all W : Strehl = 0.8

$$\begin{aligned}\text{Strehl} &= 1 - 4\pi^2 \left((\overline{W^2}) - (\bar{W})^2 \right) \\ &= 1 - (2\pi W_{rms})^2\end{aligned}$$



Approximations for the Strehl Ratio

Bi-quadratic approximation

$$D_{s,bq} \approx \left[1 - 2\pi^2 \cdot \left(\frac{W_{rms}}{\lambda} \right)^2 \right]^2$$

Exponential approximation

$$D_{s,exp} \approx \exp \left(-4\pi^2 \left(\frac{W_{rms}}{\lambda} \right)^2 \right)$$

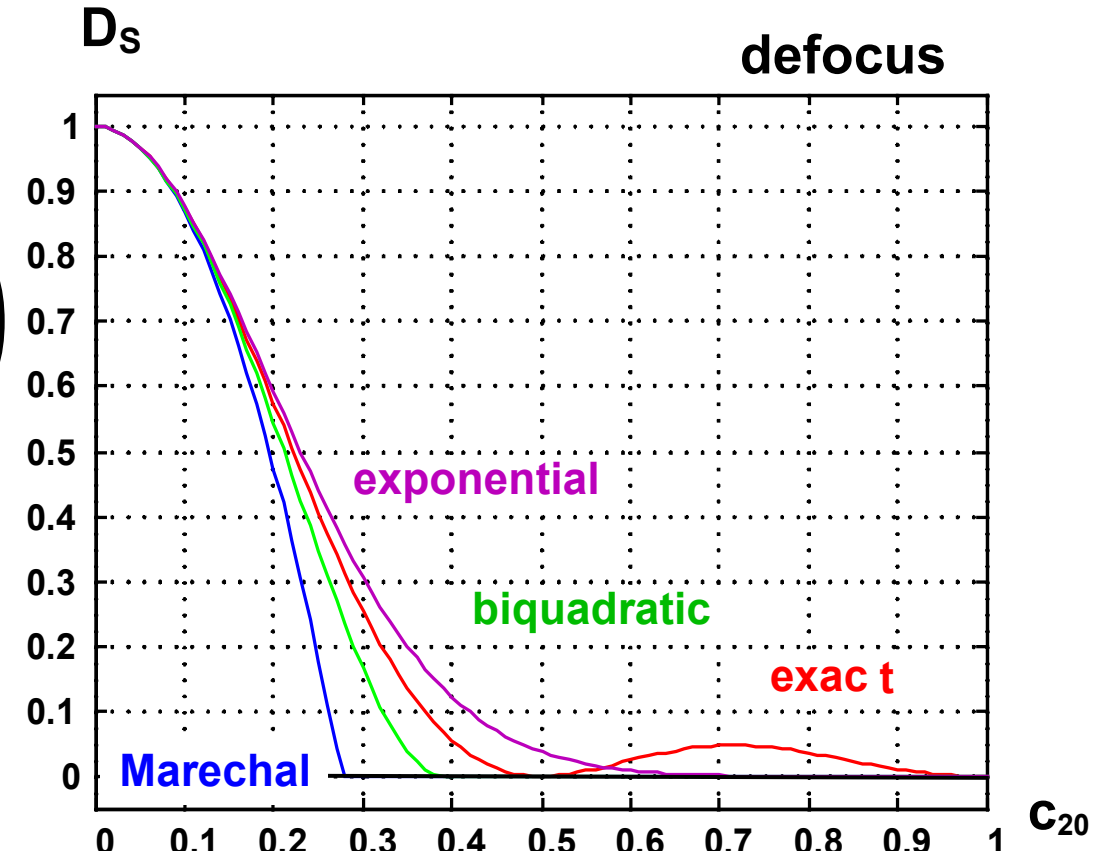
Approximation of Marechal:

(useful only for “good systems”, $D_s > 0.8$)

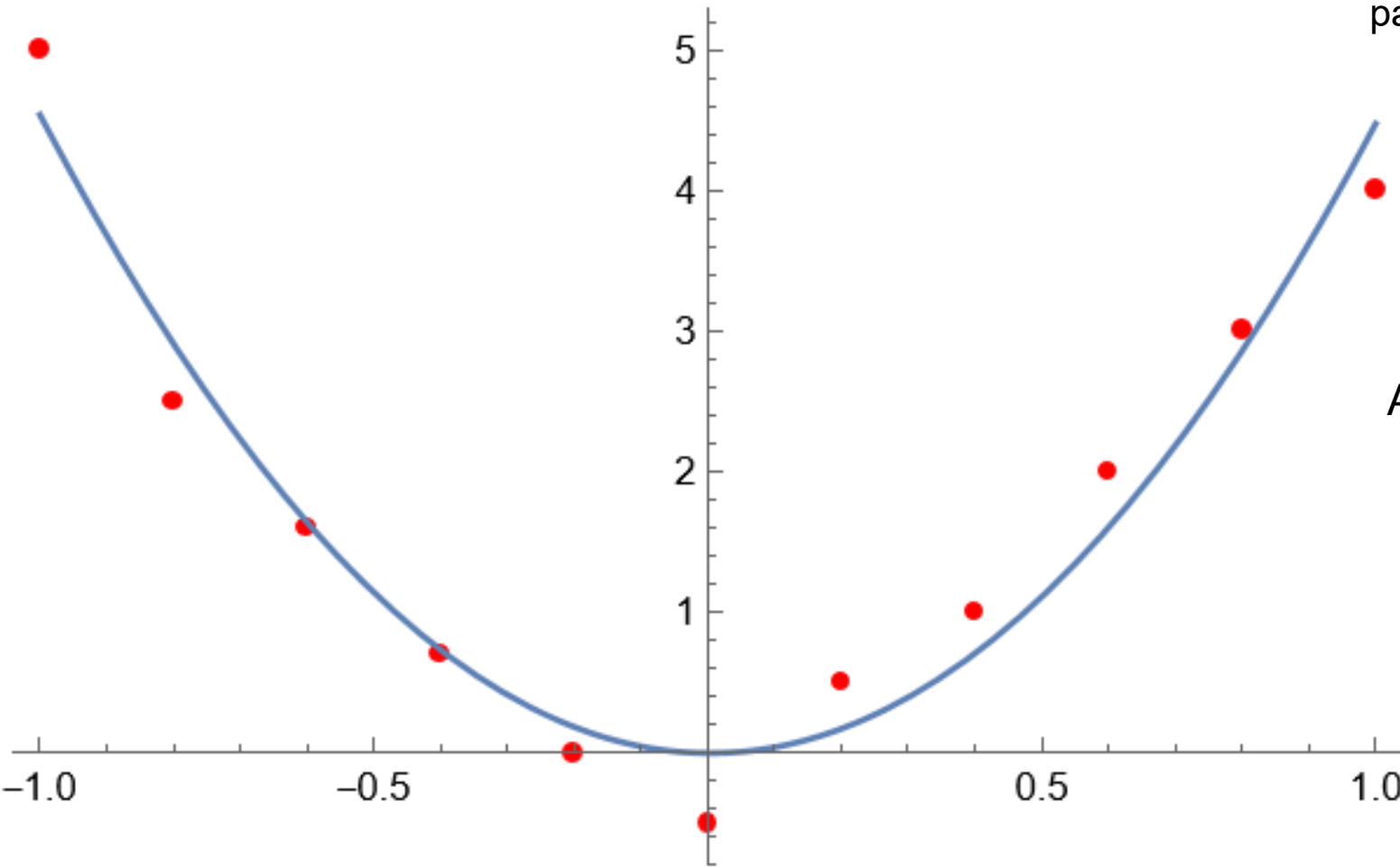
$$D_{s,M} \approx 1 - 4\pi^2 \left(\frac{W_{rms}}{\lambda} \right)^2$$

Marechal approximation expressed with Zernike coefficients

$$D_s = 1 - \left(\frac{2\pi}{\lambda} \right)^2 \cdot \left[\sum_{n=1}^N \frac{c_{n0}^2}{n+1} + \frac{1}{2} \sum_{n=1}^N \sum_{m=0}^n \frac{c_{nm}^2}{n+1} \right]$$



Fit of data points with Legendre Polynomial (Orthonormal set of functions on interval [-1,1])

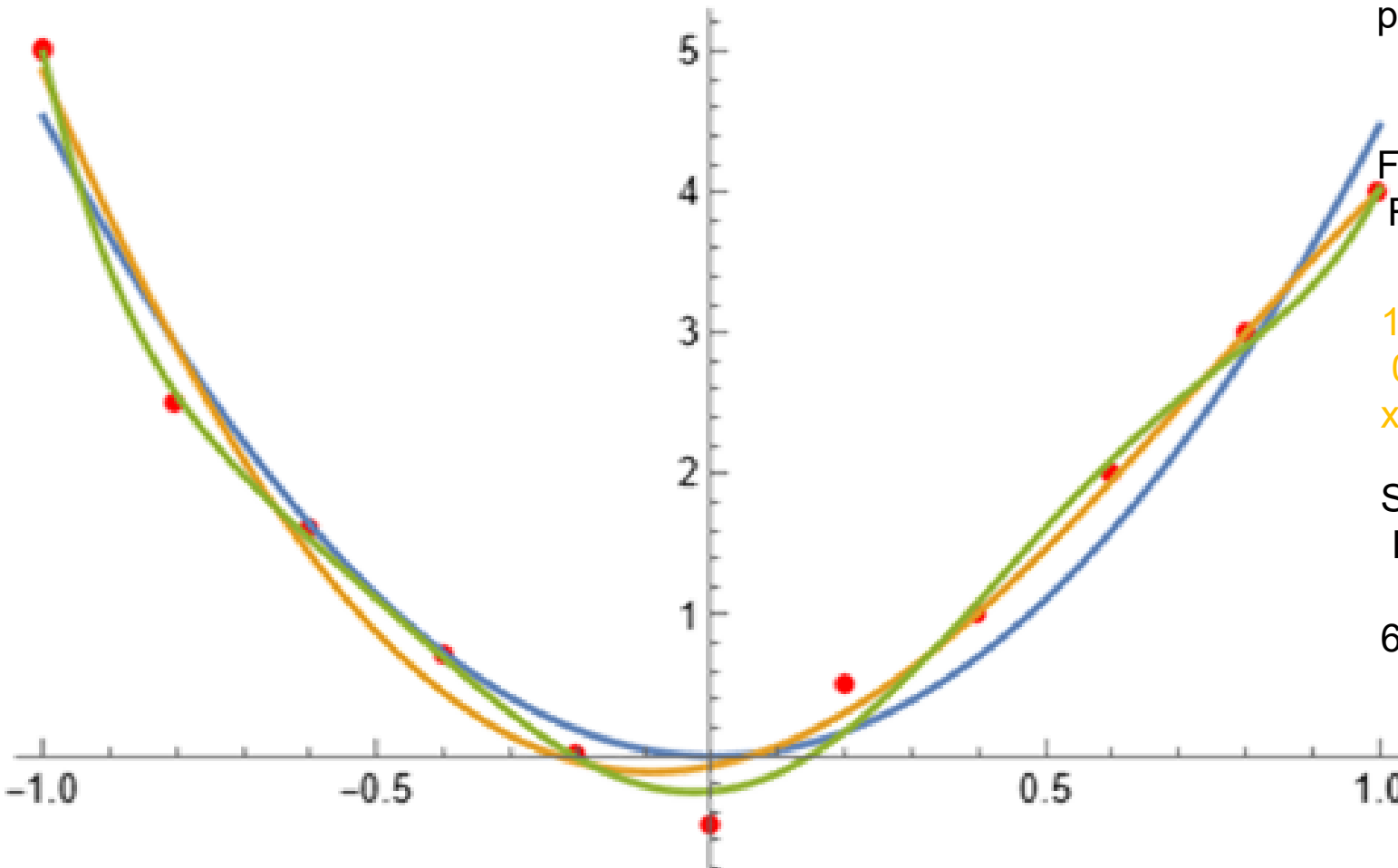


parabolicfit=Fit[data,{1,x,0.5 (3 x^2-1)},x]
1.54422 - 0.134426 x + 1.53541 (-1 + 3 x^2)

Approximation minimizes square deviation

$$\sum_{i=1}^k \left[\sum_{j=1}^n c_j f_j(\alpha_i) - W(\alpha_i) \right]^2 \rightarrow \min$$

Fit of data points with Legendre Polynomial (Orthonormal set of functions on interval [-1,1])



parabolicfit=Fit[data,{1,x,0.5 (3 x^2-1)},x]

$$1.54422 - 0.134426 x + 1.53541 (-1 + 3 x^2)$$

FourthOrderFit =

$$\text{Fit}[\text{data}, \{1, x, 0.5 (3 x^2 - 1), 1/2 (-3 x + 5 x^3), 1/8 (3 - 30 x^2 + 35 x^4)\}, x]$$

$$1.51039 + 0.119658 x + 1.53114 (-1 + 3 x^2) - 0.270493 (-3 x + 5 x^3) - 0.0171703 (3 - 30 x^2 + 35 x^4)$$

SixthOrderFit =

$$\text{Fit}[\text{data}, \{1, x, 0.5 (3 x^2 - 1), 1/2 (-3 x + 5 x^3), 1/8 (3 - 30 x^2 + 35 x^4), 1/8 (15 x - 70 x^3 + 63 x^5), 1/16 (-5 + 105 x^2 - 315 x^4 + 231 x^6)\}, x]$$

$$1.48203 + 0.161905 x + 1.46282 (-1 + 3 x^2) - 0.220636 (-3 x + 5 x^3) - 0.0440144 (3 - 30 x^2 + 35 x^4) - 0.0254375 (15 x - 70 x^3 + 63 x^5) + 0.0279626 (-5 + 105 x^2 - 315 x^4 + 231 x^6)$$

Fit of data points with Legendre Polynomial (Orthonormal set of functions on interval [-1, 1]), approximation error

x	data	LegendreFit x^2	LegendreFit x^4	LegendreFit x^6	ApprError Legendre x^2	ApprError Legendre x^4	ApprError Legendre x^6
-1	5	4,5363682	4,8566356	4,9858234	-0,4636318	-0,1433644	-0,0141766
-0,8	2,5	2,90727216	2,898596719	2,559052524	0,40727216	0,398596719	0,059052524
-0,6	1,6	1,63878332	1,422375299	1,532651467	0,03878332	-0,177624701	-0,067348533
-0,4	0,7	0,73090168	0,443822111	0,688231992	0,03090168	-0,256177889	-0,011768008
-0,2	0	0,18362724	-0,044288957	-0,016348998	0,18362724	-0,044288957	-0,016348998
0	-0,5	-0,00304	-0,0722609	-0,2526462	0,49696	0,4277391	0,2473538
0,2	0,5	0,17089996	0,306526403	0,170364682	-0,32910004	-0,193473597	-0,329635318
0,4	1	0,70544712	1,015616191	1,095924872	-0,29455288	0,015616191	0,095924872
0,6	2	1,60060148	1,955474819	2,106777787	-0,39939852	-0,044525181	0,106777787
0,8	3	2,85636304	3,003491759	2,910101644	-0,14363696	0,003491759	-0,089898356
1	4	4,4727318	4,0139790	4,0200894	0,4727318	0,0139796	0,0200894
				rms_appr:	1,123684416	0,708095051	0,455589176



Convergence of wavefront approximation by orthogonal functional systems

Approximation error (local):

$$\delta(r, \varphi) = W(r, \varphi) - W_{appr}(r, \varphi) = \sum_{j=N+1}^{\infty} c_j f_j(r, \varphi)$$

The mean quadratic error is:

$$\begin{aligned}\Delta_N &= \int_{r=0}^1 \int_{\varphi=0}^{2\pi} [\delta(r, \varphi)]^2 r dr d\varphi \\ &= \int_{r=0}^1 \int_{\varphi=0}^{2\pi} \left[W(r, \varphi) - \sum_{j=1}^N c_j f_j(r, \varphi) \right]^2 r dr d\varphi \\ &= \int_{r=0}^1 \int_{\varphi=0}^{2\pi} [W(r, \varphi)]^2 r dr d\varphi \\ &\quad - 2 \sum_{j=1}^N c_j \int_{r=0}^1 \int_{\varphi=0}^{2\pi} W(r, \varphi) f_j(r, \varphi) r dr d\varphi + \sum_{j=1}^N c_j^2 \int_{r=0}^1 \int_{\varphi=0}^{2\pi} [f_j(r, \varphi)]^2 r dr d\varphi \\ &= \int_{r=0}^1 \int_{\varphi=0}^{2\pi} [W(r, \varphi)]^2 r dr d\varphi - \underbrace{\sum_{j=1}^N c_j^2}_{\text{increases with } j}\end{aligned}$$

monotonously decreasing!

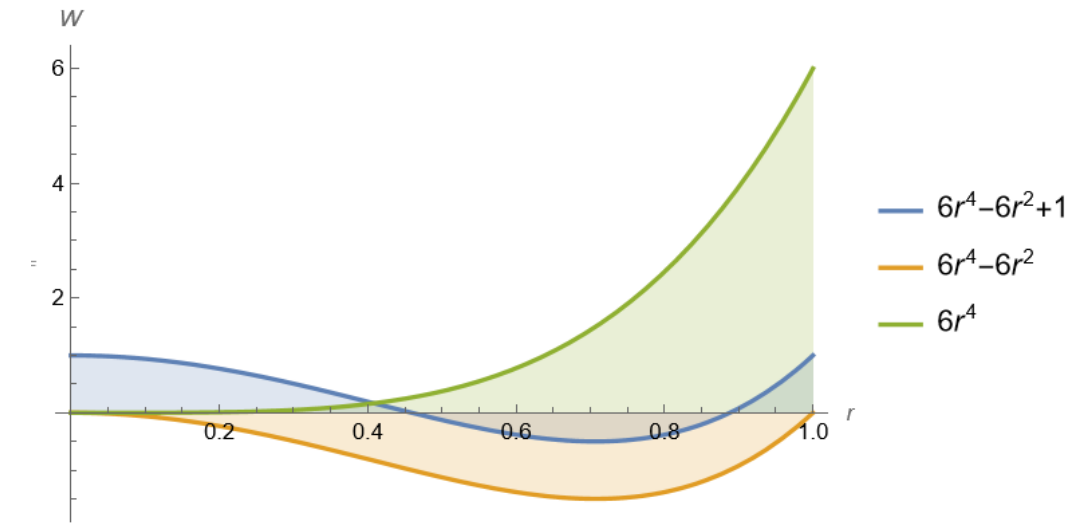
→ using more orders of the
orthogonal functions guarantees
better approximation

Balance of Lower Orders by Zernike Polynomials

Zernike functions minimize W_{rms} per order

Spherical aberration (fig. Z9):

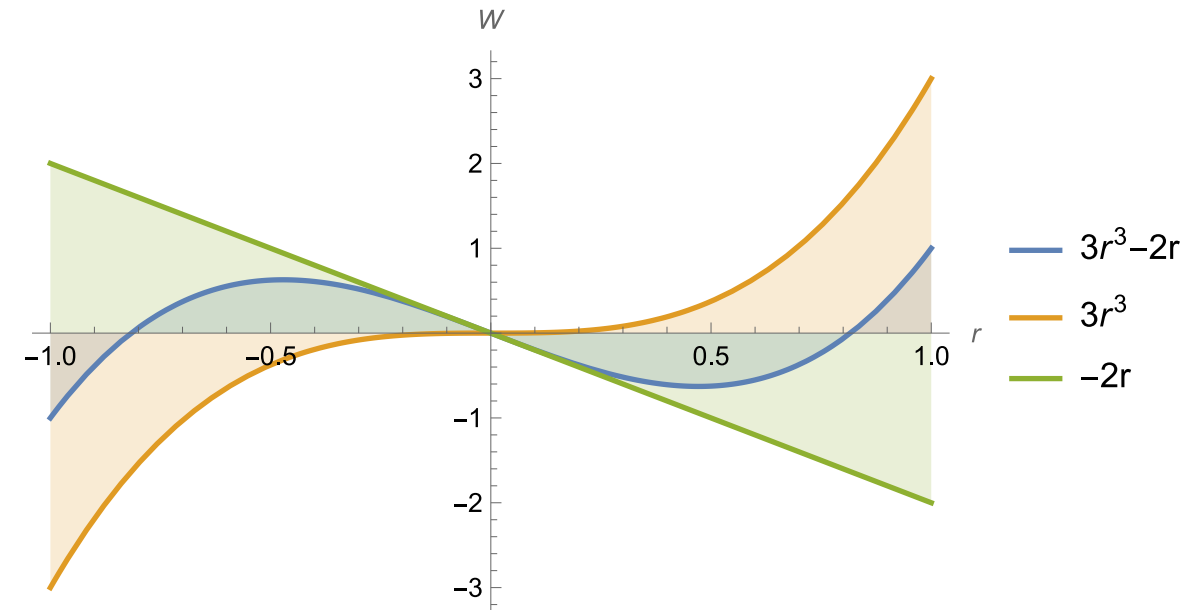
1. Spherical 4th order “Seidel” monomial
2. Additional quadratic expression:
Optimal defocusing
3. Additional absolute term
Minimum value of W_{rms}



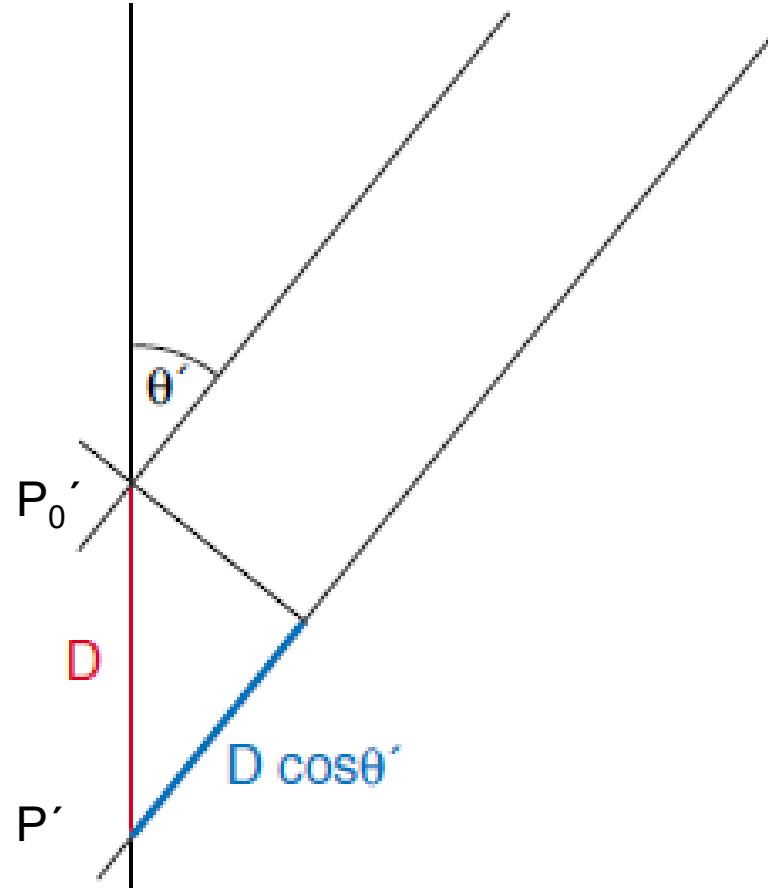
Coma (fig: Z7 along tangential direction)

Balancing by tilt contribution,

corresponds to shift between peak and centroid



Calculation of wavefront deformation for defocus



Optical path difference $OPD = D - D \cos \vartheta'$

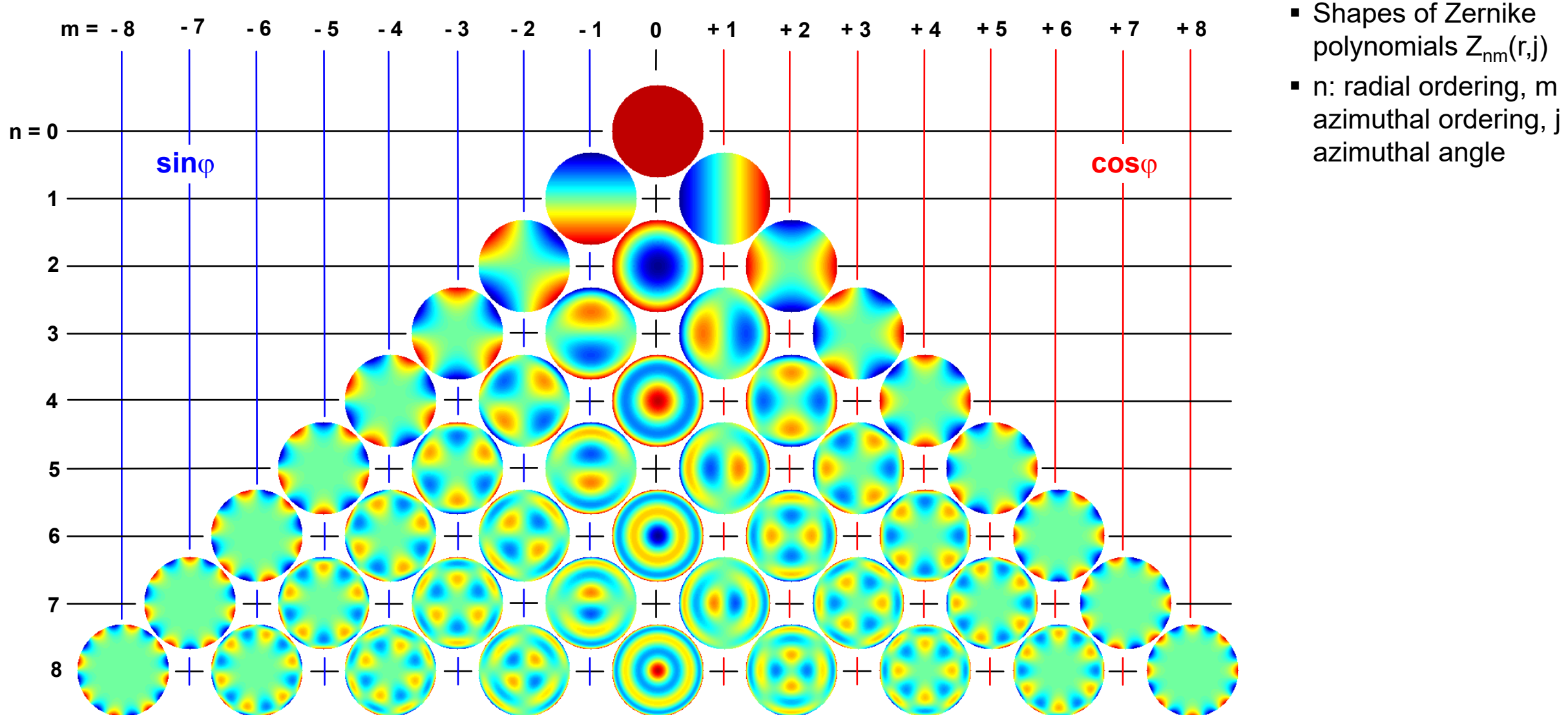
Expressed in normalized pupil coordinates
 $NA' \alpha$ pupil ($NA' = \sin \vartheta'$; $0 \leq |\alpha| \leq 1$):

$$OPD = D \left(1 - \sqrt{1 - \sin^2 \vartheta'} \right)$$
$$= D \left(1 - \sqrt{1 - NA'^2 \alpha^2} \right)$$

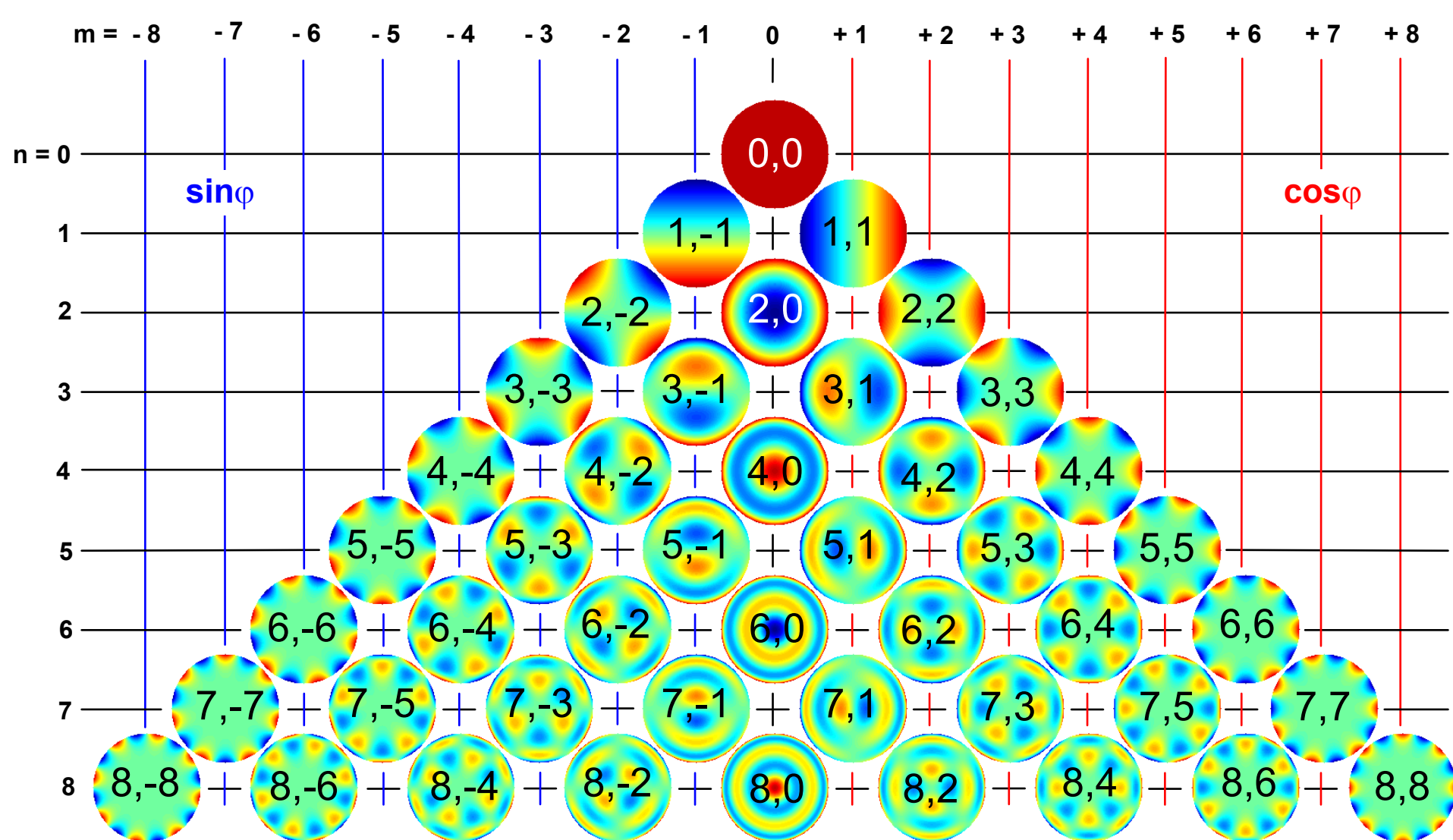
Zernike-fit vs NA'

parabolic term (Z4) dominant?
→ homework exercise

Zernike Functions

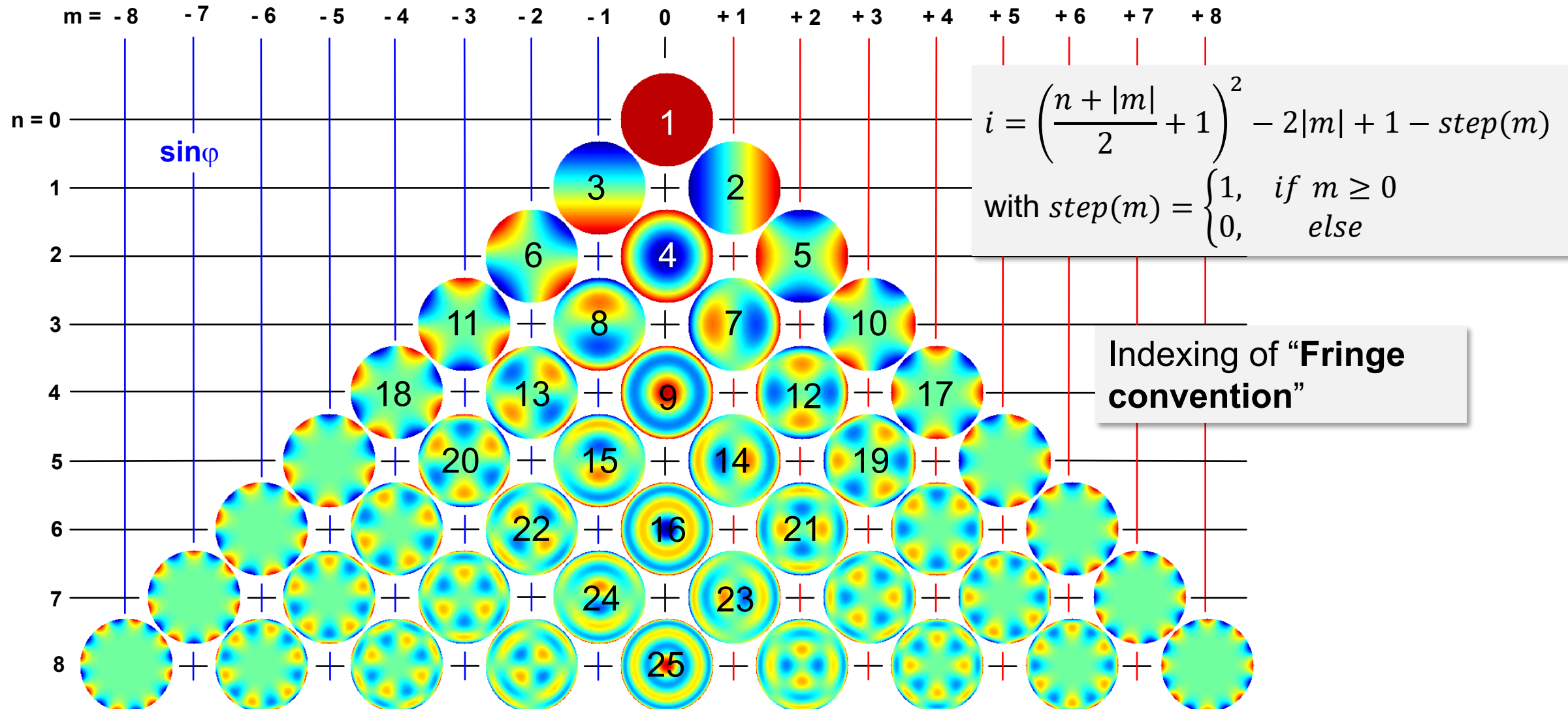


Zernike Functions

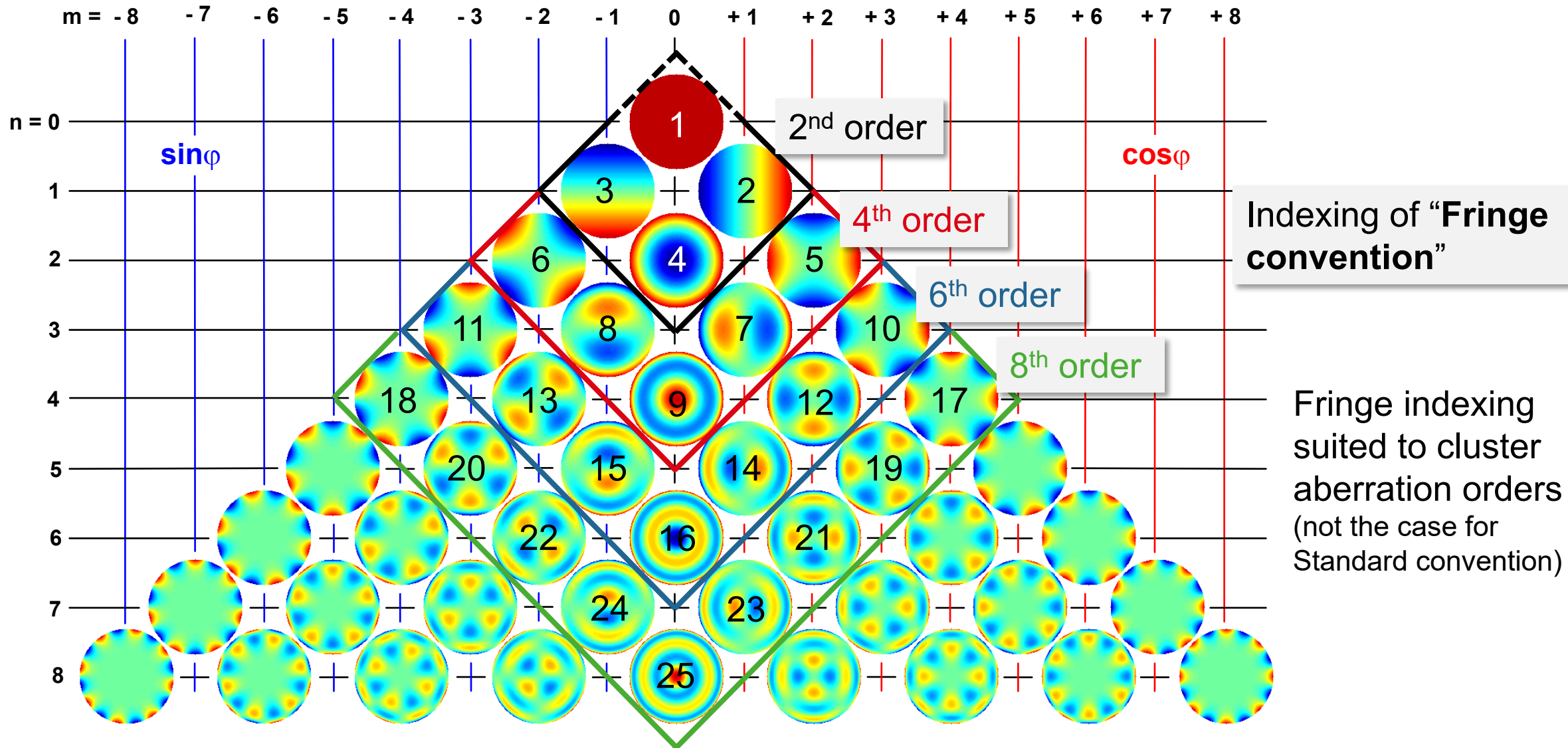


- Shapes of Zernike polynomials $Z_{nm}(r,\phi)$
- n : radial ordering, m azimuthal ordering, ϕ azimuthal angle

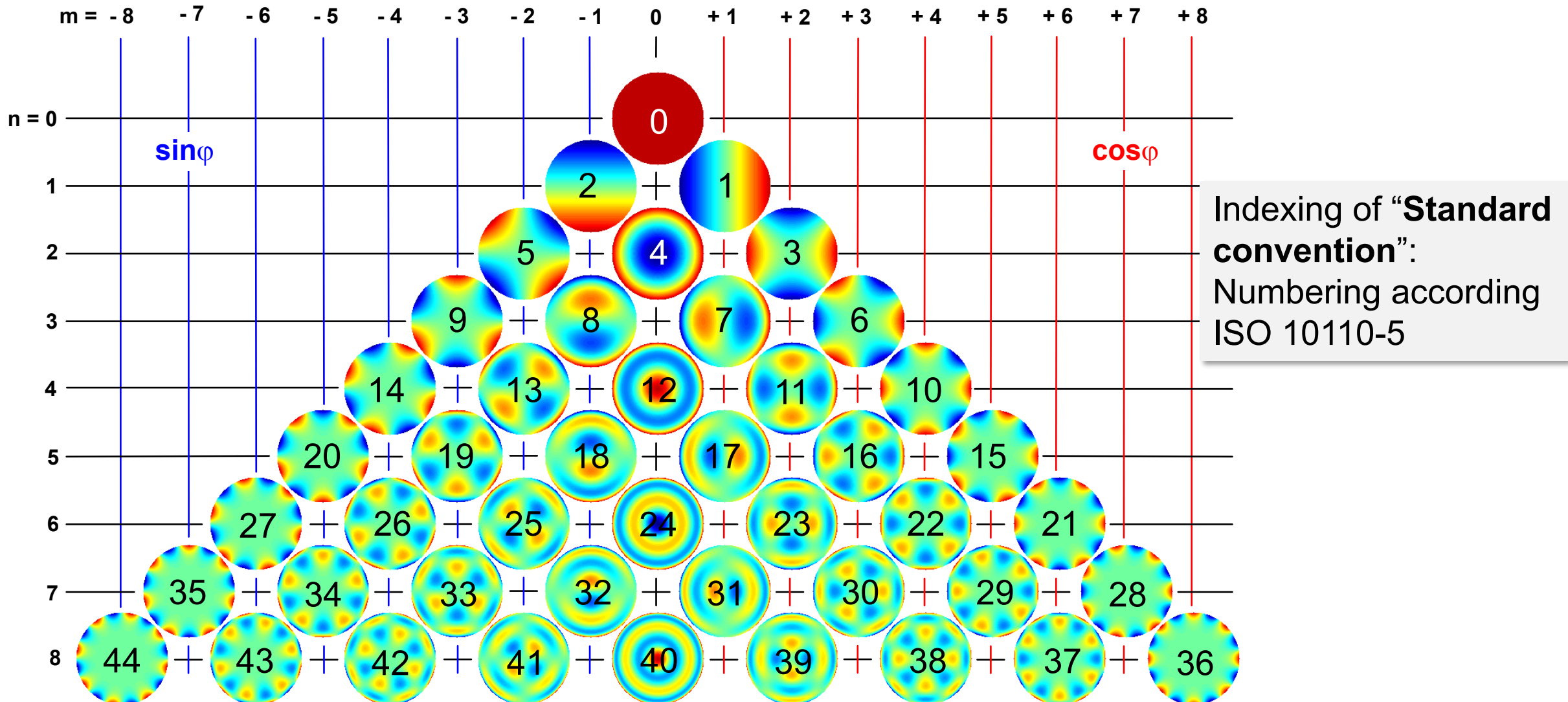
Zernike Functions – Fringe convention numbering



Zernike Functions – Fringe convention numbering



Zernike Functions – Standard convention numbering



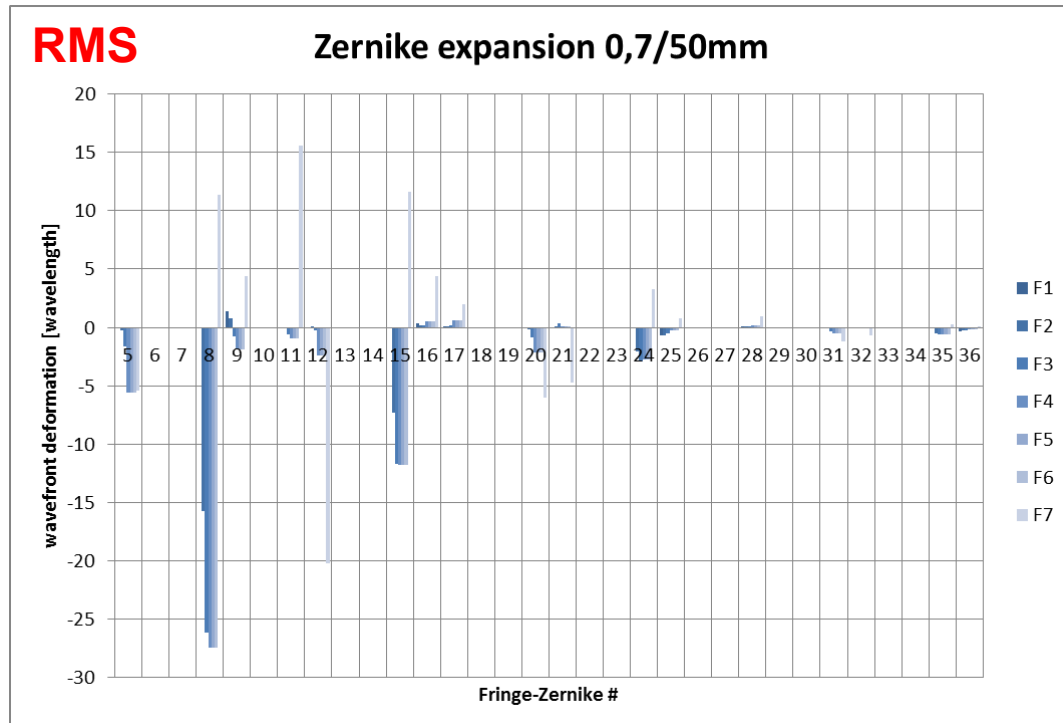
Zernike polynomials: Original, Fringe and Standard Convention

	Nijboer-Zernike	Fringe	Standard
indexing	Double index (n,m); Radial $R_n(p)$; Azimuth $\sin/\cos(m\varphi)$	$i = \left(\frac{n + m }{2} + 1 \right)^2 - 2 m + 1 - \text{step}(m)$ with $\text{step}(m) = \begin{cases} 1, & \text{if } m \geq 0 \\ 0, & \text{else} \end{cases}$	$j = \frac{n(n + 2) + m}{2}$
Indexing rule of thumb	Direct straightforward max. radial order n and azimuthal order m	Quadratic numbers: rotational symmetric, decreasing index → increasing azimuthal order	cos / sin “fir tree diagram” read line by line
scaling	$\text{rms} = 1/2\pi$	Maximum +1	$\text{rms} = 1$

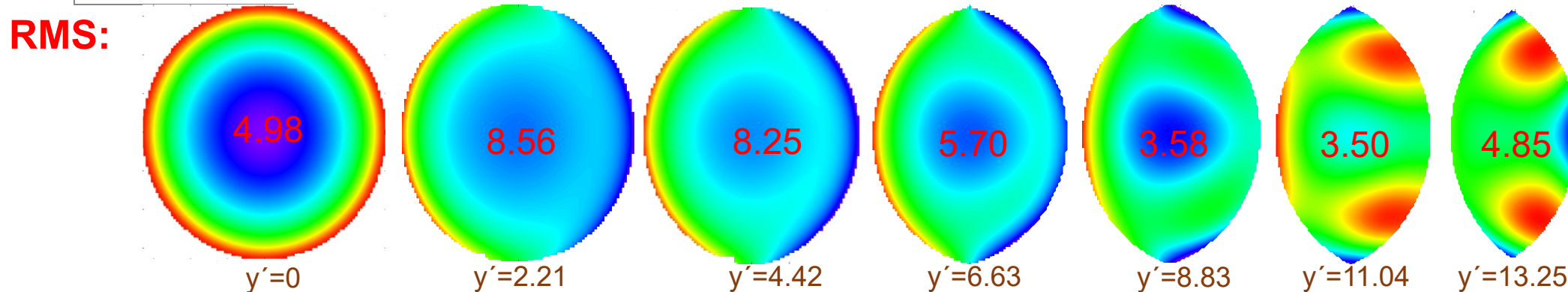
Fringe convention standard in optical lithography. In other application areas conventions might be mixed up, especially if wavefront evaluations are not used on a daily base.

Check carefully with suppliers or optical engineers from different application areas which convention is used!

Zernike expansion of lens pupil data over field



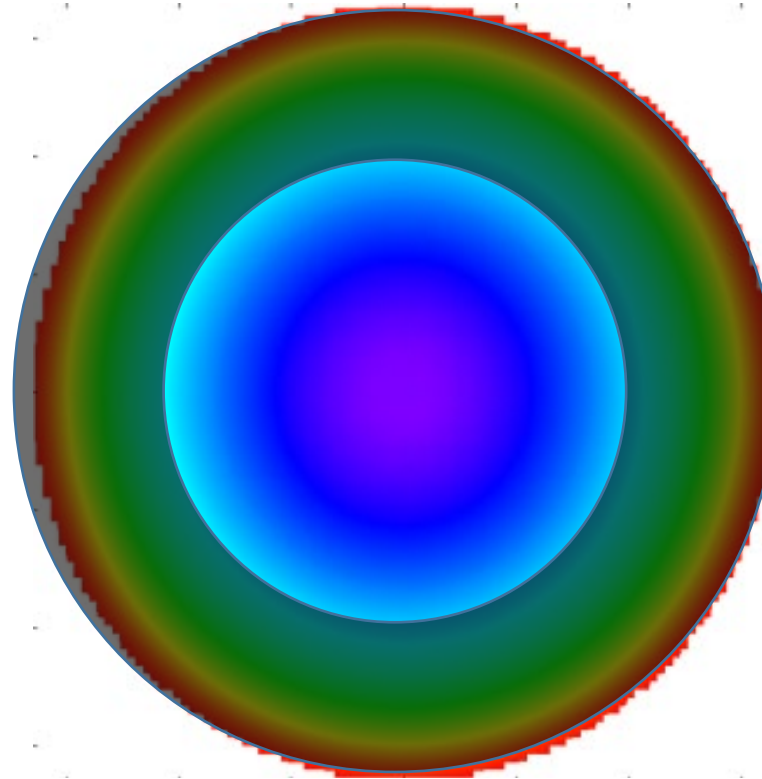
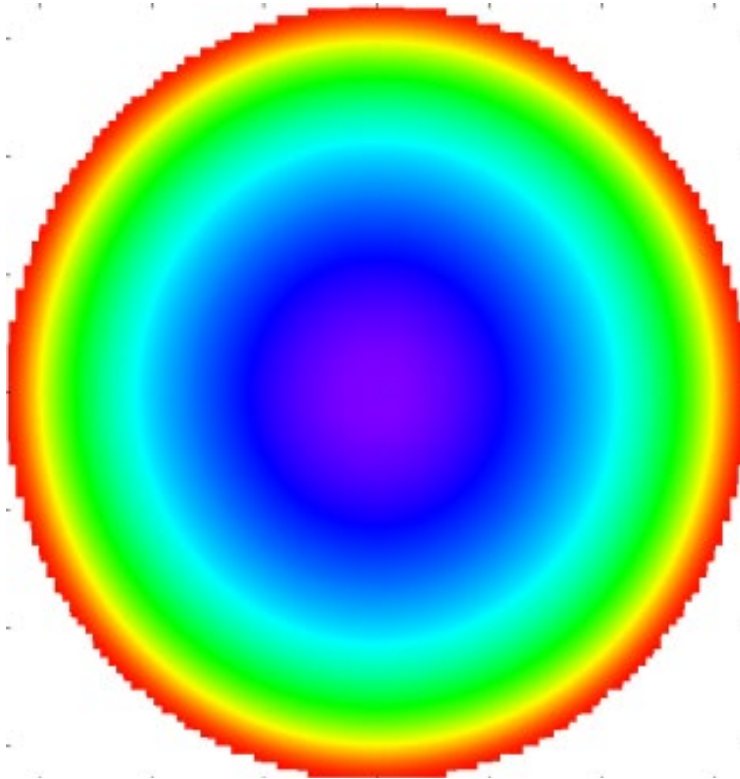
- off-axis pupils have significant amount of coma (Z8, Z15, Z24)
- pupil is vignetted → Zernike-expansion is done on spherical region which is larger than actual pupil → off-axis Zernike-expansion values tend to be large (especially high pupil orders)
- Zernike-expansion not suited for performance evaluation of vignetted pupils (qualitative analysis only)



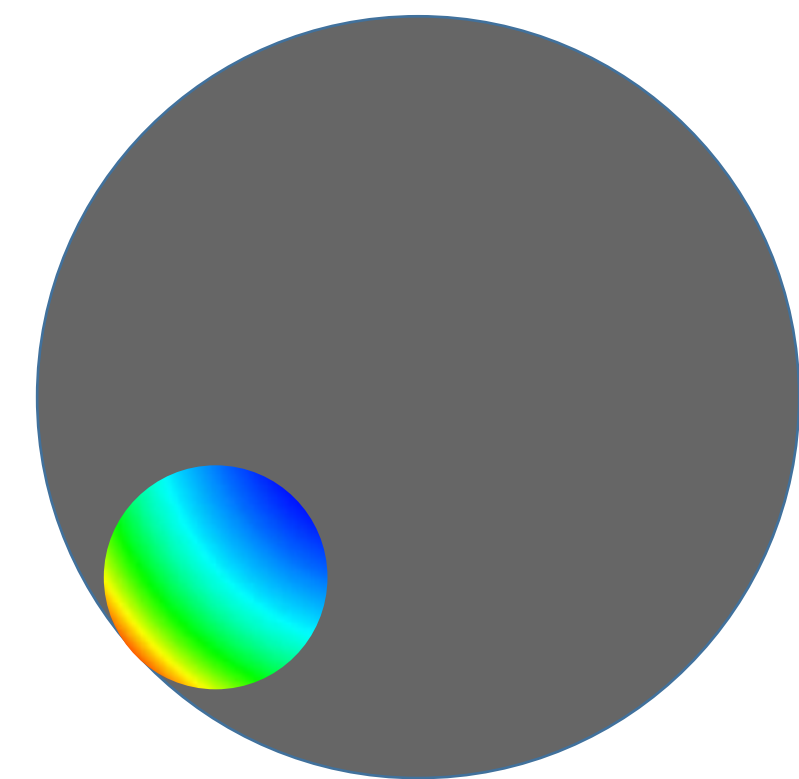
Computation of Zernike fit over any subaperture from Fit over full aperture

Given: wavefront approximation W_{appr}
 $= \sum c_j Z_j$ by Zernike polynomial

Wavefront approximation of any subaperture
can be calculated from W_{appr} directly!



Reduced aperture (on-axis subaperture)

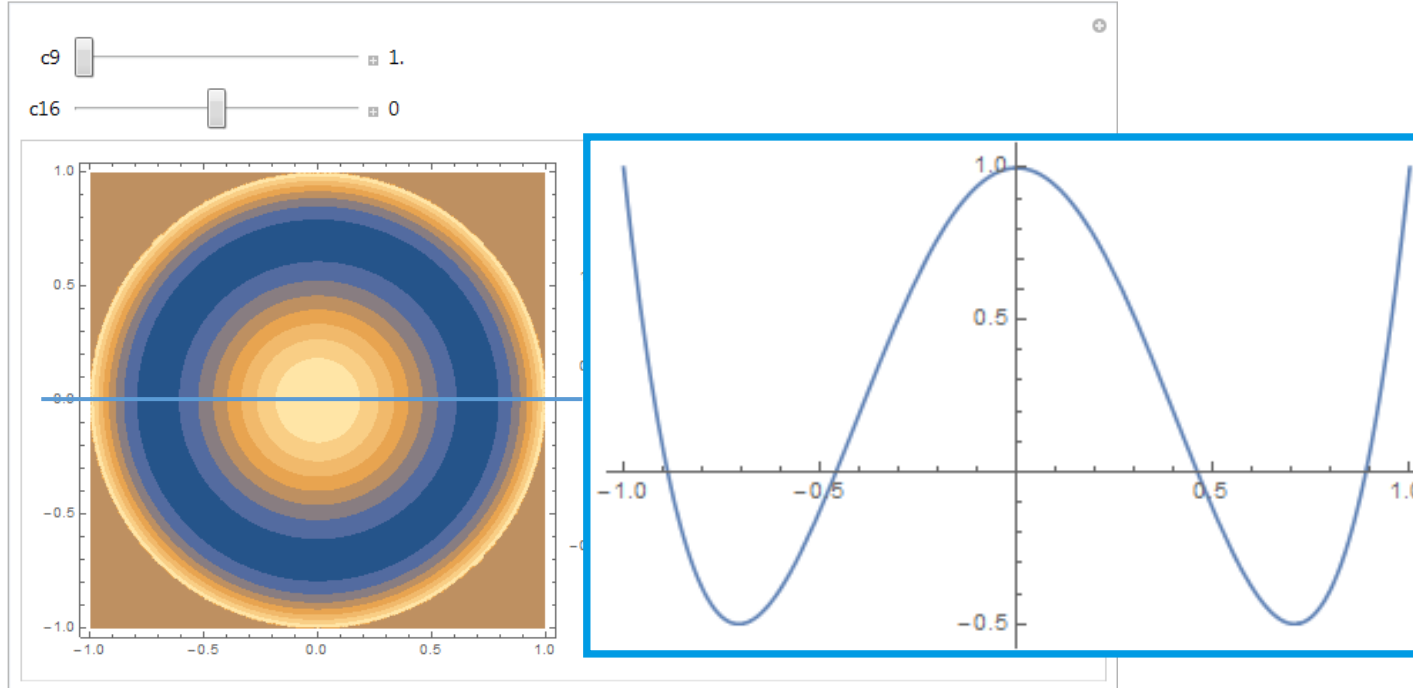


Subaperture at any position

Effect on wavefront deformation of change in aperture

For any subaperture of diameter s in the ratio to the original lens aperture the Zernike expansion for this subaperture can be calculated from the original data in terms of Zernike expansion data. Especially for the center subaperture, i.e. when changing the lens numerical aperture, the Zernike expansion on the subaperture Z^s is:

$$Z_{n,m}^s(r,\vartheta) = N_{n,m} \sum_{n,m} \left(\int_{\rho=0}^1 \int_{\phi=0}^{2\pi} d\phi d\rho \rho \ W(s\rho, \phi) Z_{n,m}(\rho, \phi) \right) Z_{n,m}(r, \vartheta)$$

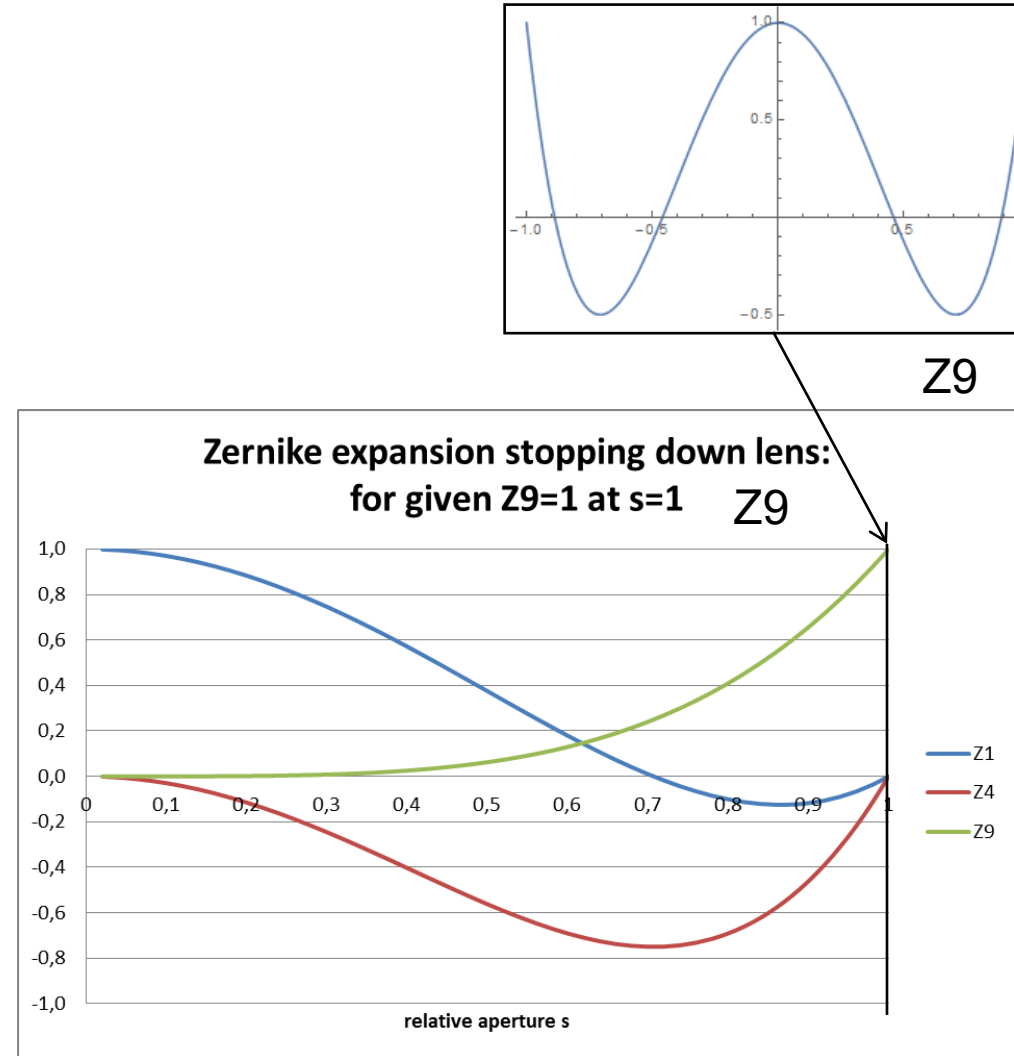


Example “spherical aberration” Z9

Effect on wavefront deformation of change in aperture

Example $Z_{4,0}$ (Fringe-Zernike Z9);

Given $Z9=1$ at nominal aperture ($s=1$).
When stopping down the Z9 splits into contributions in $Z9$ (sph. aberr.), $Z4$ (defocus), $Z1$ (offset)



Effect on wavefront deformation of change in aperture

Wavefront deformation

Aperture function

Wavefront deformation

Aperture function

Wavefront deformation

Aperture function

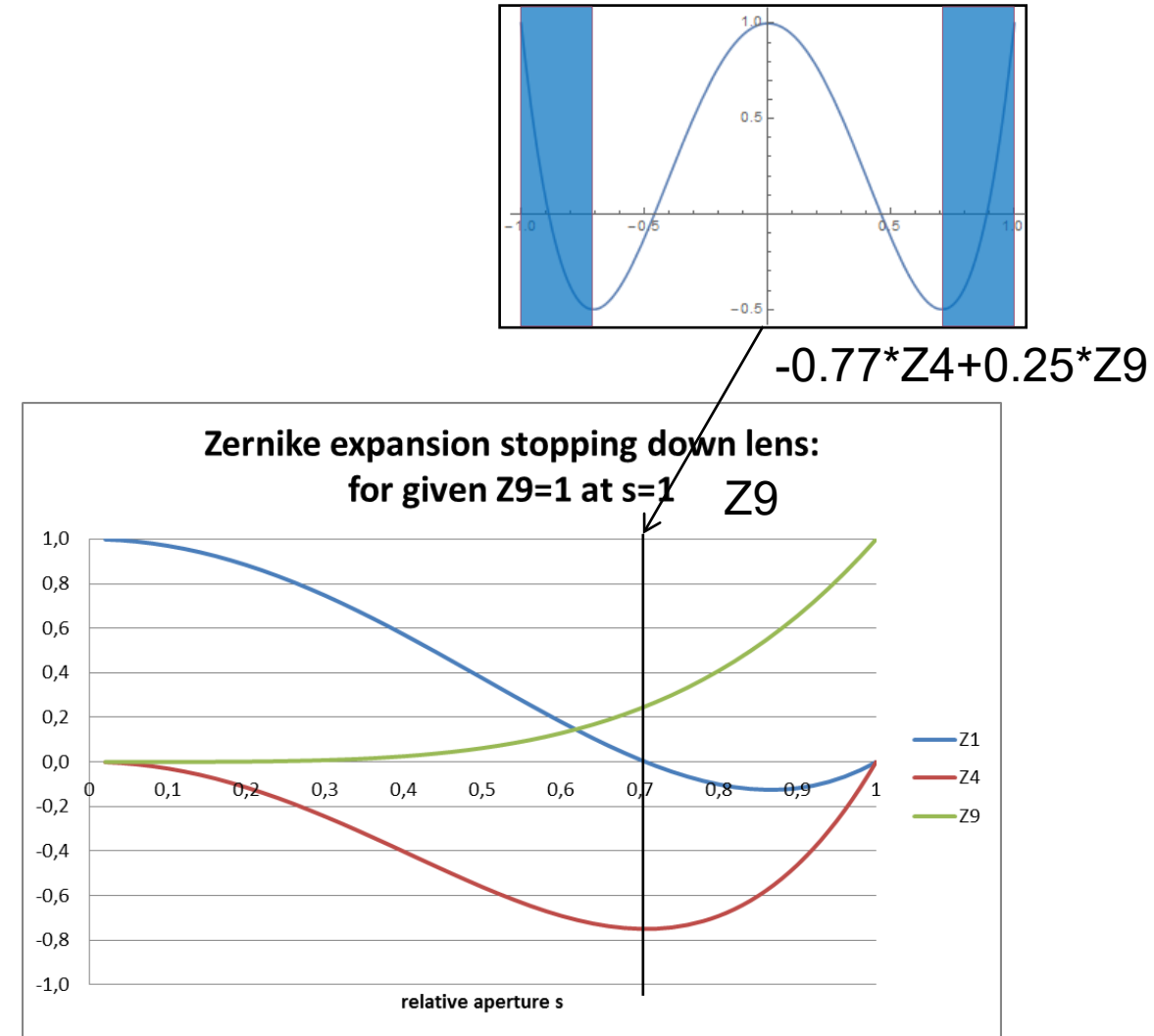
Wavefront deformation

Aperture function

Wavefront deformation

Example $Z_{4,0}$ (Fringe-Zernike Z9);

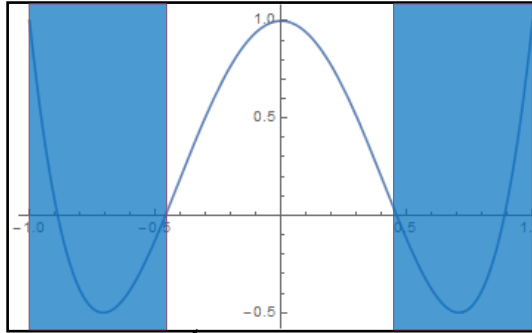
Given $Z9=1$ at nominal aperture ($s=1$).
When stopping down the Z9 splits into contributions in $Z9$ (sph. aberr.), $Z4$ (defocus), $Z1$ (offset)



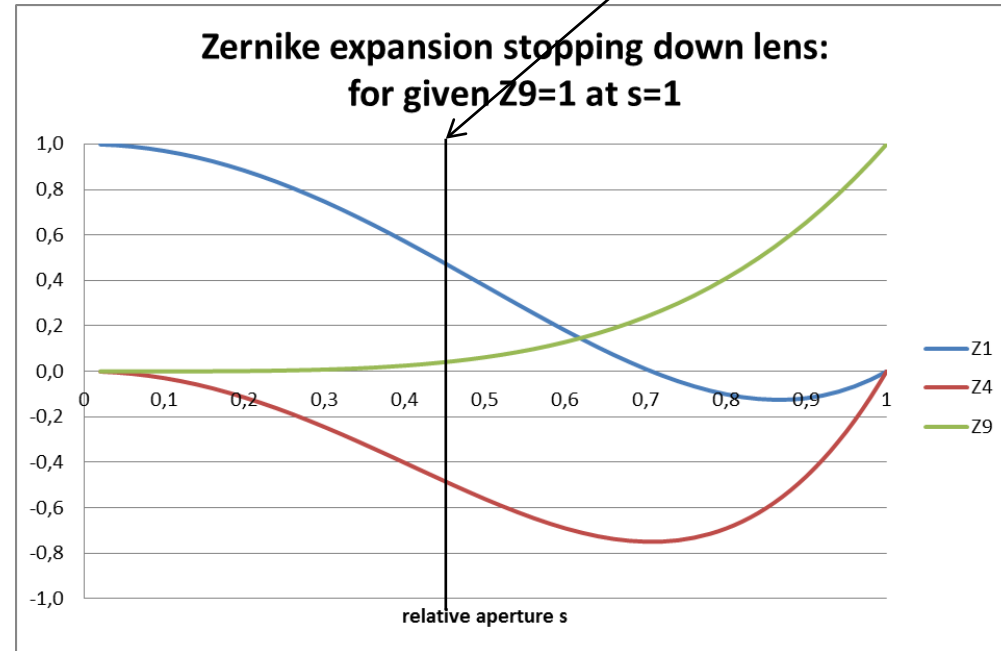
Effect on wavefront deformation of change in aperture

Example $Z_{4,0}$ (Fringe-Zernike Z9);

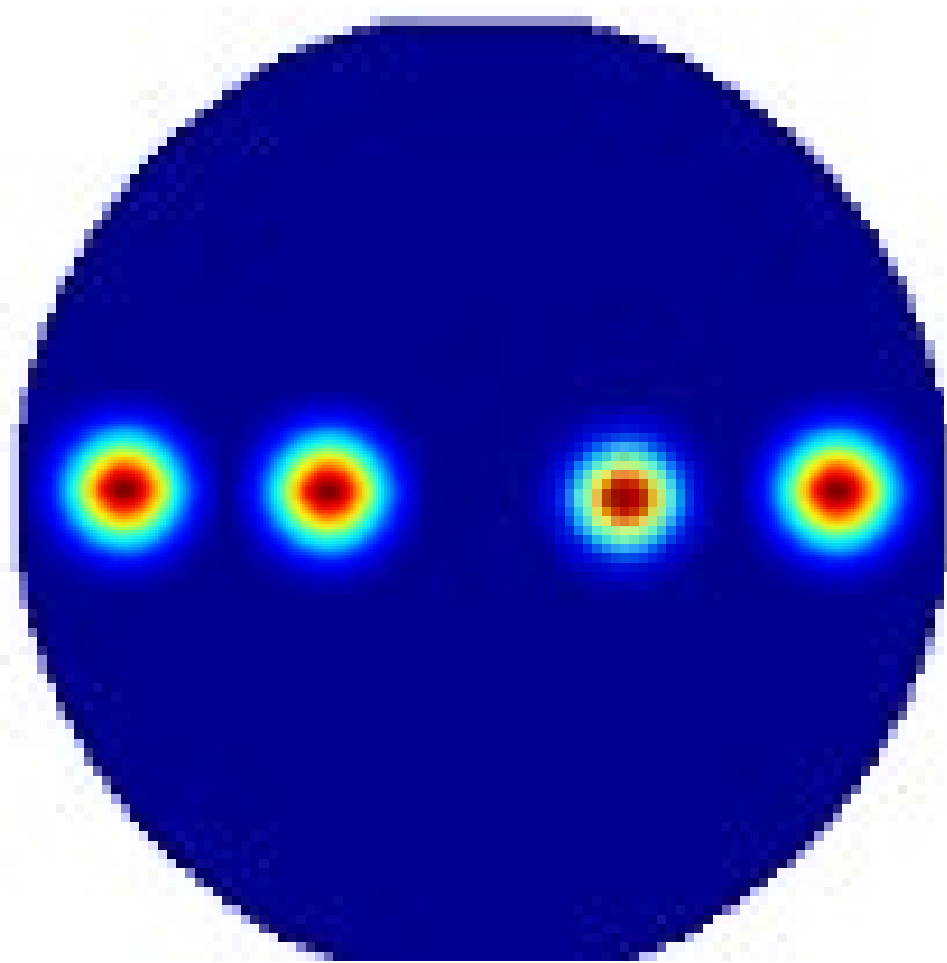
Given $Z_9=1$ at nominal aperture ($s=1$).
When stopping down the Z_9 splits into contributions in Z_9 (sph. aberr.), Z_4 (defocus), Z_1 (offset)



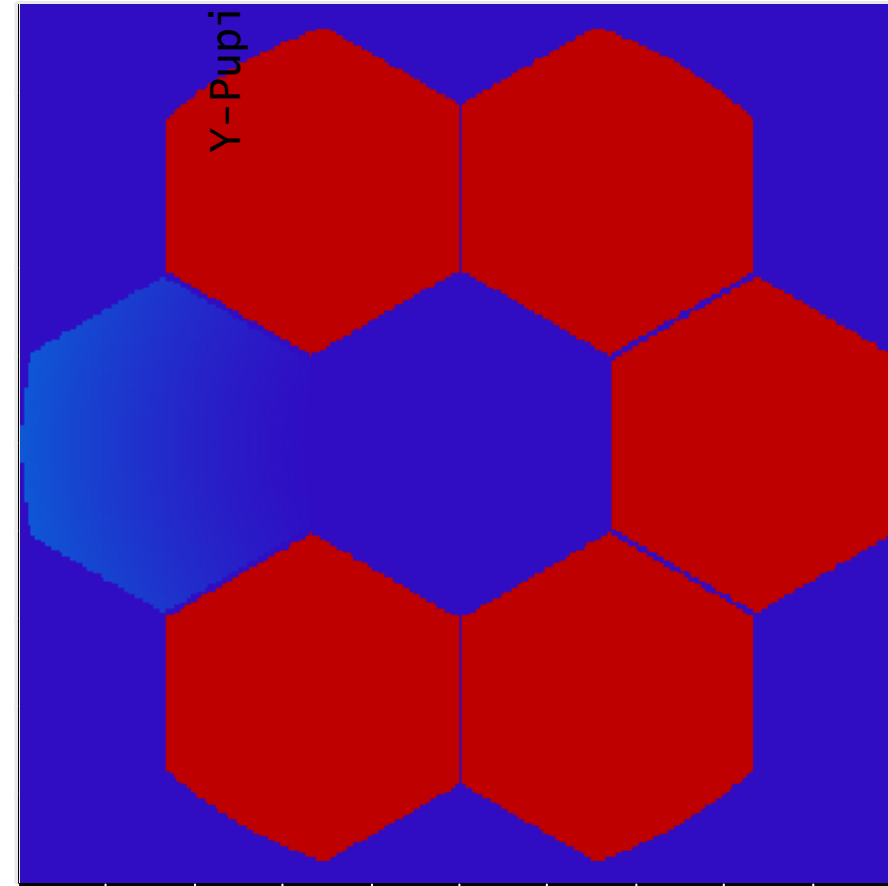
$$0.48*Z_1 - 0.47*Z_4 + 0.04*Z_9$$



Wavefront deformation unsuited for Zernike approximation

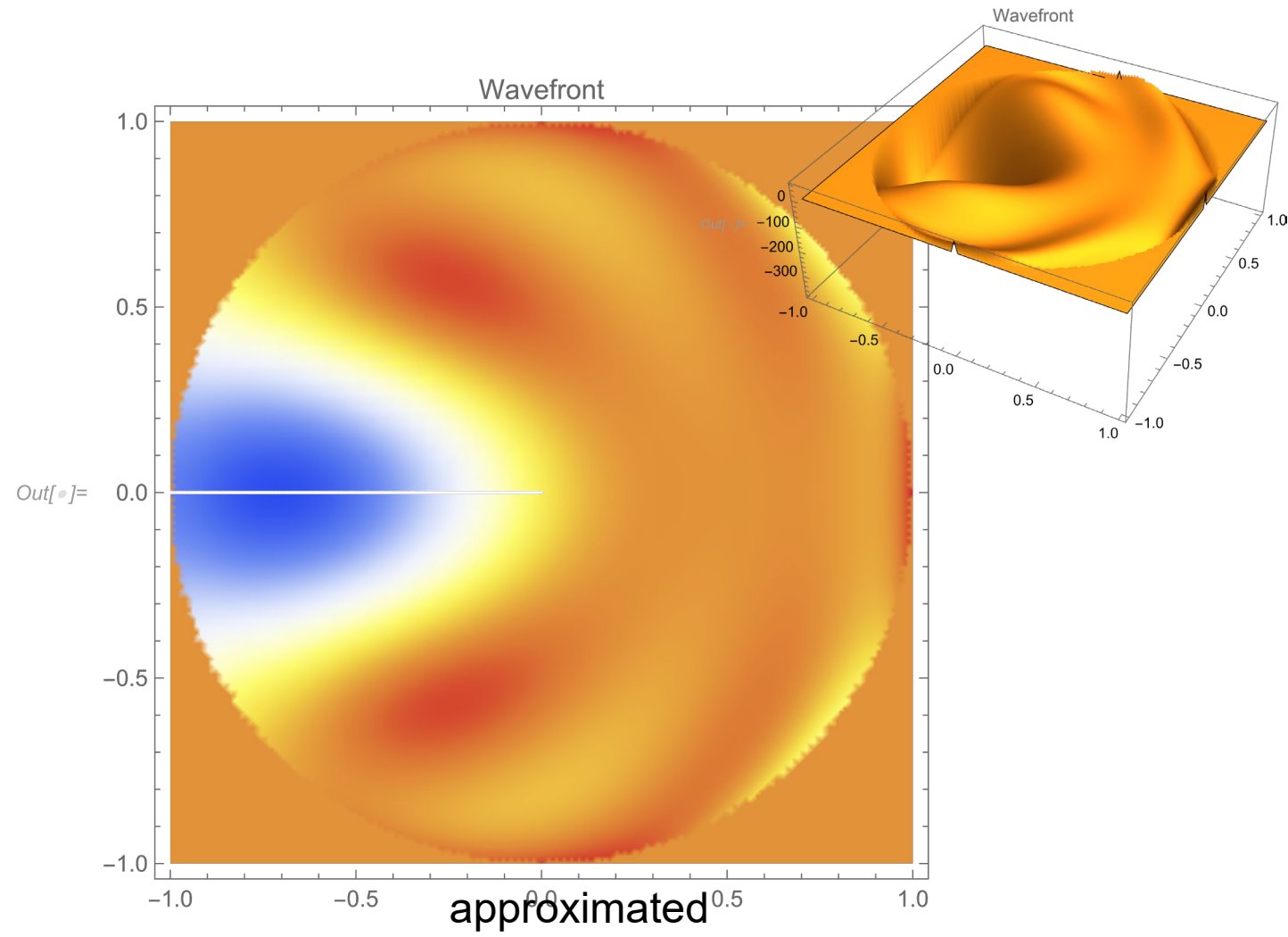
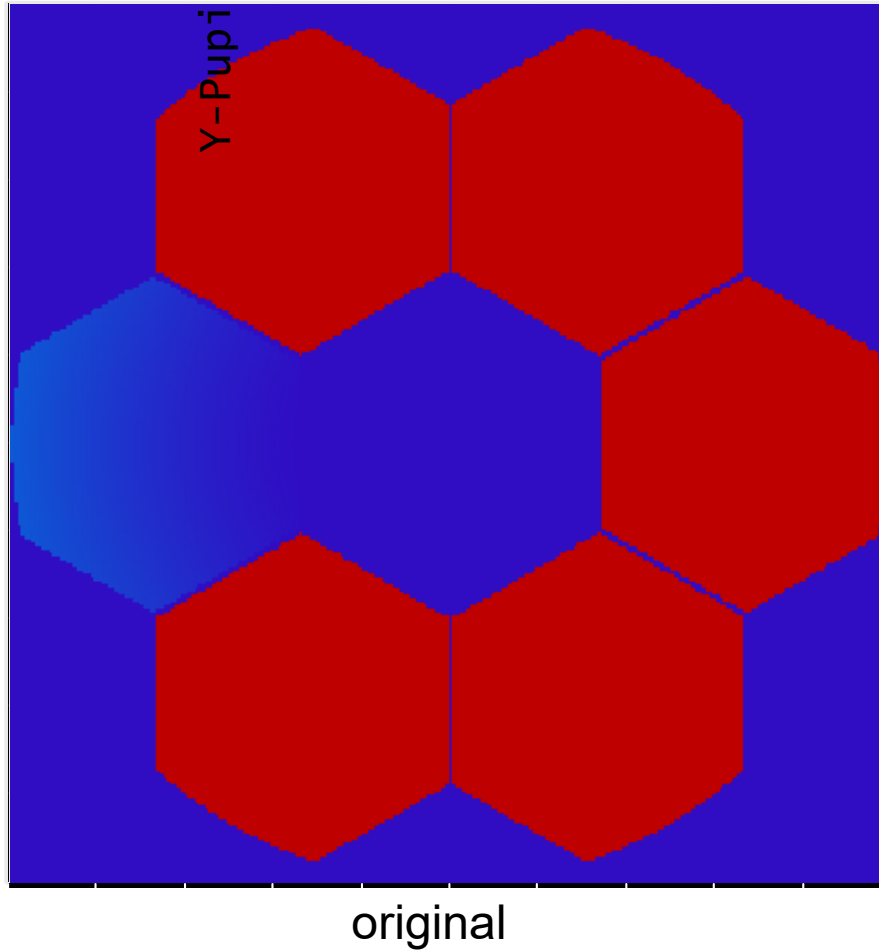


Local “hot spots” (e.g. lens heating with local illumination settings and periodic functions)

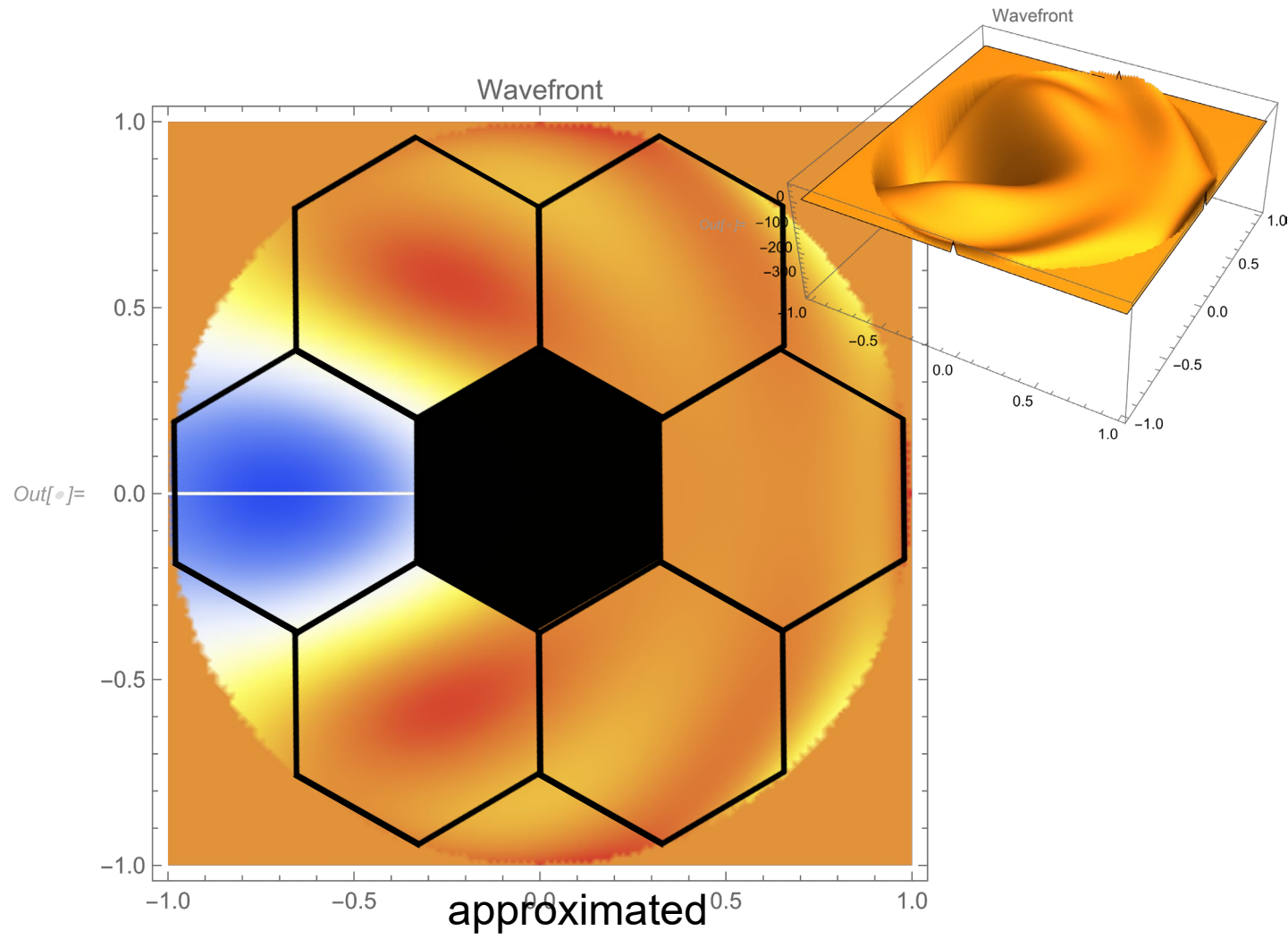
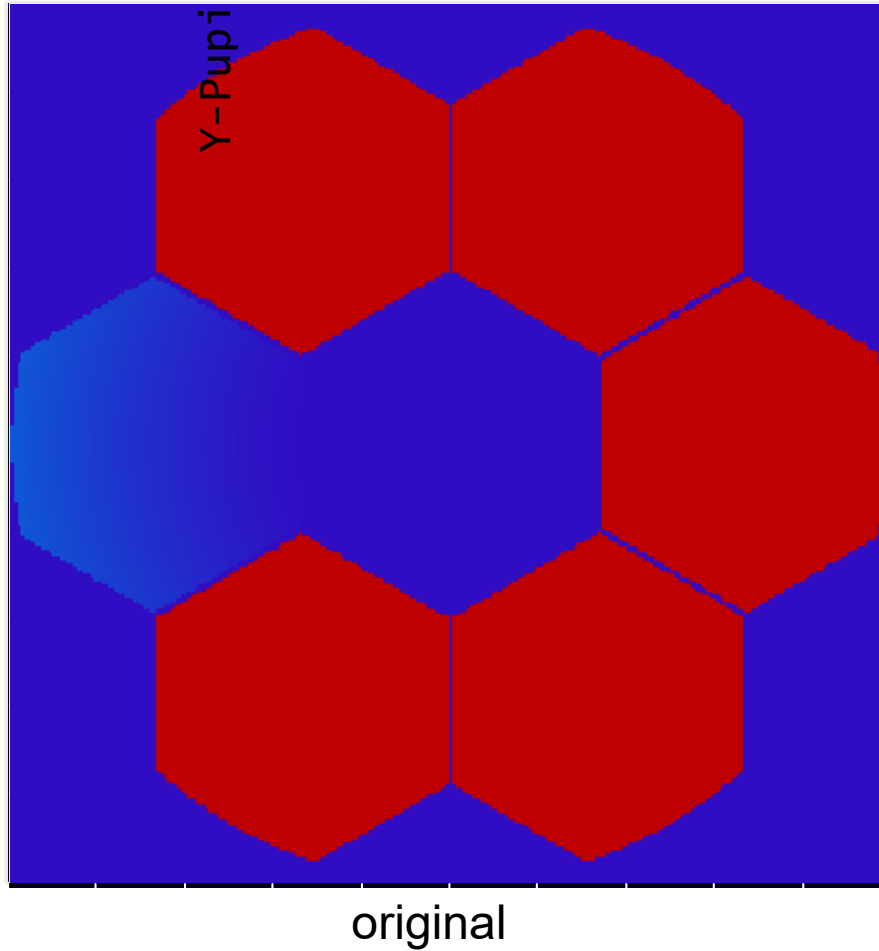


Segmented pupil (e.g. deployable mirror telescope)

Original wavefront (Pupil WF deformation) and Zernike approximated wavefront (first 37 Zernike Polynomials)

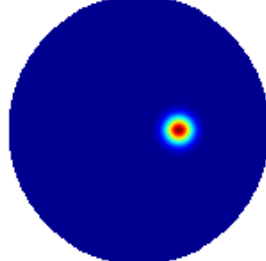


Original wavefront (Pupil WF deformation) and Zernike approximated wavefront (first 37 Zernike Polynomials)



Zernike approximation of “hot spot pupil”

original



Source: H. Gross

N = 36

Rms = 0.0237

PV = 0.378

N = 64

0.0193

0.307

N = 100

0.0149

0.235

N = 144

0.0109

0.170

N = 225

0.00624

0.0954

N = 324

0.00322

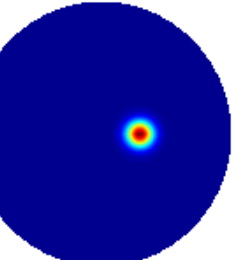
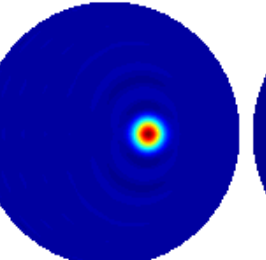
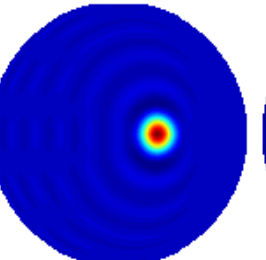
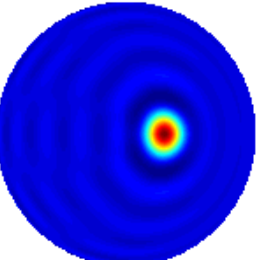
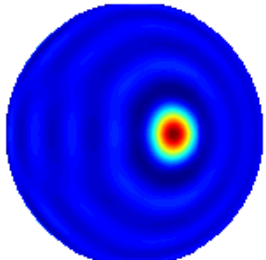
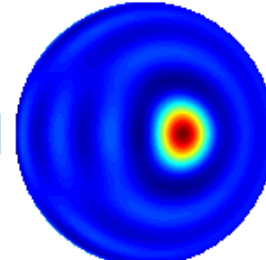
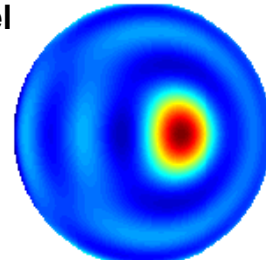
0.0475

N = 625

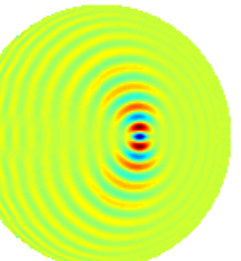
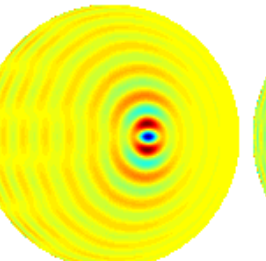
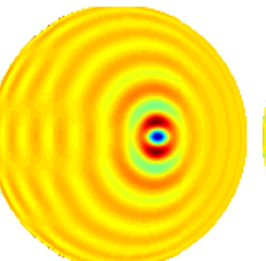
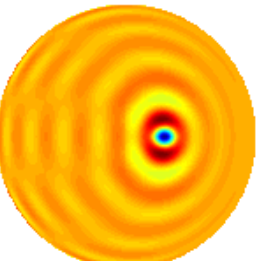
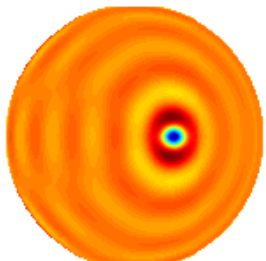
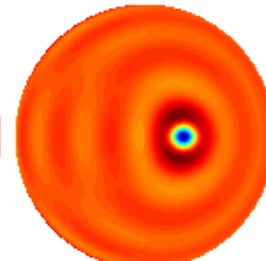
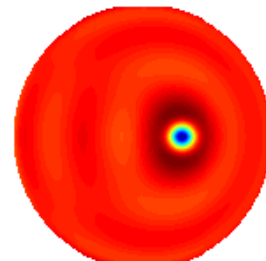
0.00047

0.0063

model



error



Gerlich-Schomaecker orthonormal functional system as alternative to Zernike Polynomials

Publications also by Rolf Wartmann

The differential operator of the oscillating membrane is the Laplace-Operator and writes in polar coordinates:

$$\Delta = \frac{\partial^2}{\partial r^2} + \frac{1}{r} \frac{\partial}{\partial r} + \frac{1}{r^2} \frac{\partial^2}{\partial \varphi^2}$$

It is self-adjoint on the unit circle $0 \leq |r| \leq 1$:

Solving the eigenvalue equation $\Delta \Phi = -\lambda \Phi$ with the separation ansatz $\Phi(r, \varphi) = y(r)h(\varphi)$ leads to the following solution for the azimuthal part:

$$h(\varphi) = a \cos m\varphi + b \sin m\varphi$$

For the radial part we obtain the Bessel differential equation: $r^2 y'' + ry' + (r^2 \lambda - m^2)y = 0$

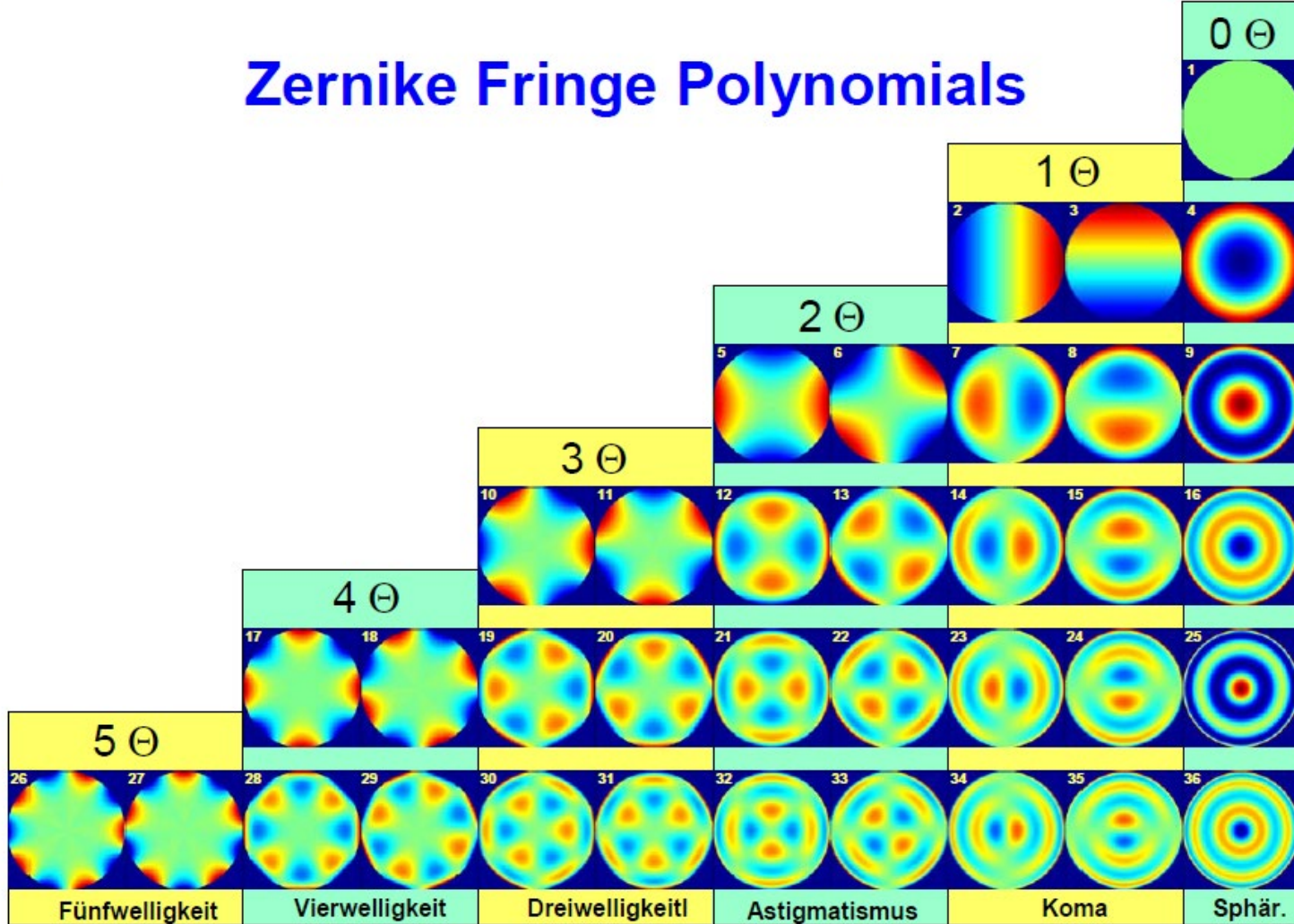
The general solutions of this differential equation are the Bessel functions: $y(r) = J_m(k_n^m r)$

The coefficients k_n^m are obtained with the inhomogeneous boundary conditions
(Courant/Hilbert (1968), p. 261) $\left. \frac{\partial W}{\partial r} \right|_{r=1} = -\alpha \left. W \right|_{r=1}$

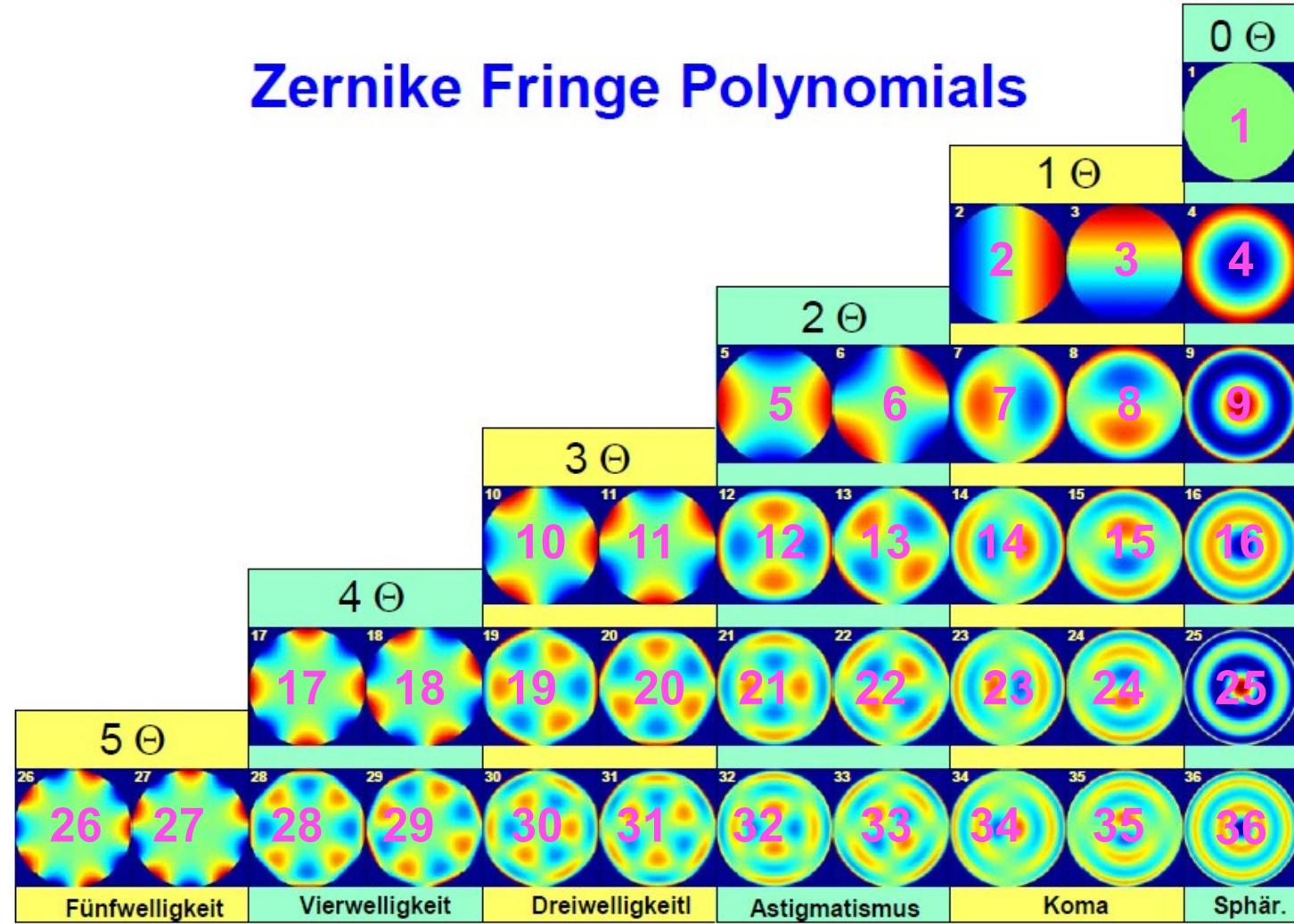
which leads to following equation to determine the values for k: $k J_n'(k) = \alpha J_n(k)$

Note that the homogeneous boundary conditions $W|_{r=1} = 0$ and $\left. \frac{\partial W}{\partial r} \right|_{r=1} = 0$ are included here coming down to determine the zero positions of the Bessel function and its derivative respectively.

Zernike Fringe Polynomials

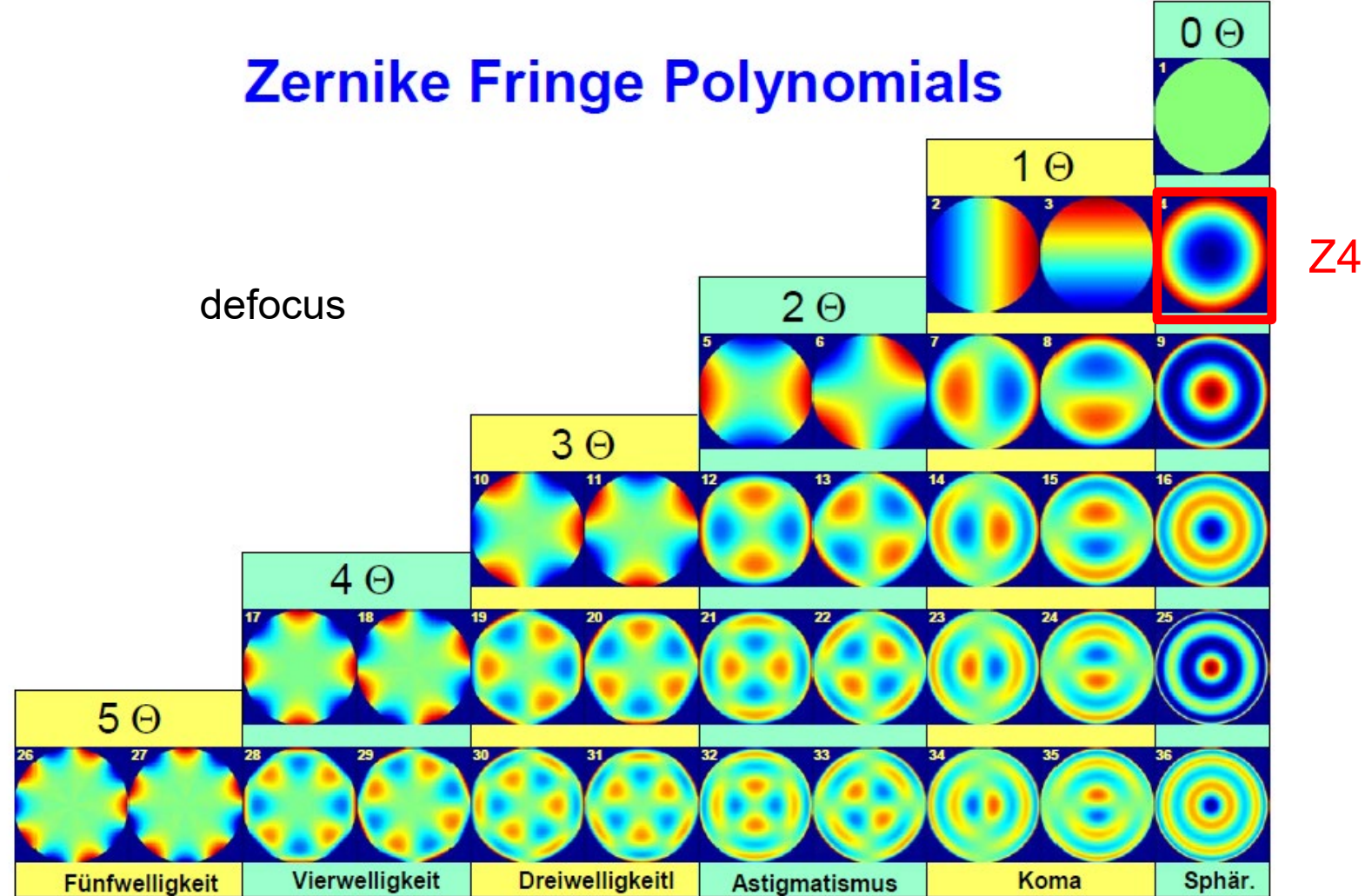


Zernike Fringe Polynomials

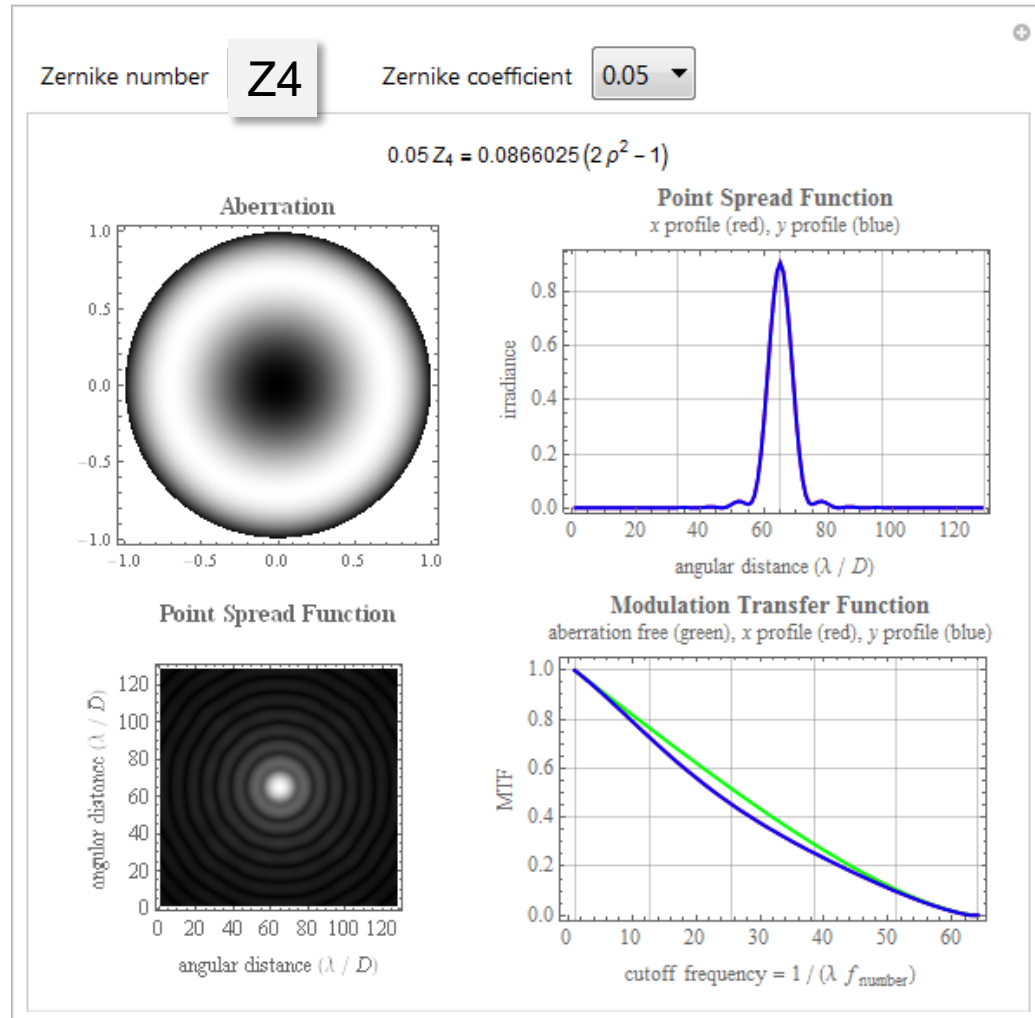


Zernike Fringe Polynomials

defocus

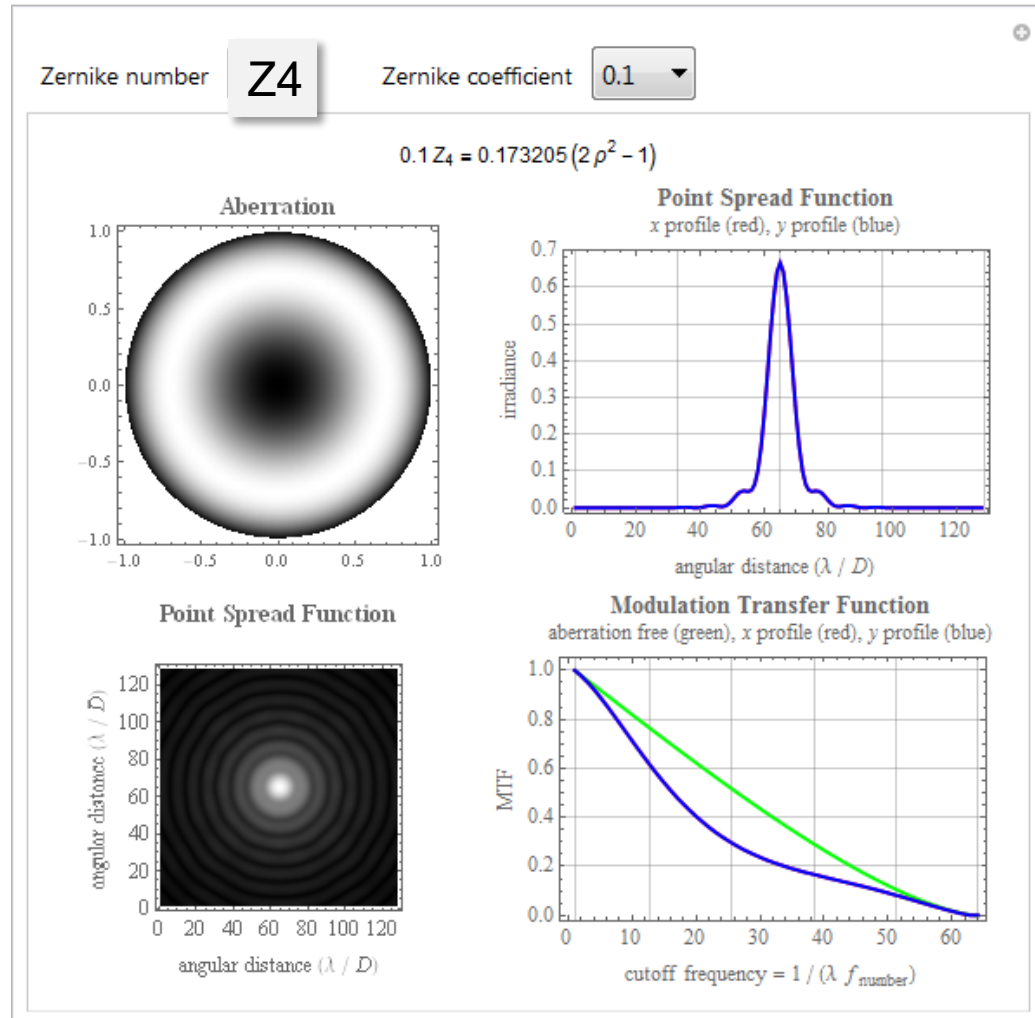


Zernike Z4 ($Z_{2,0}$), „defocus“ PSF, MTF



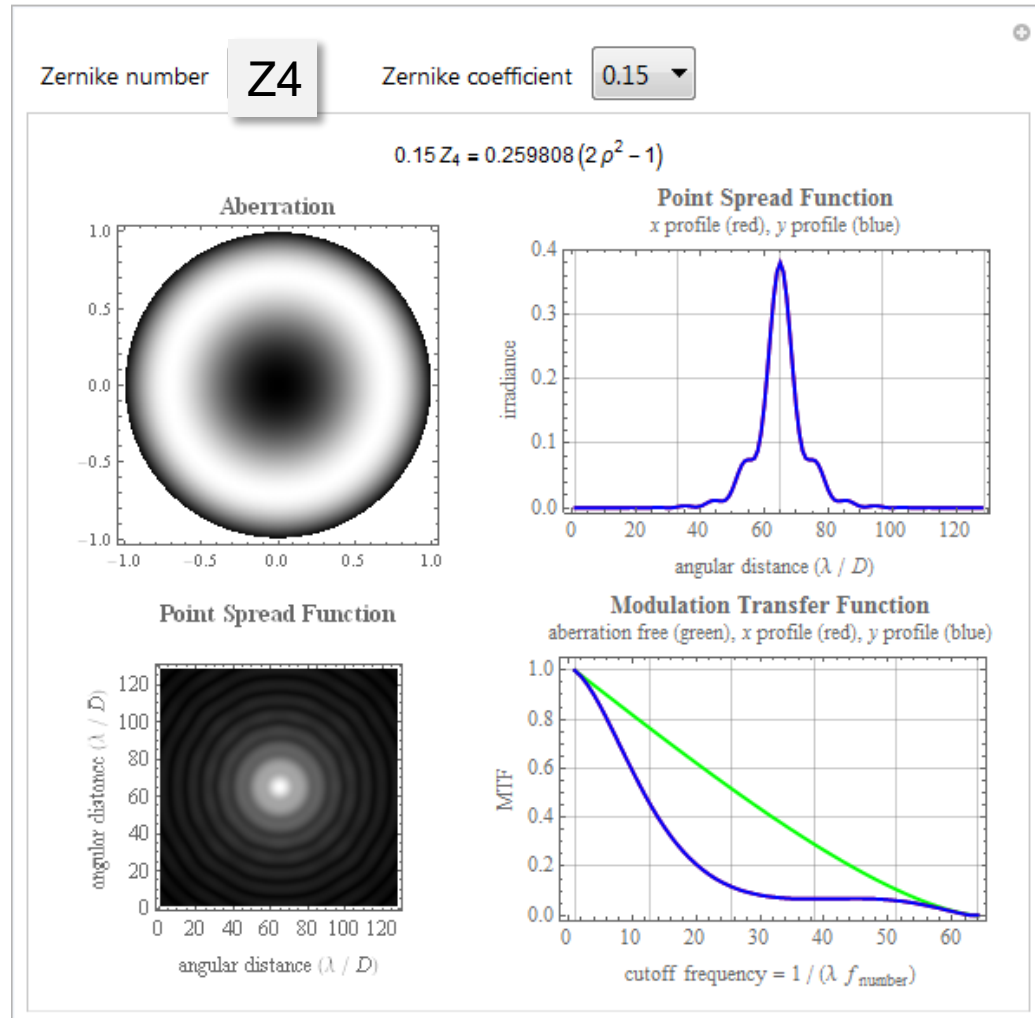
defocus

Zernike Z4 ($Z_{2,0}$), „defocus“ PSF, MTF



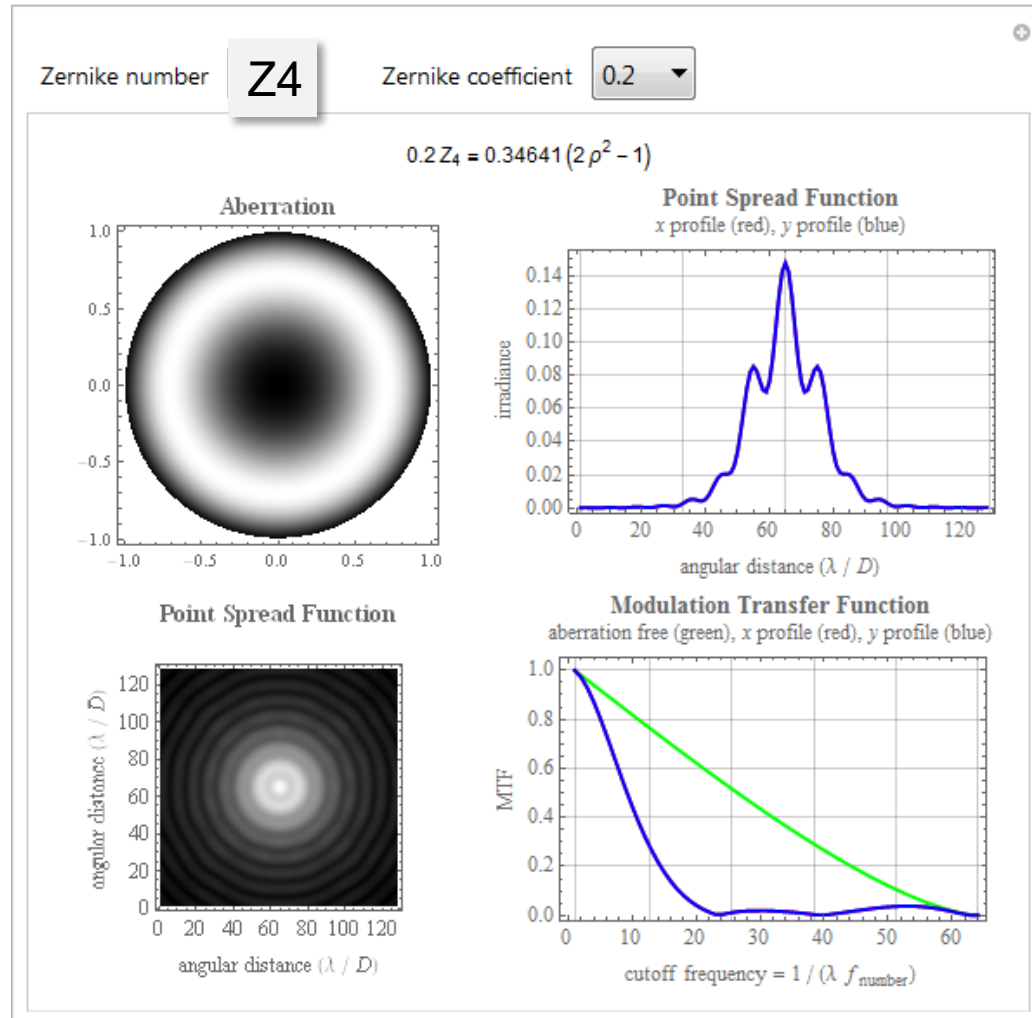
defocus

Zernike Z4 ($Z_{2,0}$), „defocus“ PSF, MTF



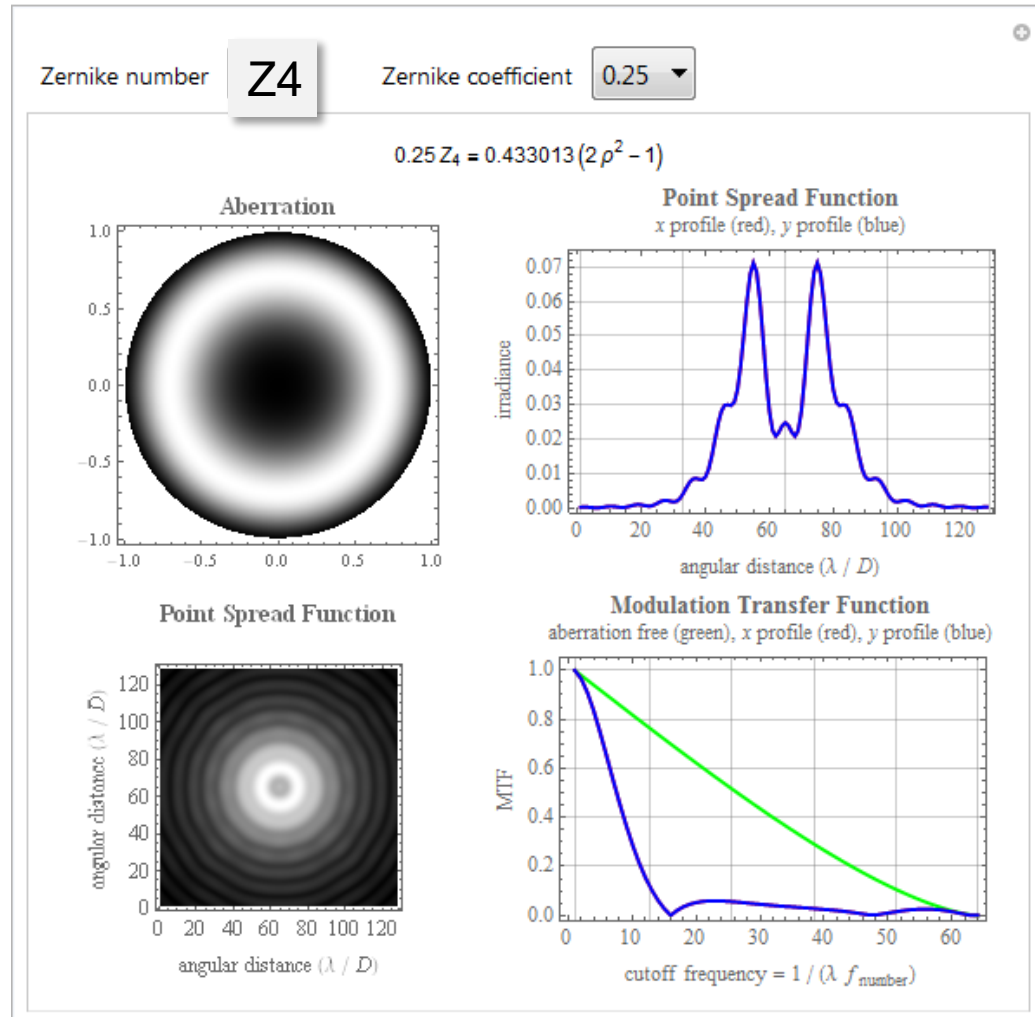
defocus

Zernike Z4 ($Z_{2,0}$), „defocus“ PSF, MTF



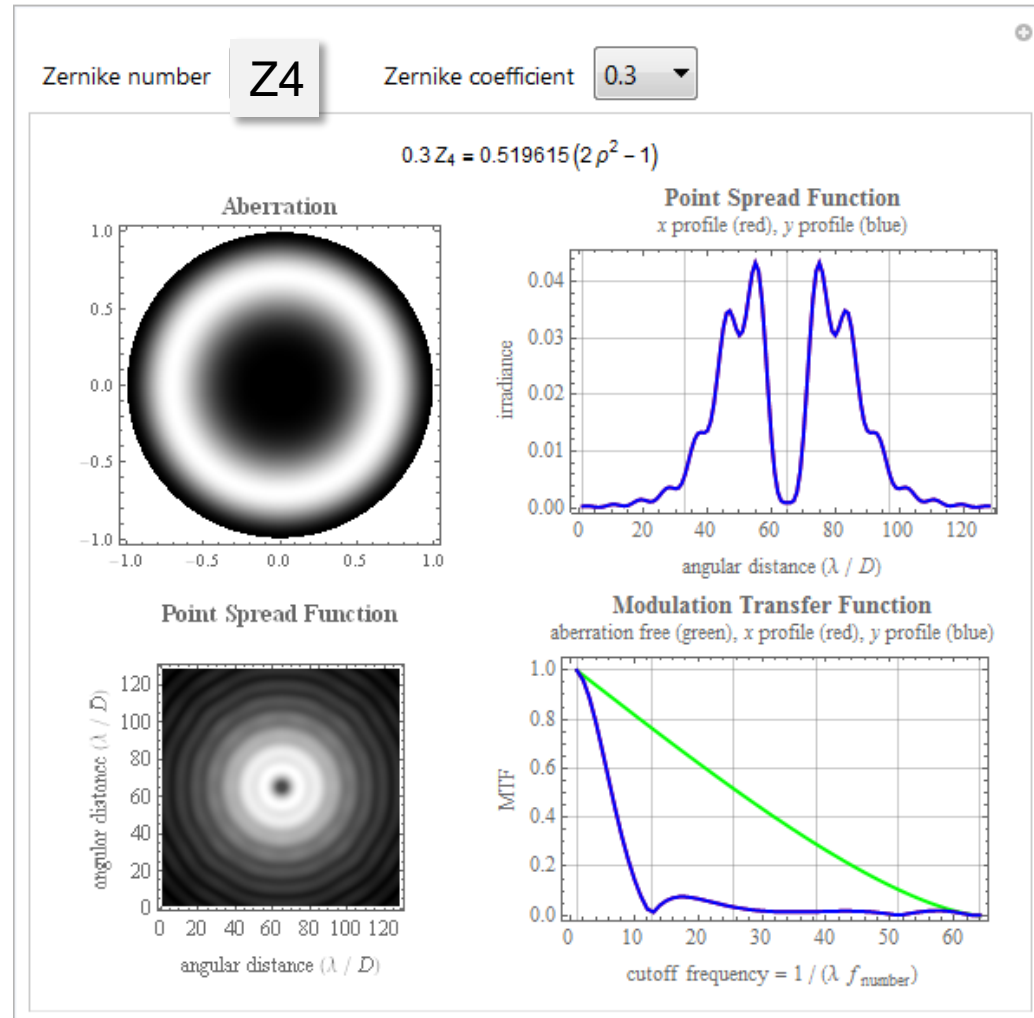
defocus

Zernike Z4 ($Z_{2,0}$), „defocus“ PSF, MTF



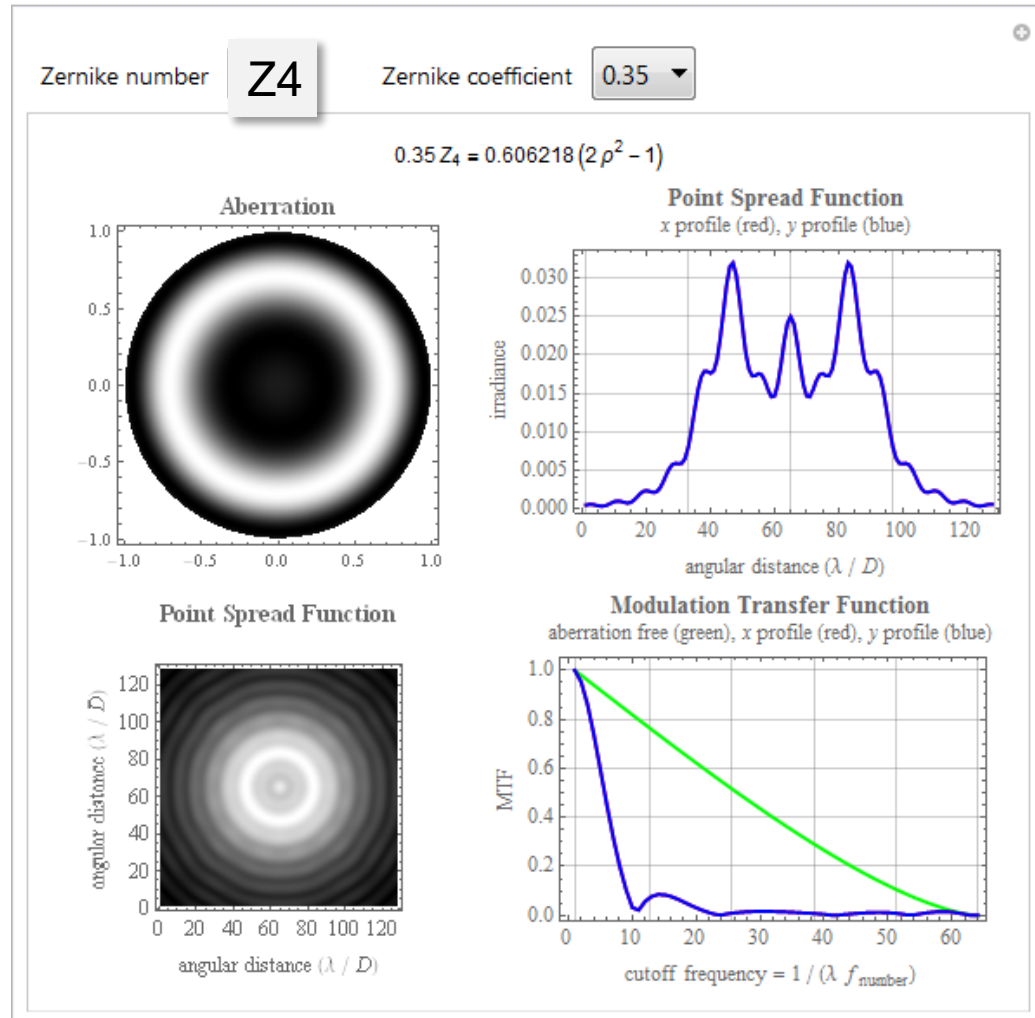
defocus

Zernike Z4 ($Z_{2,0}$), „defocus“ PSF, MTF



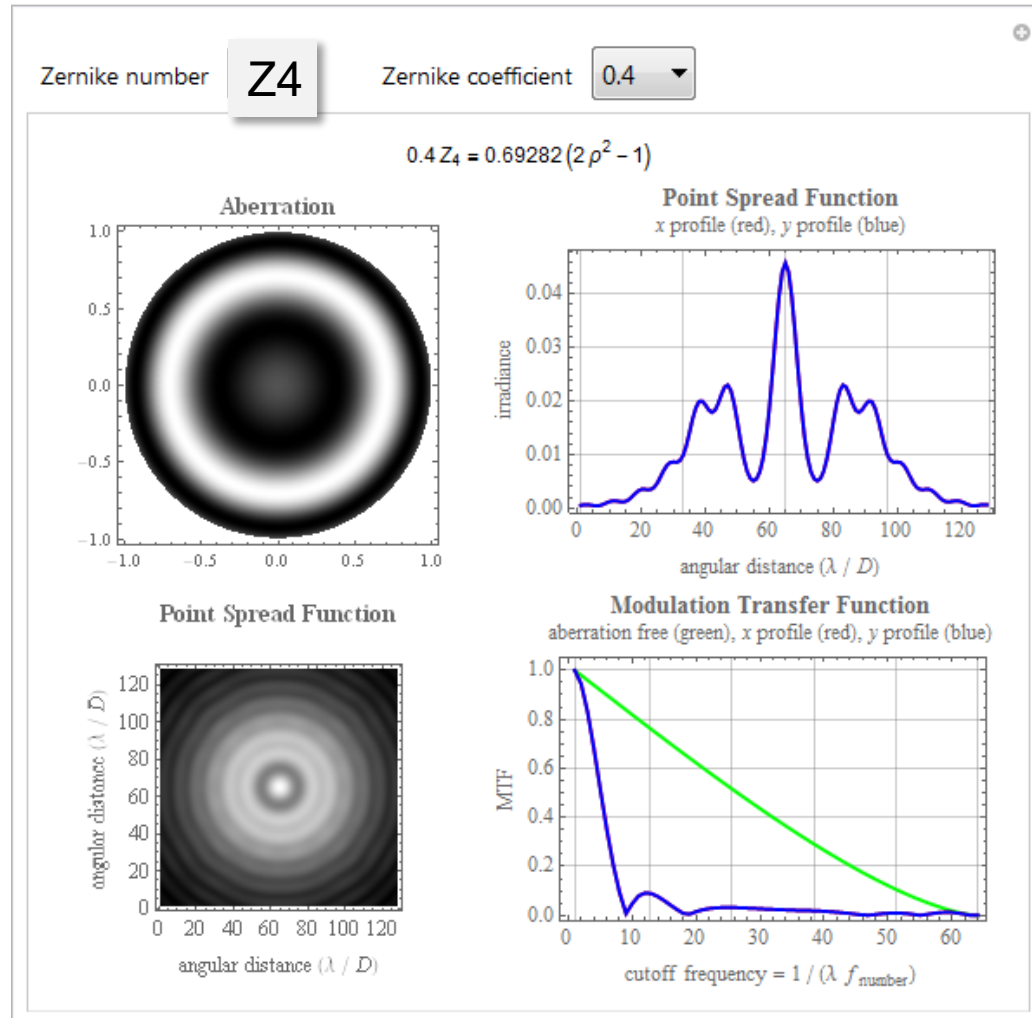
defocus

Zernike Z4 ($Z_{2,0}$), „defocus“ PSF, MTF



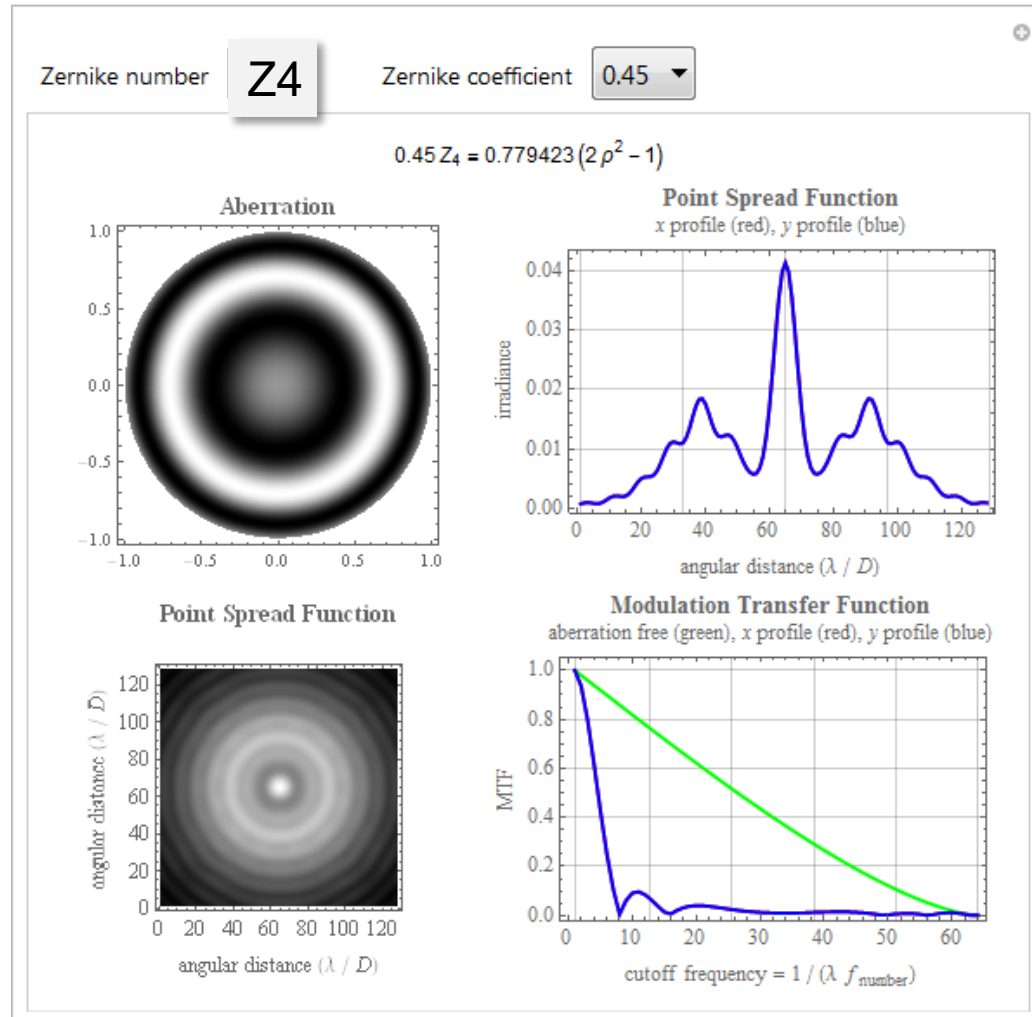
defocus

Zernike Z4 ($Z_{2,0}$), „defocus“ PSF, MTF



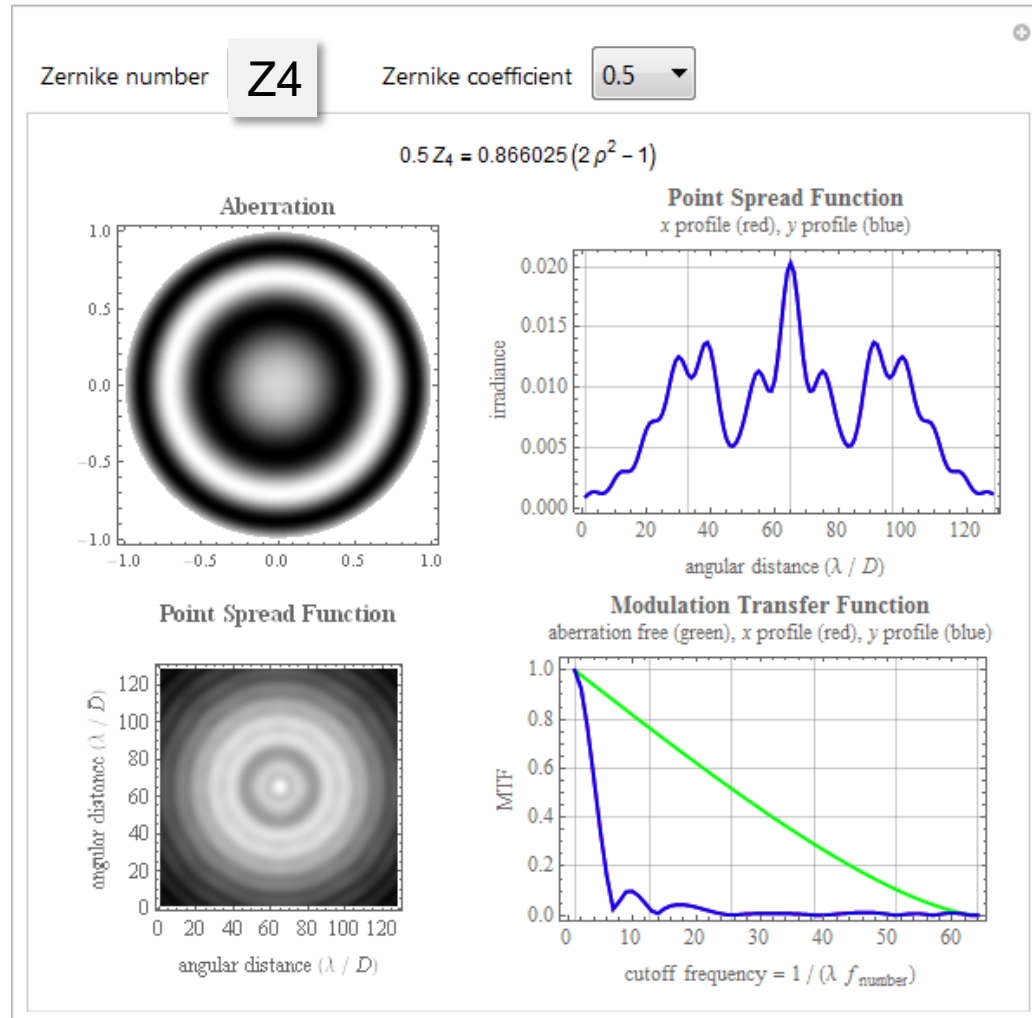
defocus

Zernike Z4 ($Z_{2,0}$), „defocus“ PSF, MTF



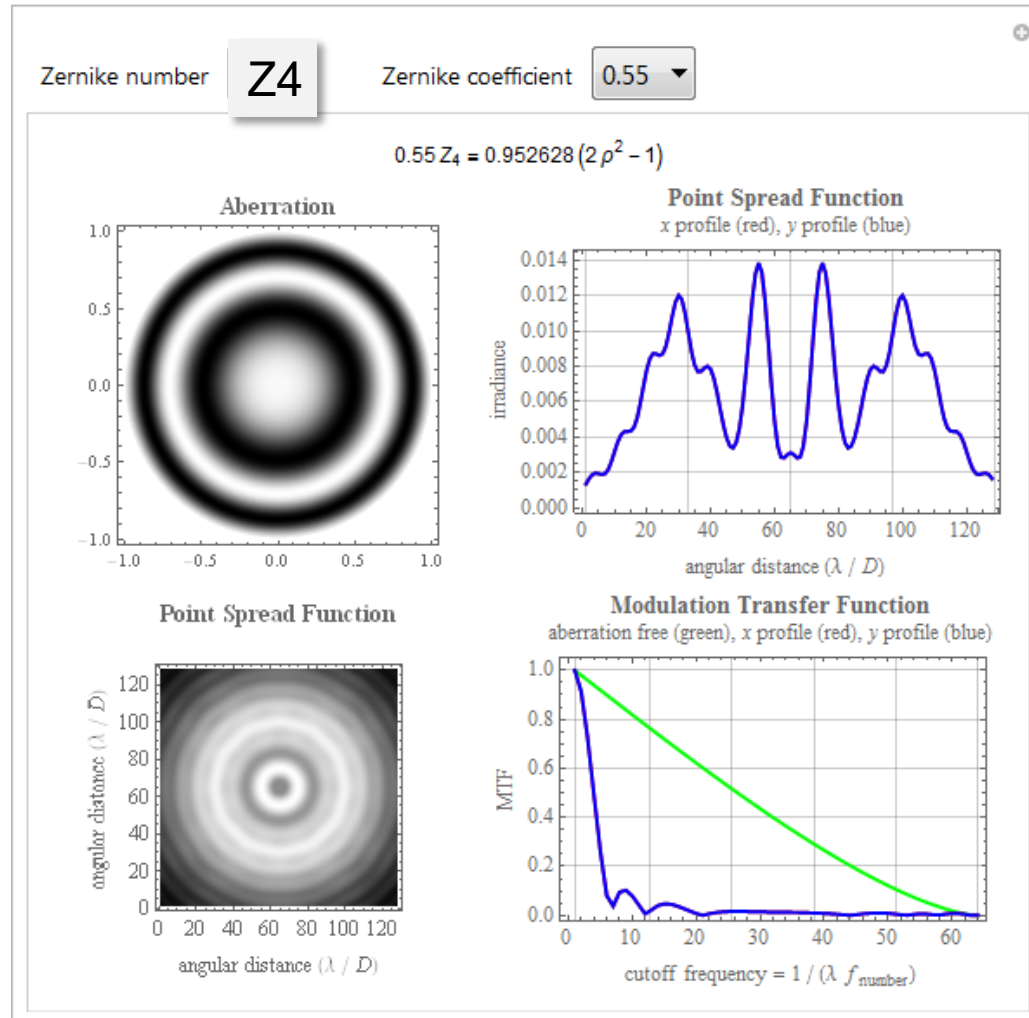
defocus

Zernike Z4 ($Z_{2,0}$), „defocus“ PSF, MTF



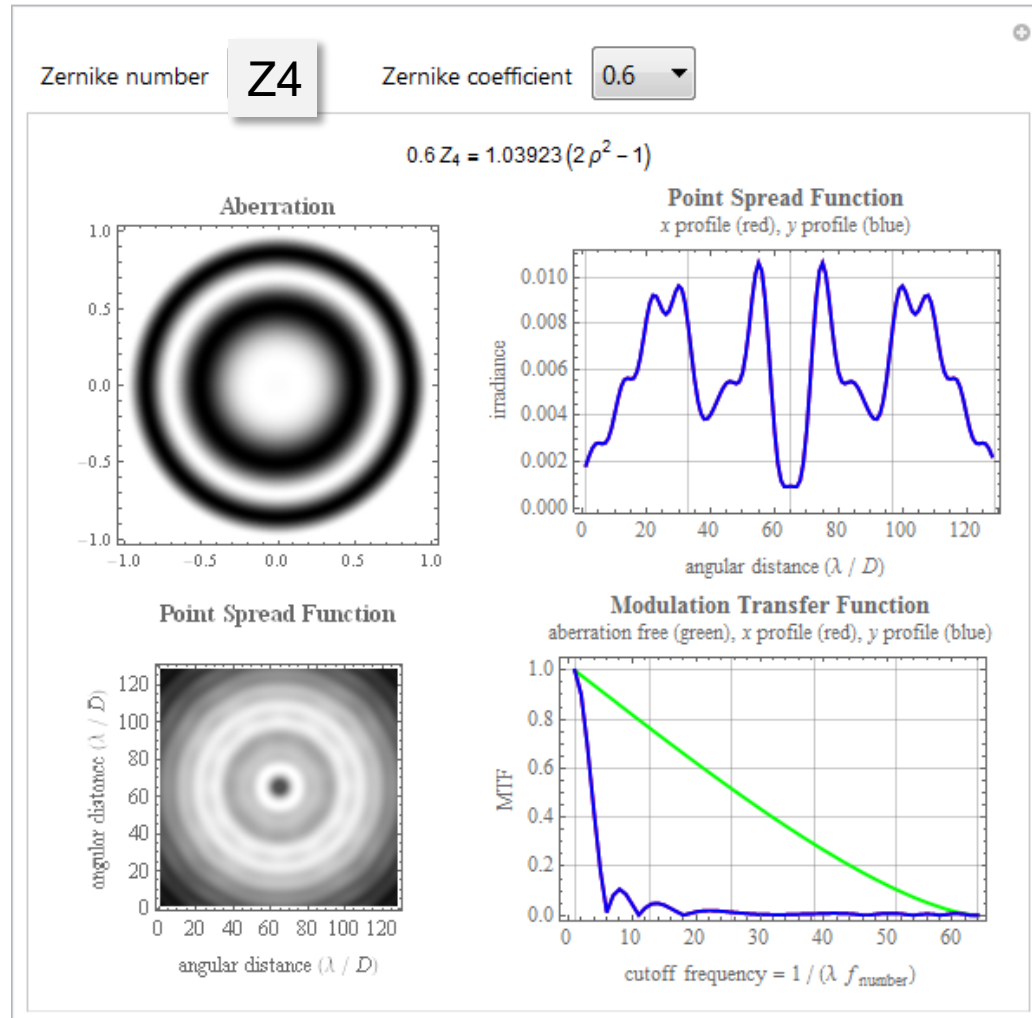
defocus

Zernike Z4 ($Z_{2,0}$), „defocus“ PSF, MTF



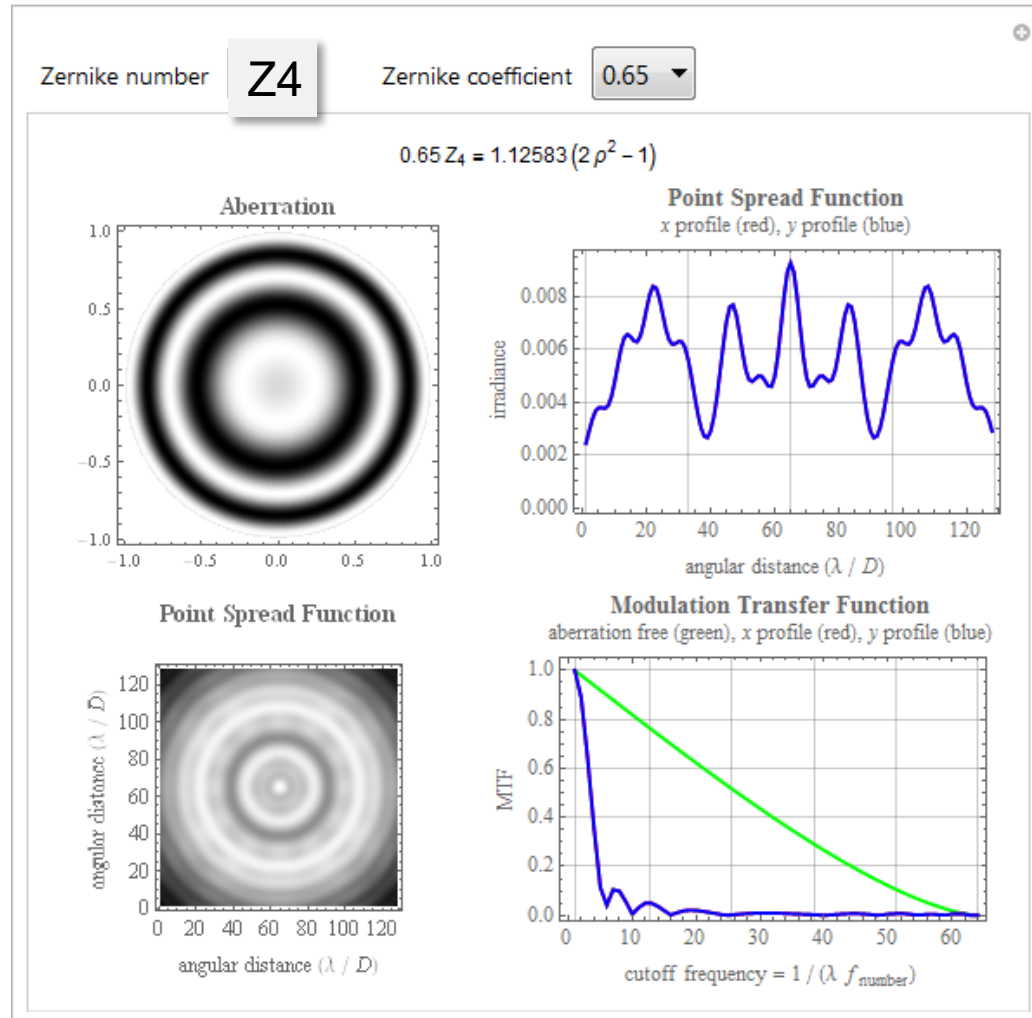
defocus

Zernike Z4 ($Z_{2,0}$), „defocus“ PSF, MTF



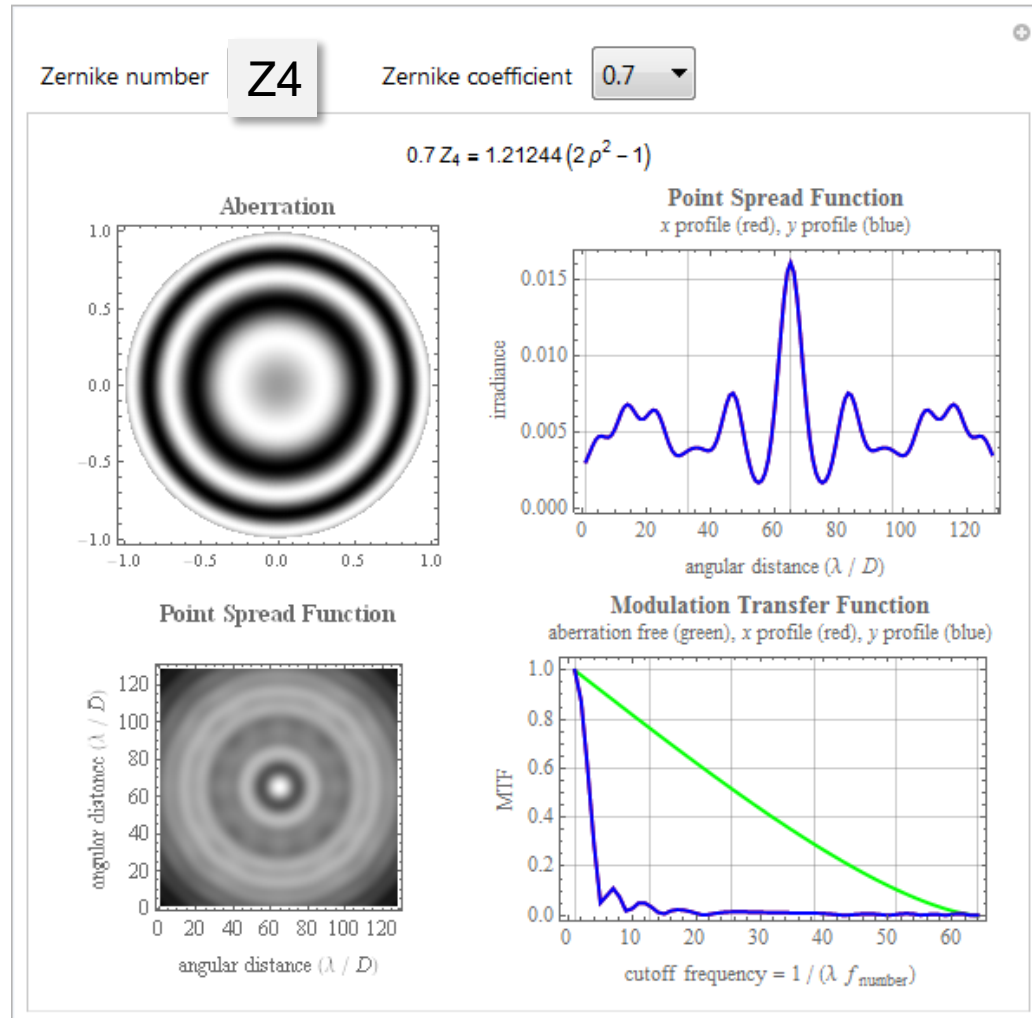
defocus

Zernike Z4 ($Z_{2,0}$), „defocus“ PSF, MTF



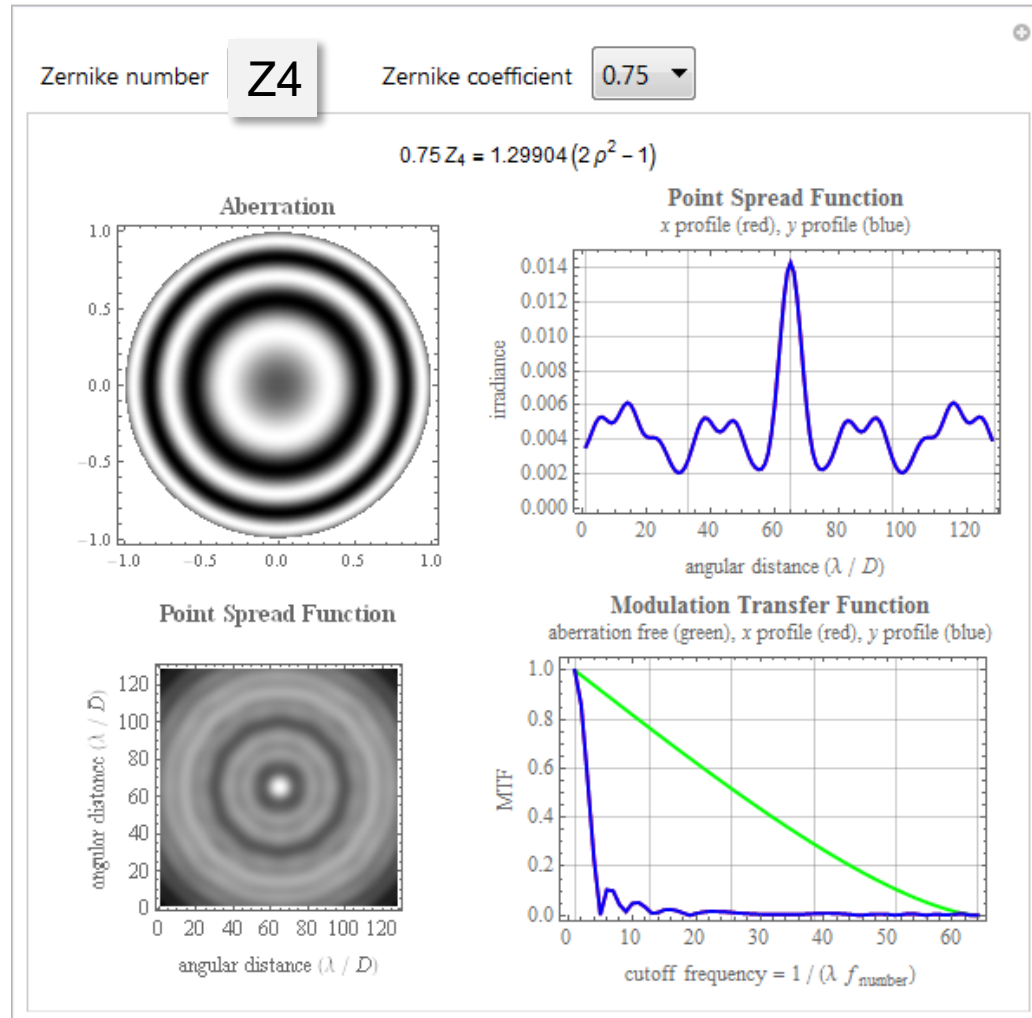
defocus

Zernike Z4 ($Z_{2,0}$), „defocus“ PSF, MTF



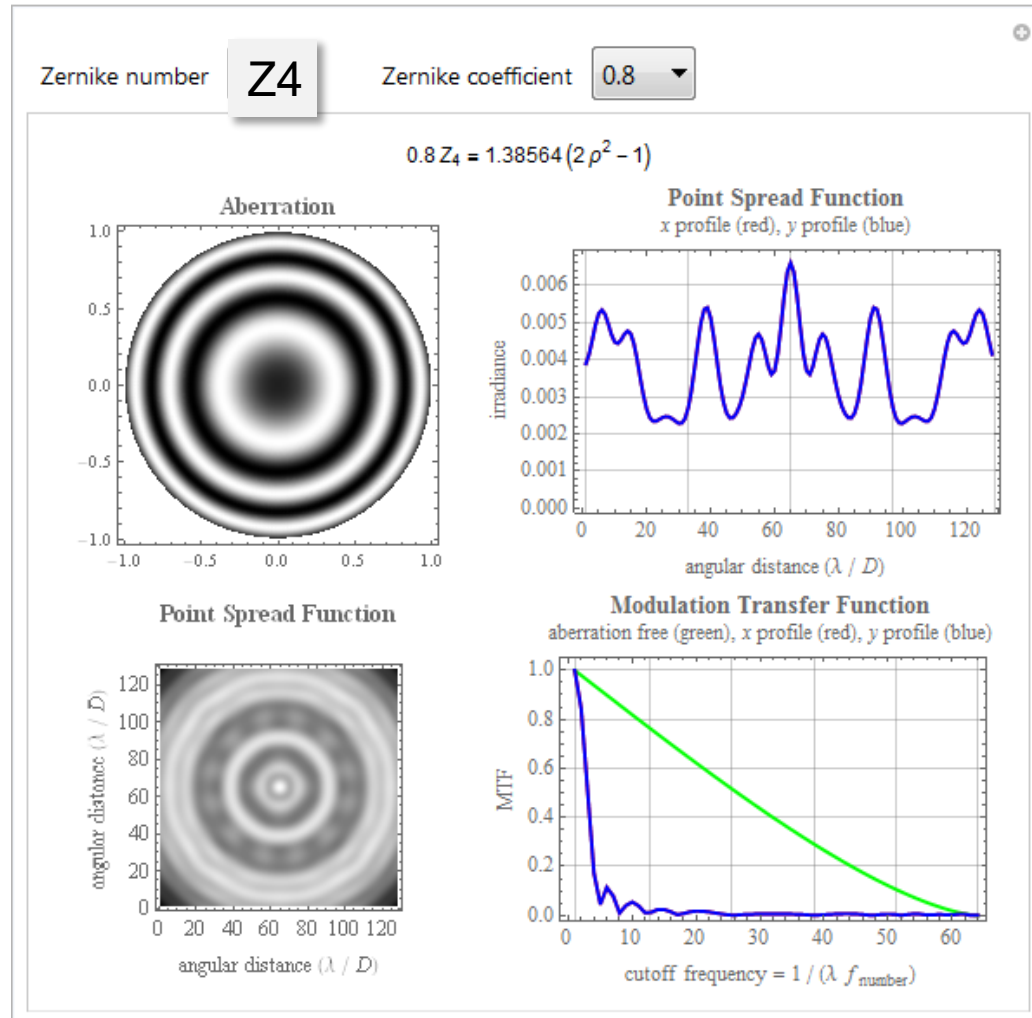
defocus

Zernike Z4 ($Z_{2,0}$), „defocus“ PSF, MTF



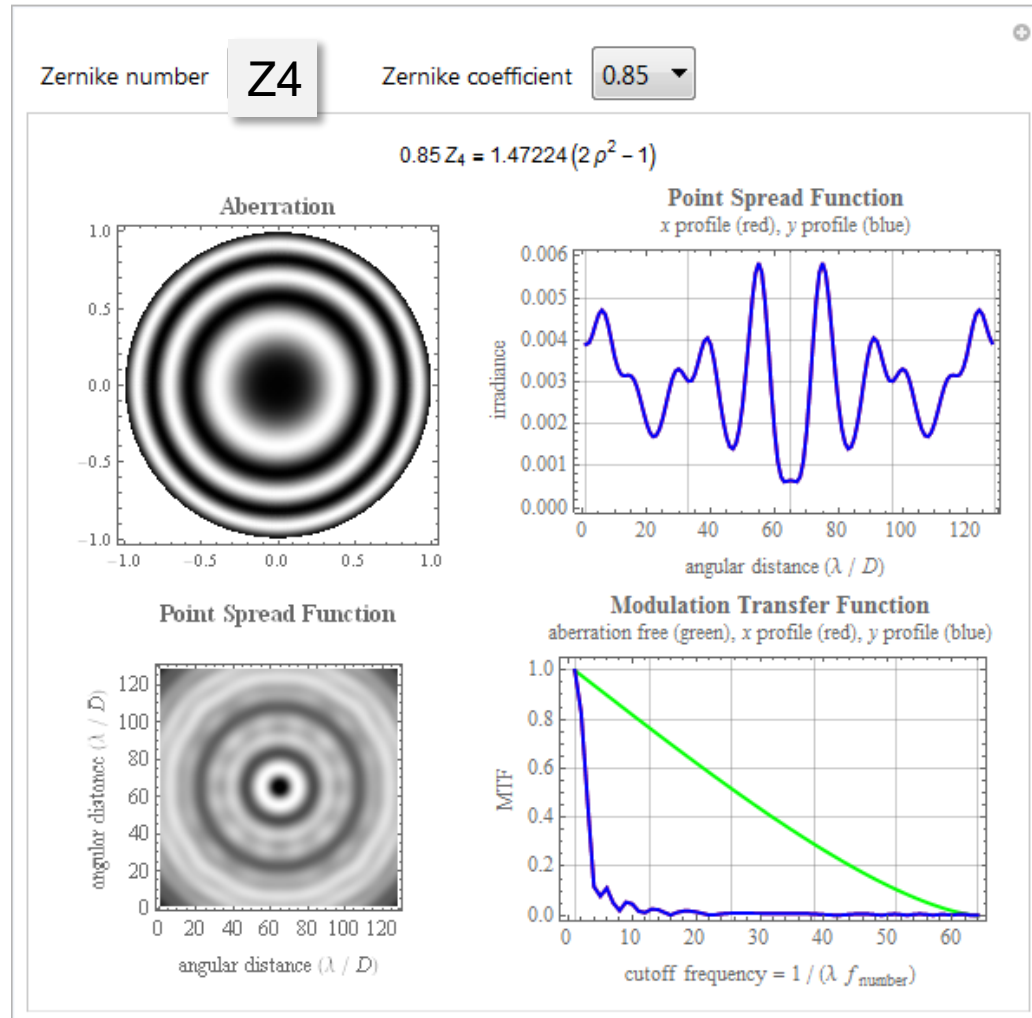
defocus

Zernike Z4 ($Z_{2,0}$), „defocus“ PSF, MTF



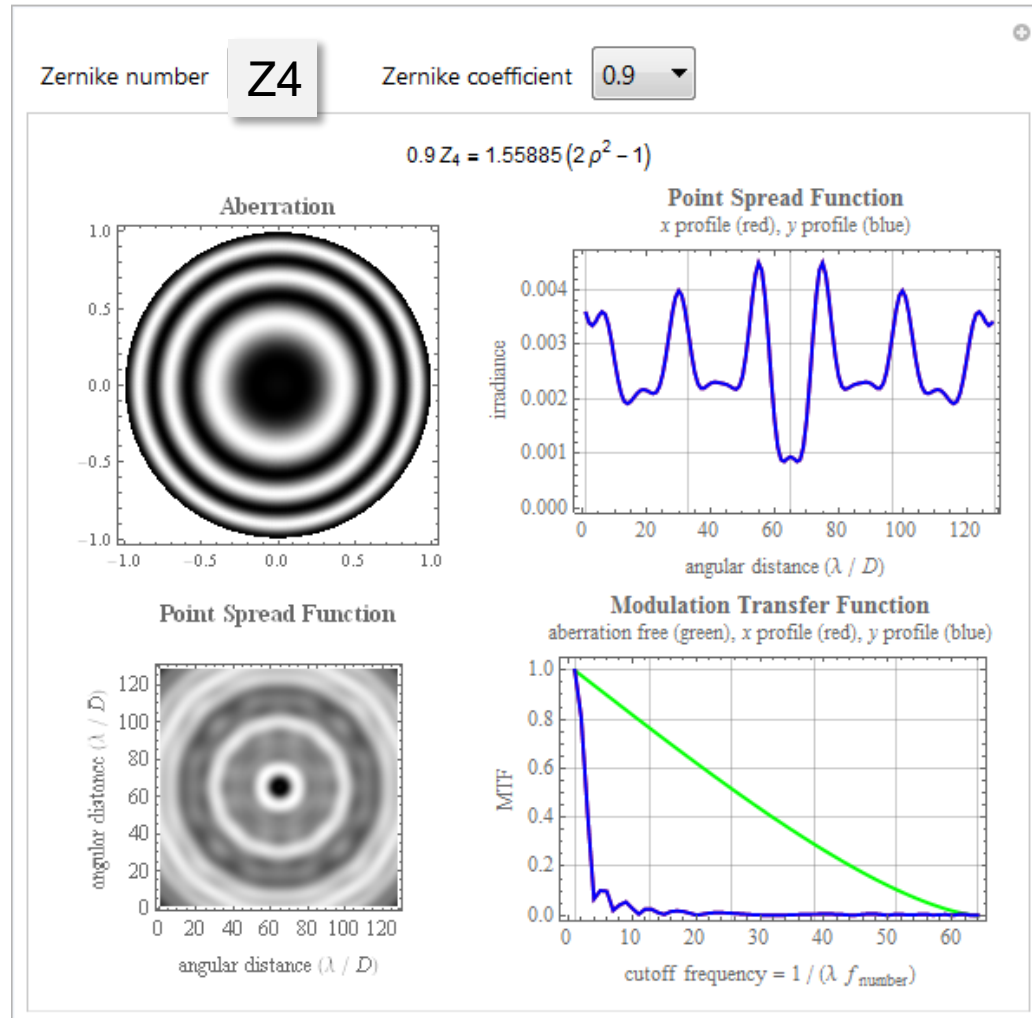
defocus

Zernike Z4 ($Z_{2,0}$), „defocus“ PSF, MTF



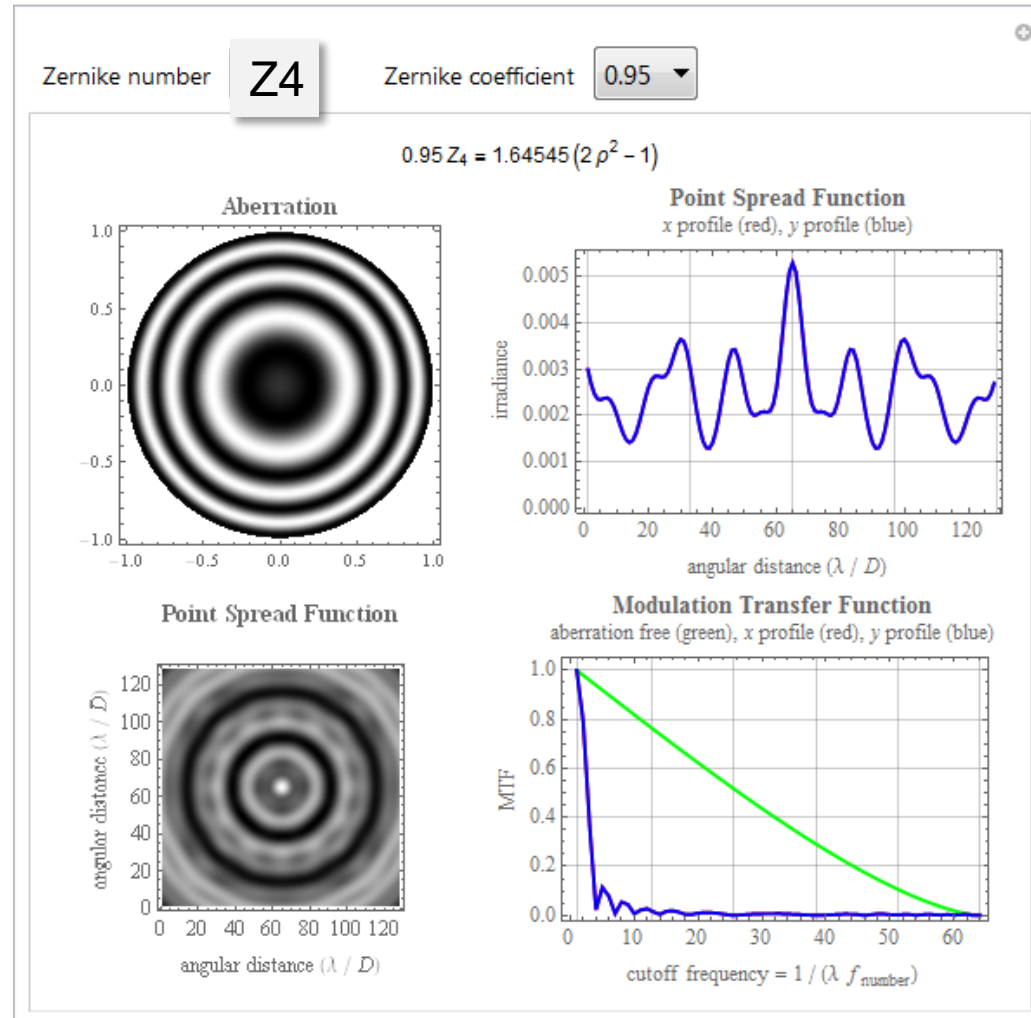
defocus

Zernike Z4 ($Z_{2,0}$), „defocus“ PSF, MTF



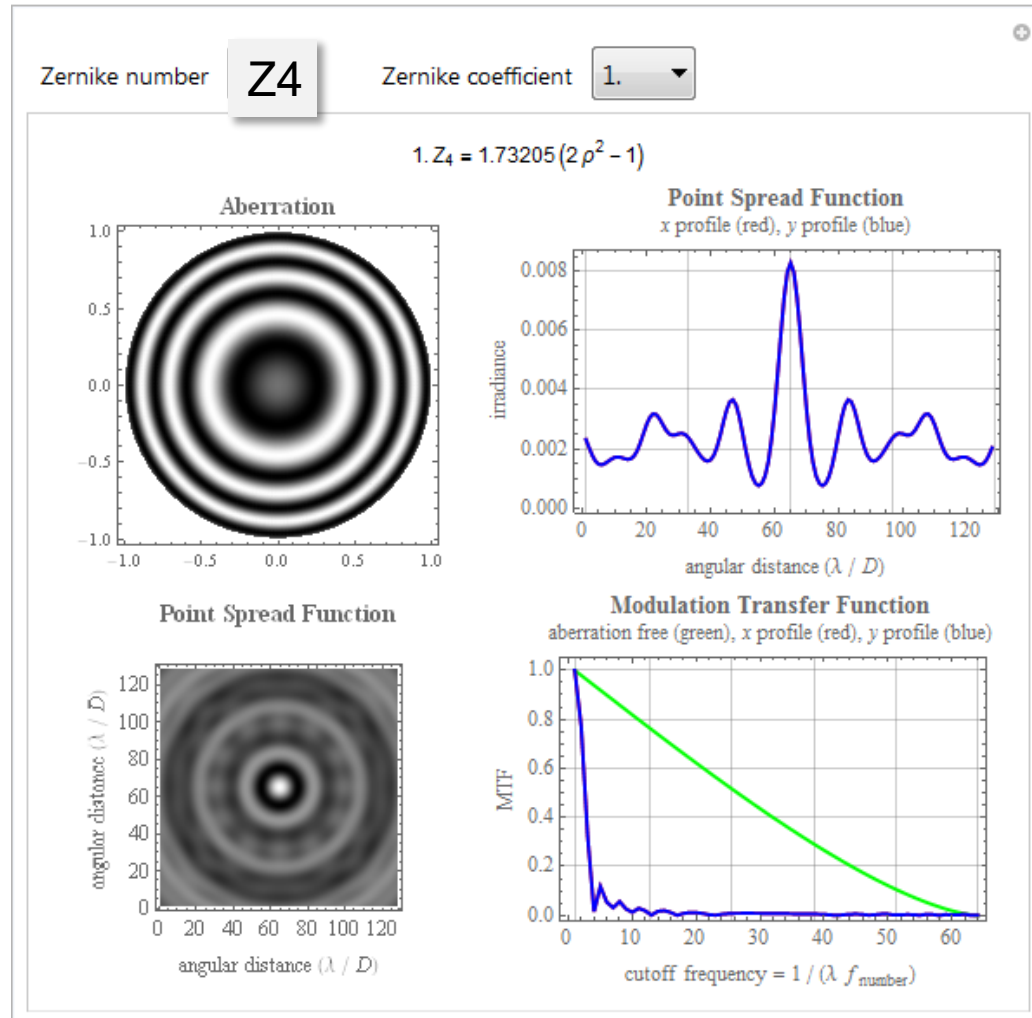
defocus

Zernike Z4 ($Z_{2,0}$), „defocus“ PSF, MTF



defocus

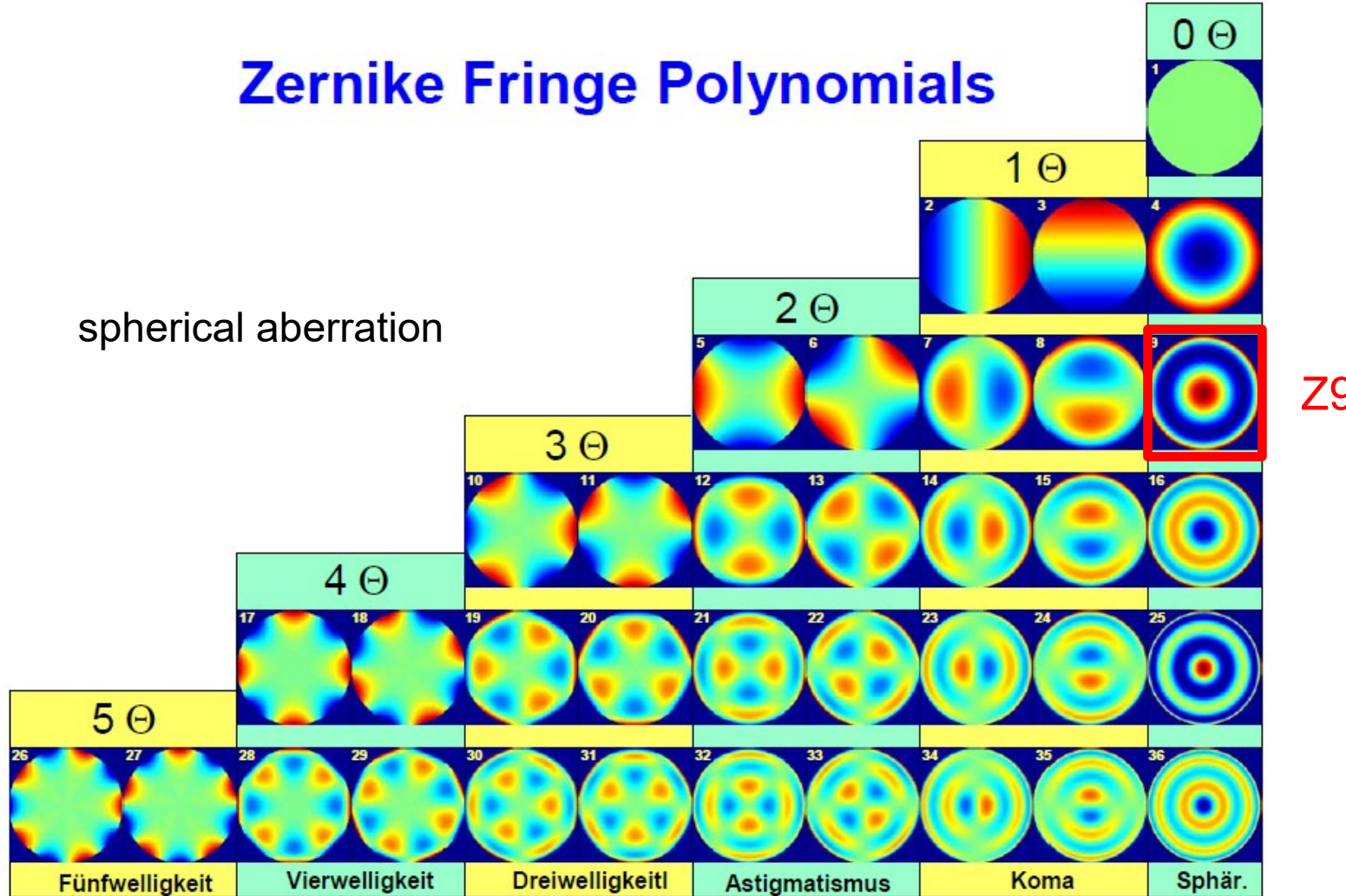
Zernike Z4 ($Z_{2,0}$), „defocus“ PSF, MTF



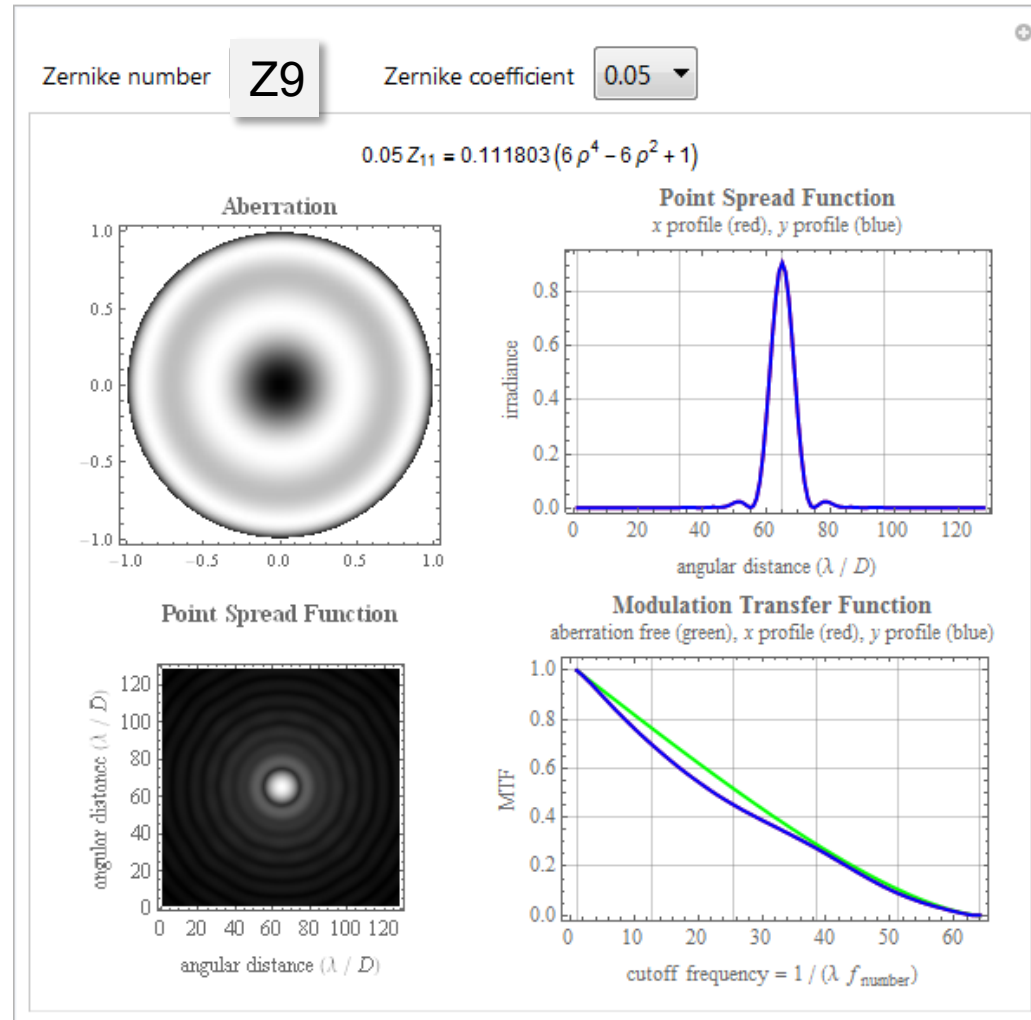
defocus

Zernike Fringe Polynomials

spherical aberration

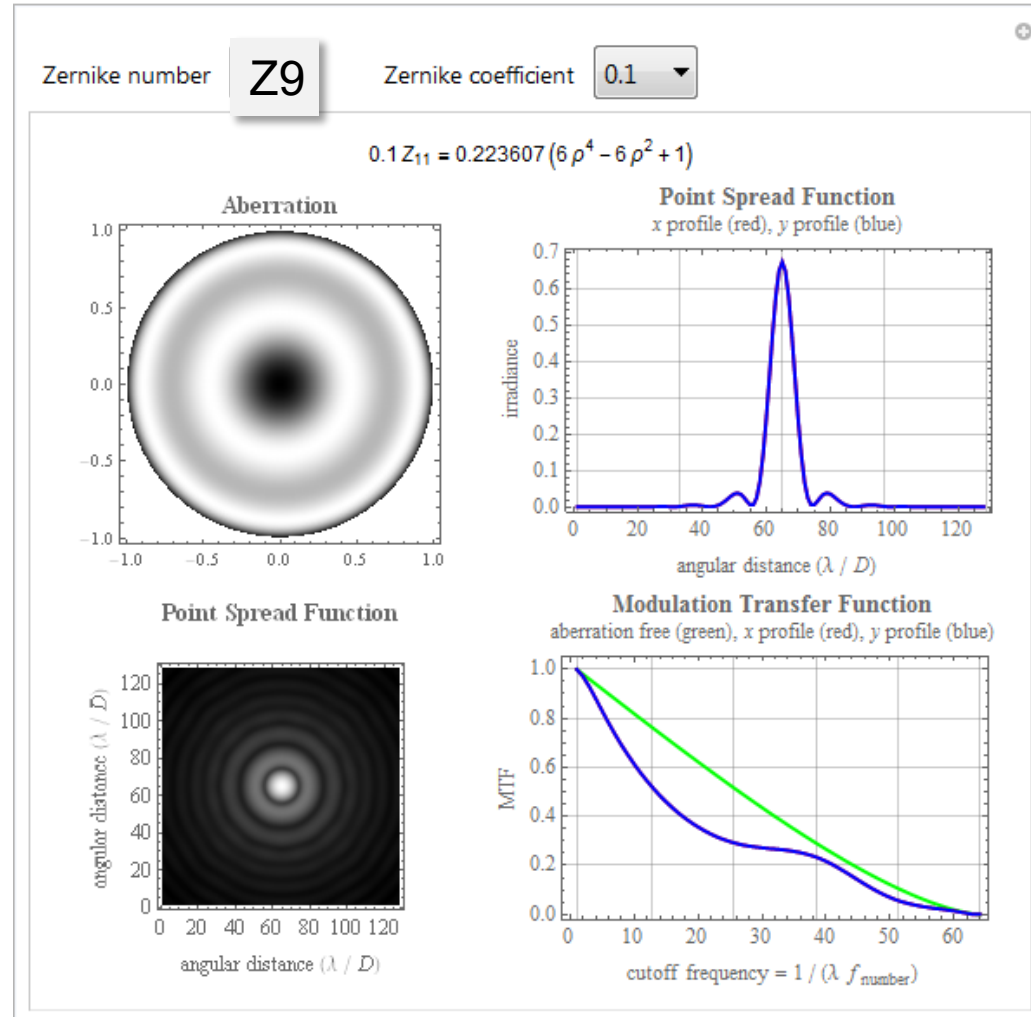


Zernike Z9 ($Z_{4,0}$), „spherical aberration“ PSF, MTF



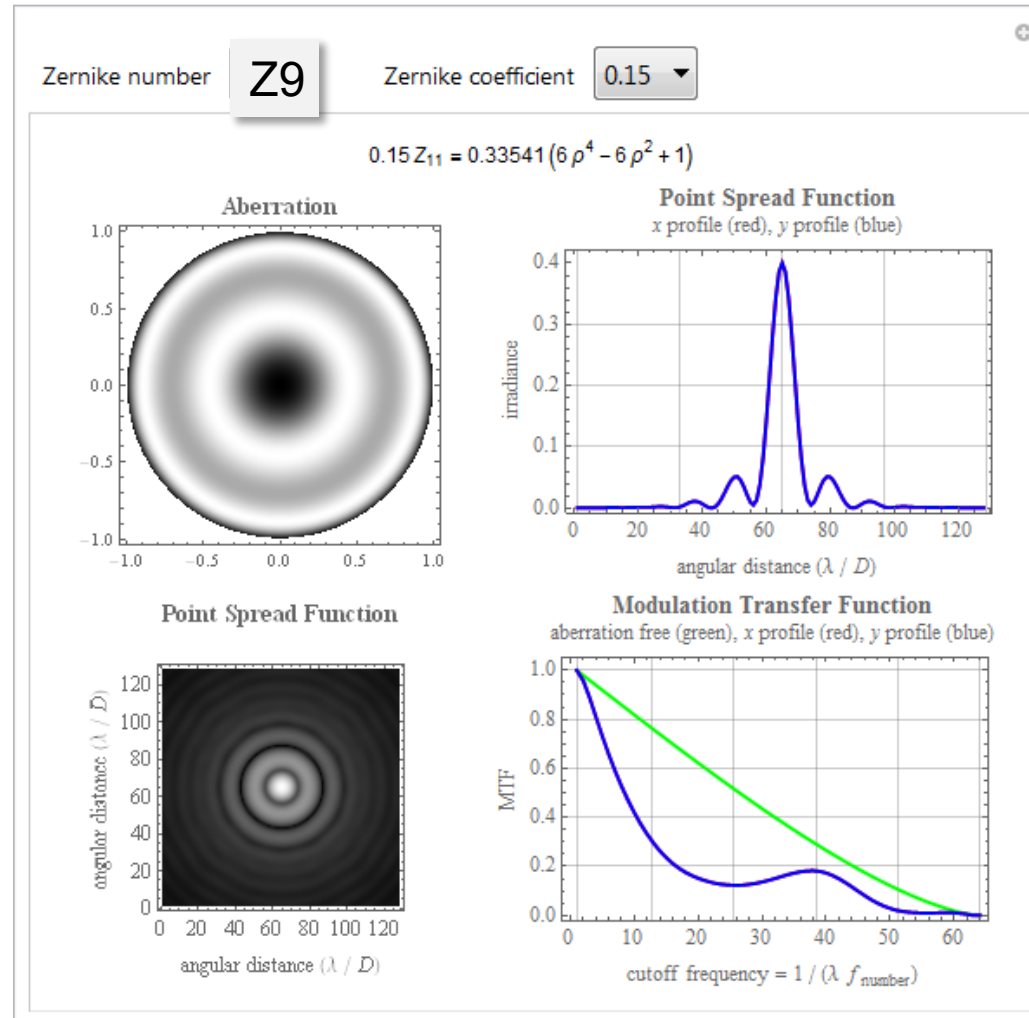
spherical aberration

Zernike Z9 ($Z_{4,0}$), „spherical aberration“ PSF, MTF



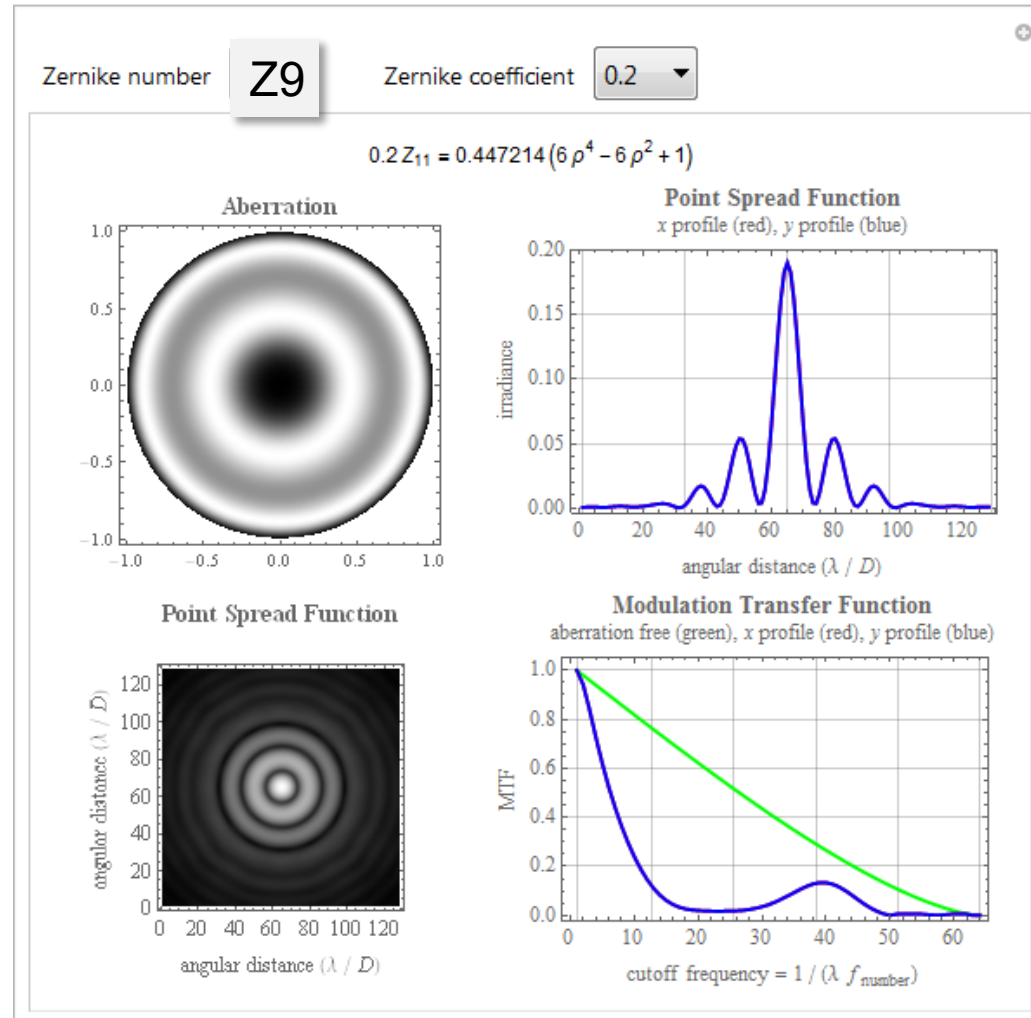
spherical aberration

Zernike Z9 ($Z_{4,0}$), „spherical aberration“ PSF, MTF



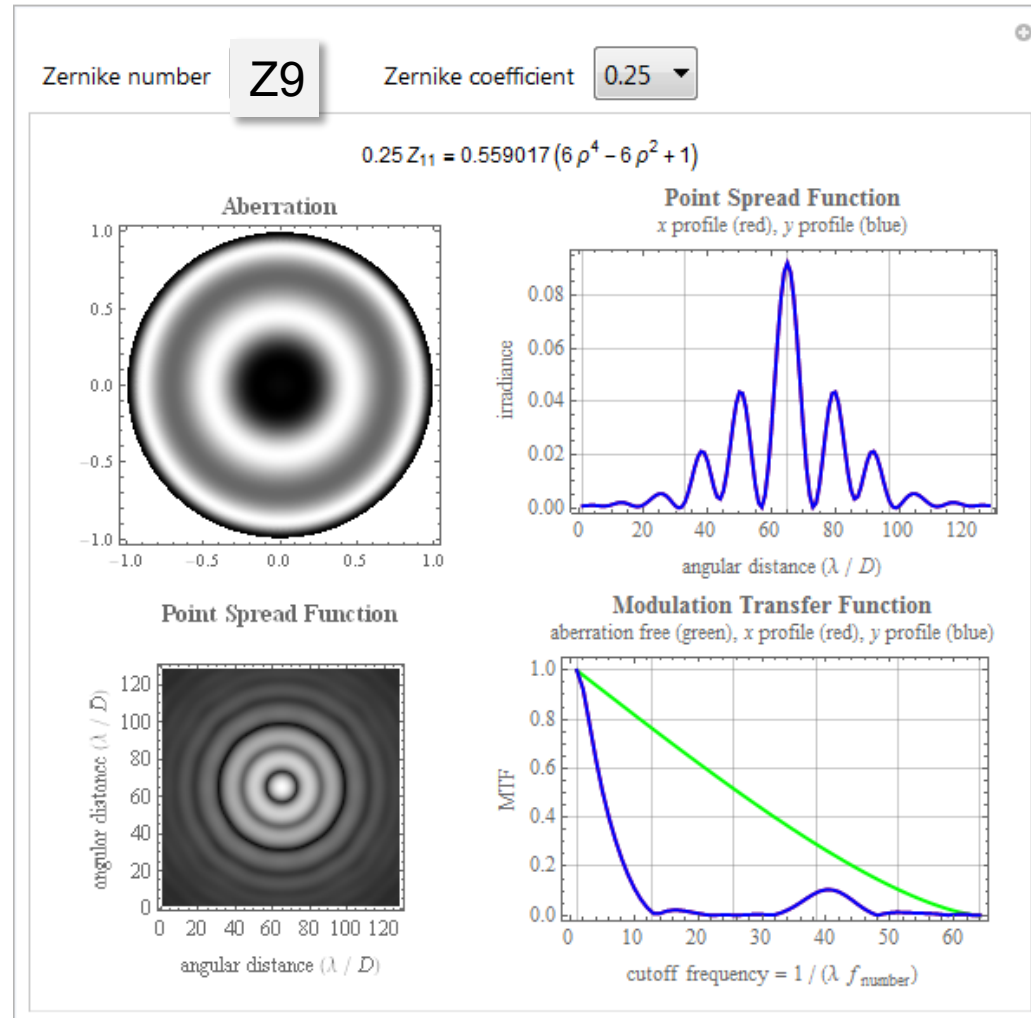
spherical aberration

Zernike Z9 ($Z_{4,0}$), „spherical aberration“ PSF, MTF



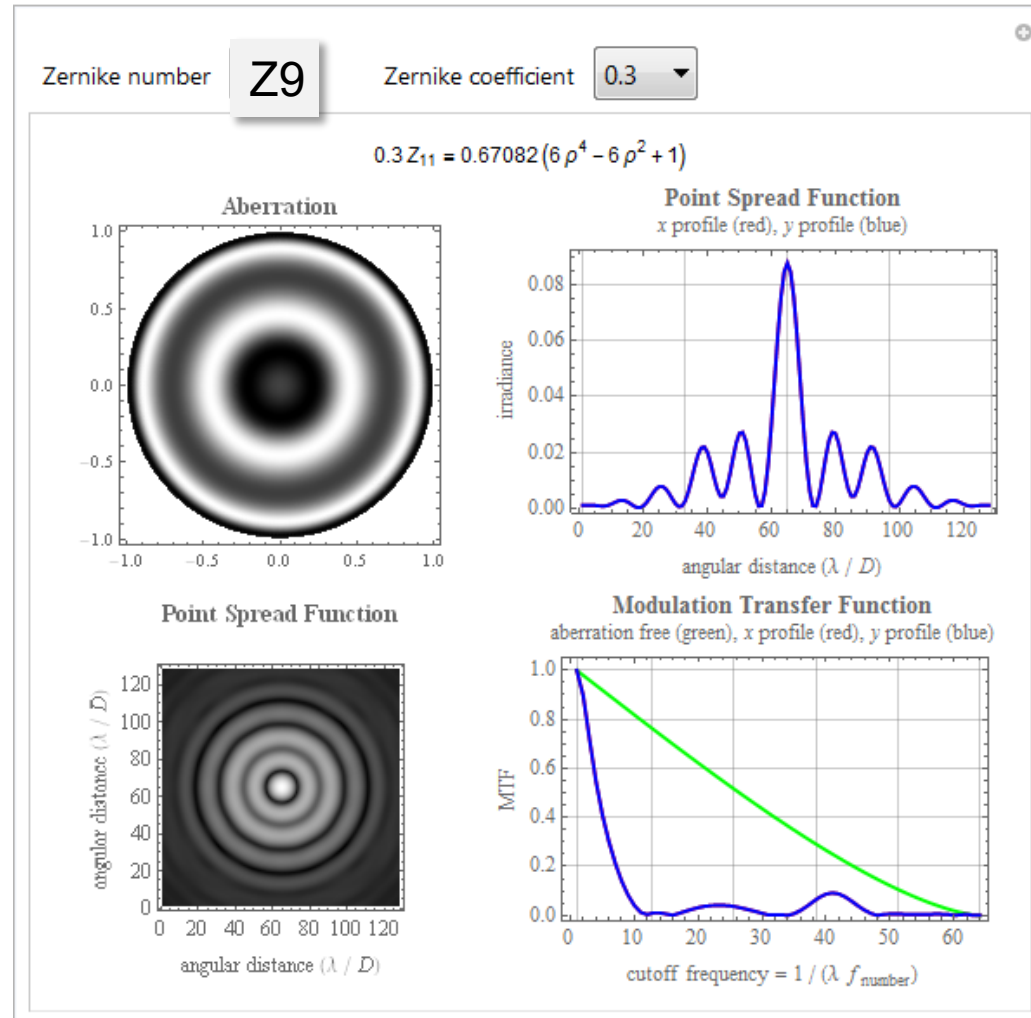
spherical aberration

Zernike Z9 ($Z_{4,0}$), „spherical aberration“ PSF, MTF



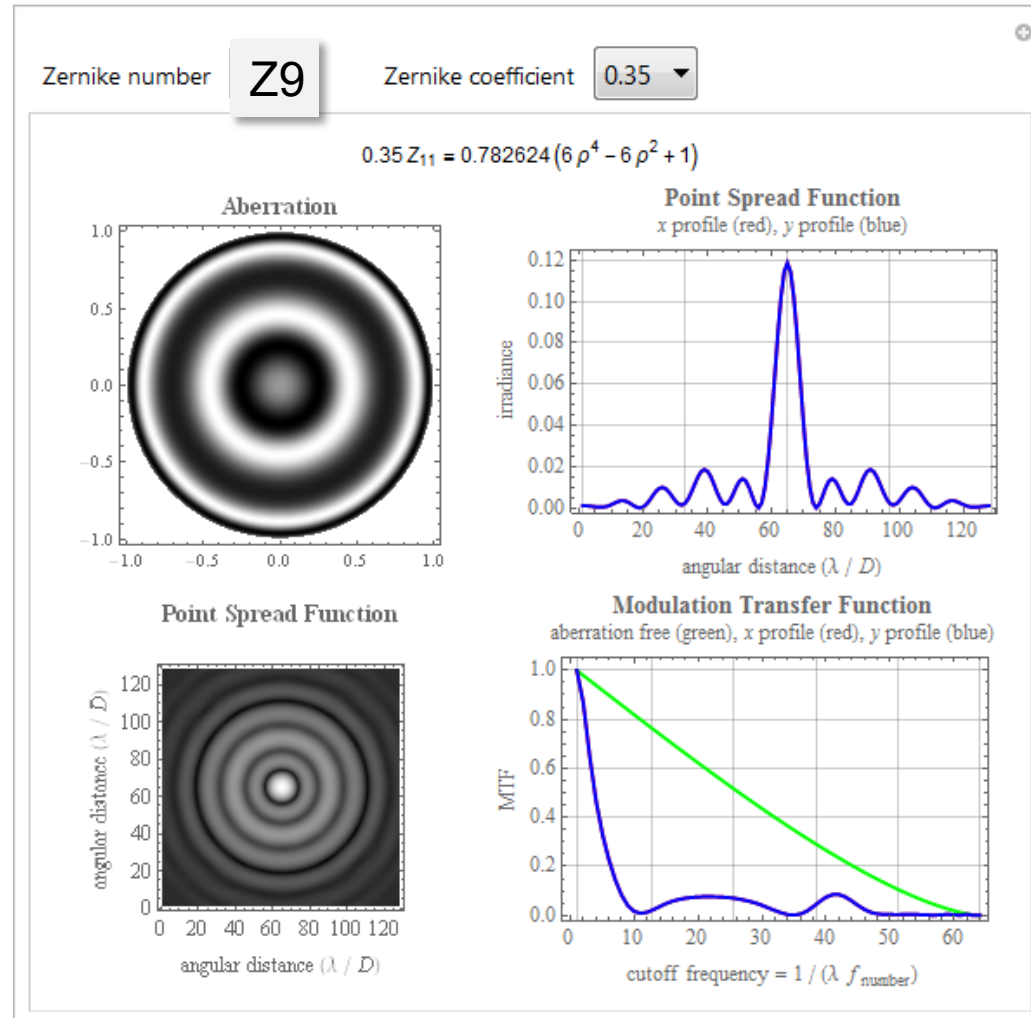
spherical aberration

Zernike Z9 ($Z_{4,0}$), „spherical aberration“ PSF, MTF



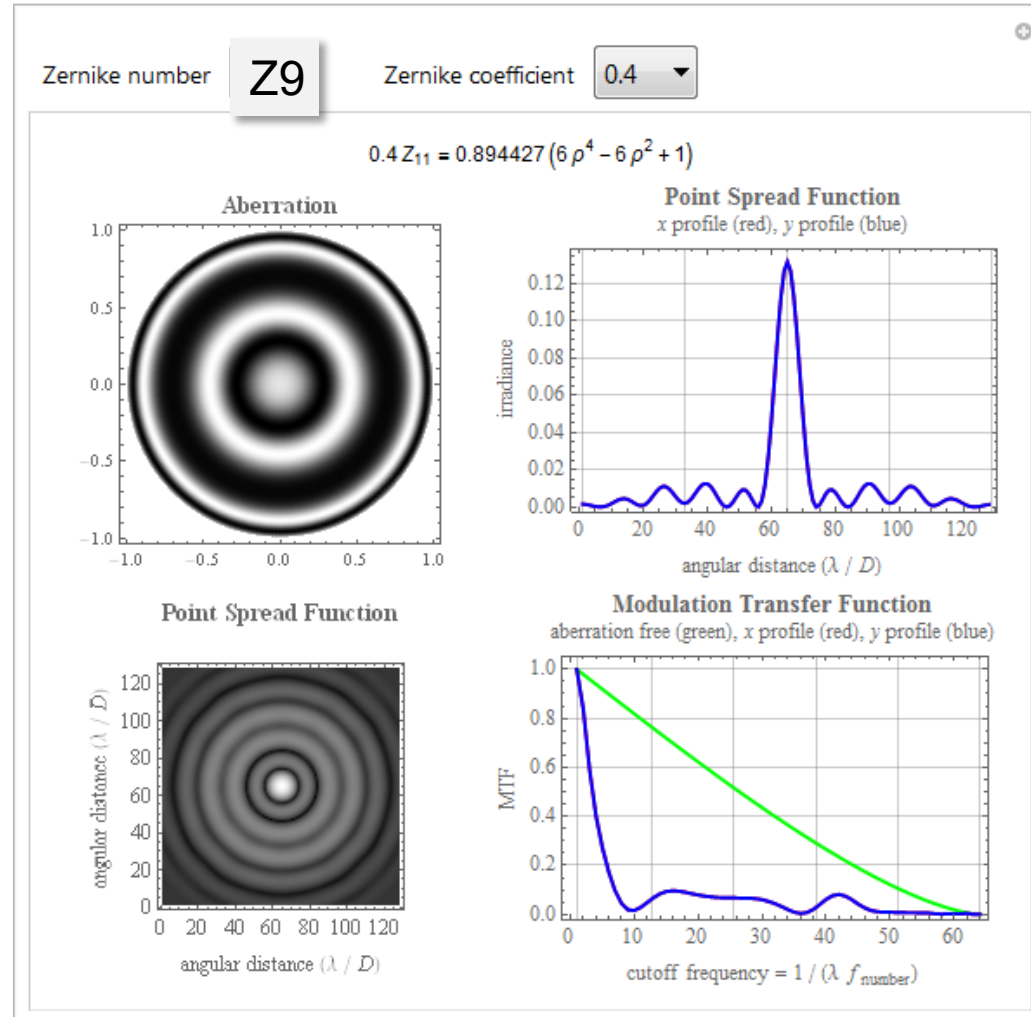
spherical aberration

Zernike Z9 ($Z_{4,0}$), „spherical aberration“ PSF, MTF



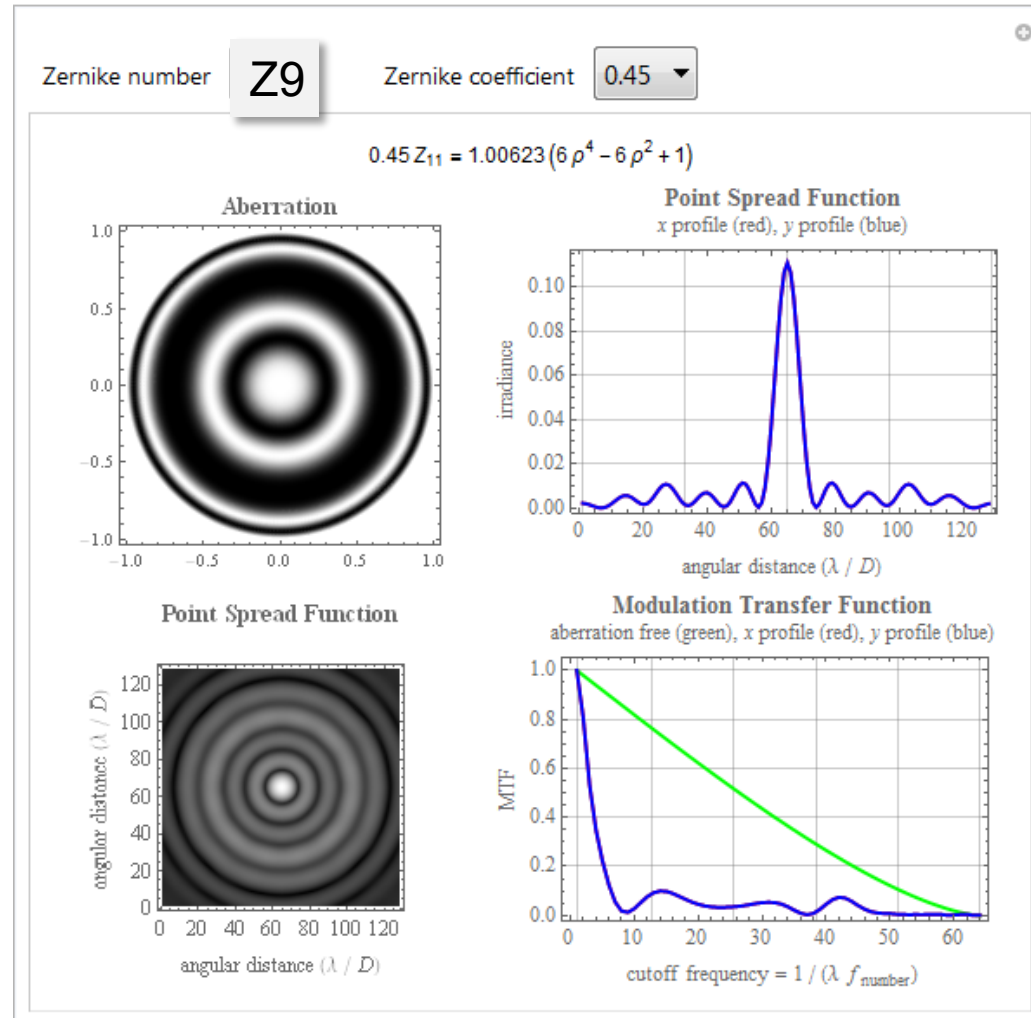
spherical aberration

Zernike Z9 ($Z_{4,0}$), „spherical aberration“ PSF, MTF



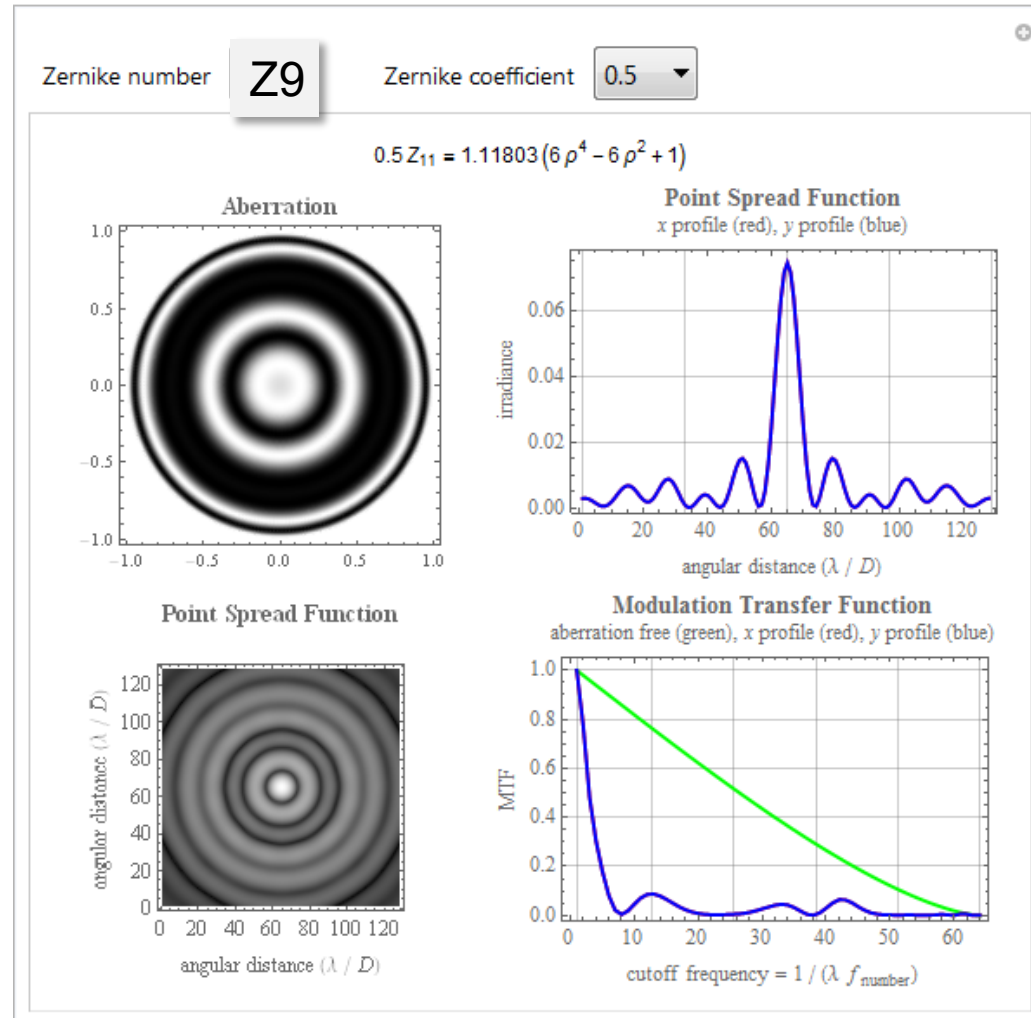
spherical aberration

Zernike Z9 ($Z_{4,0}$), „spherical aberration“ PSF, MTF



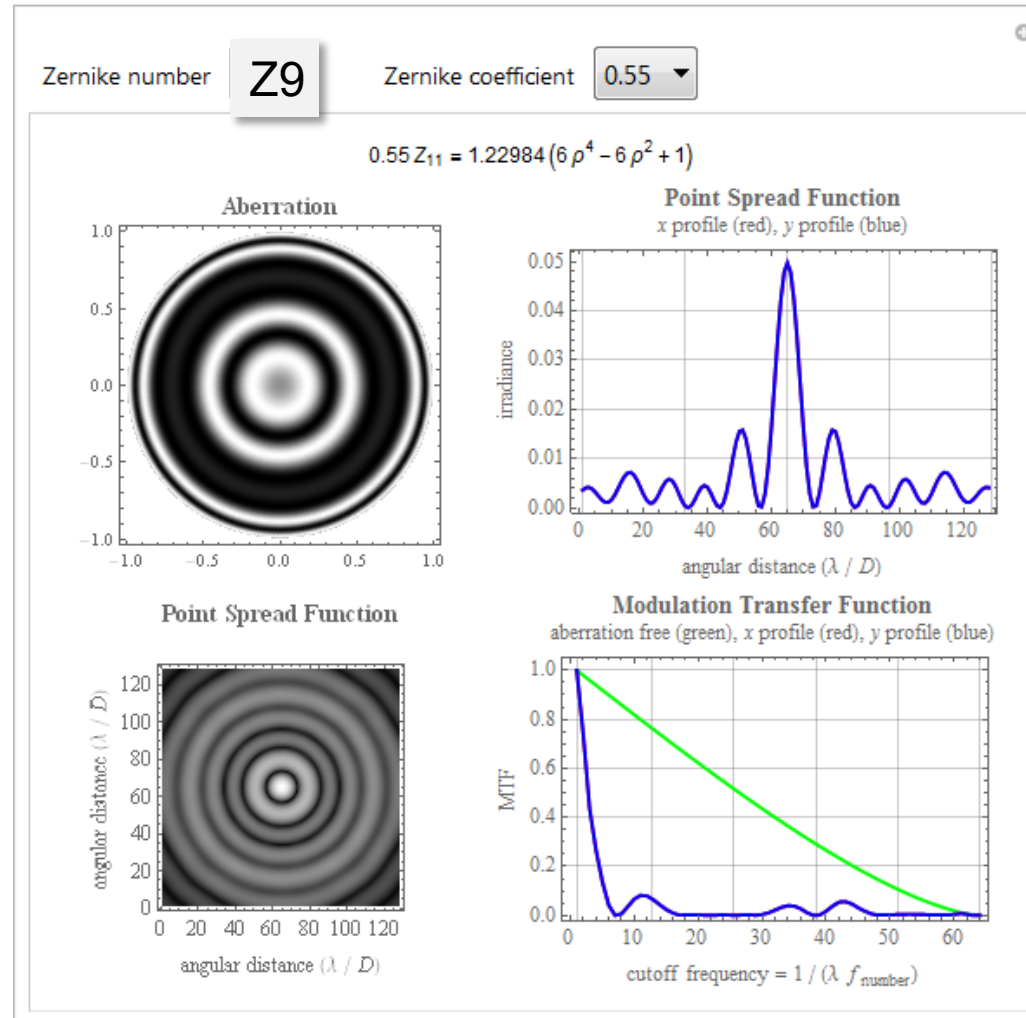
spherical aberration

Zernike Z9 ($Z_{4,0}$), „spherical aberration“ PSF, MTF



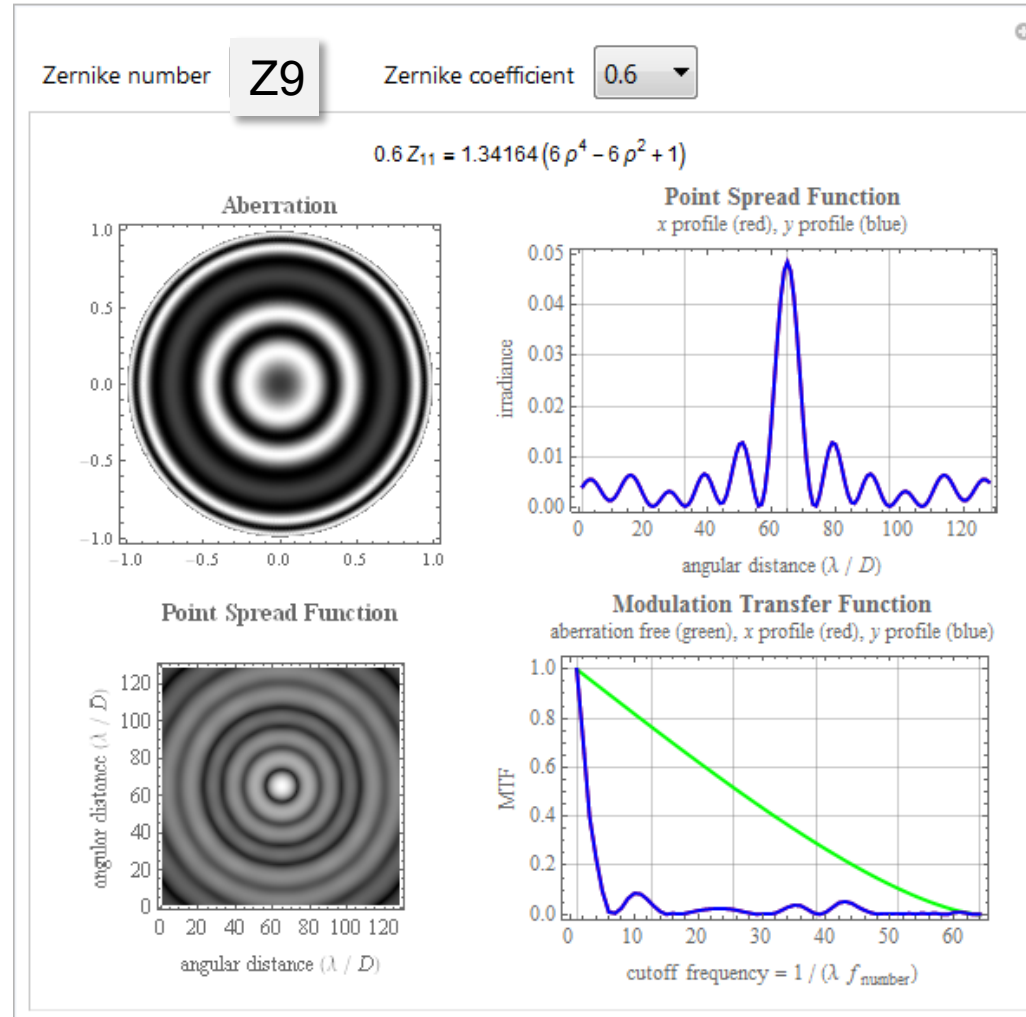
spherical aberration

Zernike Z9 ($Z_{4,0}$), „spherical aberration“ PSF, MTF



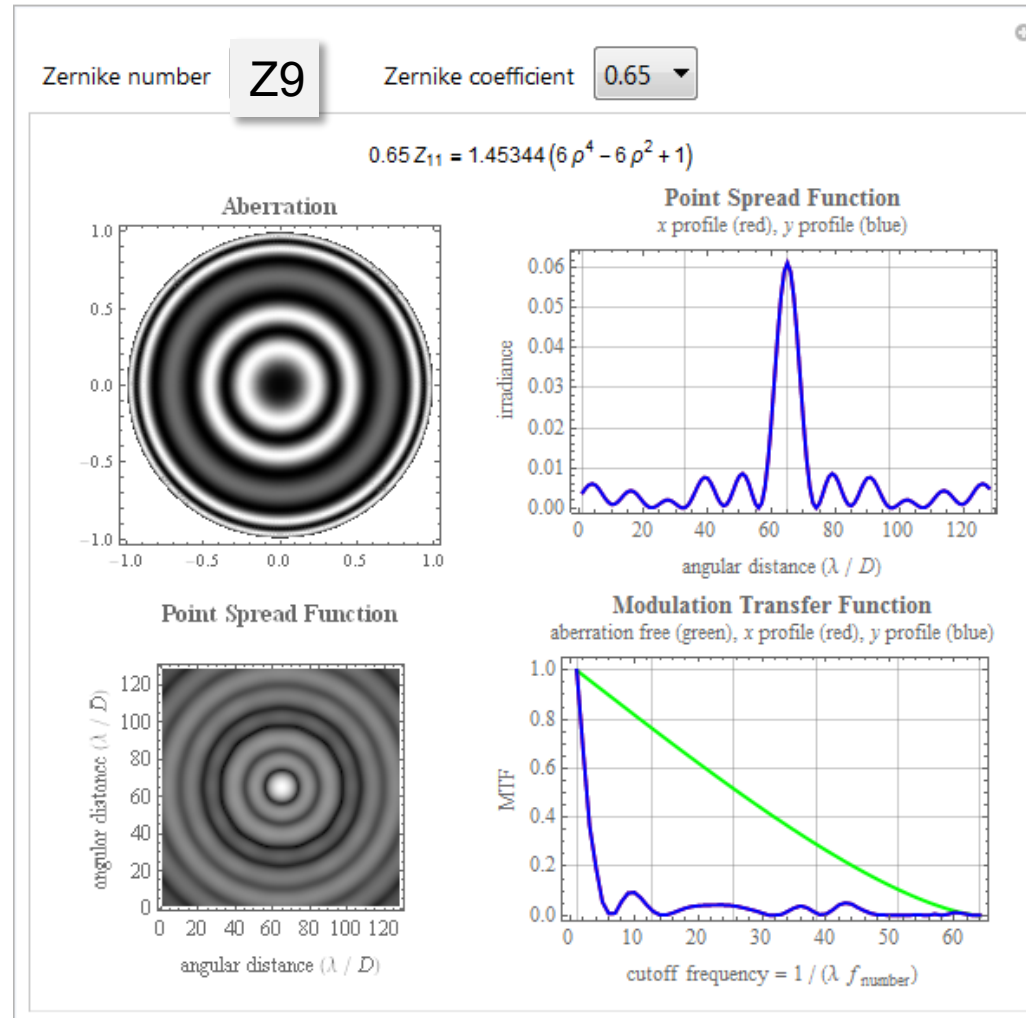
spherical aberration

Zernike Z9 ($Z_{4,0}$), „spherical aberration“ PSF, MTF



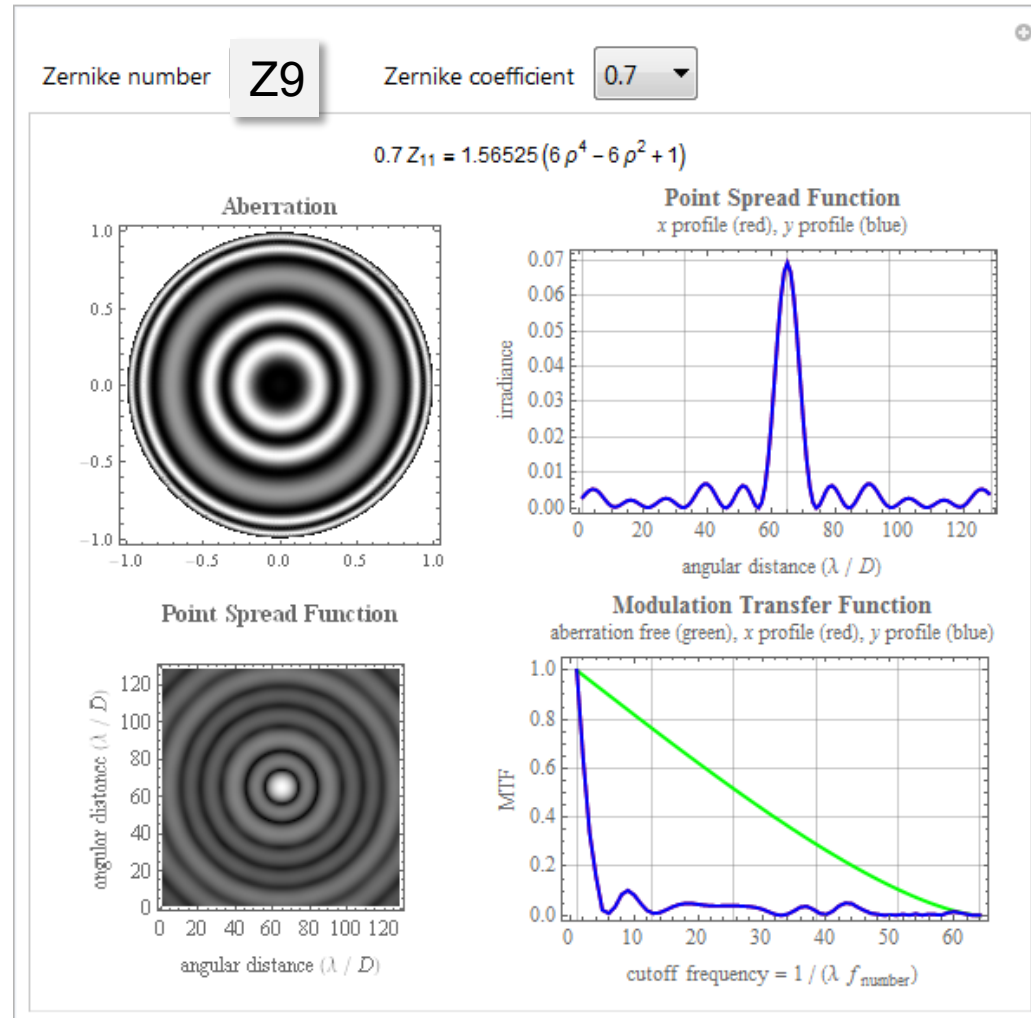
spherical aberration

Zernike Z9 ($Z_{4,0}$), „spherical aberration“ PSF, MTF



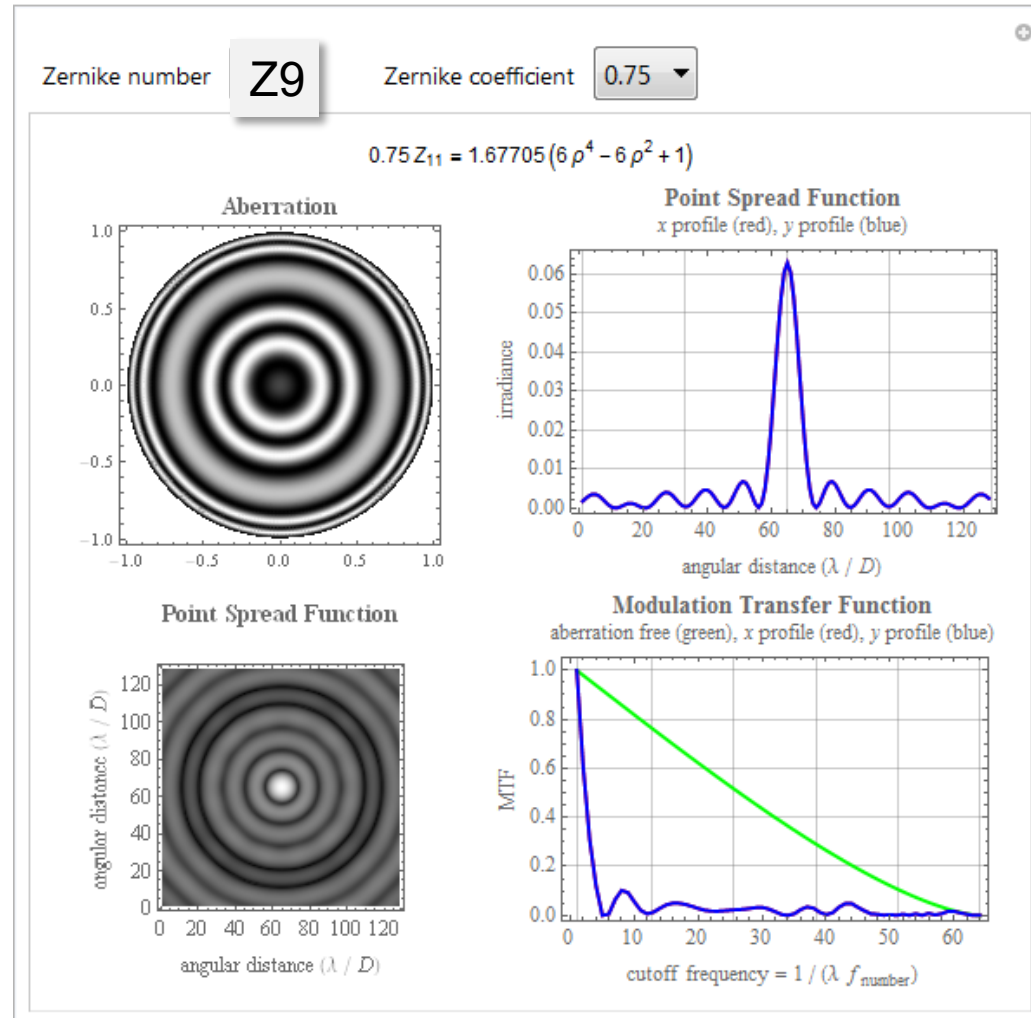
spherical aberration

Zernike Z9 ($Z_{4,0}$), „spherical aberration“ PSF, MTF



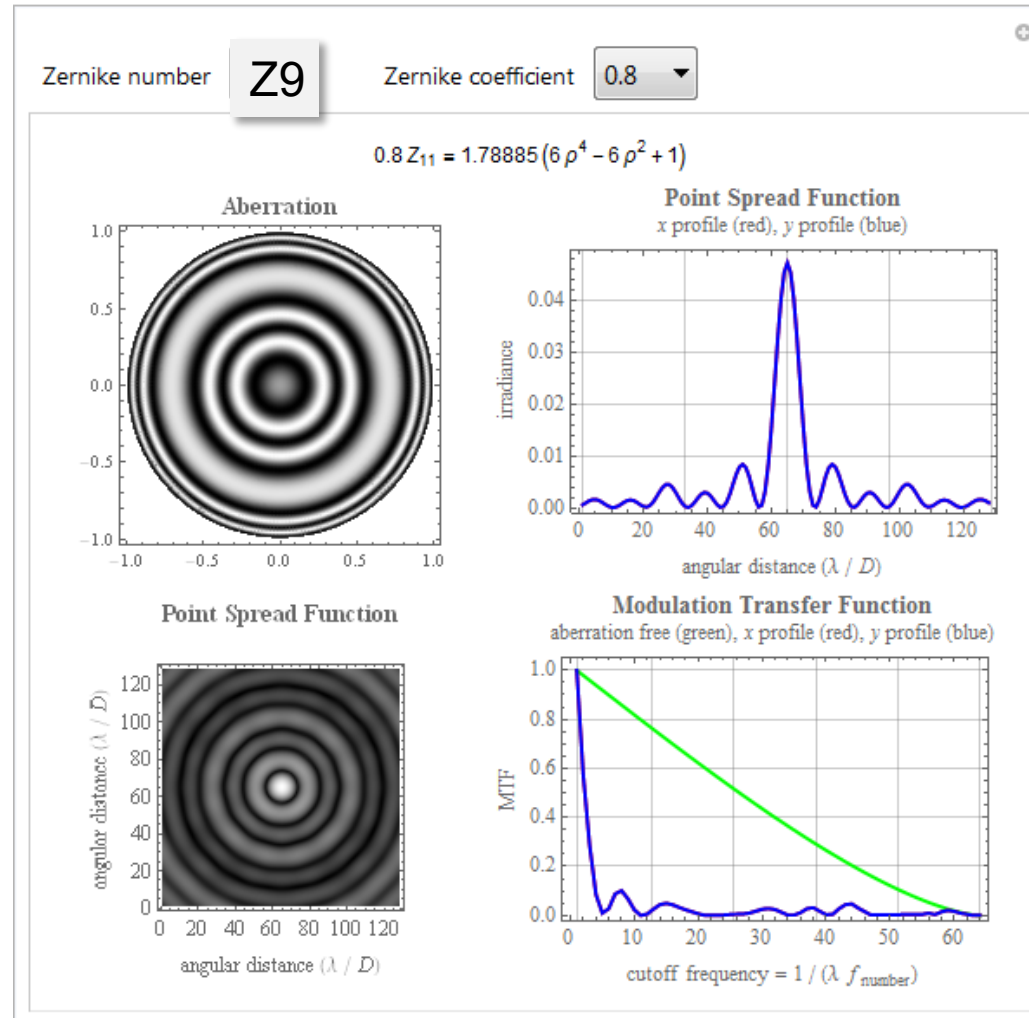
spherical aberration

Zernike Z9 ($Z_{4,0}$), „spherical aberration“ PSF, MTF



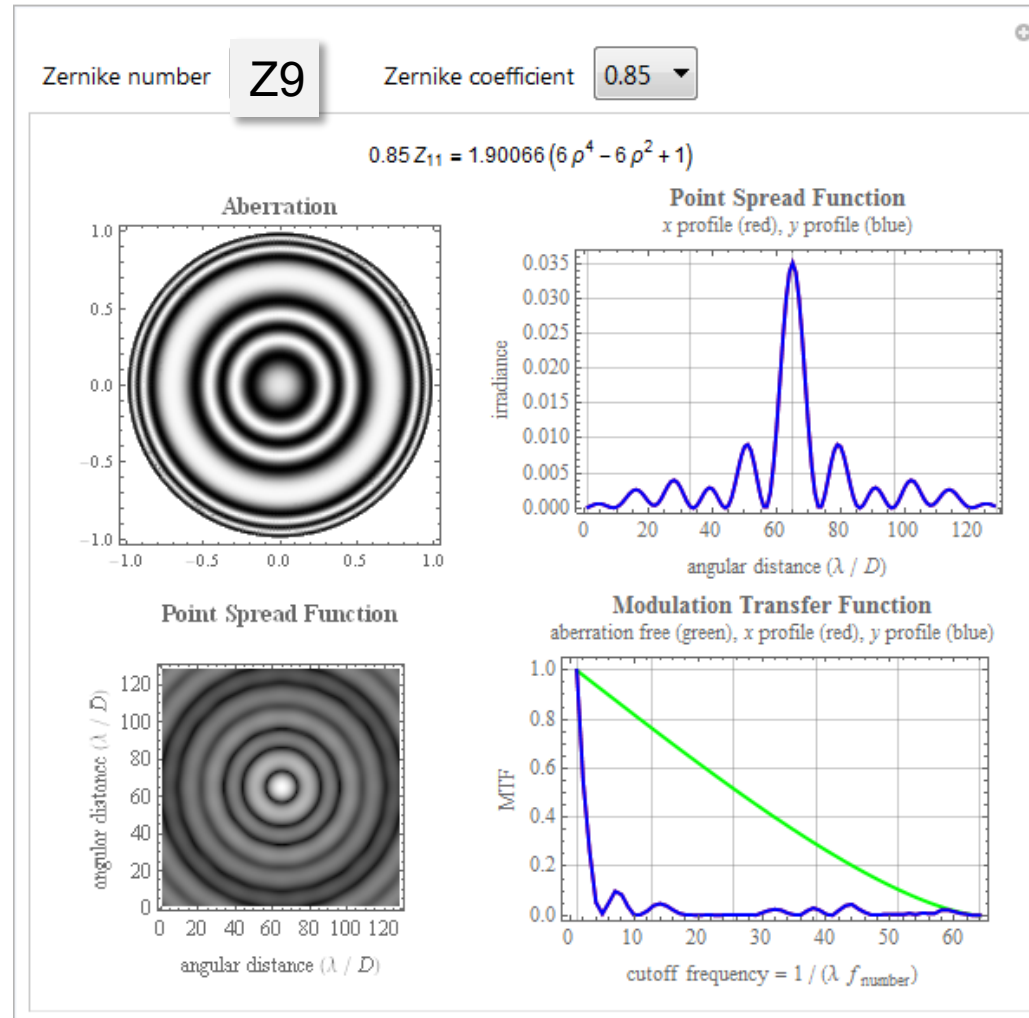
spherical aberration

Zernike Z9 ($Z_{4,0}$), „spherical aberration“ PSF, MTF



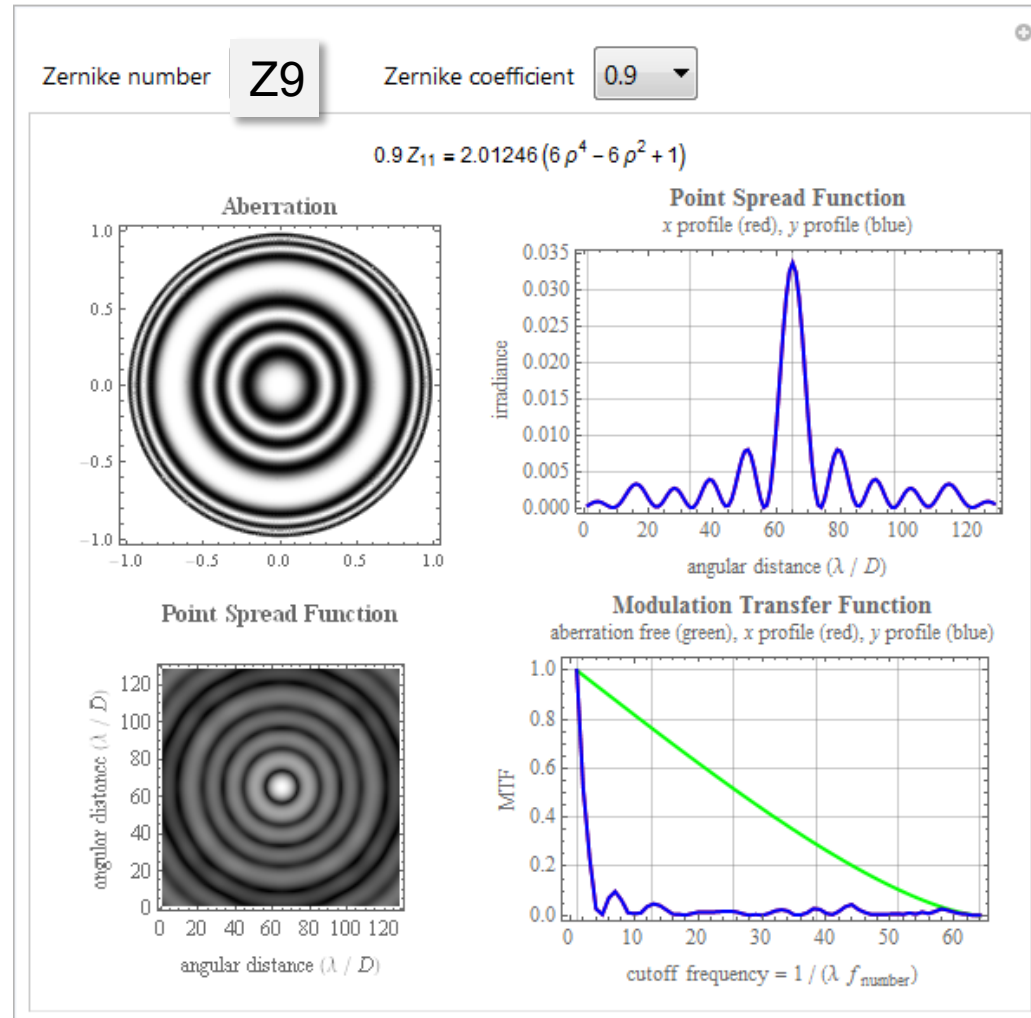
spherical aberration

Zernike Z9 ($Z_{4,0}$), „spherical aberration“ PSF, MTF



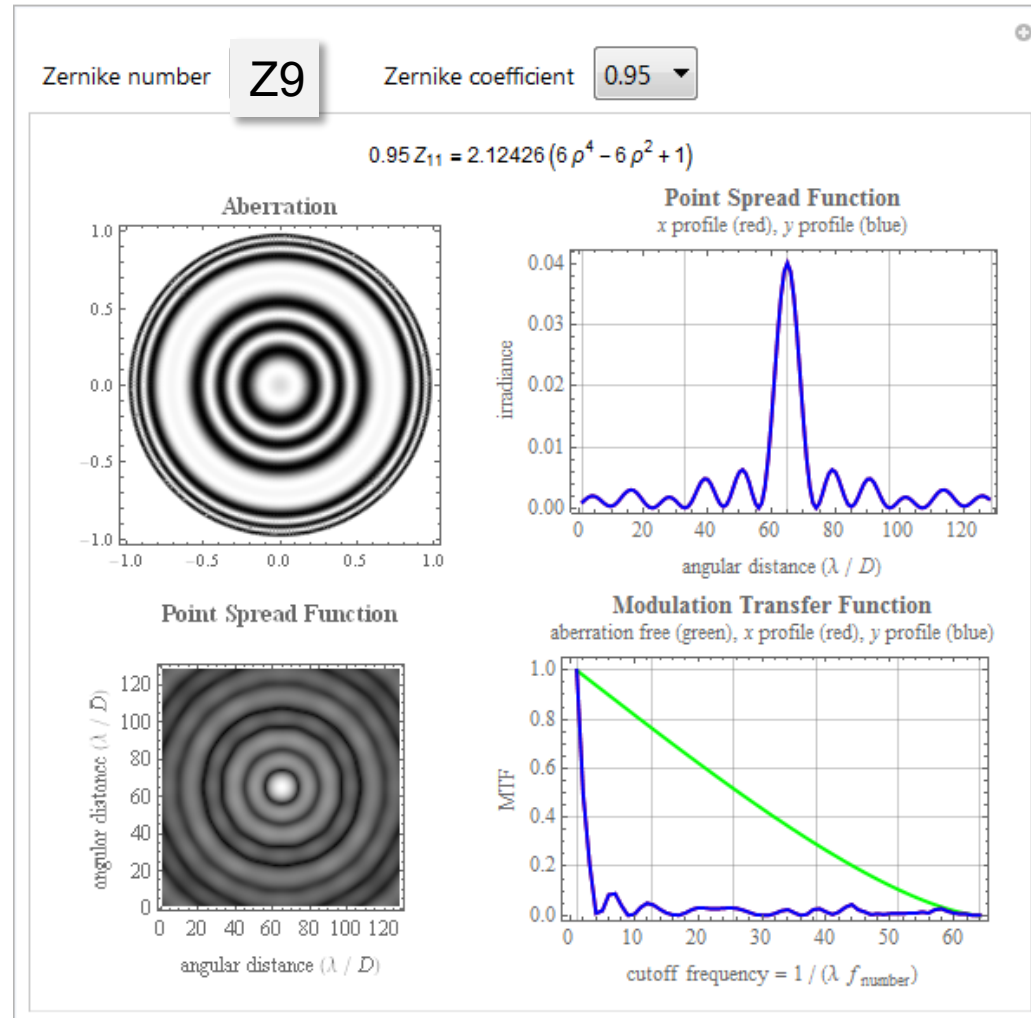
spherical aberration

Zernike Z9 ($Z_{4,0}$), „spherical aberration“ PSF, MTF



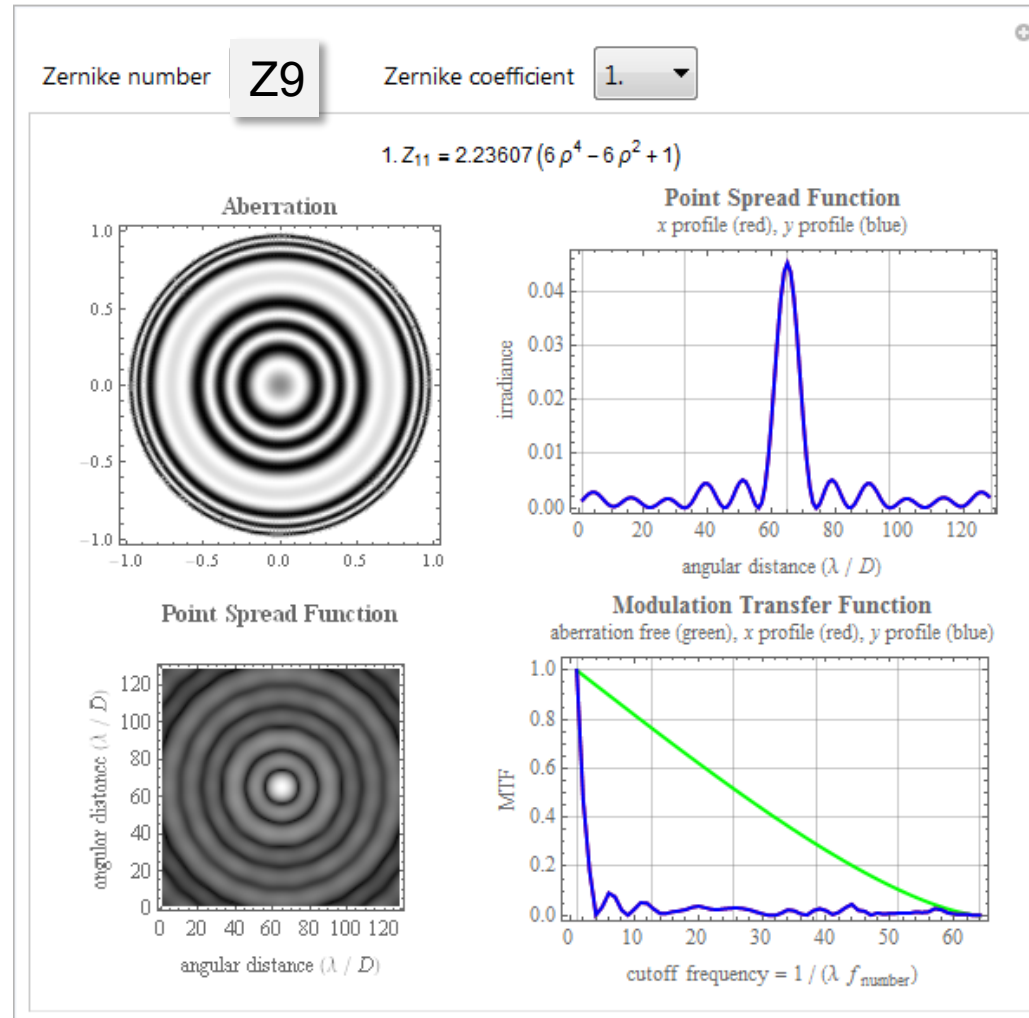
spherical aberration

Zernike Z9 ($Z_{4,0}$), „spherical aberration“ PSF, MTF



spherical aberration

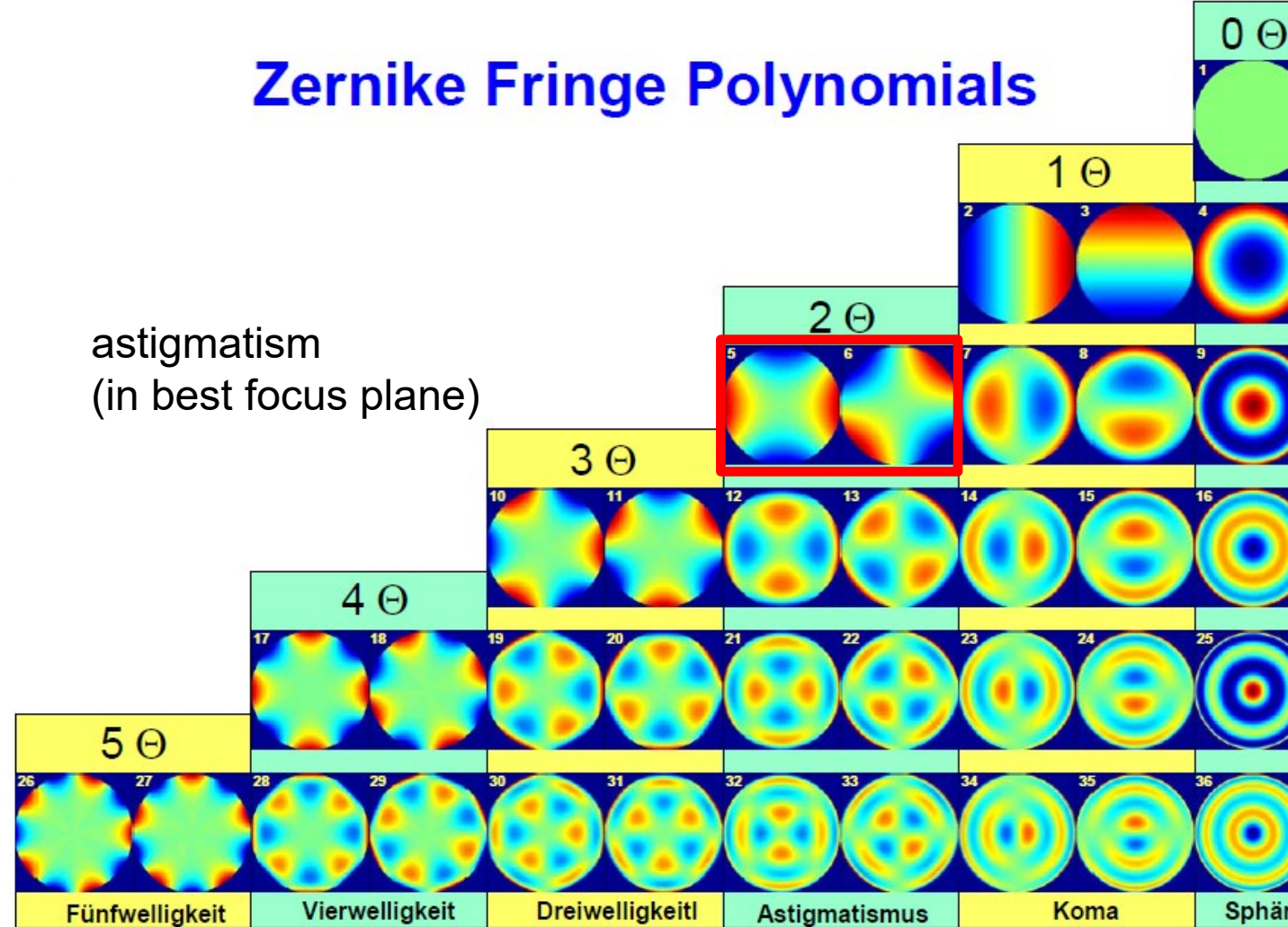
Zernike Z9 ($Z_{4,0}$), „spherical aberration“ PSF, MTF



spherical aberration

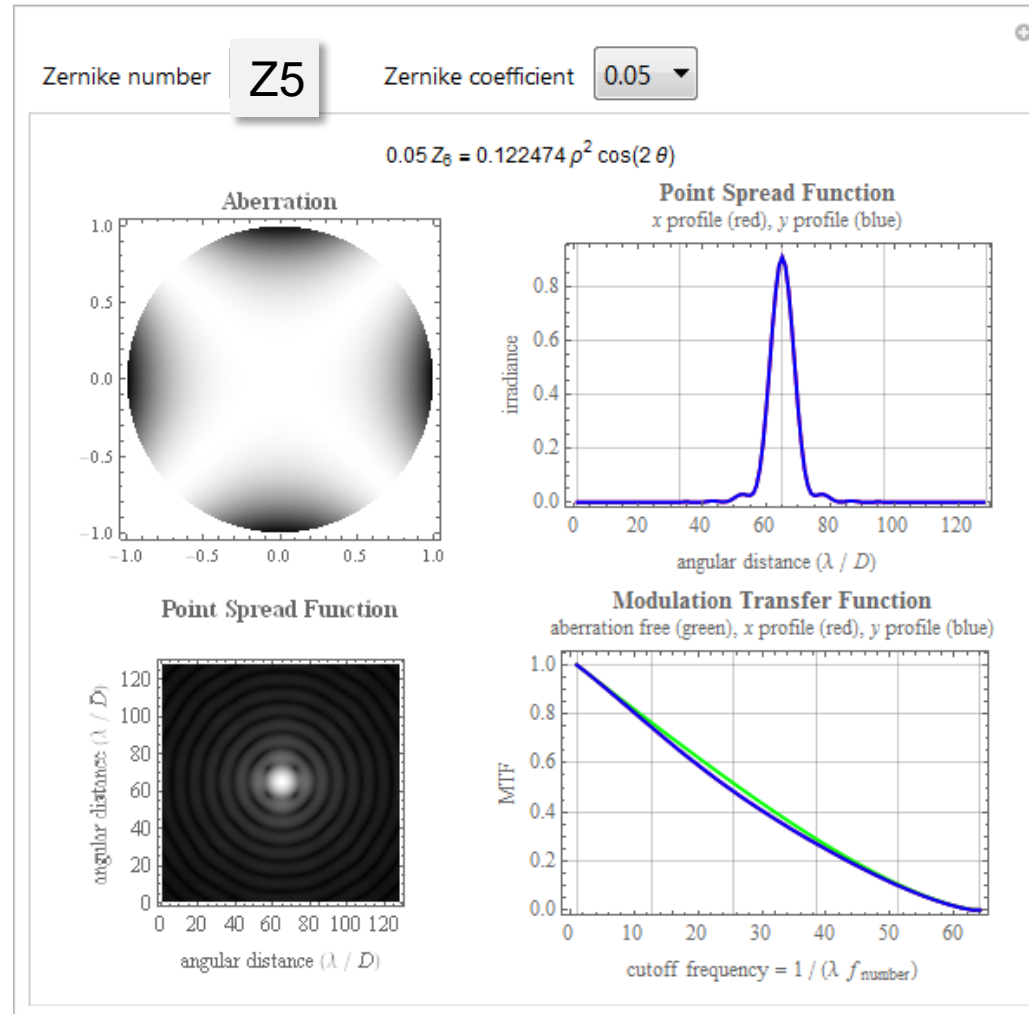
Zernike Fringe Polynomials

astigmatism
(in best focus plane)



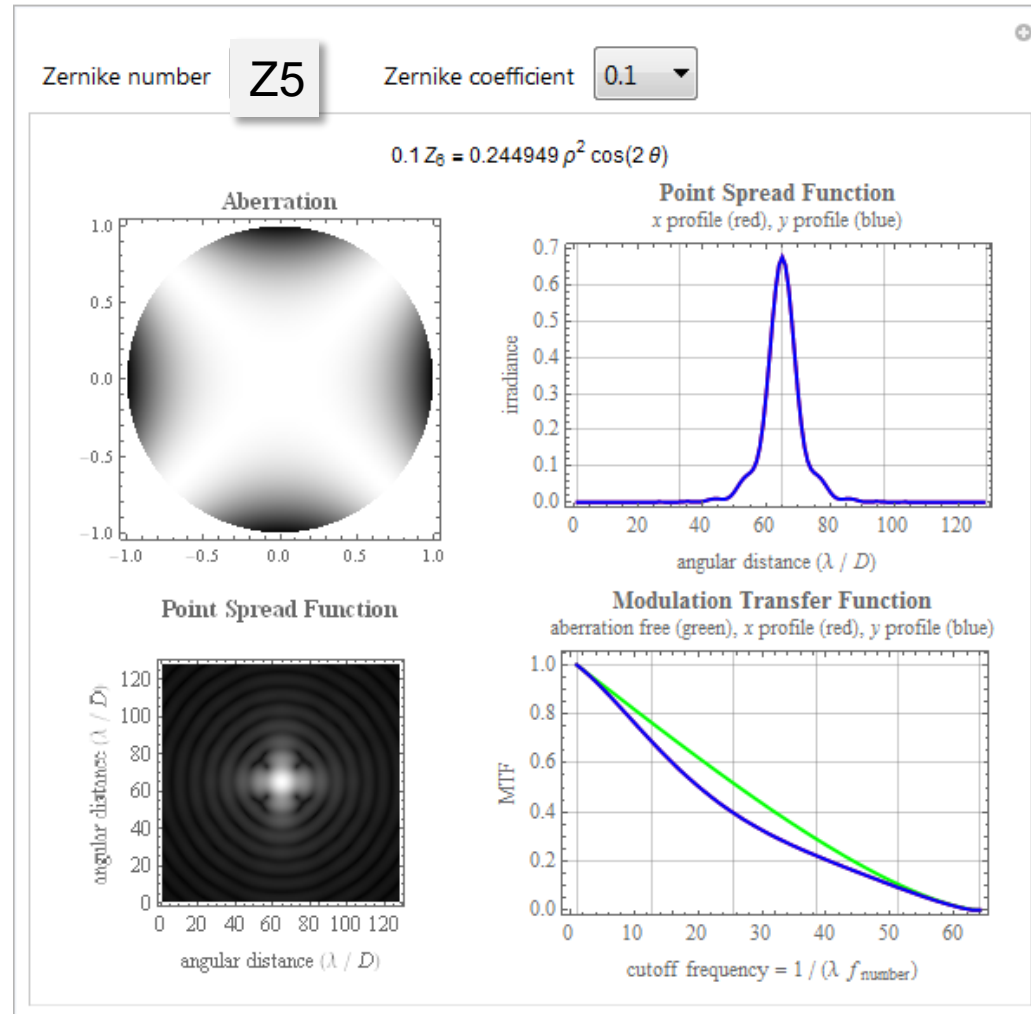
Z5/6

Zernike Z5 ($Z_{2,2}$), „astigmatism“ PSF, MTF



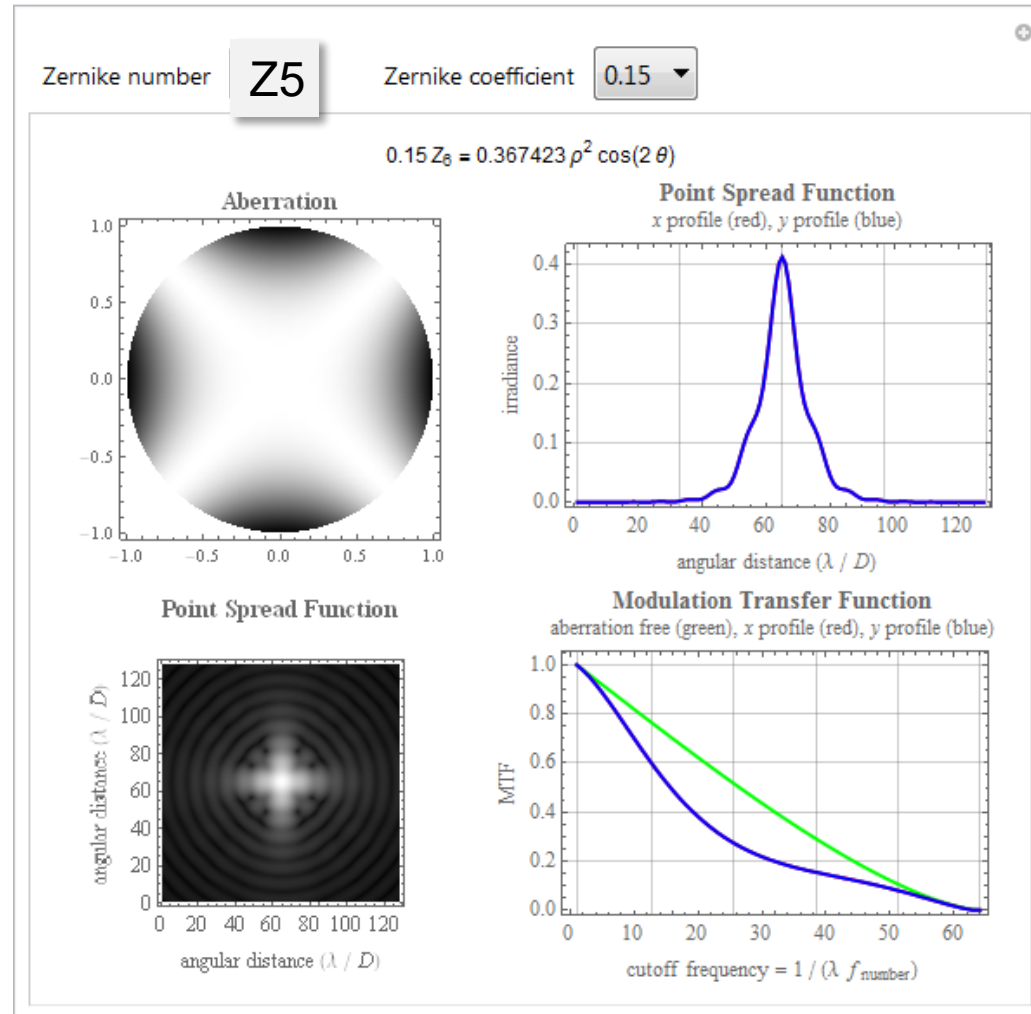
astigmatism
(in best focus plane)

Zernike Z5 ($Z_{2,2}$), „astigmatism“ PSF, MTF



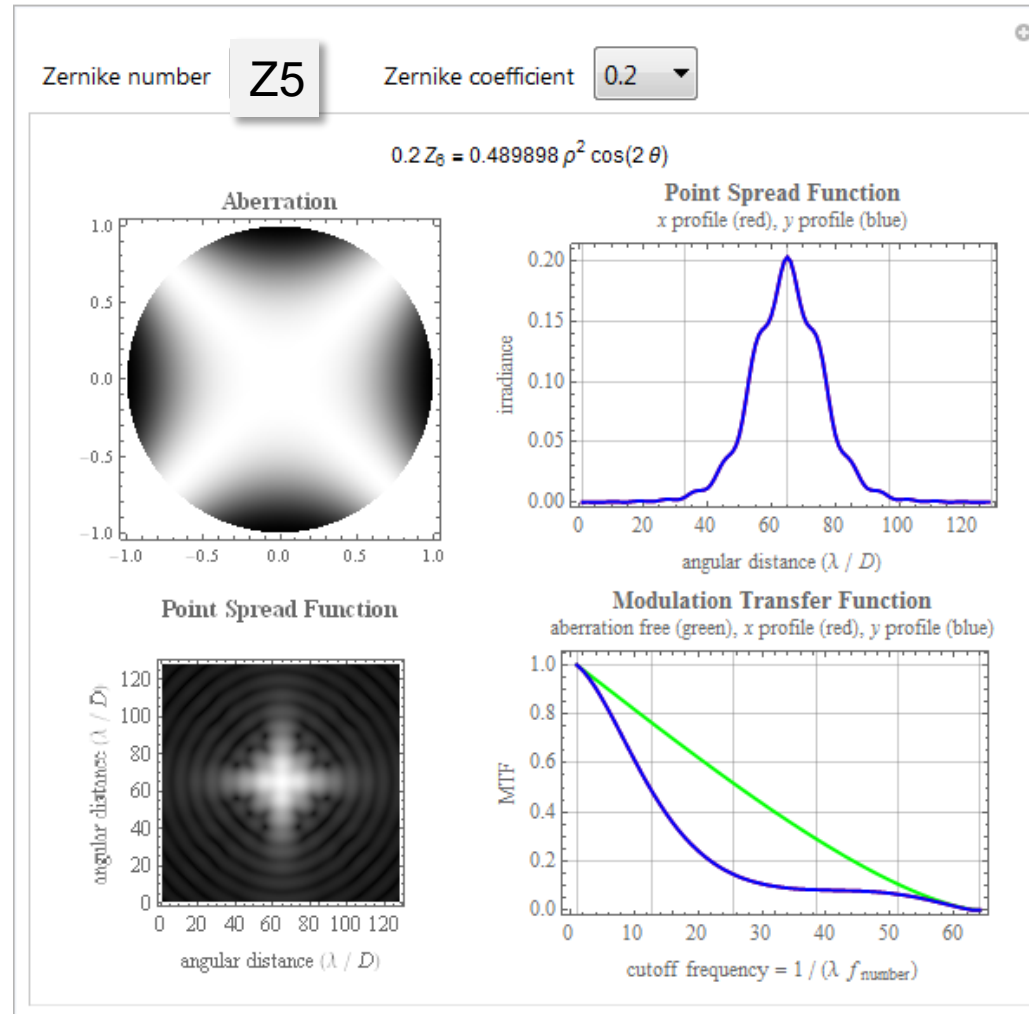
astigmatism
(in best focus plane)

Zernike Z5 ($Z_{2,2}$), „astigmatism“ PSF, MTF



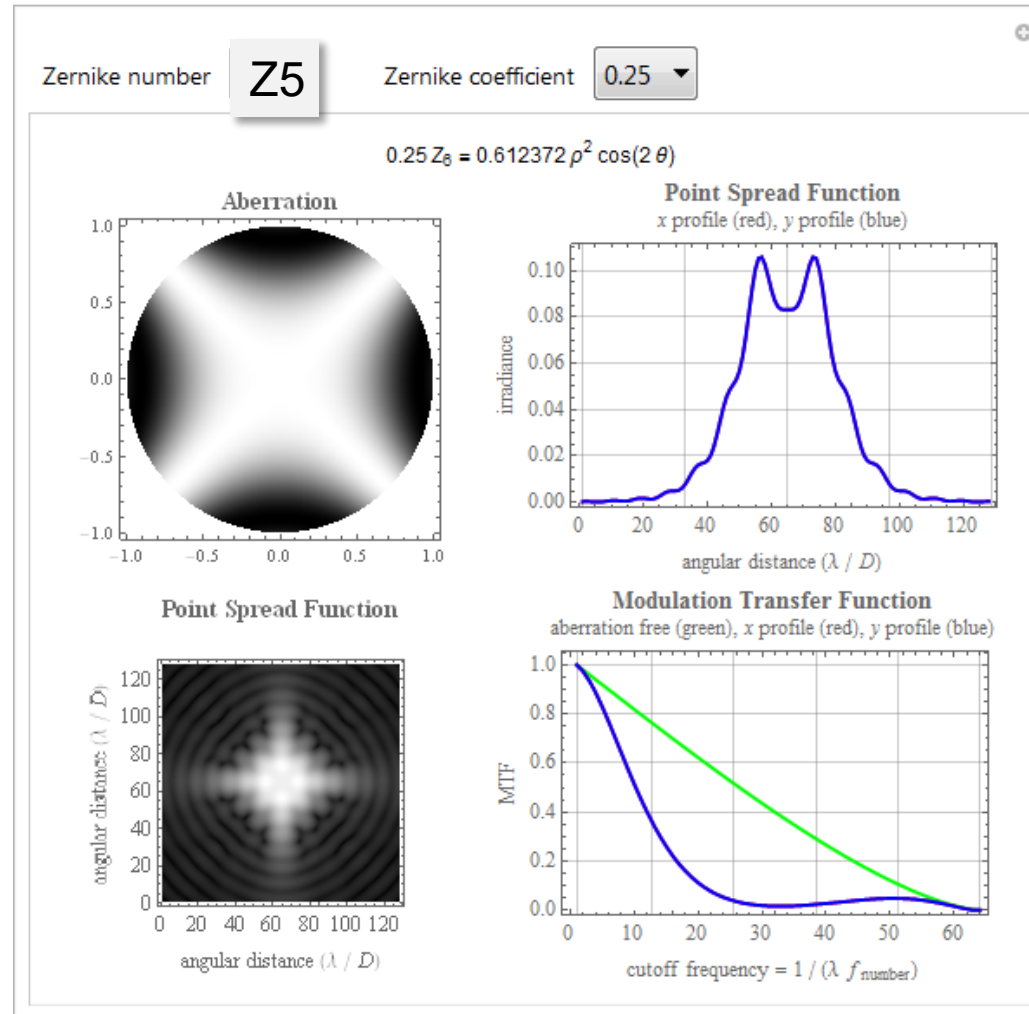
astigmatism
(in best focus plane)

Zernike Z5 ($Z_{2,2}$), „astigmatism“ PSF, MTF



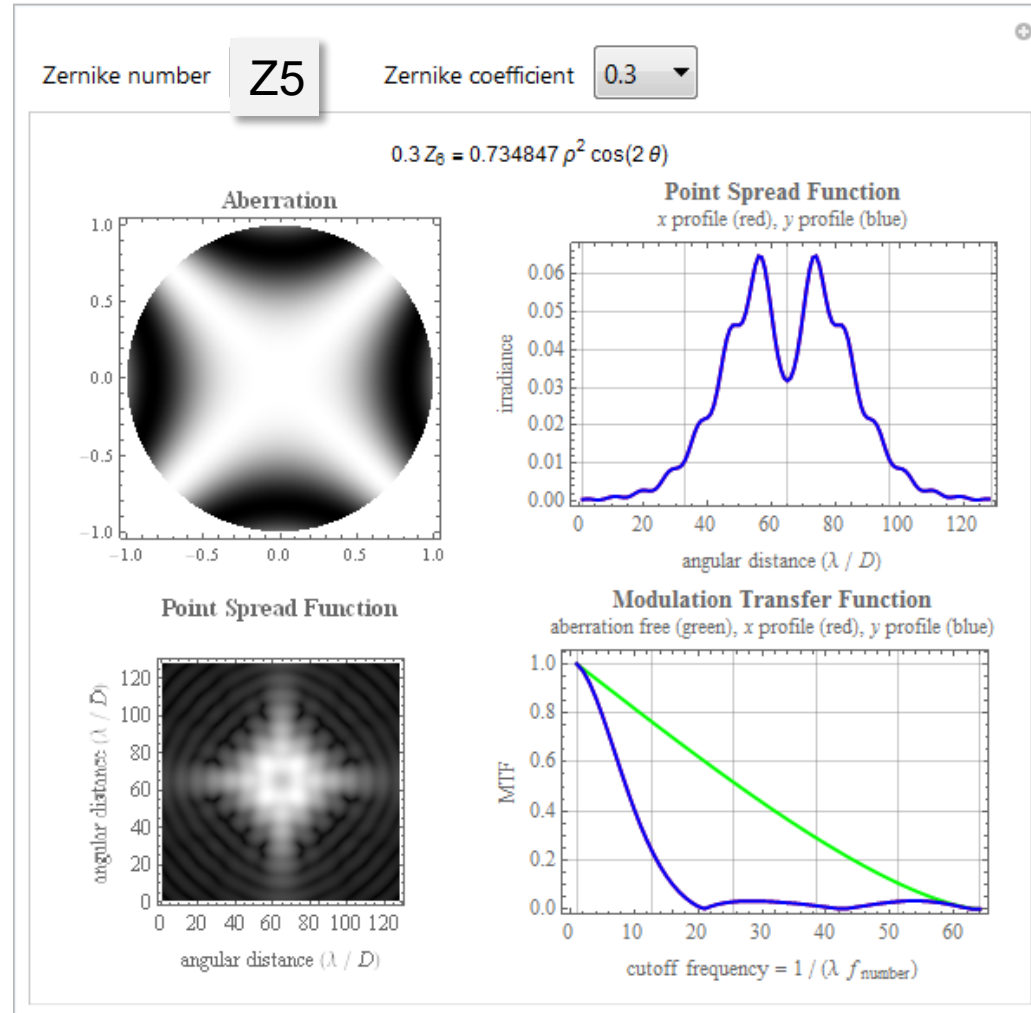
astigmatism
(in best focus plane)

Zernike Z5 ($Z_{2,2}$), „astigmatism“ PSF, MTF



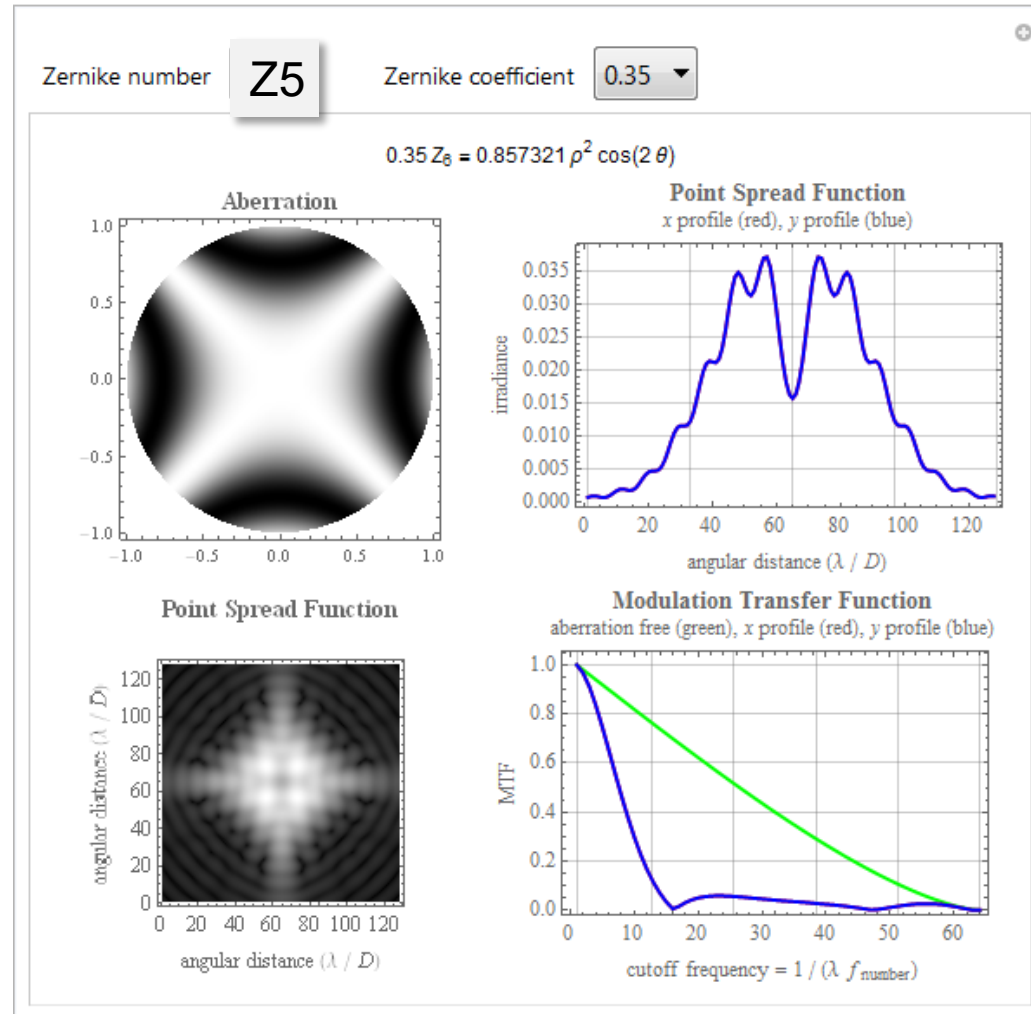
astigmatism
(in best focus plane)

Zernike Z5 ($Z_{2,2}$), „astigmatism“ PSF, MTF



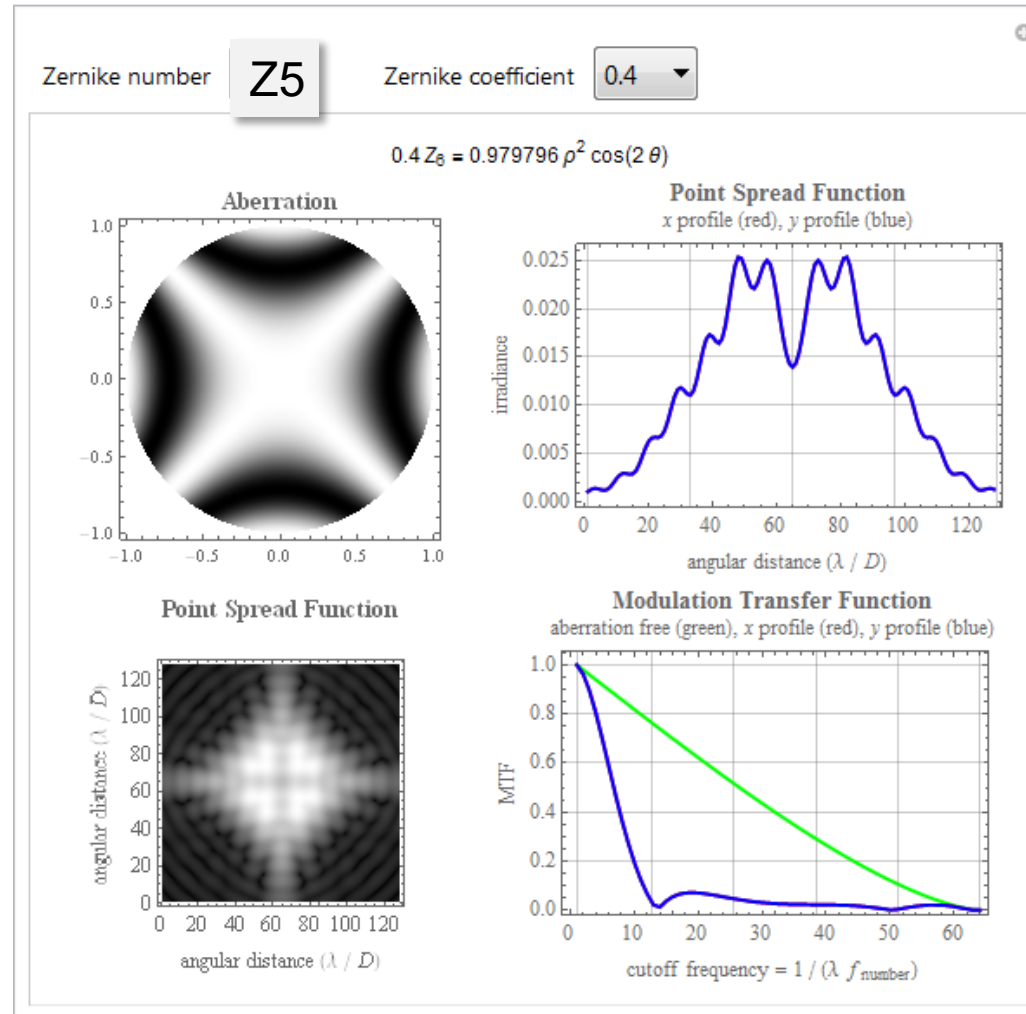
astigmatism
(in best focus plane)

Zernike Z5 ($Z_{2,2}$), „astigmatism“ PSF, MTF



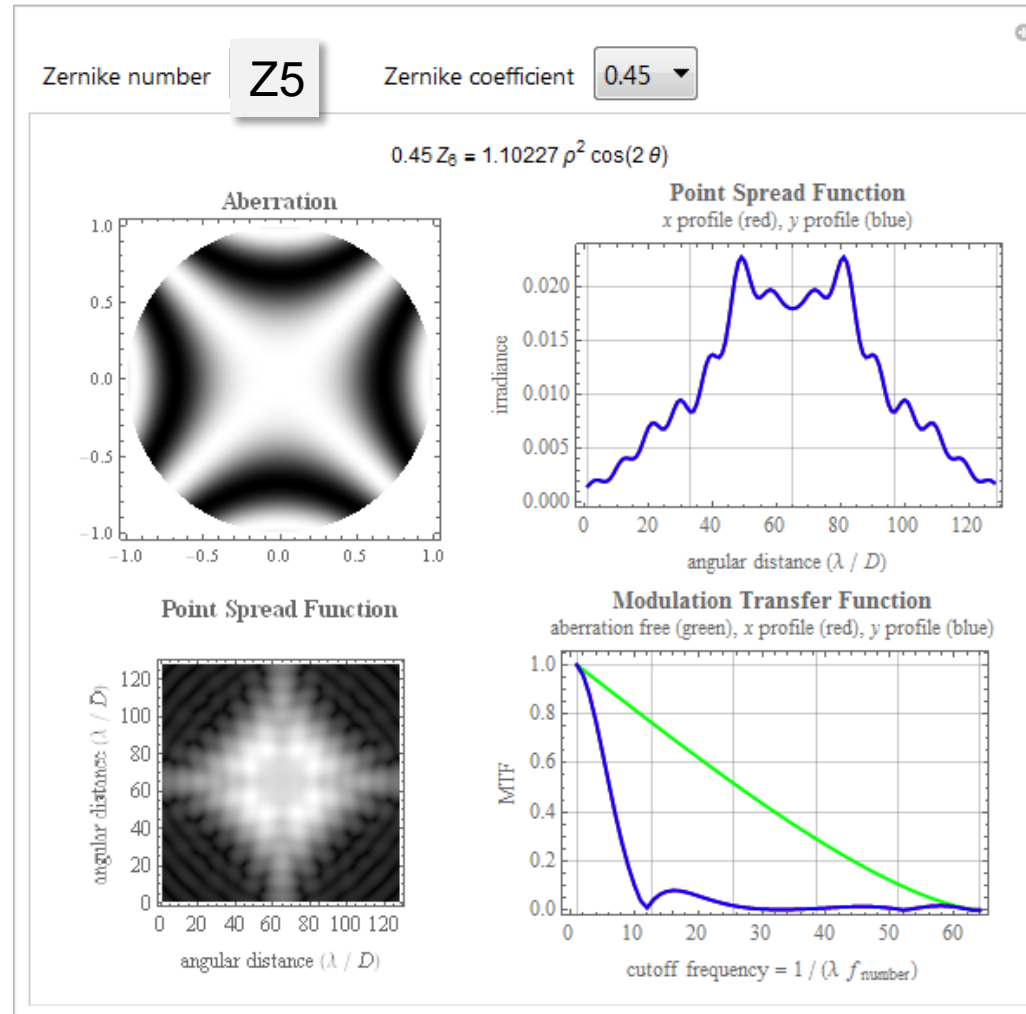
astigmatism
(in best focus plane)

Zernike Z5 ($Z_{2,2}$), „astigmatism“ PSF, MTF



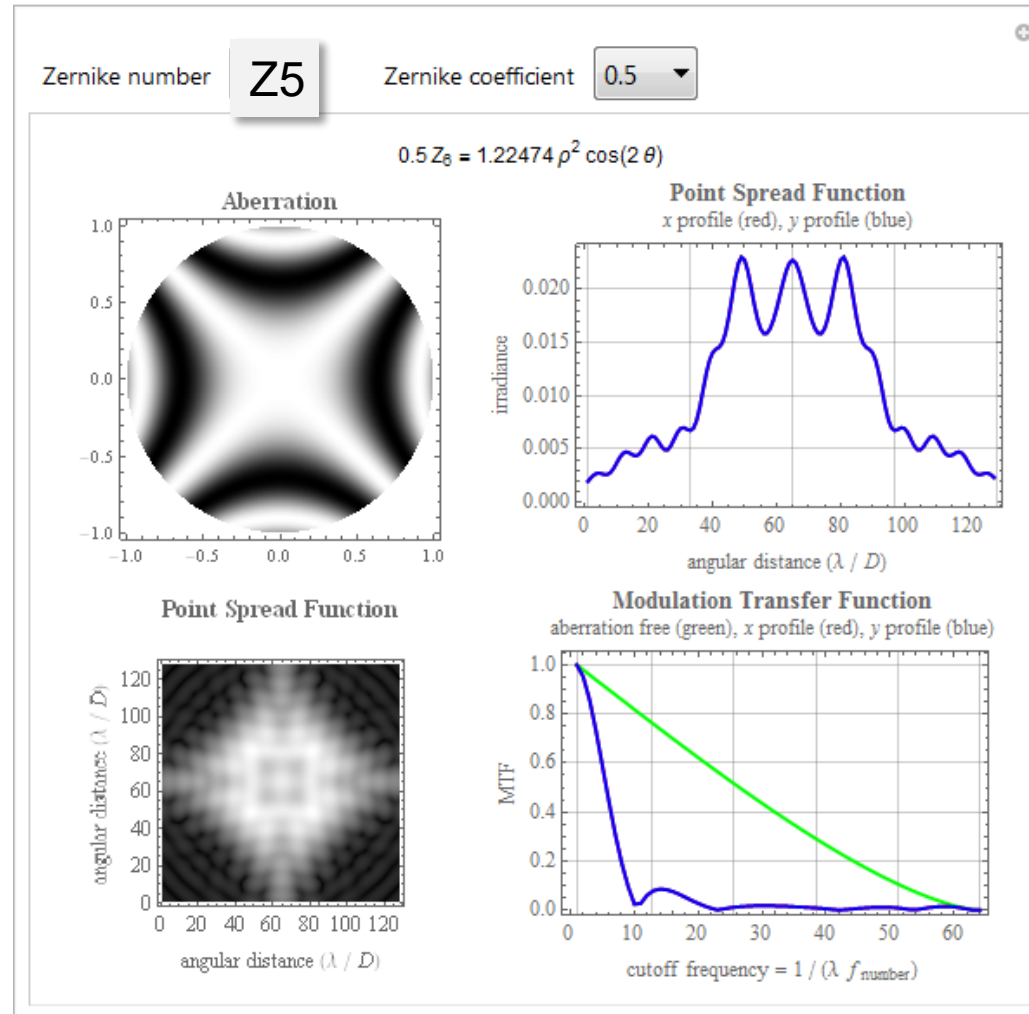
astigmatism
(in best focus plane)

Zernike Z5 ($Z_{2,2}$), „astigmatism“ PSF, MTF



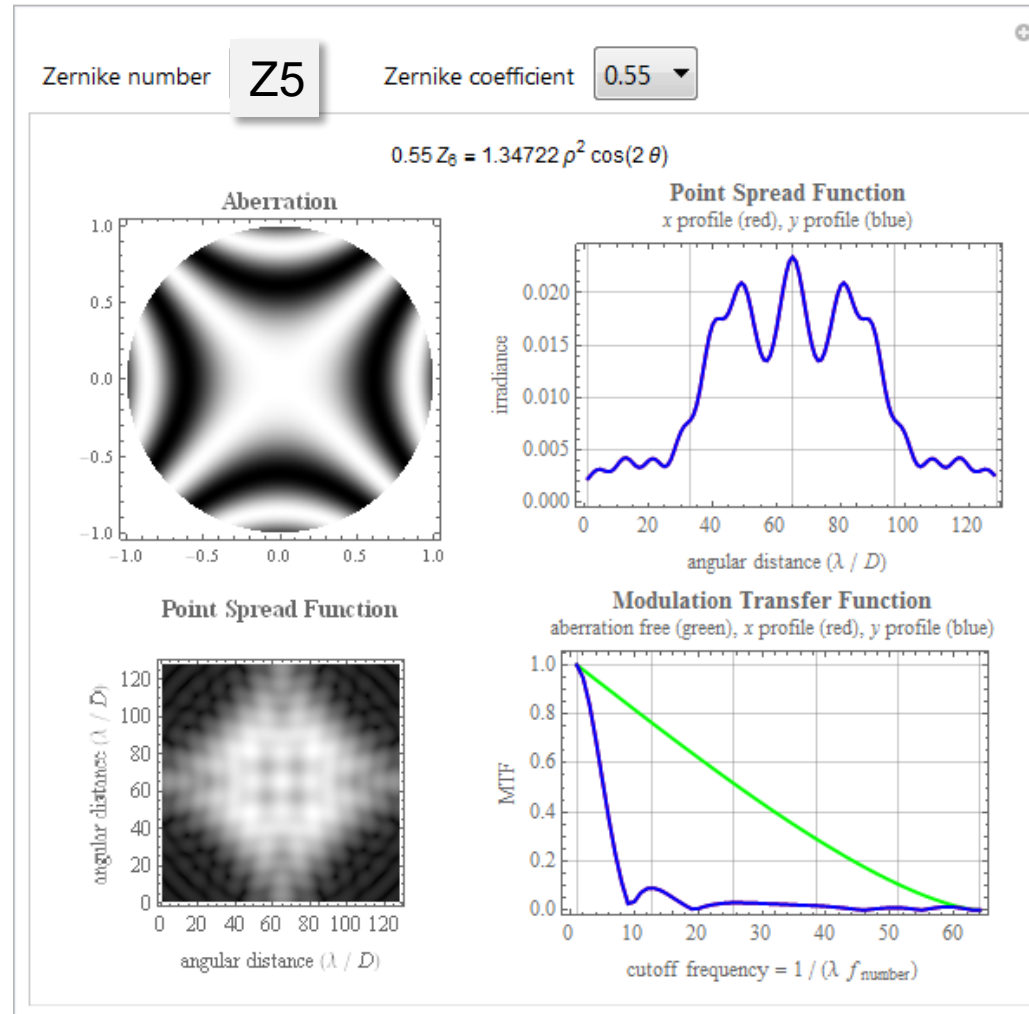
astigmatism
(in best focus plane)

Zernike Z5 ($Z_{2,2}$), „astigmatism“ PSF, MTF



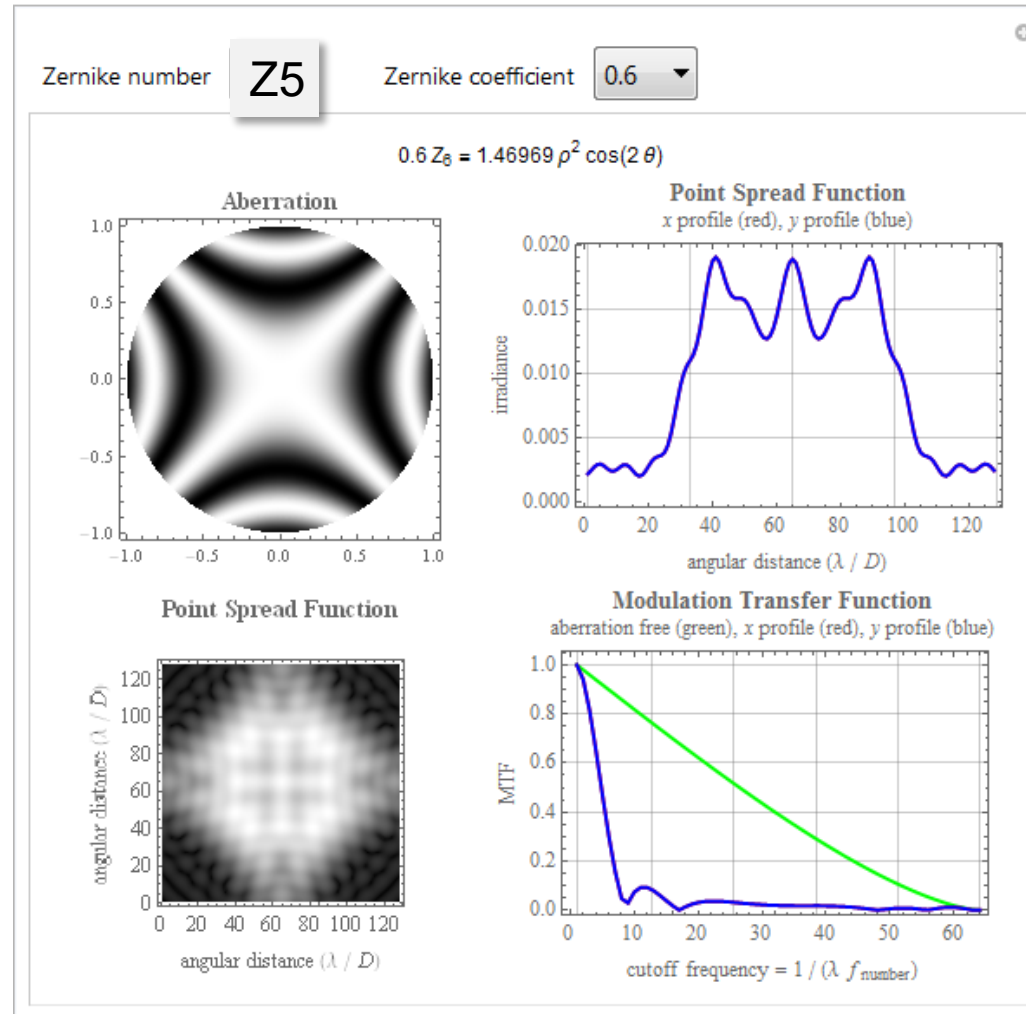
astigmatism
(in best focus plane)

Zernike Z5 ($Z_{2,2}$), „astigmatism“ PSF, MTF



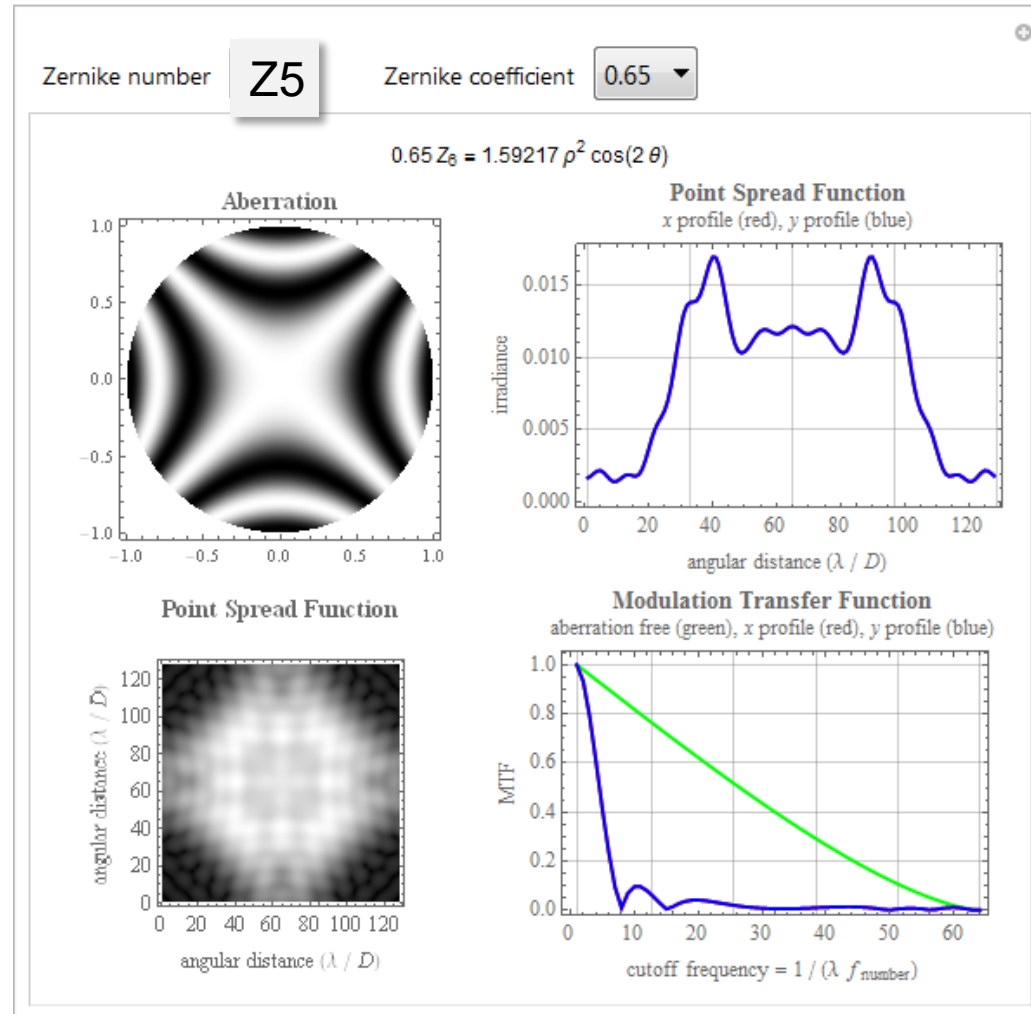
astigmatism
(in best focus plane)

Zernike Z5 ($Z_{2,2}$), „astigmatism“ PSF, MTF



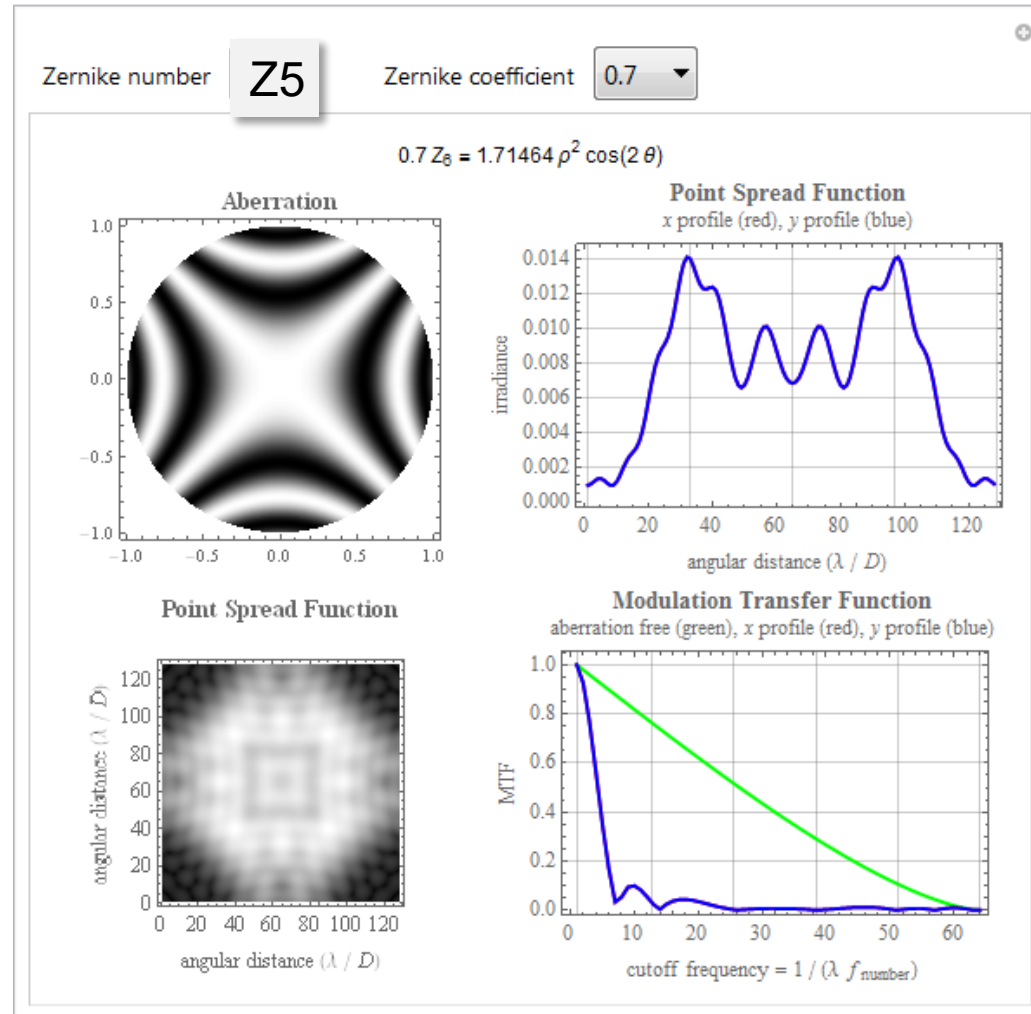
astigmatism
(in best focus plane)

Zernike Z5 ($Z_{2,2}$), „astigmatism“ PSF, MTF



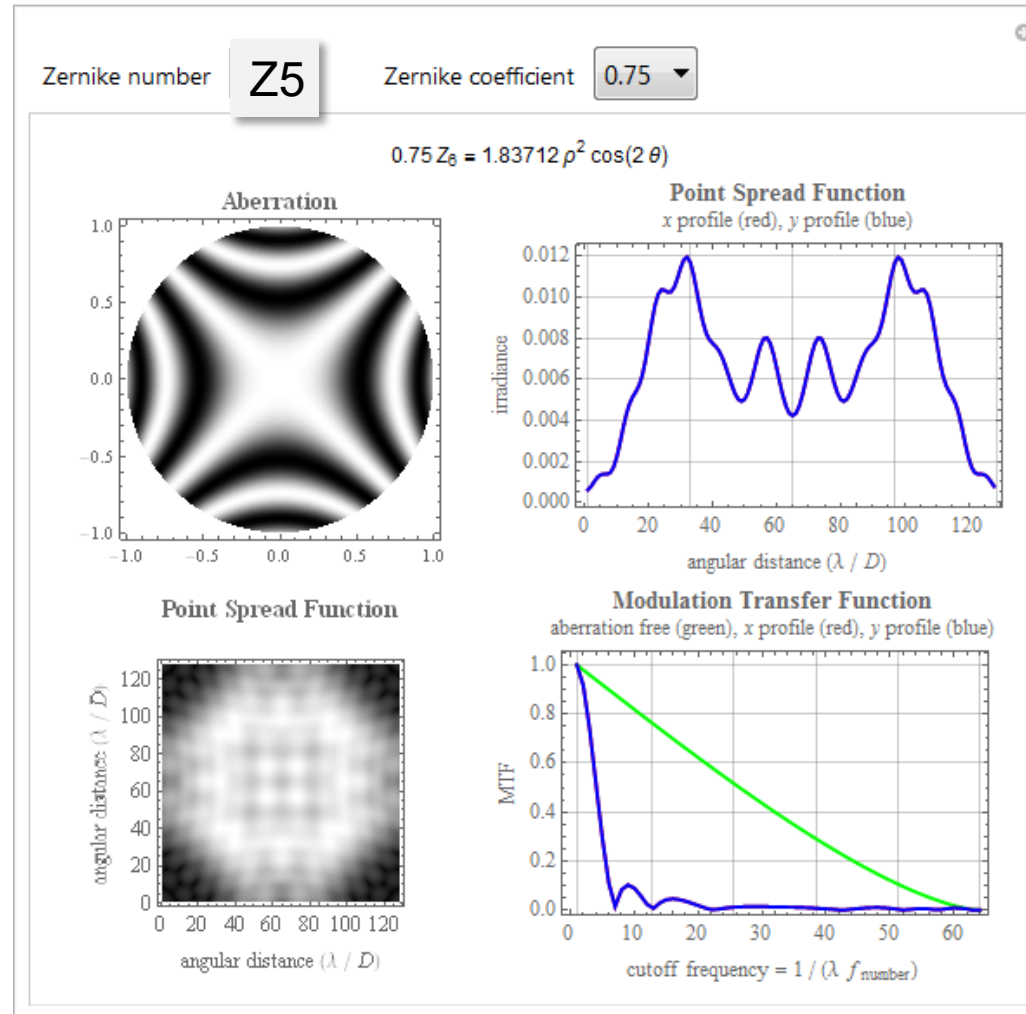
astigmatism
(in best focus plane)

Zernike Z5 ($Z_{2,2}$), „astigmatism“ PSF, MTF



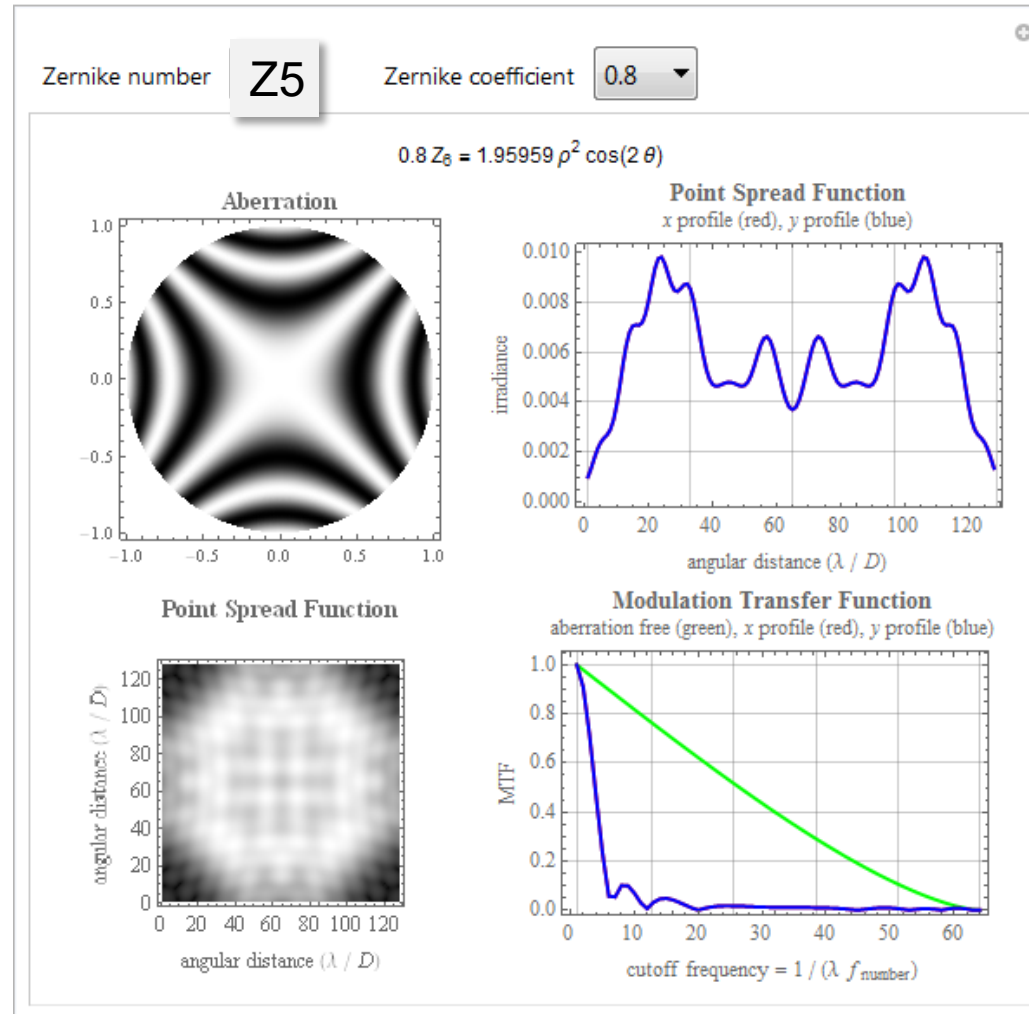
astigmatism
(in best focus plane)

Zernike Z5 ($Z_{2,2}$), „astigmatism“ PSF, MTF



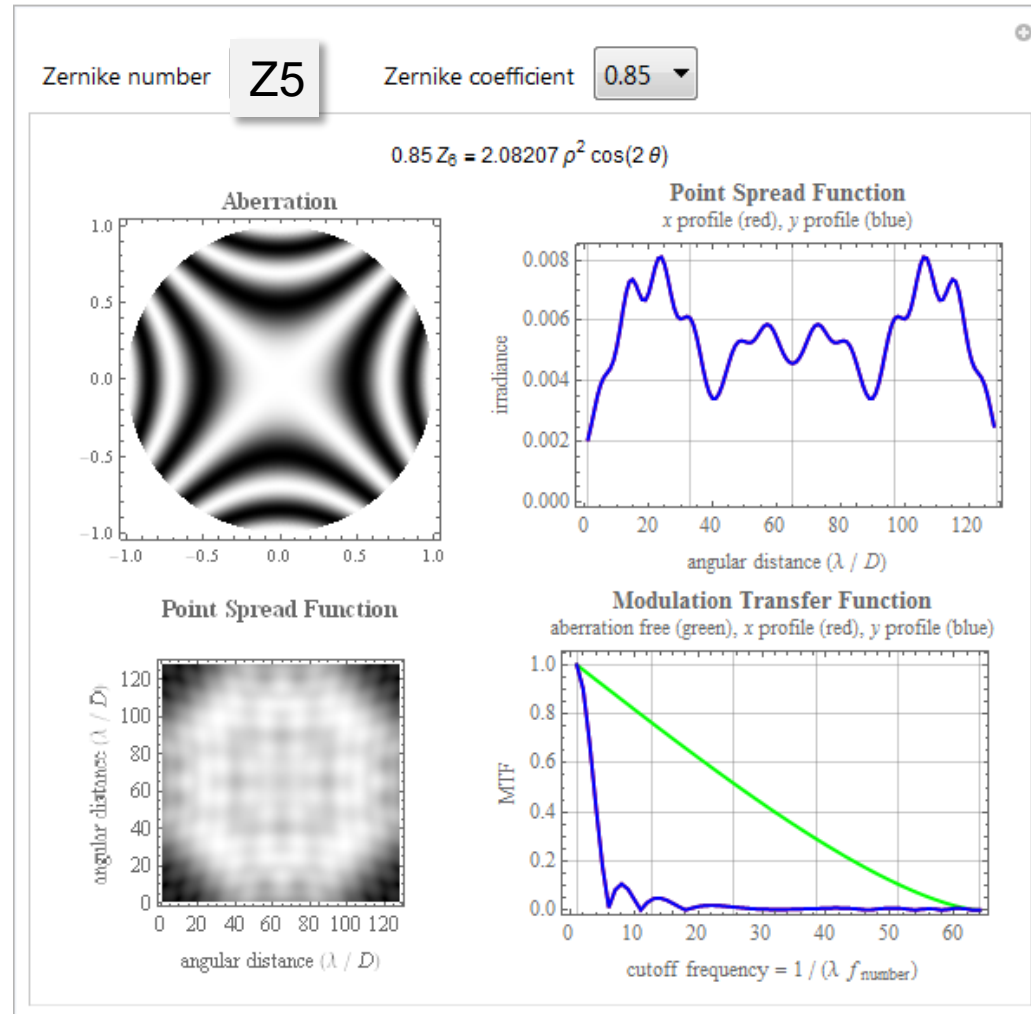
astigmatism
(in best focus plane)

Zernike Z5 ($Z_{2,2}$), „astigmatism“ PSF, MTF



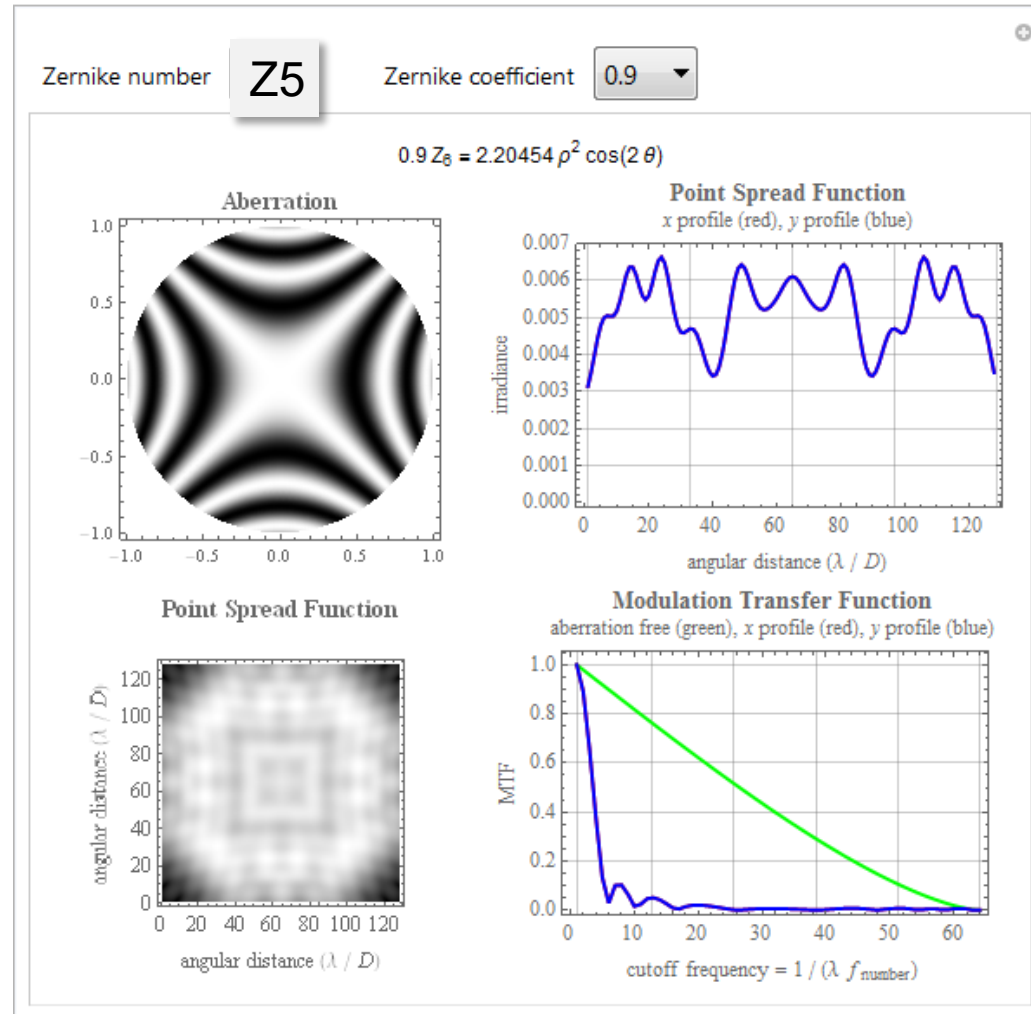
astigmatism
(in best focus plane)

Zernike Z5 ($Z_{2,2}$), „astigmatism“ PSF, MTF



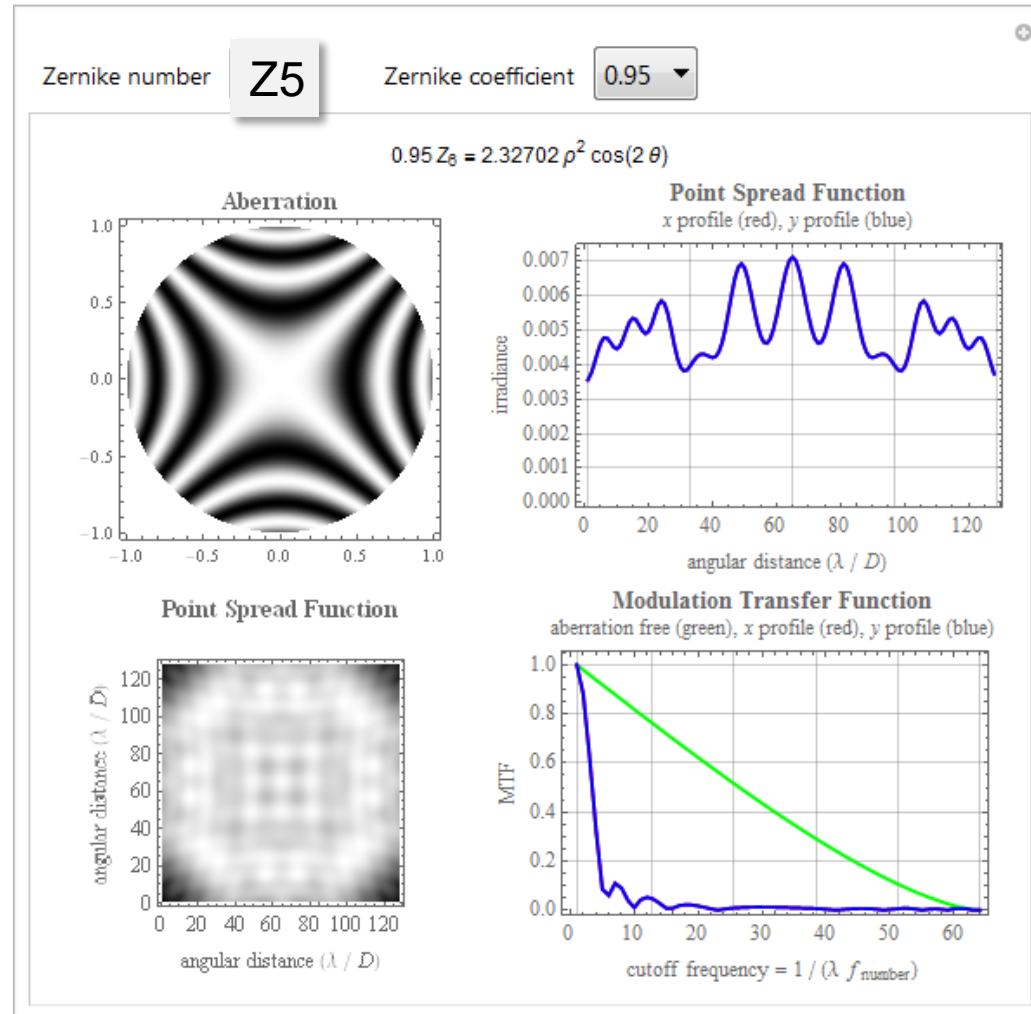
astigmatism
(in best focus plane)

Zernike Z5 ($Z_{2,2}$), „astigmatism“ PSF, MTF



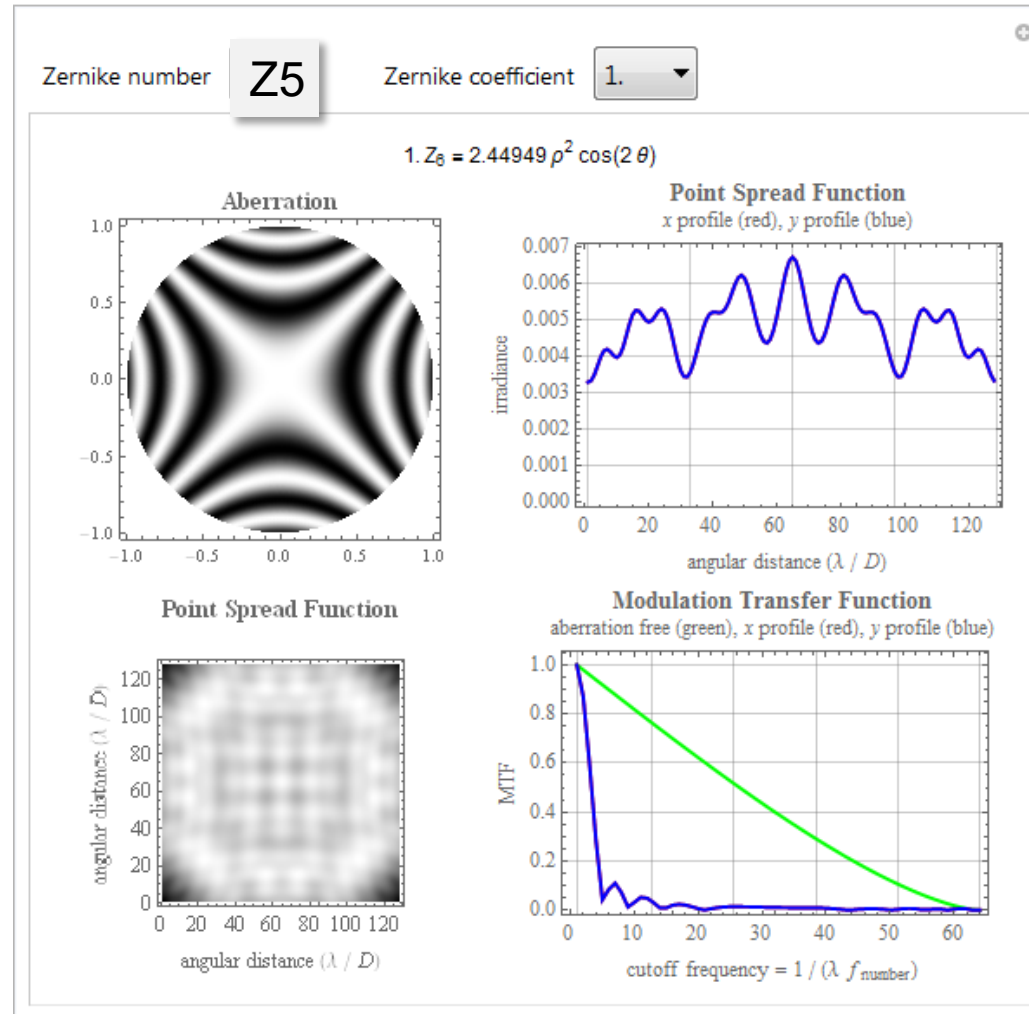
astigmatism
(in best focus plane)

Zernike Z5 ($Z_{2,2}$), „astigmatism“ PSF, MTF



astigmatism
(in best focus plane)

Zernike Z5 ($Z_{2,2}$), „astigmatism“ PSF, MTF

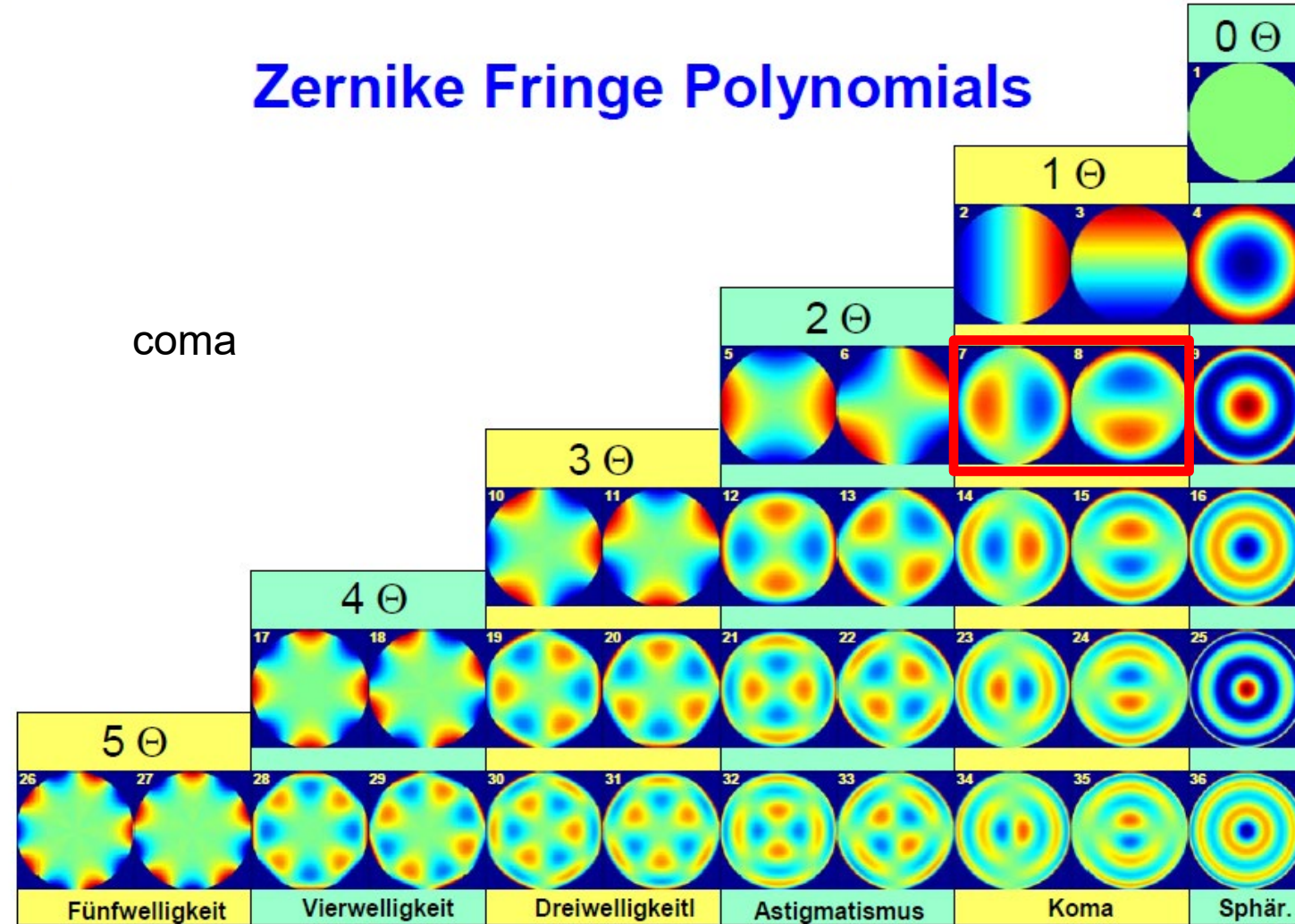


astigmatism
(in best focus plane)

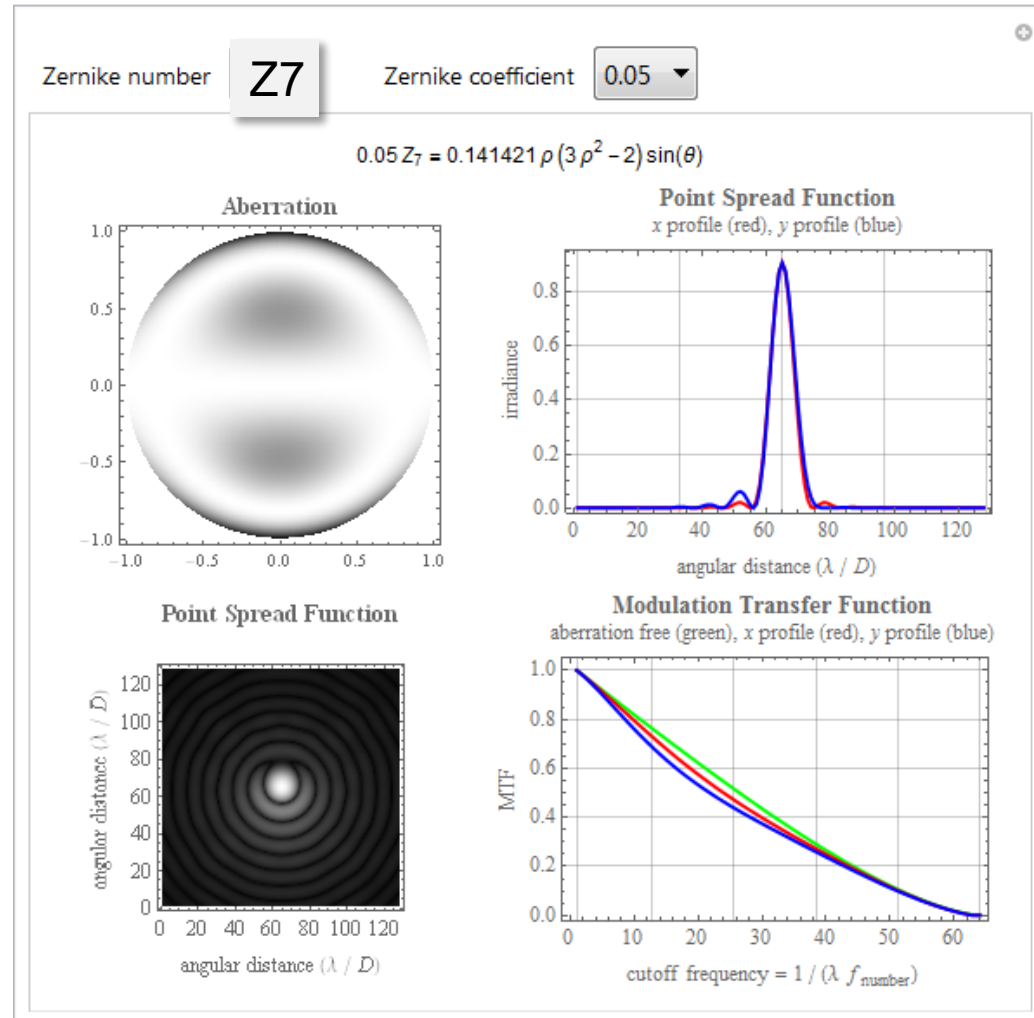
Zernike Fringe Polynomials

coma

Z7/8

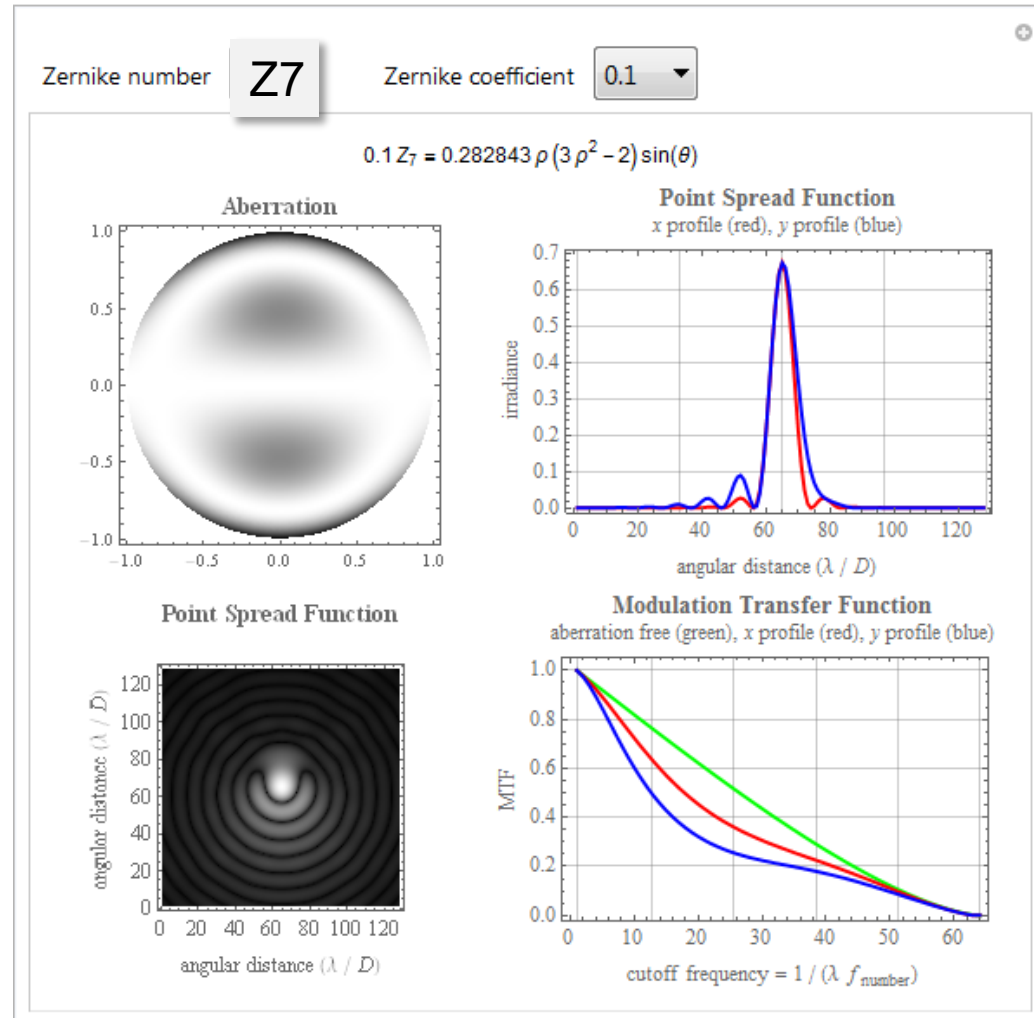


Zernike Z7 ($Z_{3,1}$), „coma“ PSF, MTF



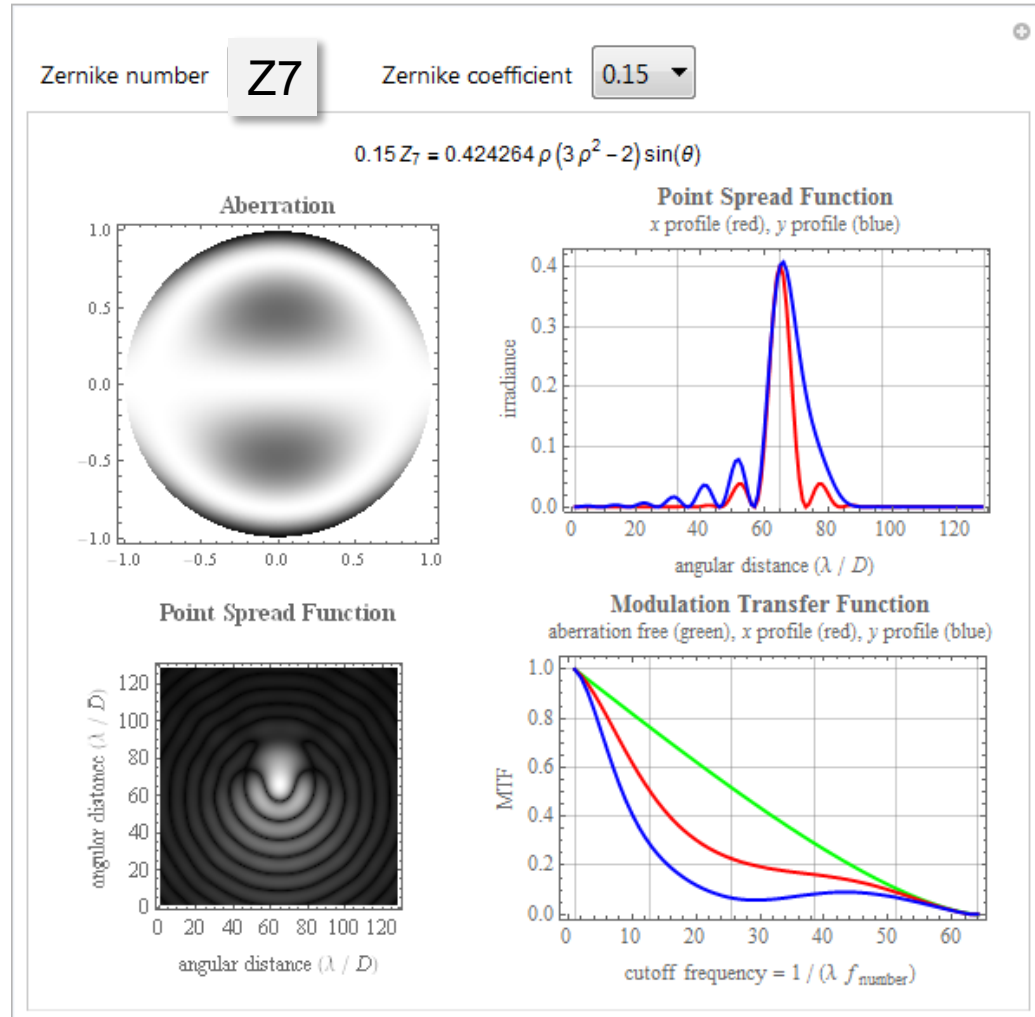
coma

Zernike Z7 ($Z_{3,1}$), „coma“ PSF, MTF



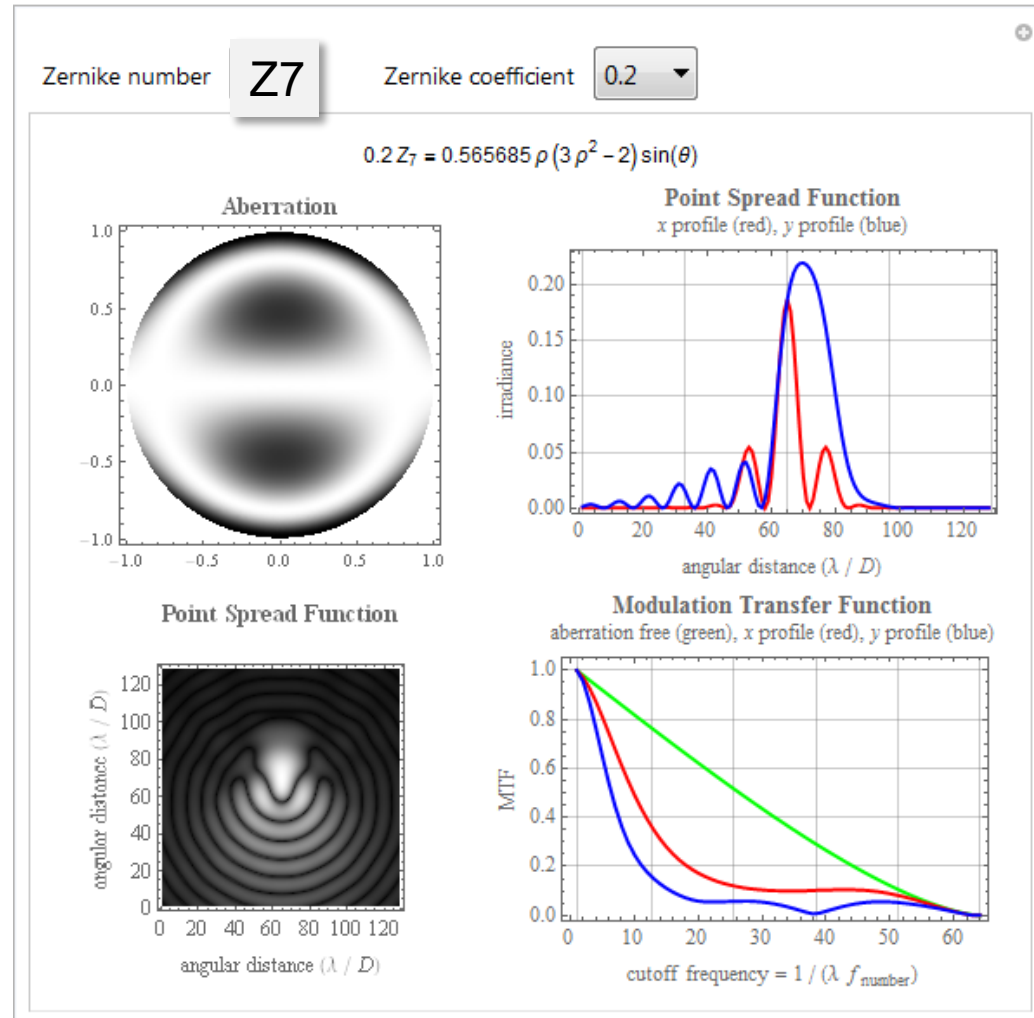
coma

Zernike Z7 ($Z_{3,1}$), „coma“ PSF, MTF



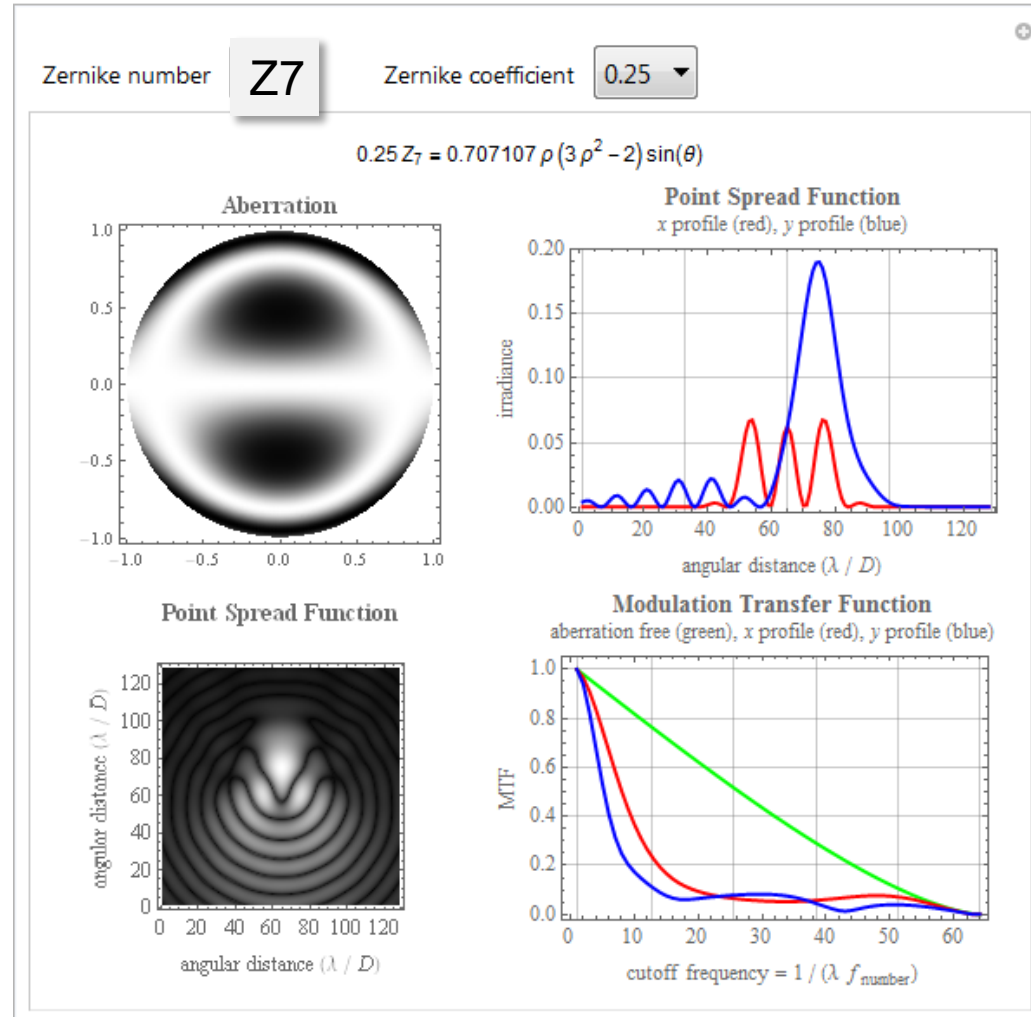
coma

Zernike Z7 ($Z_{3,1}$), „coma“ PSF, MTF



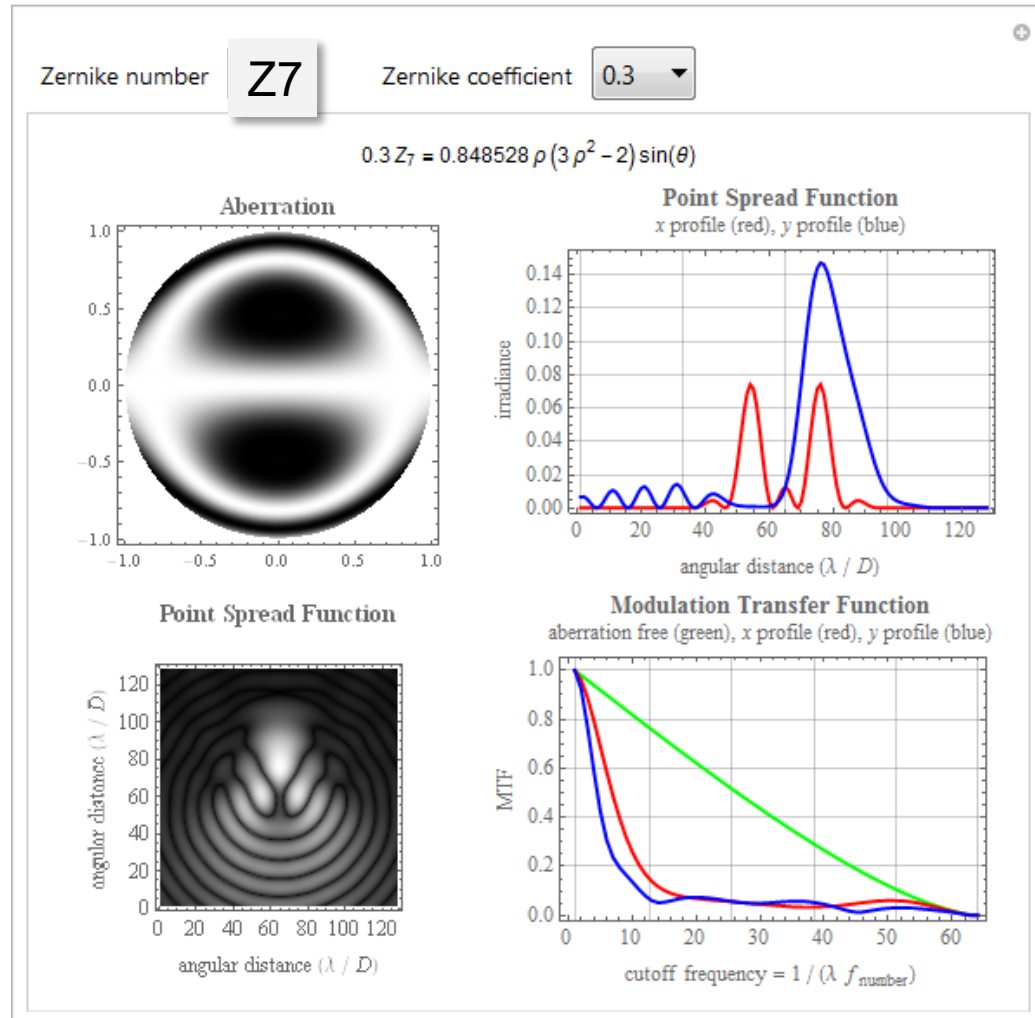
coma

Zernike Z7 ($Z_{3,1}$), „coma“ PSF, MTF



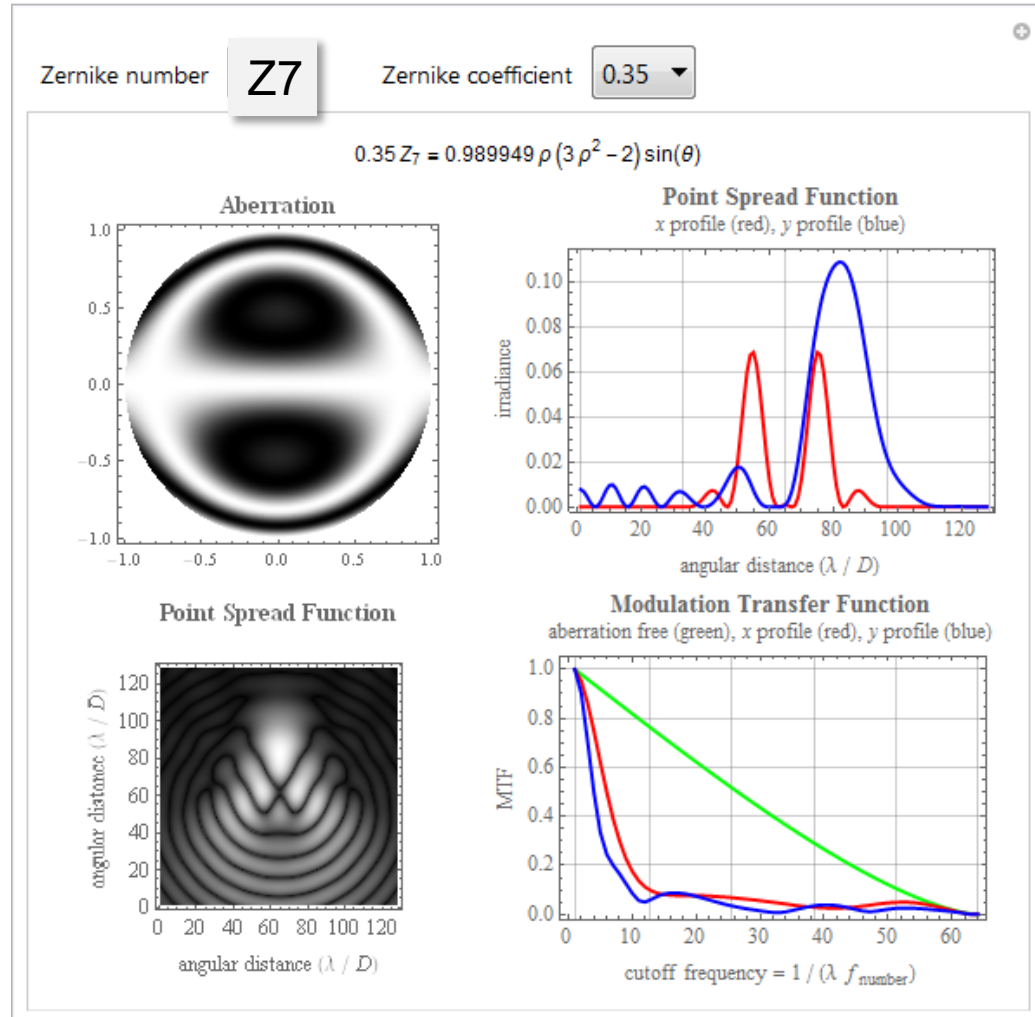
coma

Zernike Z7 ($Z_{3,1}$), „coma“ PSF, MTF



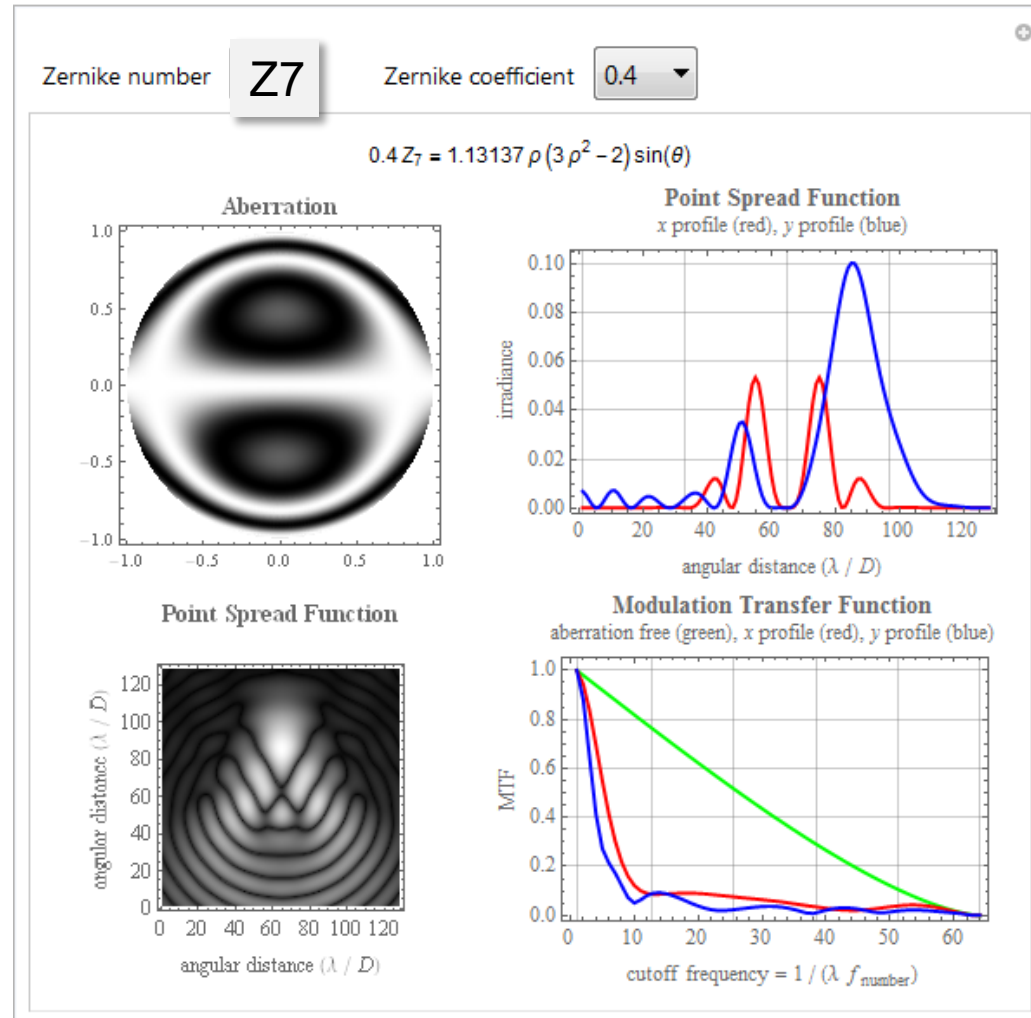
coma

Zernike Z7 ($Z_{3,1}$), „coma“ PSF, MTF



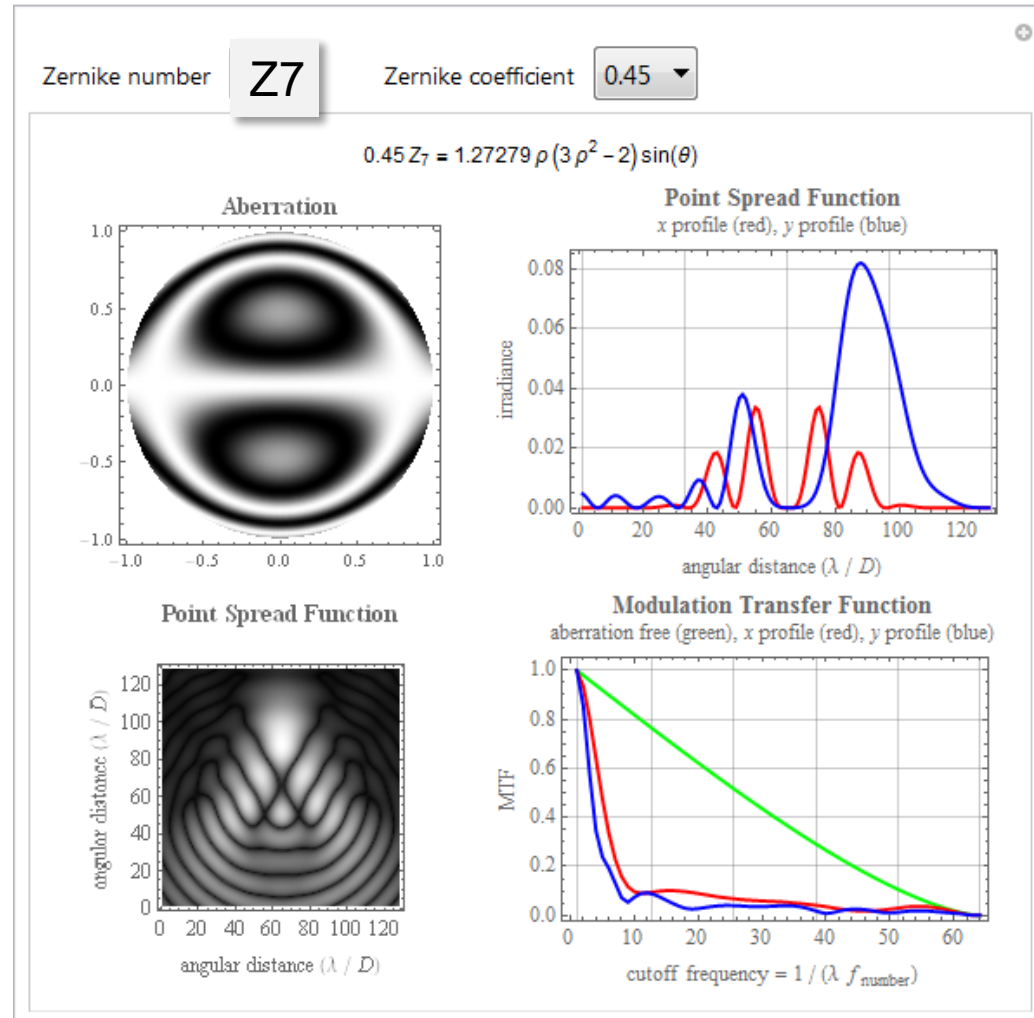
coma

Zernike Z7 ($Z_{3,1}$), „coma“ PSF, MTF



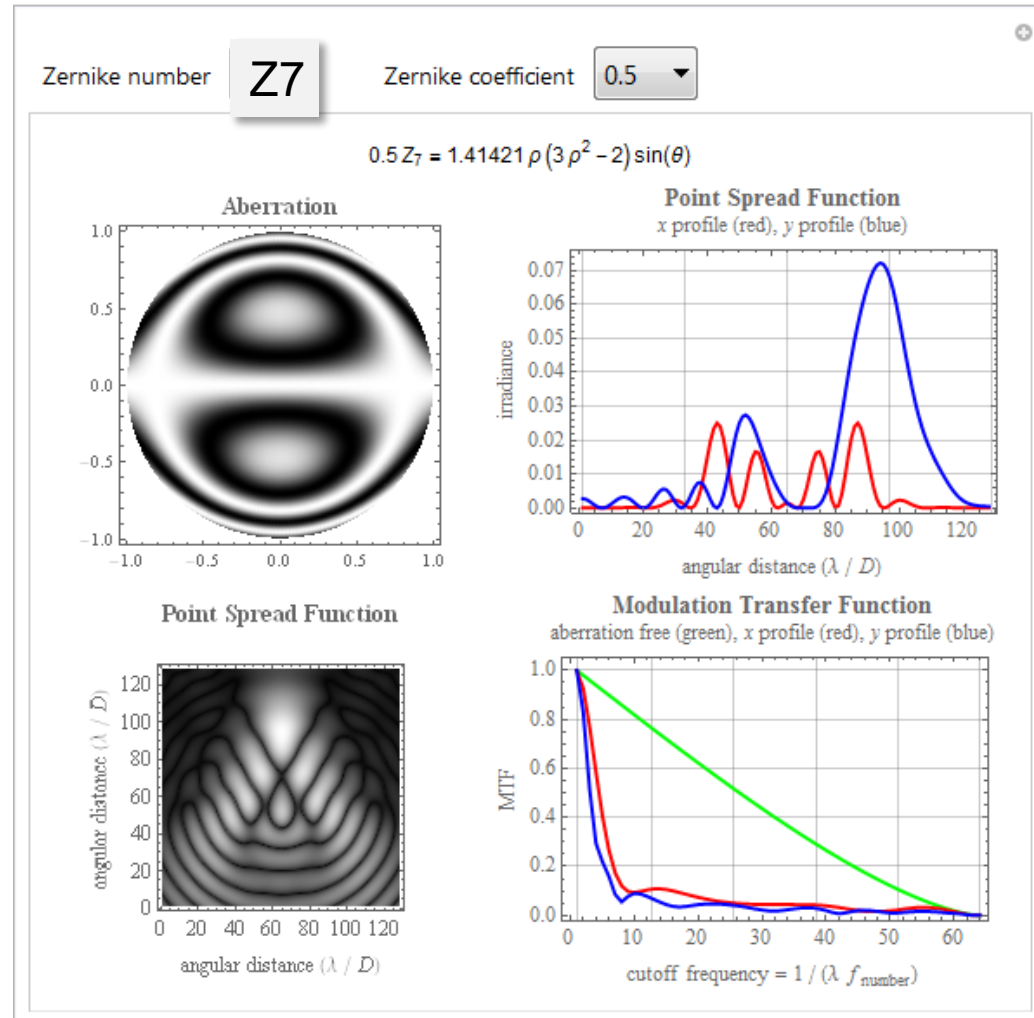
coma

Zernike Z7 ($Z_{3,1}$), „coma“ PSF, MTF



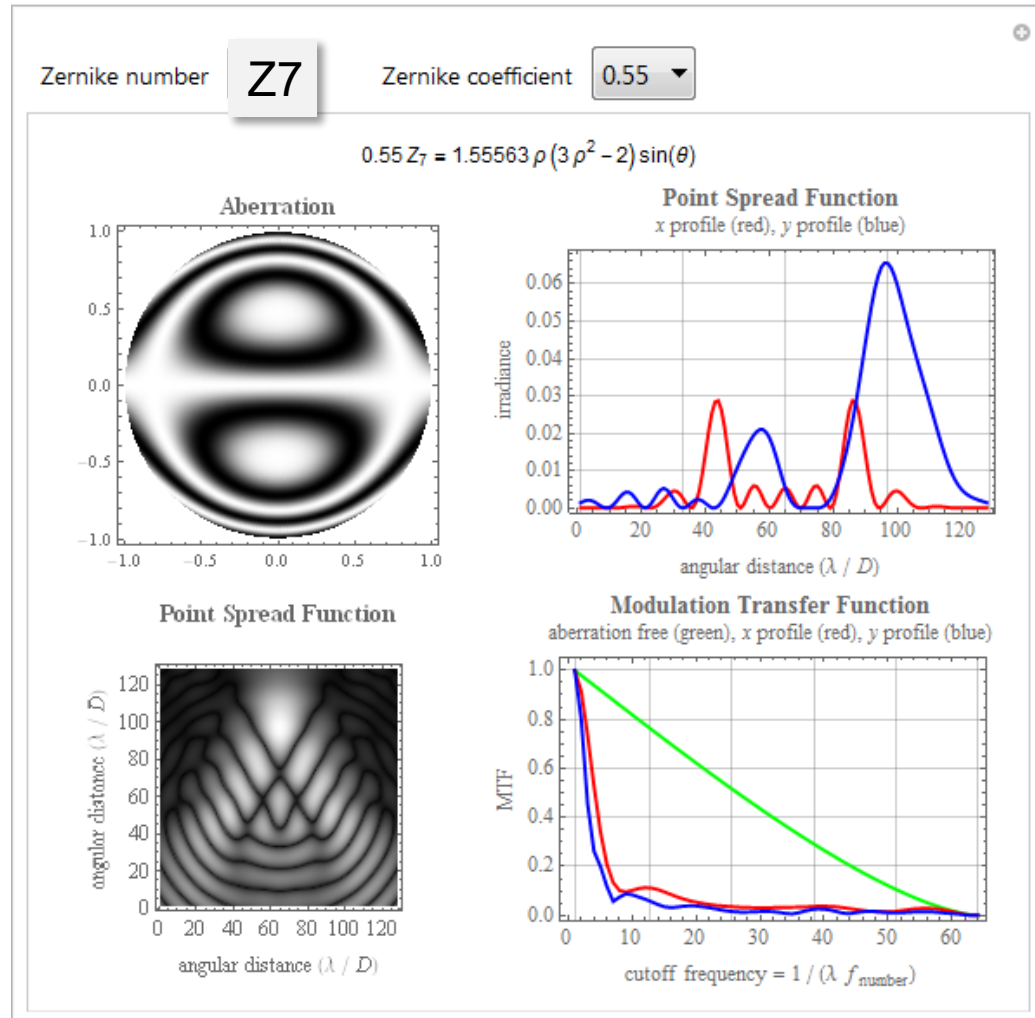
coma

Zernike Z7 ($Z_{3,1}$), „coma“ PSF, MTF



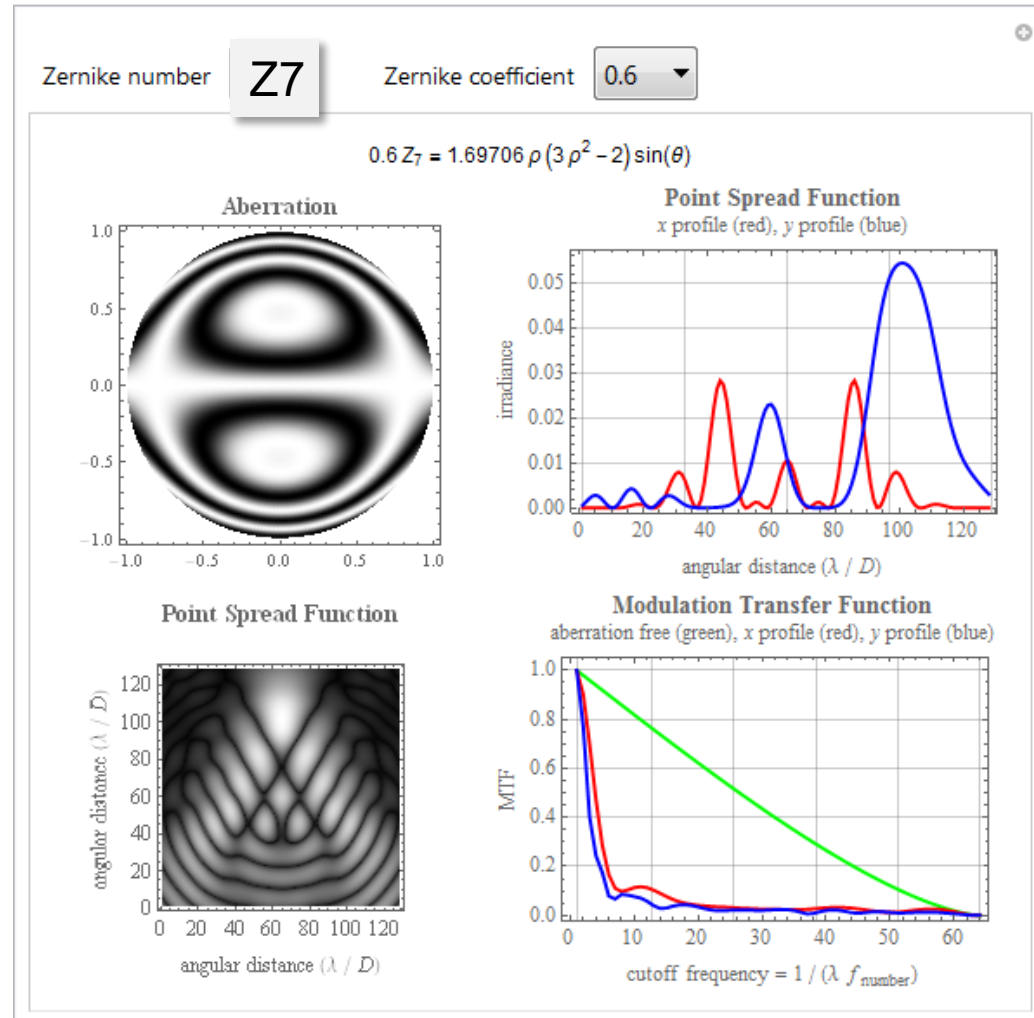
coma

Zernike Z7 ($Z_{3,1}$), „coma“ PSF, MTF



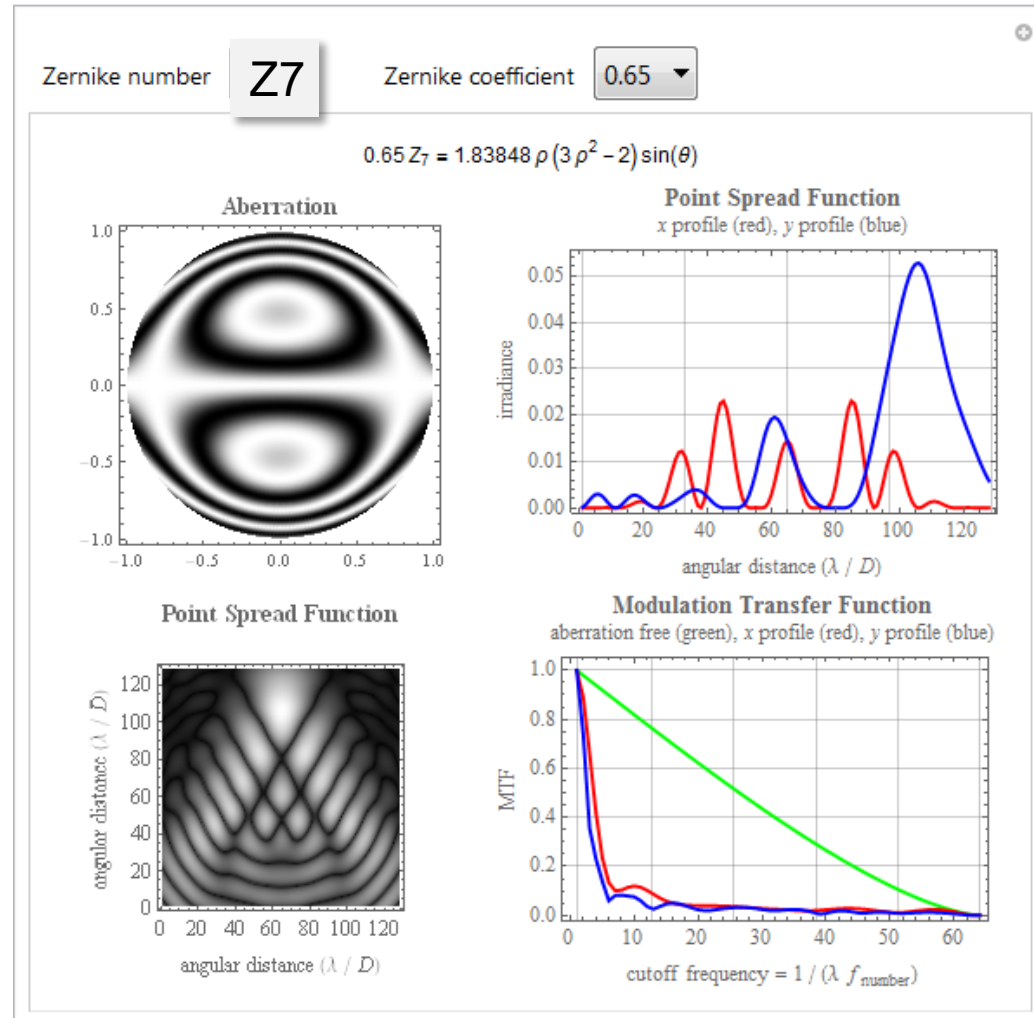
coma

Zernike Z7 ($Z_{3,1}$), „coma“ PSF, MTF



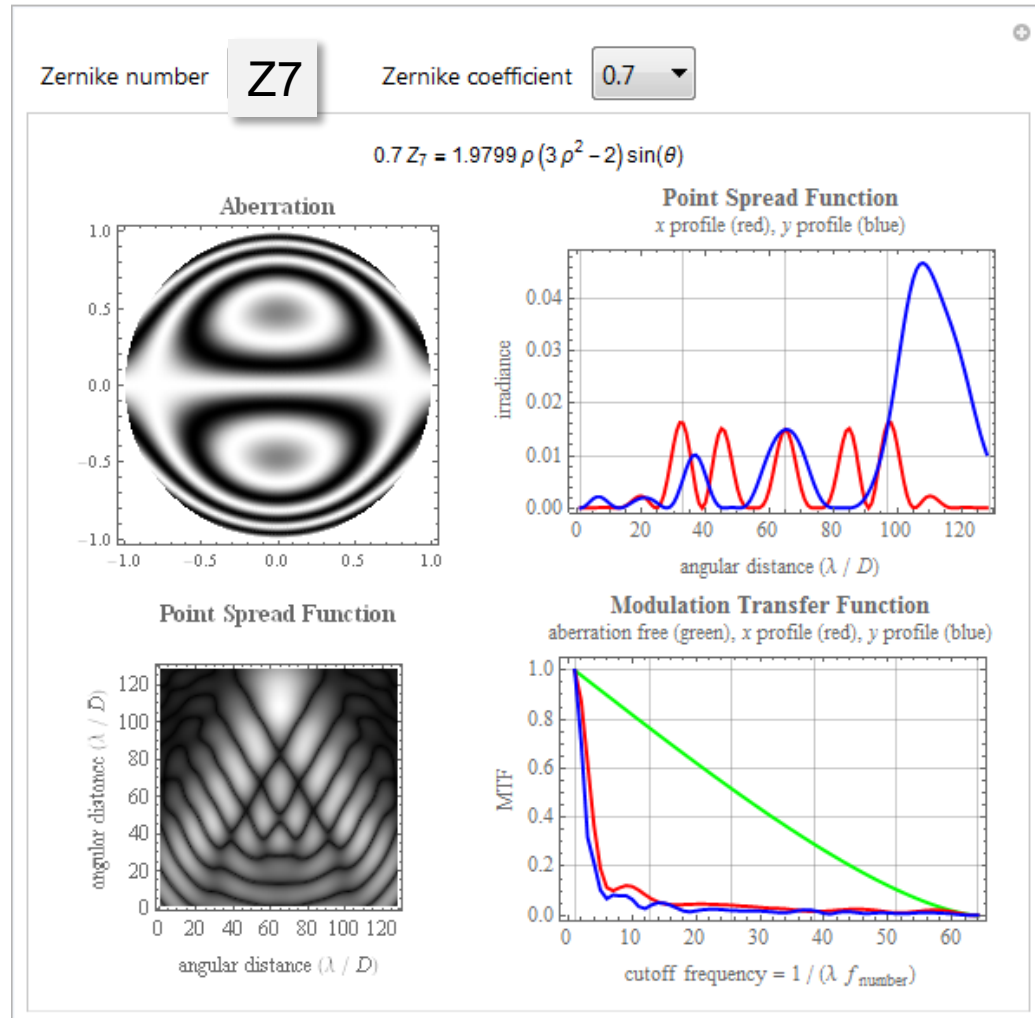
coma

Zernike Z7 ($Z_{3,1}$), „coma“ PSF, MTF



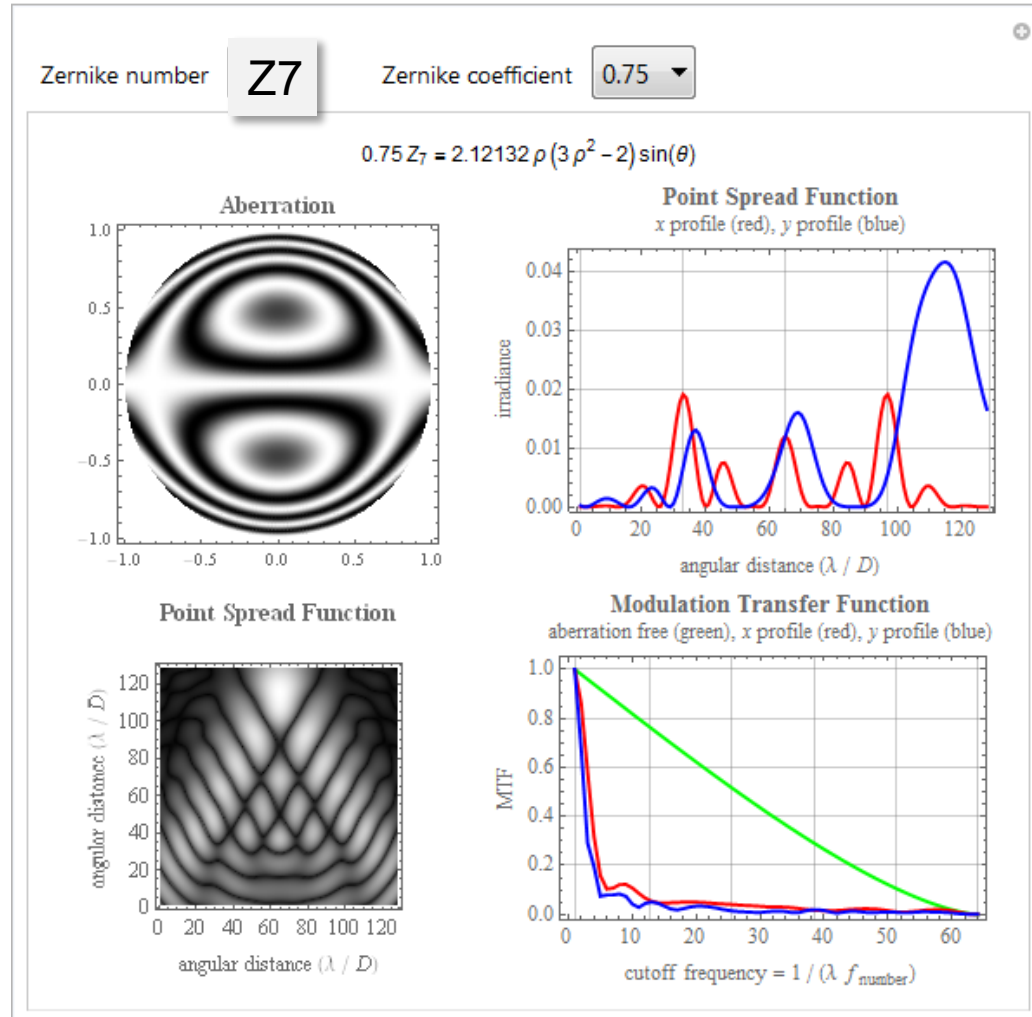
coma

Zernike Z7 ($Z_{3,1}$), „coma“ PSF, MTF



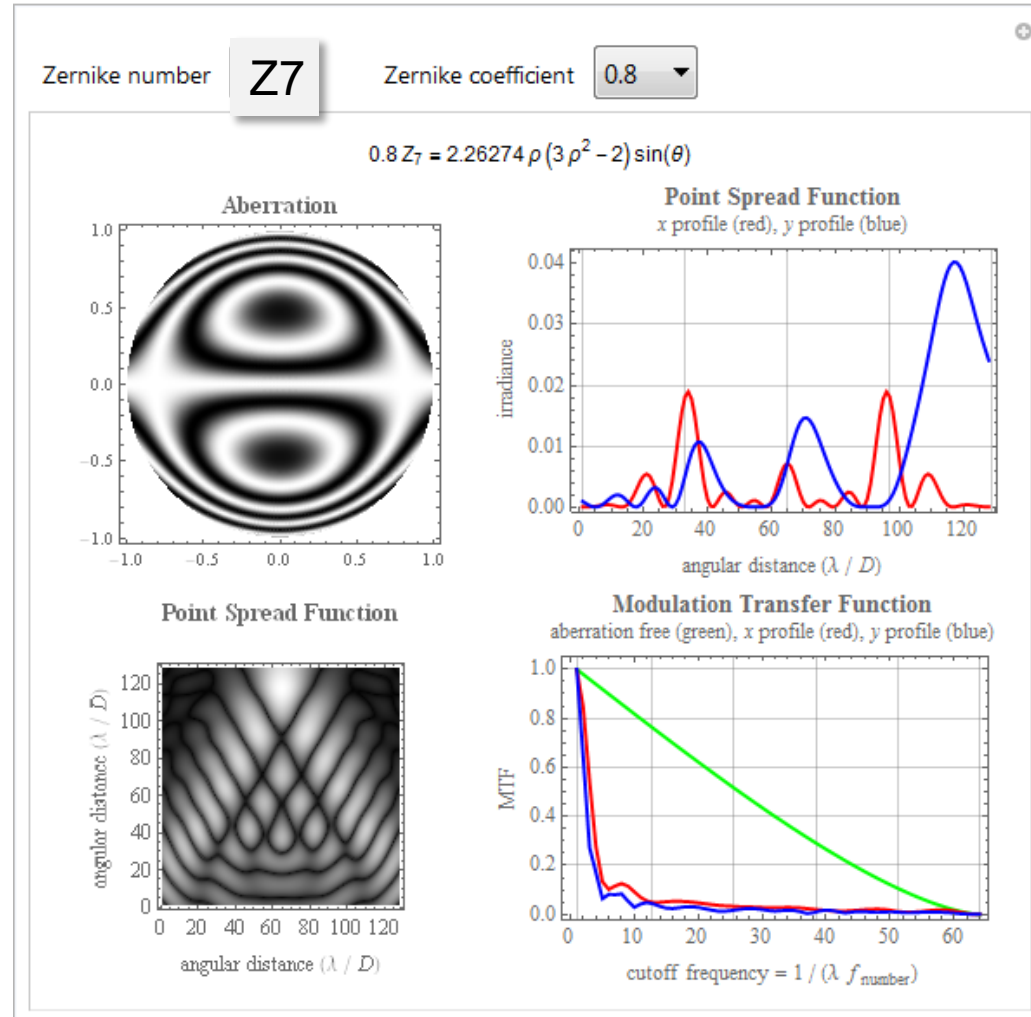
coma

Zernike Z7 ($Z_{3,1}$), „coma“ PSF, MTF



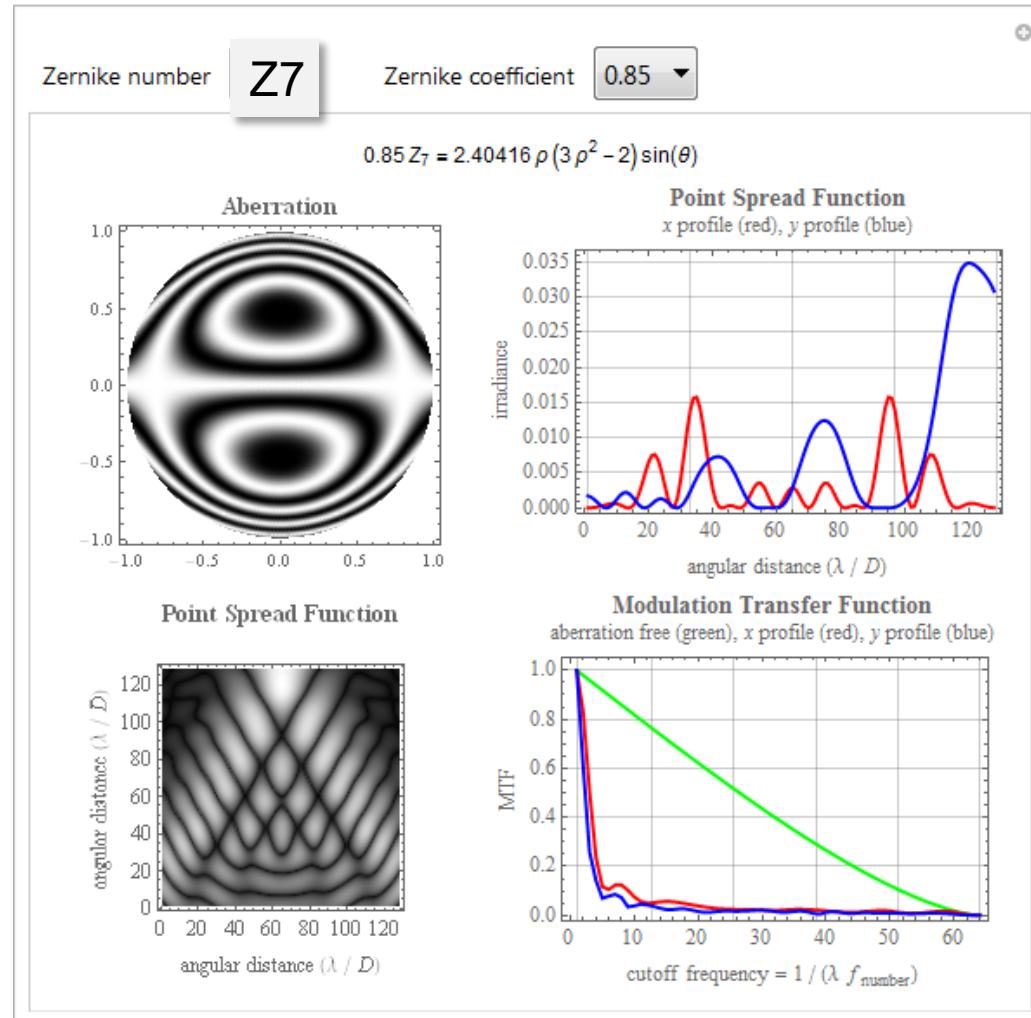
coma

Zernike Z7 ($Z_{3,1}$), „coma“ PSF, MTF



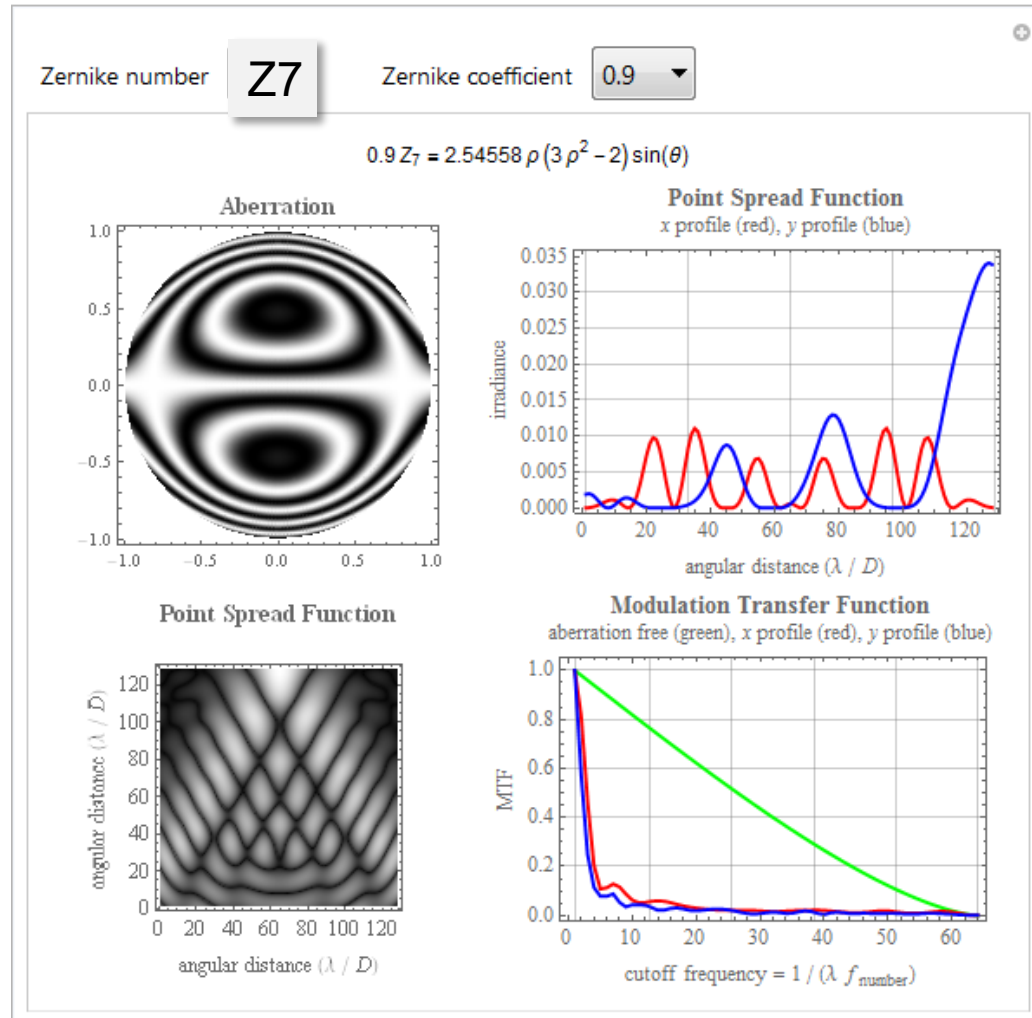
coma

Zernike Z7 ($Z_{3,1}$), „coma“ PSF, MTF



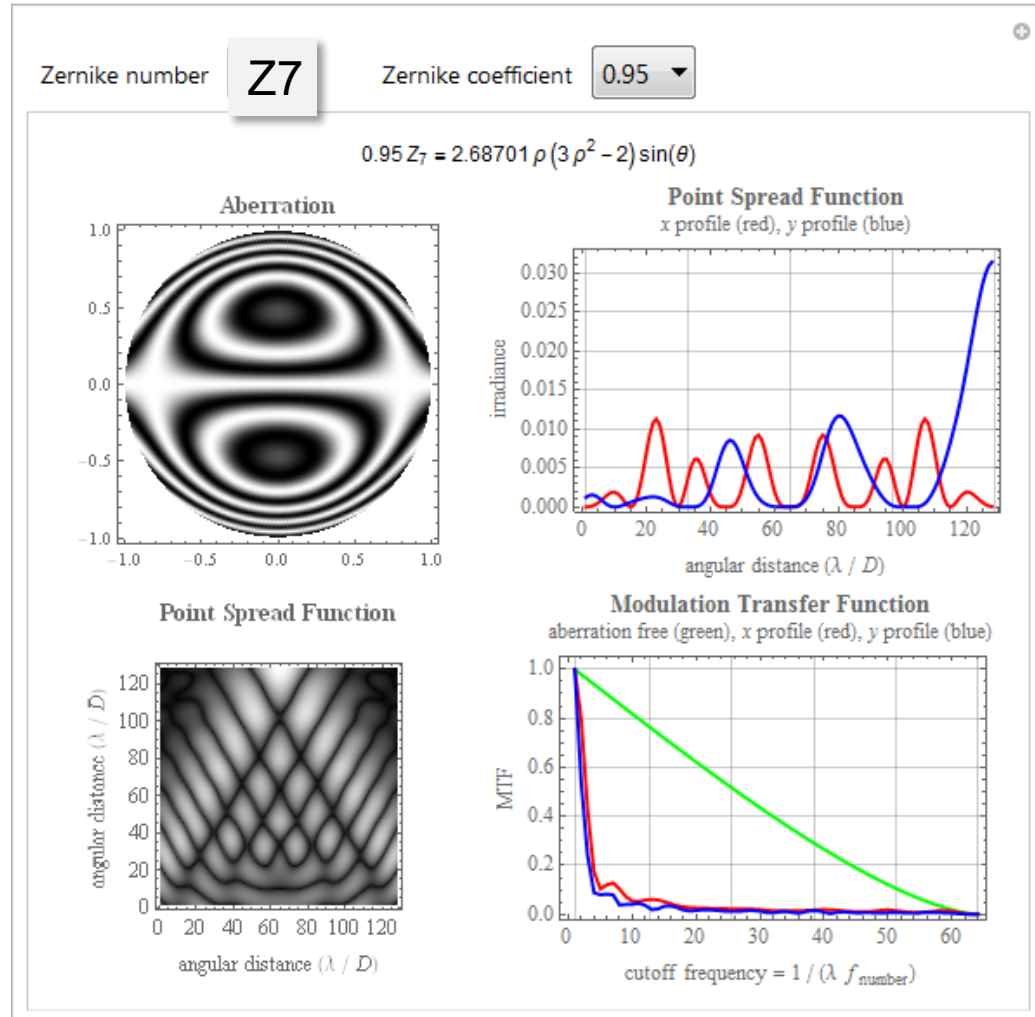
coma

Zernike Z7 ($Z_{3,1}$), „coma“ PSF, MTF



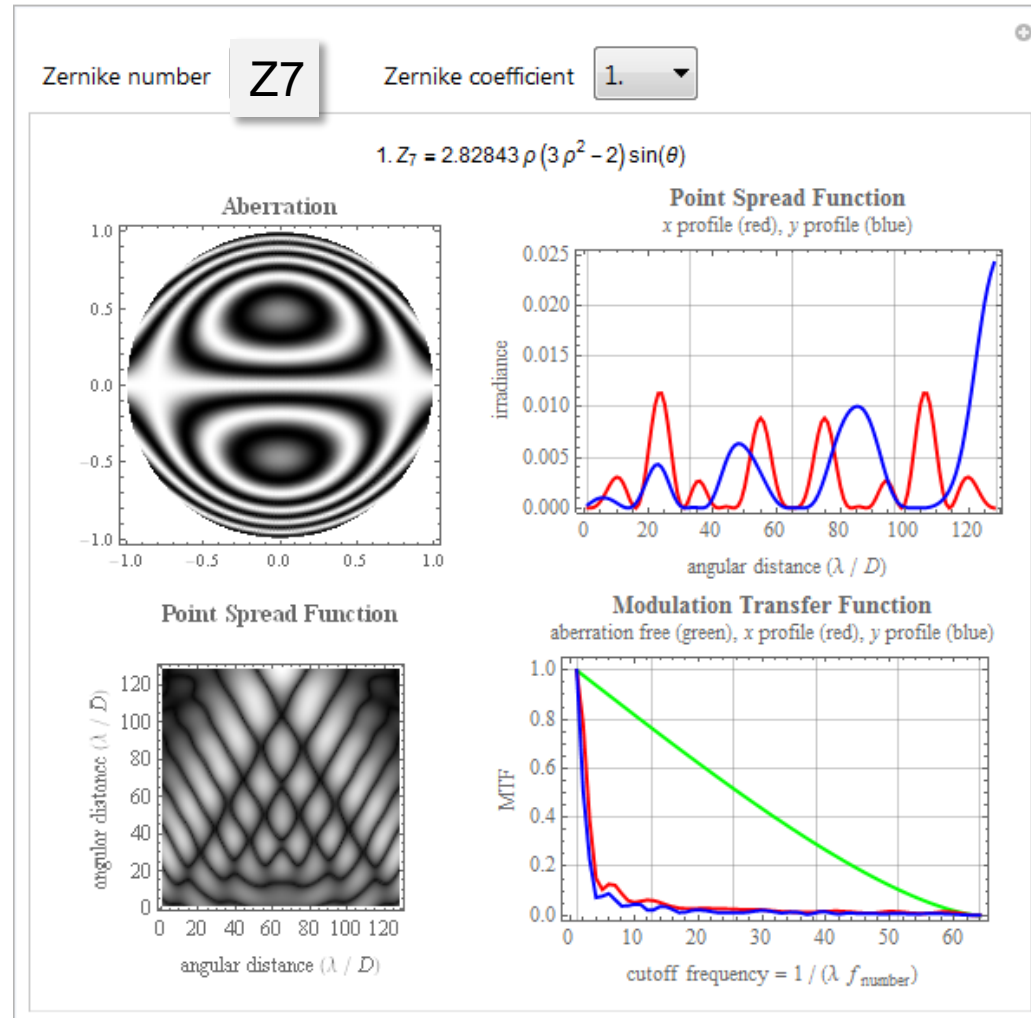
coma

Zernike Z7 ($Z_{3,1}$), „coma“ PSF, MTF



coma

Zernike Z7 ($Z_{3,1}$), „coma“ PSF, MTF

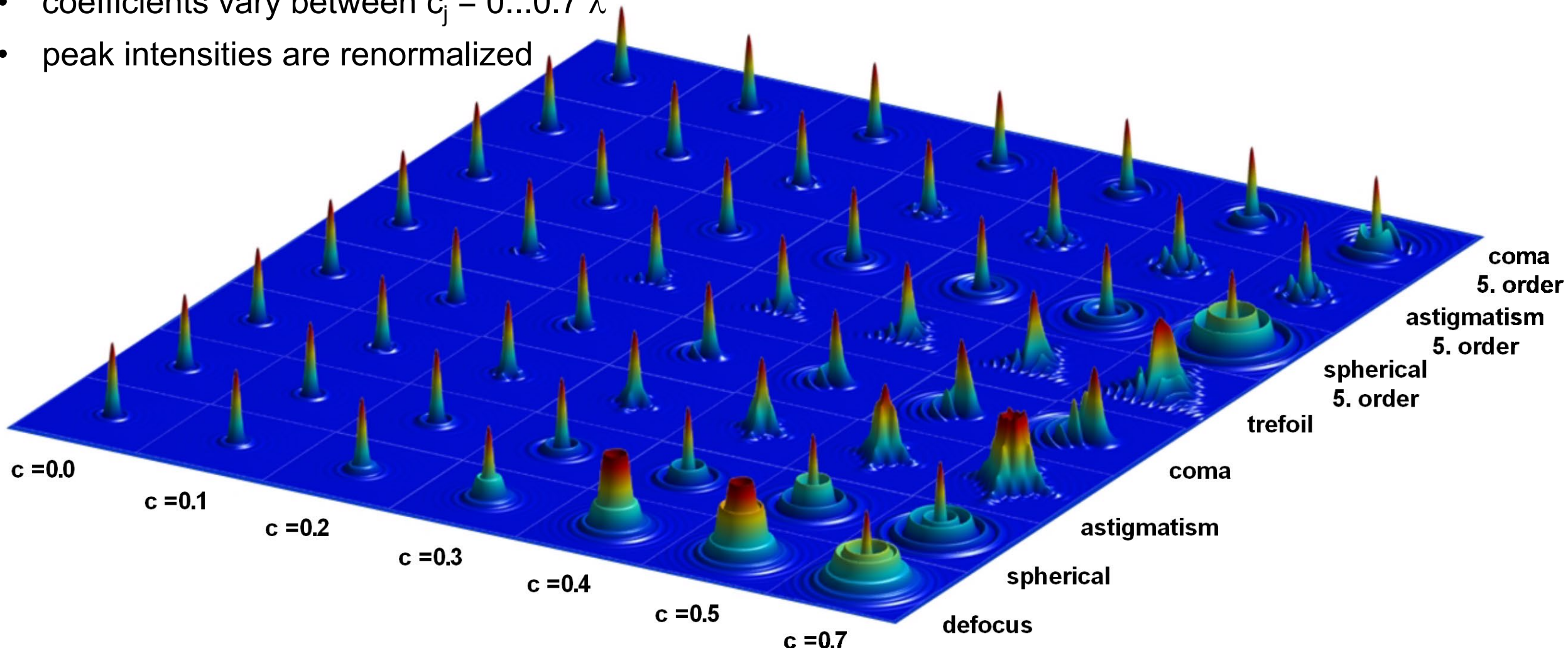


coma

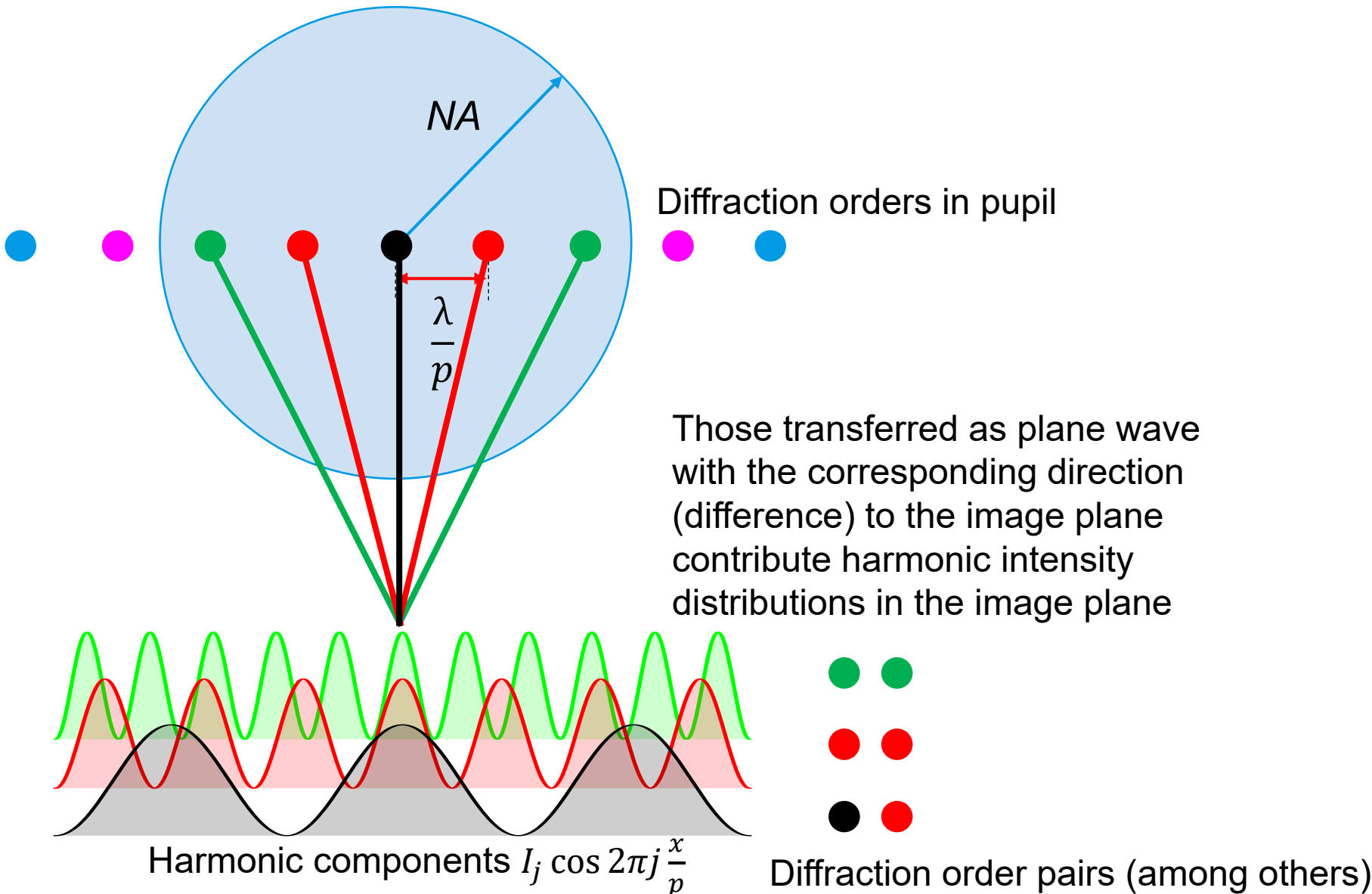
PSF with aberrations

- PSF of low order Zernike coefficients
- coefficients vary between $c_j = 0 \dots 0.7 \lambda$
- peak intensities are renormalized

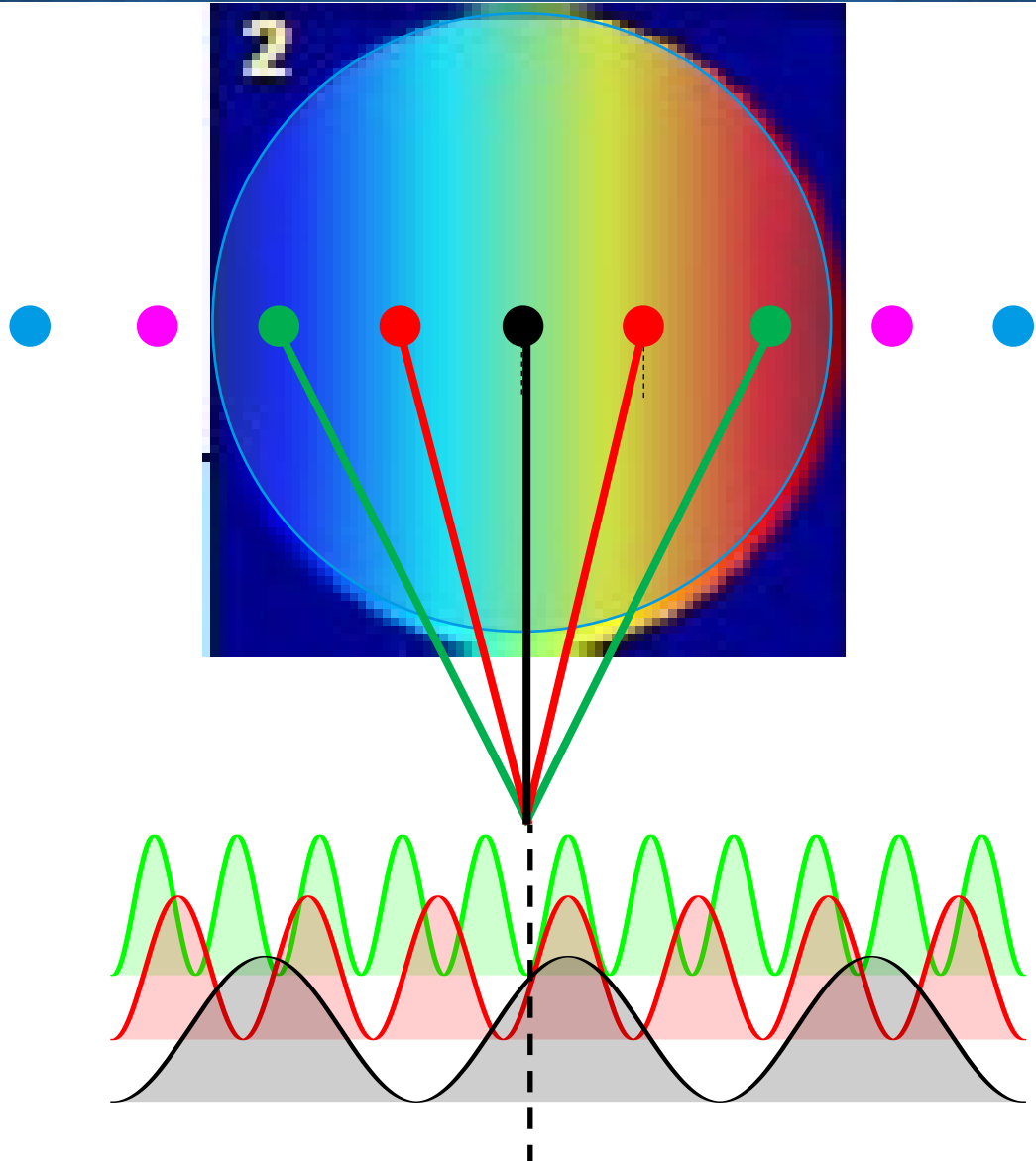
Source: H. Gross



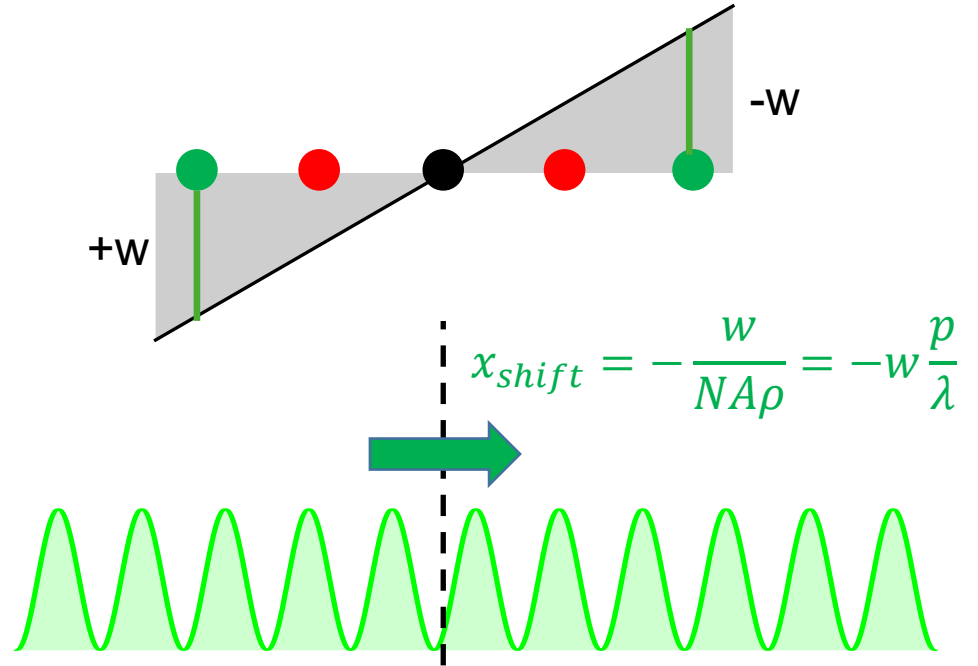
Imaging of periodic structure (ideal)



Imaging of periodic structure (wavefront tilt, Z2)

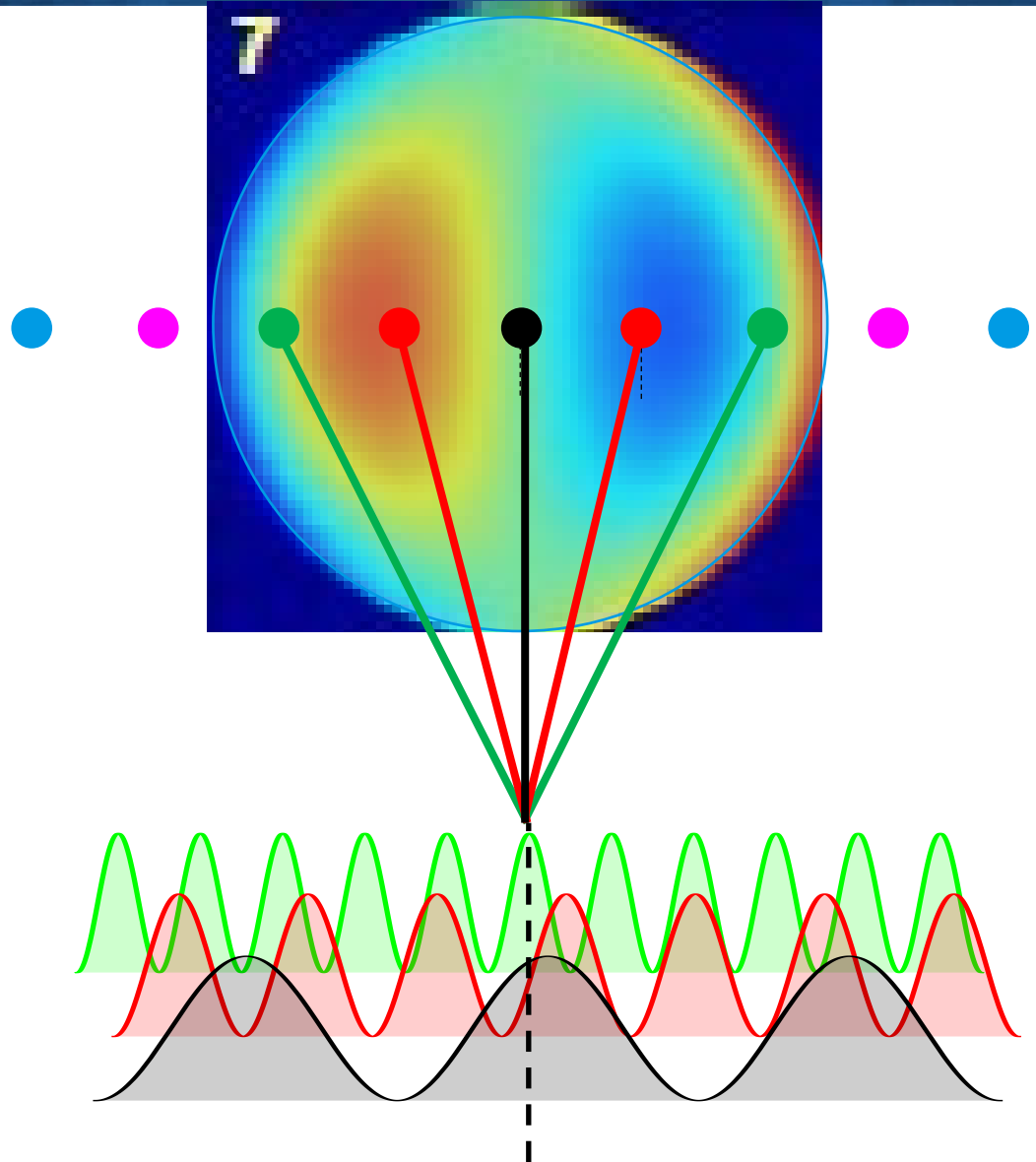


Zernike Z2:
wavefront tilt

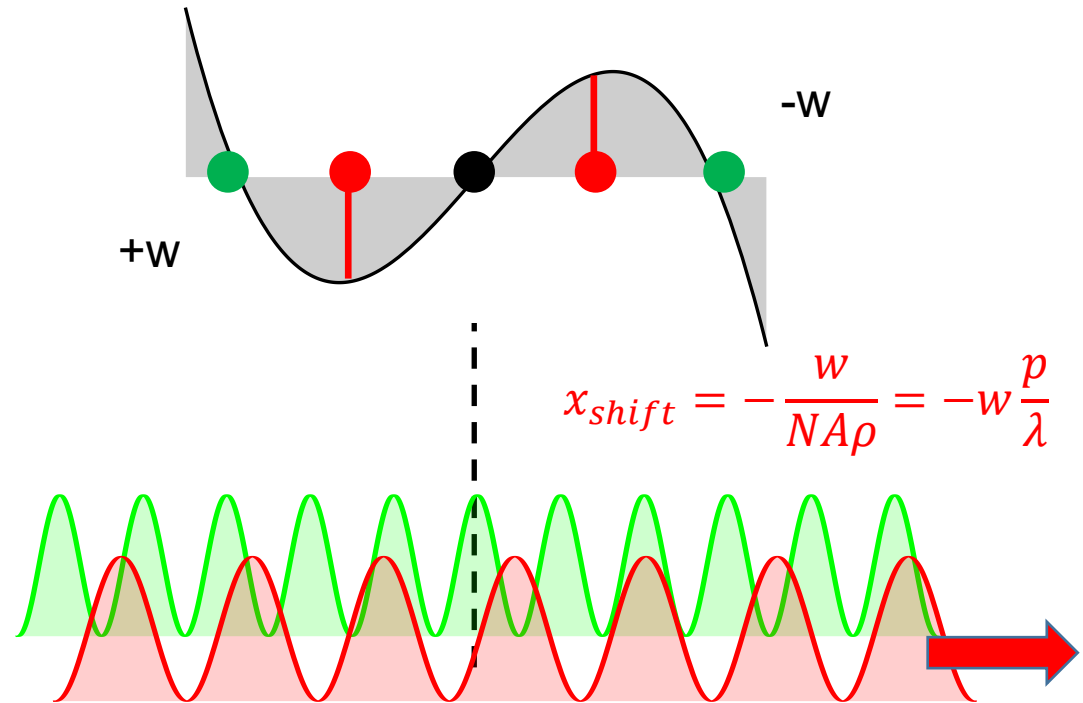
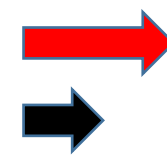


Wavefront tilt shifts all harmonics laterally by the same amount (independent on j/p). Intensity distribution unchanged, just shifted.

Imaging of periodic structure (coma, Z7)

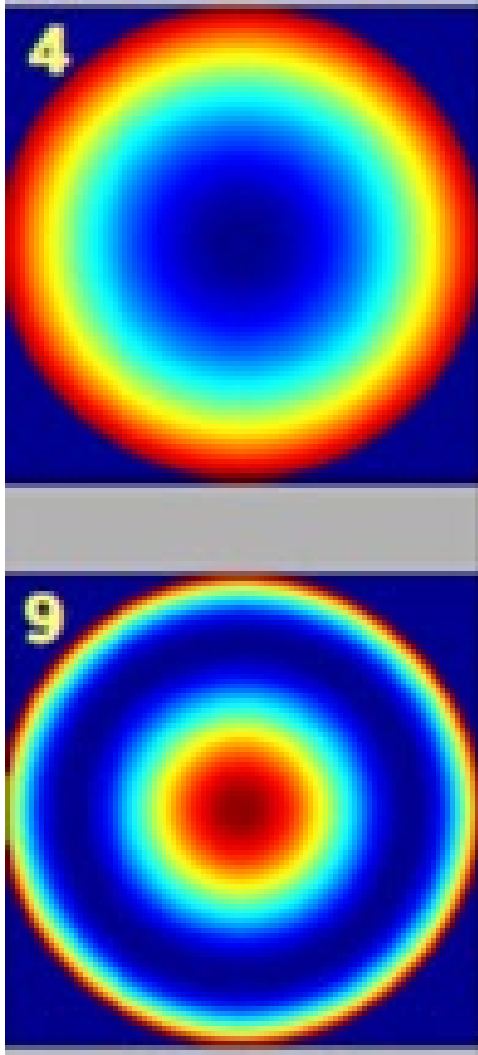


Zernike Z7:
coma



$$x_{shift} = -\frac{w}{NA\rho} = -w \frac{p}{\lambda}$$

Different wavefront tilts depending on diffraction pair: different lateral image shifts for different image harmonics (also different directions possible).
→ change of intensity distribution, as well as mean shift of intensity pattern



Zernike Z4:
defocus

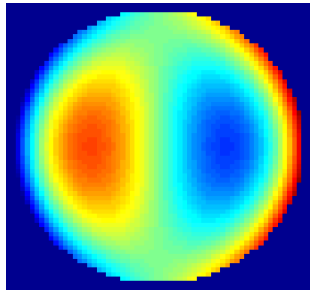
- No lateral shift of any harmonic component
- Axial shift: same amount of z-shift for all harmonics (approximately for low/moderate NA)

Zernike Z9:
spherical aberration

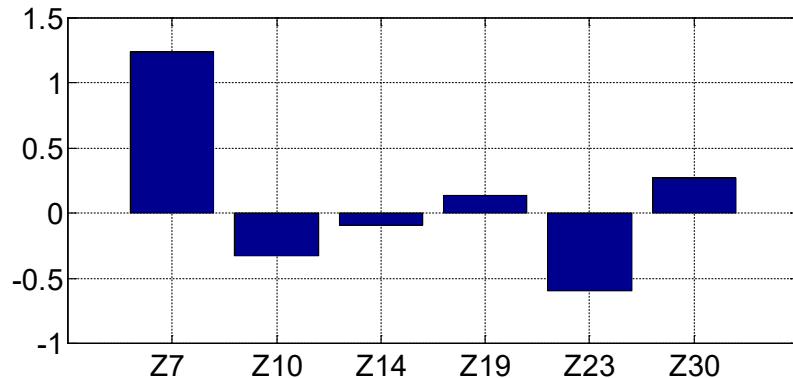
- No lateral shift of any harmonic component
- Axial shift: different amount of z-shift for different harmonics (approximately for low/moderate NA)

Litho tests & systematic approach to break down tool errors effect on litho print errors, Example: two-line test (coma sensitive)

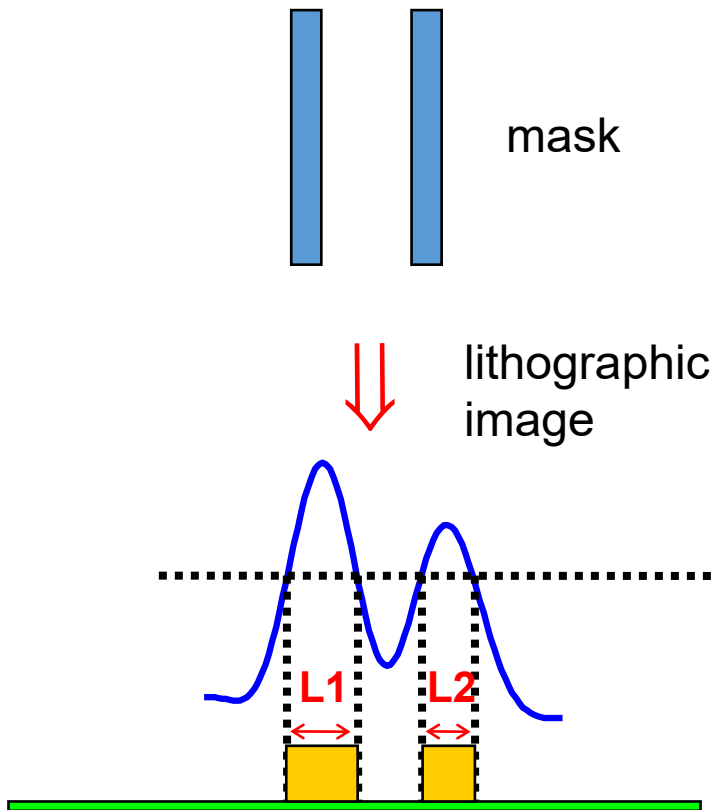
x-coma (Zernike polynomial Z7):



Sensitivities NA0.93, annular 0.65-0.9
L1-L2 [nm] / Zernike [nm]



Lines of equal width on mask:



Critical spec for optical lithography:

- Deviations in linewidths ("CD", critical dimension)
- Deviations in position (overlay)

For all performance quantities like specific

- aberrations,
- straylight,
- illumination distribution deviations, etc.

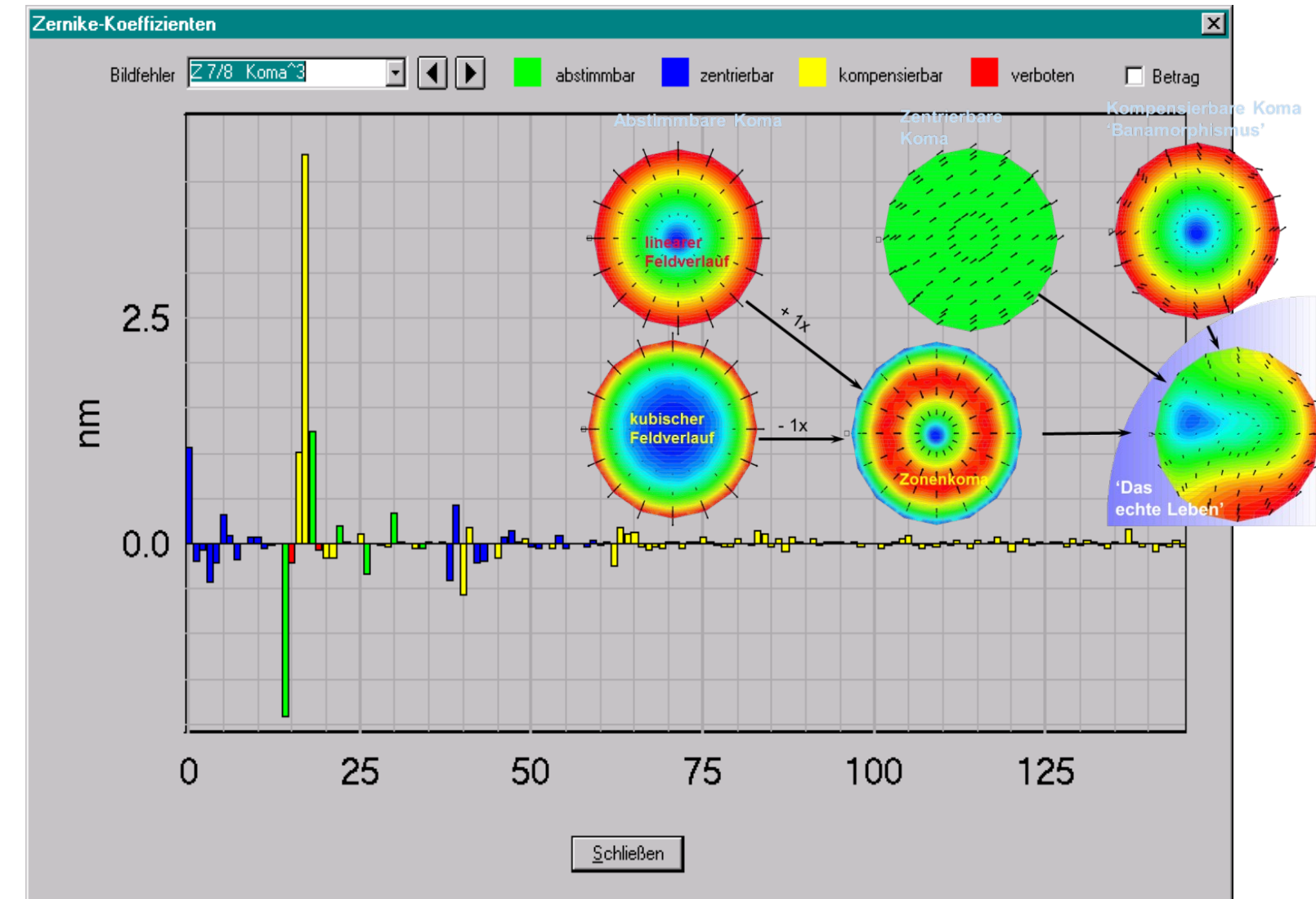
sensitivities are simulated for different structure types are generated for specific illumination / lens settings.

Basis for specifications.

Analysis Tool Systematic Assembly Process

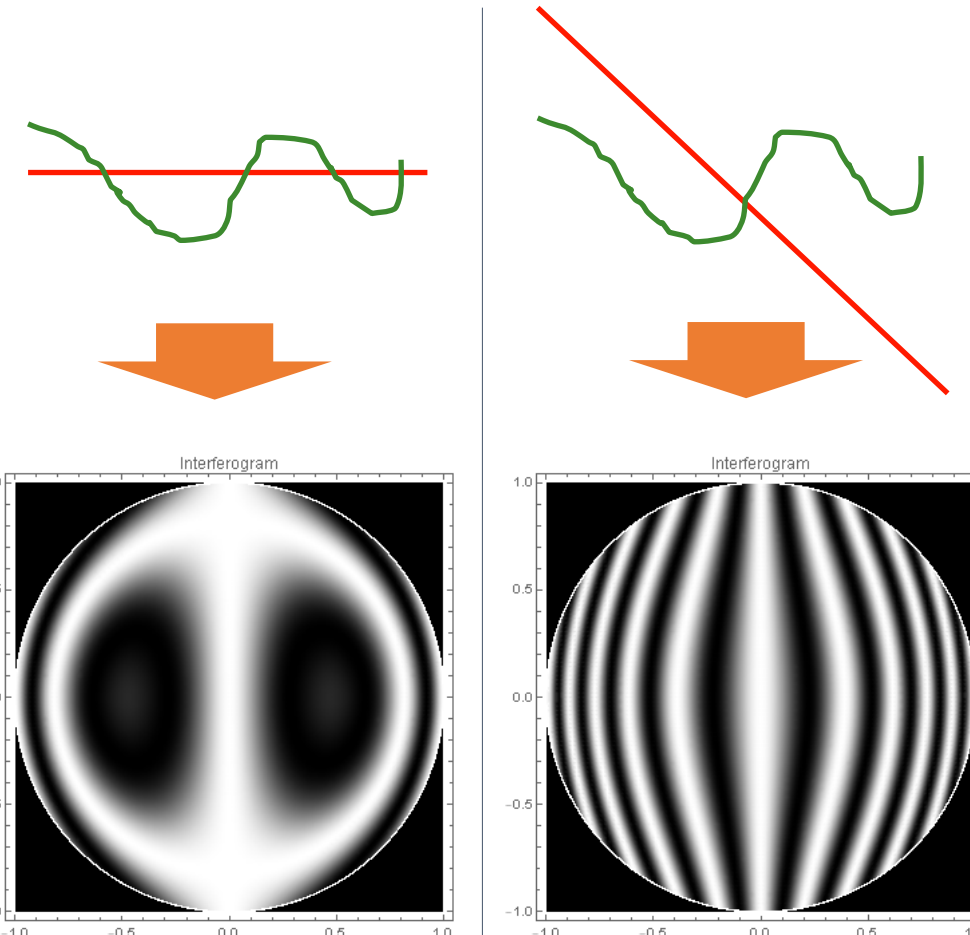
Field-Pupil Aberration (4D function) Coefficients: Data Analysis

Which aberration types dominate?



Interferogram from wavefronts

superposed wavefronts
@image sensor:

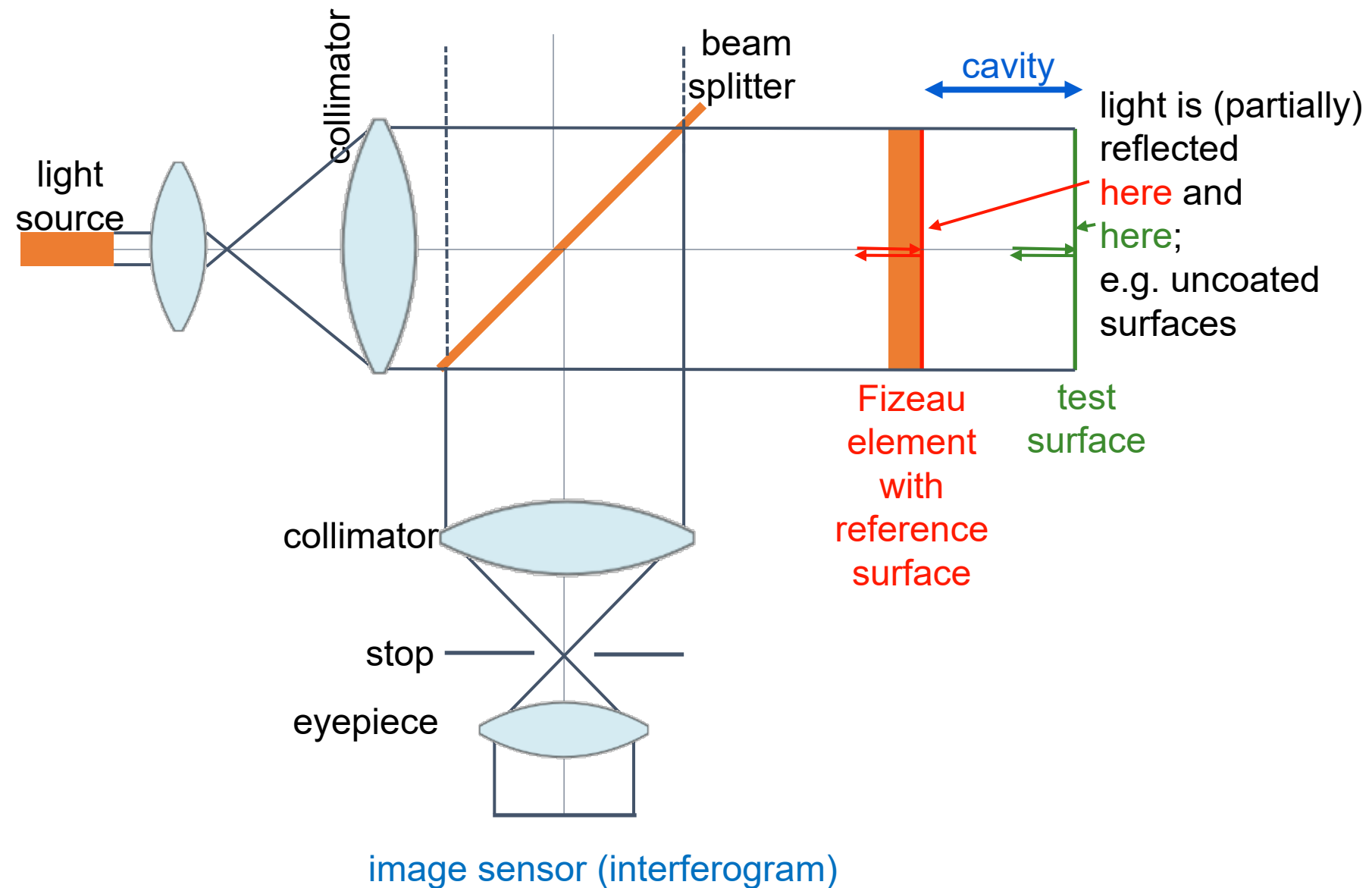


Interferogram

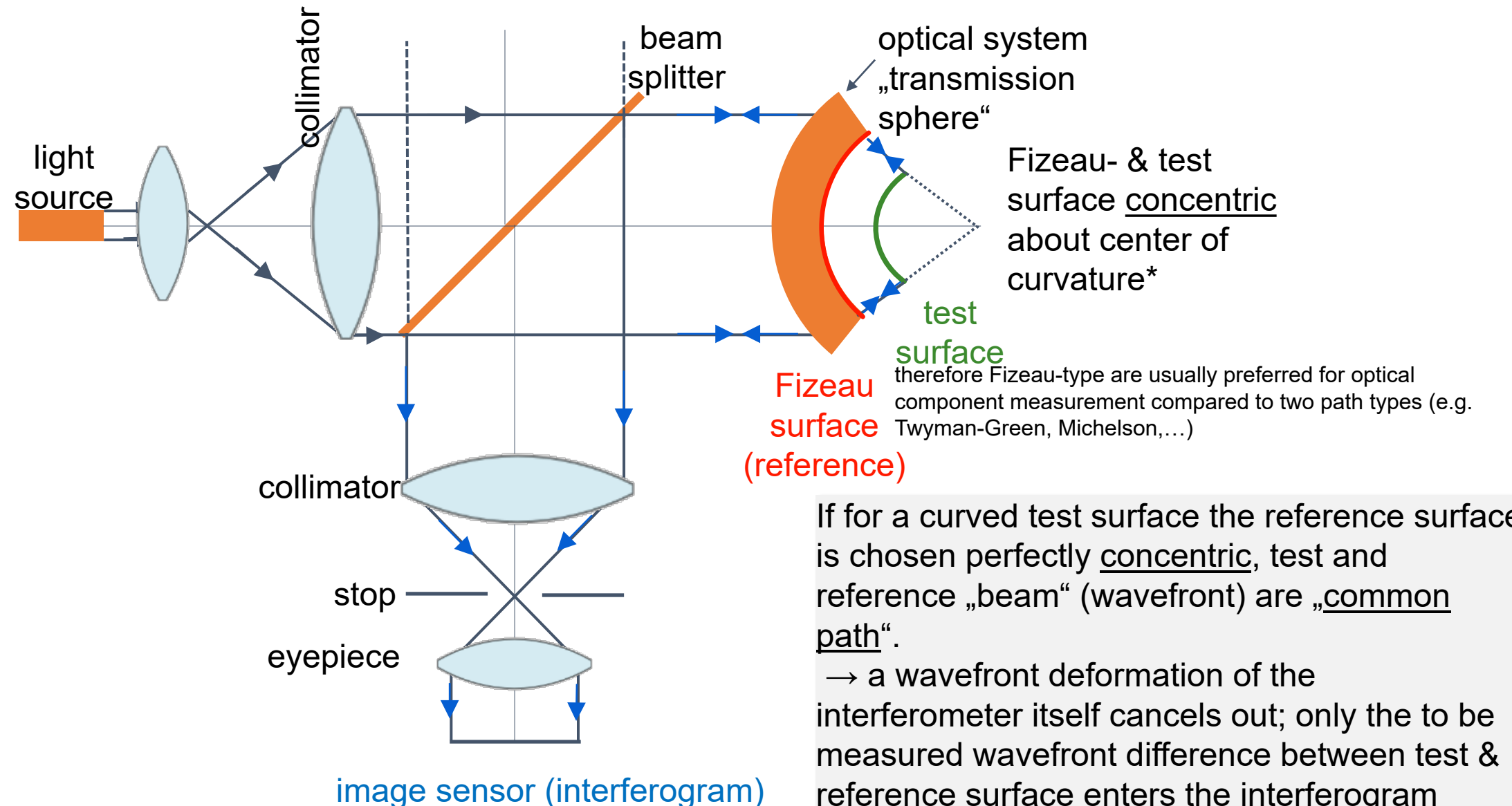
two-beam coherent
superposition gives
intensity distribution
@image sensor:

$$I(x) = | \exp(iT(x)) + \exp(iR(x)) |^2$$

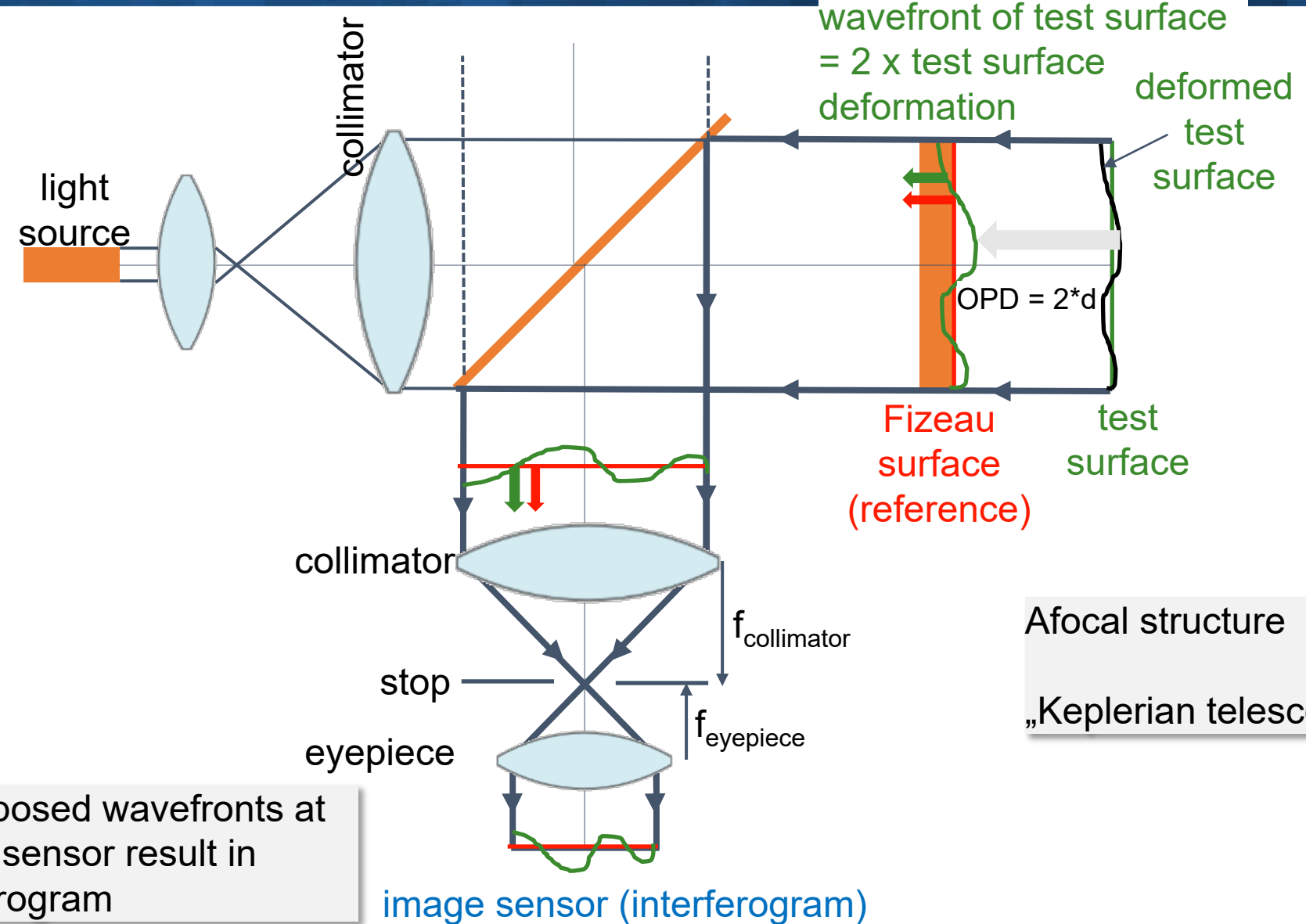
Fizeau interferometer setup (coherent)



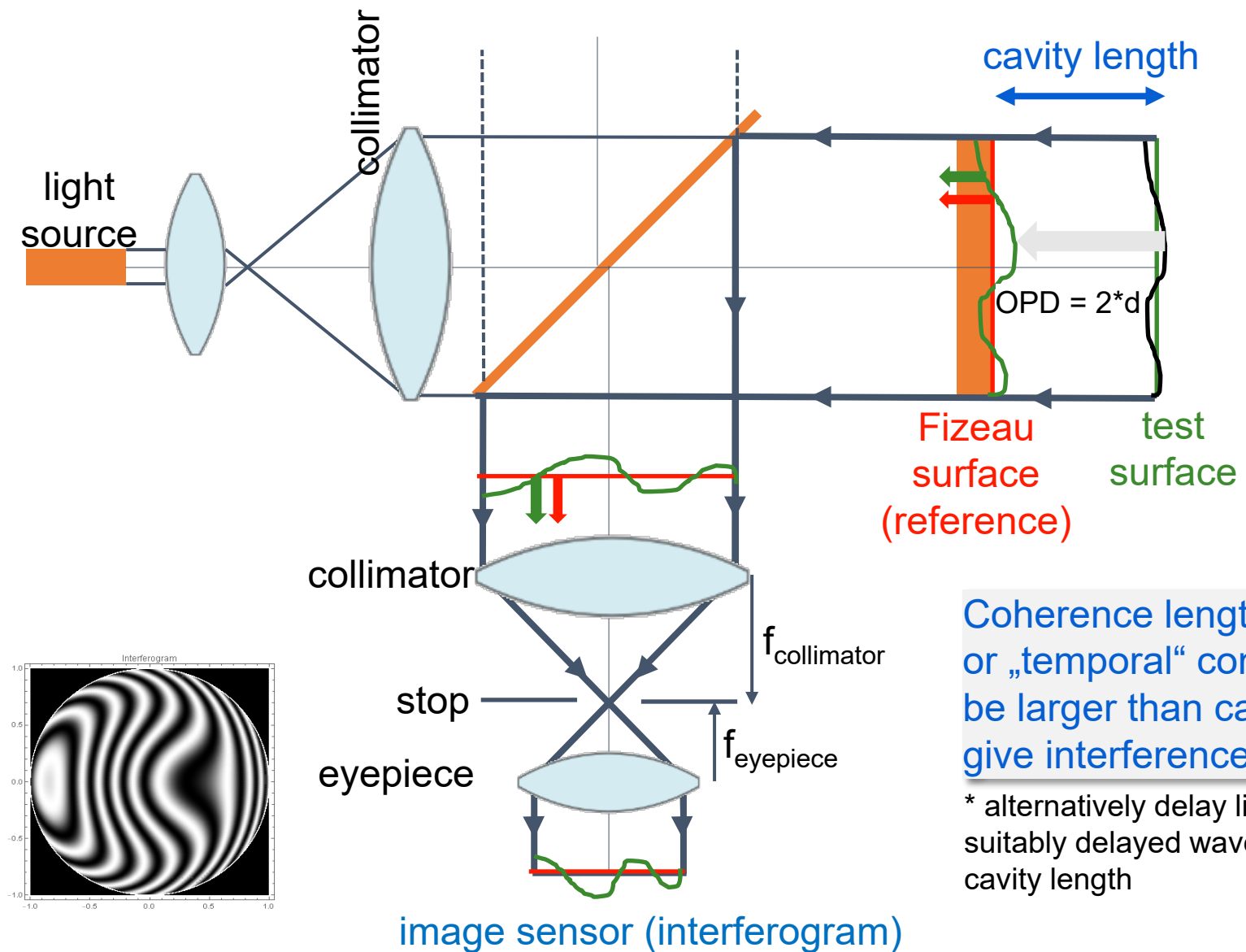
Fizeau interferometer setup (coherent) curved surface



Fizeau interferometer setup (coherent)



Fizeau interferometer setup (coherent)

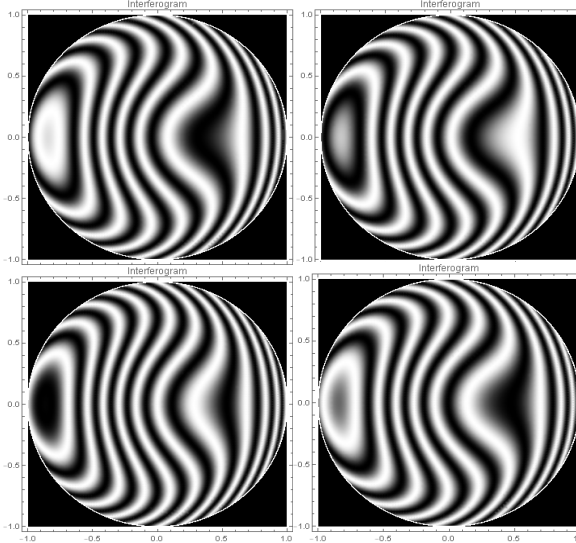


Coherence length („longitudinal“ or „temporal“ component) must be larger than cavity length to give interference pattern.

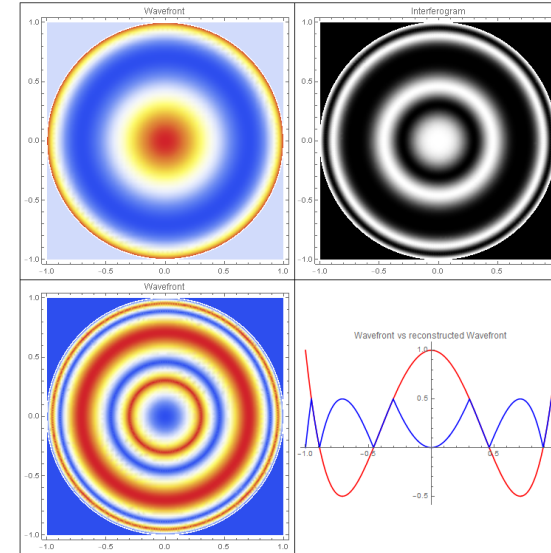
* alternatively delay line introducing suitably delayed waves according to the cavity length

Reconstruction of wavefront from set of interferograms

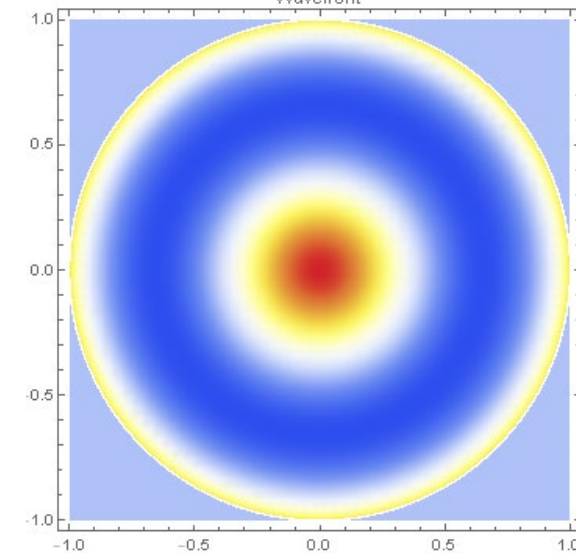
Set of interferograms



Reconstruction algorithm



Reconstructed wavefront



e.g. phase shifted by 90°, 180°, ...

$$\varphi(x, y) = \arctan \frac{Z(I_1, \dots, I_M)}{N(I_1, \dots, I_M)}$$

$$a = \frac{1}{M} \sum_{i=1}^M I_i \quad b = \frac{\sqrt{Z^2 + N^2}}{2}$$

$$A_1(x, y) = \sqrt{\frac{1}{2}(a + \sqrt{a^2 - b^2})}$$

$$A_2(x, y) = \sqrt{\frac{1}{2}(a - \sqrt{a^2 - b^2})}$$

Reconstruction & image processing &
calibration steps

Born, M. / Wolf, E. (1980). Principles of Optics.

Gross, H., Zügge, H., Peschka, M., Blechinger, F. (2007). Handbook of Optical Systems: “Aberration Theory and Correction of Optical Systems”, vol. 3.

Nijboer, B.R.A. (1943 / 47). The diffraction theory of optical images. Published in Optica.

Sasian, J. (2013). Introduction to Aberrations in Optical Systems.

Schomäcker, U. (2002). *Objekthöhenabhängige Wellenfrontdeformationen*, Dissertation am Institut für Mathematische Physik der TU Braunschweig.

Zernike, F. (1934). *Beugungstheorie des Schneidenverfahrens und seiner verbesserten Form, der Phasenkontrastmethode*, Physica I, S. 689-704.

- Wavefront aberrations are commonly represented by a series of Zernike polynomials, which are a set of orthonormal function on the unit circle with respect to the L^2 scalar product
- Choosing a set of orthogonal functions for numerical approximation of sample data (wavefront data) guarantees a monotonic improvement of approximation with an increased number of functions
- Zernike expansions are also suited for vigneted pupils
- Given a Zernike approximation of a surface, the wavefront on any subaperture (circular subsurface) can directly be computed from the given coefficient for the full aperture
- Zernike polynomials are unsuited for local or very high-order or segmented pupils
- unfortunately different conventions are specified in official norms as well as common usage (“Fringe”, “standard” etc) which can lead to confusion and errors in practice
- The symmetry of aberration representations helps to understand and predict the properties of images, e.g. for periodic images by superposition of lateral and axial shifts of harmonic image components
- systematic optical system assembly is enabled with suitable parametrization of aberrations

- Aberrations are a function of both pupil and field, e.g. the wavefront deformation $W(\vec{\alpha}, \vec{\xi}) = W(\alpha, \beta, \xi, \eta)$ depends in general on four parameters
- For rotational symmetric optical systems the number of variables reduces to 3, e.g. $W(\vec{\alpha} \cdot \vec{\alpha}, \vec{\alpha} \cdot \vec{\xi}, \vec{\xi} \cdot \vec{\xi})$
- the Seidel form of aberrations is an expansion of W as polynomial series expansion
$$W(\vec{\alpha} \cdot \vec{\alpha}, \vec{\alpha} \cdot \vec{\xi}, \vec{\xi} \cdot \vec{\xi}) = \sum_{l=0}^{\infty} \sum_{k=0}^{\infty} \sum_{j=0}^{\infty} c_{2j,k,2l} |\vec{\xi}|^{2j} (\vec{\xi} \cdot \vec{\alpha})^k |\vec{\alpha}|^{2l}$$
- Aberrations of rotationally symmetric systems are described with respect to the tangential plane including object and image point, chief ray and the optical axis; and the sagittal plane perpendicular to the tangential plane containing also object and image point, chief ray, but not the optical axis – aberrations in sagittal direction are symmetric with respect to the tangential plane, therefore aberration diagram of the sagittal branch can be reduced to positive values
- Spot diagrams and ray aberration diagrams show ray intersection points in the image points in the image plane omitting an analysis of optical path lengths; ray aberration diagrams show the ray deviations in the image plane in tangential and sagittal plane only, but give a quick overview of dominating aberration types including several wavelengths